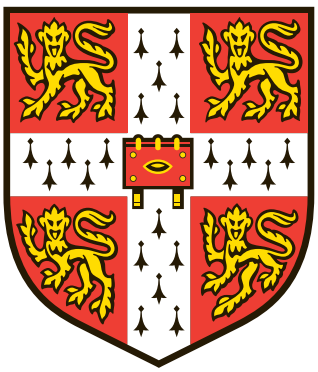

Imaging innate immune cell behaviour in lymphoid organs

Laurence Si Chong Lok
Jesus College
May 2020

Supervisors: Professor Edwin Chilvers, Professor Menna Clatworthy
Department of Medicine, University of Cambridge

This thesis is submitted for the degree of Doctor of Philosophy

Declaration

This thesis is the result of my own work and includes nothing which is the outcome of work done in collaboration except as declared in the Preface and specified in the text. It is not substantially the same as any that I have submitted, or, is being concurrently submitted for a degree or diploma or other qualification at the University of Cambridge or any other University or similar institution except as declared in the Preface and specified in the text. I further state that no substantial part of my thesis has already been submitted, or, is being concurrently submitted for any such degree, diploma or other qualification at the University of Cambridge or any other University or similar institution except as declared in the Preface and specified in the text. It does not exceed the prescribed word limit for the relevant Degree Committee.

Abstract

Imaging innate immune cell behaviour in lymphoid organs
Laurence Si Chong Lok

Innate immune cells generate the early host response to infection and tissue injury. Neutrophils are rapidly recruited from circulation to inflammatory tissues for pathogen killing. Type 2 innate lymphoid cells (ILC2s) mediate early responses to helminths and allergens via cytokine production. Innate immune cells interact with adaptive immune cells, for example via major histocompatibility complex class II (MHCII) expression for antigen presentation. Secondary lymphoid organs, including lymph nodes (LNs) and Peyer's patches, are ideal sites for innate-adaptive cellular interactions.

Whilst neutrophils migrate to LNs following inflammation, whether this occurs in homeostasis is unclear. I demonstrated the presence of neutrophils under homeostatic conditions in LNs from unstimulated mice and human organ donors, trafficking into LNs via blood and lymphatic vessels. LN neutrophils were located in interfollicular areas, and expressed MHCII at baseline. *Ex vivo*, immune complex (IC) stimulation upregulated neutrophil expression of MHCII and co-stimulatory molecules, and increased antigen-specific $CD4^+$ T cell activation. *In vivo*, neutrophils were capable of delivering circulating IC into LNs, and interacted with dendritic cells at baseline. Overall, these data suggest a novel role of neutrophils in homeostatic immune surveillance, routinely patrolling LNs and delivering systemic antigen to influence adaptive immunity.

To date little data exist on ILC2 behaviour in lymphoid tissues *in vivo*. Using two helminth inflammatory models, I demonstrated that ILC2s were the early source of interleukin-13. ILC2s were in T cell areas of LNs and Peyer's patches, and increased in cell number, size and speed of movement following inflammatory challenge, suggesting a potential role in cytokine distribution. Within small bowel wall ILC2s interacted with T cells, suggesting a broader role in activating tissue T cells. Overall, these data provide novel insights into ILC2 behaviour *in vivo*.

Neutrophils and ILC2s are involved in chronic inflammatory diseases, but few neutrophil- or ILC2-targeted treatments exist. These data represent new knowledge on neutrophil and ILC2 behaviour within LNs, facilitating development of therapeutic approaches to these diseases.

Contents

Abbreviations

AHR	Aryl hydrocarbon receptor
ATP	Adenosine triphosphate
BAFF	B cell activating factor
BFP	Blue fluorescent protein
BM	Bone marrow
CCL	C-C chemokine ligand
CCR	C-C chemokine receptor
CFA	Complete Freund's adjuvant
CRTH2	Chemoattractant receptor-homologous molecule expressed on Th2 cells
CXCL	C-X-C chemokine ligand
CXCR	C-X-C chemokine receptor
DAMP	Damage-associated molecular pattern
DC	Dendritic cell
dLN	Draining lymph node
dpi	Days post infection / immunisation
FALC	Fat-associated lymphoid cluster
FcγR	Fc gamma receptor (receptor for Fc portion of IgG)
FCS	Fetal calf serum
FDC	Follicular dendritic cell
fMLP	N-formyl-methionyl-leucyl-phenylalanine
fps	Frames per second
FRC	Fibroblastic reticular cell
G-CSF	Granulocyte colony-stimulating factor
GFP	Green fluorescent protein
GM-CSF	Granulocyte-macrophage colony-stimulating factor
GPCR	G-protein coupled receptor
Gr1	Myeloid differentiation antigen-1
HEL	Hen egg lysozyme
HEV	High endothelial venule
HLA	Human leukocyte antigen
IC	Immune complex
ICAM	Intercellular adhesion molecule-1
ICOS	Inducible T cell costimulator
Id	Inhibitor of DNA binding
IFN	Interferon
Ig	Immunoglobulin

IL	Interleukin
ILC	Innate lymphoid cell
IMDM	Iscove's Modified Dulbecco's Media
ITAM	Immunoreceptor tyrosine-based activation motif
ITIM	Immunoreceptor tyrosine-based inhibitory motif
JAM	Junctional adhesion molecule
KLRG	Killer-cell lectin like receptor G1
LFA	Lymphocyte function-associated antigen-1
LN	Lymph node
LPS	Lipopolysaccharide
LT	Leukotriene
LTi	Lymphoid tissue inducer
Ly6G	Lymphocyte antigen 6 complex locus G
LysM	Lysozyme M
LYVE-1	Lymphatic vessel endothelial hyaluronan receptor 1
Mac-1	Macrophage-1 antigen
MFI	Median fluorescence intensity
MHC	Major histocompatibility complex
NADPH	Nicotinamide adenine dinucleotide phosphate
NCR	Natural cytotoxicity receptor
NET	Neutrophil extracellular trap
NK	Natural killer
NMS	Normal mouse serum
OVA	Ovalbumin
OVAIC	Ovalbumin immune complex
PAMP	Pathogen-associated molecular pattern
PBS	Phosphate-buffered saline
PE	Phycoerythrin
PEIC	Phycoerythrin immune complex
PFA	Paraformaldehyde
PMN	Polymorphonuclear leukocyte
PNAd	Peripheral node addressin
PRR	Pattern recognition receptor
ROR	Retinoic acid receptor-related orphan receptor
ROS	Reactive oxygen species
RT-PCR	Reverse-transcriptase polymerase chain reaction
SCS	Subcapsular sinus
SEM	Standard error of mean

SHG	Second harmonic generation
TCR	T cell receptor
Th	T helper
TLR	Toll-like receptor
TNF	Tumour necrosis factor
TSLP	Thymic stromal lymphopoietin
WT	Wild type
YFP	Yellow fluorescent protein

Chapter 1. Introduction

1.1. Overview of the immune system

The immune system consists of a number of leukocyte subsets that work together to defend the body against a diverse range of microbial and inflammatory challenges. Traditionally, the immune system is considered to have two arms, namely innate immunity and adaptive immunity. The innate immune response is present in all multicellular organisms and, together with anatomical barriers such as skin and respiratory tract mucociliary layer, forms the early host defence against invading pathogens (1). Innate immune cells, including neutrophils, eosinophils, macrophages and dendritic cells (DCs), respond rapidly to stimuli by expressing a range of receptors that recognise molecular patterns common to pathogens and damaged cells (Section 1.5.1) (2). The adaptive immune system consists of B and T lymphocytes that express antigen-specific receptors generated by somatic rearrangement of antigen receptor genes; the response is slower but more specific compared to innate immunity, and the ability to generate long term immune memory enables an effective response upon rechallenge by the same antigen (3).

The innate and adaptive systems work in conjunction to generate inflammatory responses. Innate immune cells can process and present antigen to T cells to activate adaptive immunity, and both innate and adaptive cells can produce a variety of pro- and anti-inflammatory cytokines resulting in bidirectional cellular crosstalk (4). In addition, innate lymphoid cells (ILCs) have recently been characterised; these cells originate from lymphoid progenitors and have analogous functions to T cell subsets in terms of cytokine production, but do not express antigen-specific receptors and like other innate immune cells respond rapidly to microbial and inflammatory challenges (5). Therefore, immune cell subsets form a complex network with interlinked functions.

1.1.1. Innate and adaptive immune cells

Cells of the immune system begin their development in the yolk sac and liver in the fetus, whilst in adults haematopoiesis occurs in bone marrow (BM), where haematopoietic stem cells differentiate into common lymphoid progenitors or common myeloid progenitors. Common lymphoid progenitors give rise to adaptive (B and T cells) and innate (ILCs) lymphocytes (6). Common myeloid progenitors give rise to innate immune cells including granulocytes (neutrophils, eosinophils and basophils) and monocytes / macrophages (3). DCs can develop from myeloid progenitor- or lymphoid progenitor-derived DC precursors (7).

Innate immune cells respond rapidly to infectious and inflammatory stimuli, performing roles such as pathogen killing and production of cytokines that recruit or activate other immune cells. Neutrophils and monocytes migrate from the circulation to inflammatory tissue sites, where they exert their effector functions (8). There are also tissue resident innate immune cells, such as macrophages (blood monocyte-derived or yolk sac-derived), DCs and ILCs (9,10), that respond to local inflammatory signals, and some innate immune cells such as DCs (11) and neutrophils (12) are capable of migration into secondary lymphoid organs such as lymph nodes (LNs), the sites of adaptive immune responses.

Adaptive immune cells include B and T lymphocytes. Both B cell receptor (immunoglobulin, Ig) and T cell receptor (TCR) undergo somatic rearrangement of their variable (V), diversity (D) and joining (J) gene segments, creating a diverse permutation of receptor genes enabling antigen specificity to be achieved (13). B cells produce different subclasses of immunoglobulin that can bind specifically to antigen, to neutralise antigen or opsonise antigen for ingestion by phagocytes. T cells mature in the thymus into $CD4^+$ or $CD8^+$ T cells. $CD8^+$ or cytotoxic T cells mediate cellular killing by secreting cytotoxic substances such as granzymes and perforin and triggering target cell apoptosis in a contact-dependent manner. $CD4^+$ or T helper (Th) cells differentiate into subpopulations with varying patterns of cytokine production, including Th1 cells involved in antiviral immunity, Th2 cells involved in allergy and anti-helminth immunity, and Th17 cells involved in neutrophilic inflammation (14).

The ILC subsets ILC1s, ILC2s and ILC3s have analogous functions to Th1, Th2 and Th17 cells respectively, but unlike T cells they lack antigen-specific receptors and respond rapidly to inflammatory stimuli (6).

1.1.2. Antigen presentation

TCRs recognise pathogens and cell fragments presented by major histocompatibility complex (MHC) molecules, also known as human leukocyte antigen (HLA) in humans and H2 in mice. MHC class I (MHCI) is expressed on all nucleated cells, and includes HLA-A, HLA-B and HLA-C subclasses in humans (15), and H2-D, H2-K and H2-L in mice. Endogenous antigens, such as intracellular proteins from virus-infected cells, are processed into smaller peptides and loaded onto MHCI on the cell surface. MHCI then presents the endogenous peptide to $CD8^+$ T cells with specific TCRs, thus activating cellular killing.

MHC class II (MHCII) includes HLA-DP, HLA-DQ and HLA-DR in humans (15), and H2-A, H2-E and H2-P in mice. Antigen presenting cells, for example DCs and macrophages, phagocytose exogenous antigens such as bacterial proteins and process them into peptides

for loading onto MHCII and subsequent presentation to $CD4^+$ T cells, resulting in their activation. Exogenous antigens can also be phagocytosed, loaded onto MHCI and cross-presented to $CD8^+$ T cells (3).

In addition to the binding of antigenic peptide-MHC complex to the TCR, a second, co-stimulatory signal is also required for full T cell activation, for example by the ligation of CD80 (B7.1) / CD86 (B7.2) on the antigen presenting cell to CD28 on the T cell, or that of CD40 on the antigen presenting cell to its ligand CD40L (CD154) on the T cell (16). DCs, macrophages and B cells are traditionally considered professional antigen presenting cells, with high surface expression of MHCII.

Therefore, upon activation by pathogenic stimuli, innate immune cells process and present antigenic peptides to T cells, resulting in the activation of T cell effector functions (Figure 1.1). B cells that have captured antigens by their immunoglobulin receptors also internalise and process the antigens for presentation to T cells; B cells, in return, receive reciprocal T cell help, where co-stimulatory ligand-receptor binding results in B cell maturation and isotype switching, leading to generation of antibody-producing plasma cells and memory B cells (14).

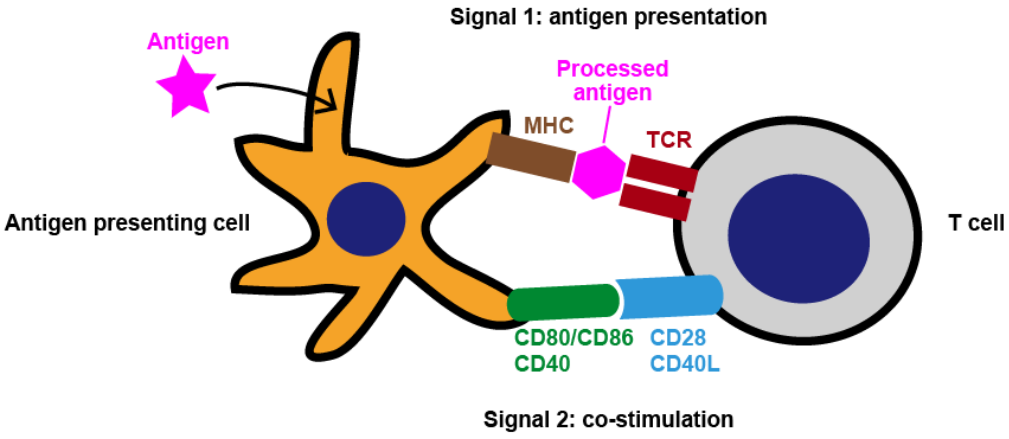

Figure 1.1. Mechanism of antigen presentation. Antigen is processed by the antigen presenting cell, loaded onto surface MHC and recognised by TCR. The antigen presenting cell also upregulates expression of co-stimulatory molecules, providing the second signal required for full T cell activation.

1.2. LNs: the anatomical site where innate and adaptive immune cells interact

Adaptive immunity involves interactions between antigen-specific cells, which are relatively rare populations within circulating leukocytes. Therefore, these interactions are concentrated in secondary lymphoid organs, stations where immune cells congregate and antigens are trapped within a confined anatomical space, increasing the probability of these cells encountering each other, and facilitating specific antigen encounter and cellular interactions. Secondary lymphoid organs include spleen, LNs, and other lymphoid tissues such as lymphoid aggregates in the small bowel known as Peyer's patches (17).

LNs are present at multiple sites throughout the body, receiving lymphatic drainage from local areas of skin, such as inguinal, popliteal and axillary LNs, or from organs, such as mediastinal LN for the lungs, and mesenteric LN for the gut. Packed with B and T lymphocytes, the LN has a specific micro-anatomical cellular structure, with innate and stromal cells contributing to the overall adaptive immune response (18).

1.2.1. LN structure and lymphocyte maturation

Each LN contains an inner medulla and an outer cortex, surrounded by a fibrous capsule with a subcapsular sinus (SCS). The supplying artery enters from the hilum of the medulla and branches outwards into capillaries in the cortex, with the draining vein leaving from the hilum. The post-capillary venules are known as high endothelial venules (HEVs) due to their specialised layer of cuboidal endothelial cells; these express peripheral node addressin (PNAd) which is used in studies to identify HEVs (19). Lymphatic fluid from peripheral tissues drains via afferent lymphatic vessels into the SCS, with protrusions extending into the LN as cortical sinuses, which in turn connect to medullary sinuses that drain into the efferent lymphatic vessel at the hilum. Lymphatic endothelial cells express lymphatic vessel endothelial hyaluronan receptor 1 (LYVE-1), which is used to identify lymphatic vessels (17,18).

B and T lymphocytes enter from blood into the LN by migration across HEVs in a multi-step process. Initial rolling is mediated by lymphocyte L-selectin (CD62L) binding to endothelial PNAd. This is followed by C-C chemokine receptor CCR7 and C-X-C chemokine receptor CXCR4 on lymphocytes binding to their respective ligands CCL19 / CCL21 and CXCL12 on the HEV lumen. Adhesion and transmigration is then mediated by lymphocyte function-associated antigen-1 (LFA-1) binding to endothelial intercellular adhesion molecule-1 (ICAM-1) (18,20). Within the LN, lymphocytes are guided to their respective locations by resident stromal cells in those areas; fibroblastic reticular cells (FRCs) produce CCL19 and CCL21 to

guide CCR7-expressing T cells to the paracortex / interfollicular areas, and follicular dendritic cells (FDCs) produce CXCL13 to guide $CXCR5^+$ B cells into the follicles, as well as $CXCR5^+$ follicular helper T cells that provide B cell help (19,21,22).

T cells are activated in the LN paracortex by antigen presented on MHC molecules together with a second co-stimulatory signal from antigen presenting cells. Early upon stimulation, $CD4^+$ T cells, known as Th0 cells, produce interleukin-2 (IL-2) driving further autocrine T cell proliferation. Th0 cells differentiate into Th cell subsets depending on the types of cytokines they are exposed to. IL-12 and interferon-gamma (IFNγ) drive differentiation into Th1 subset that produces further IFNγ and is involved in cellular immunity and response to intracellular pathogens. IL-4 drives differentiation into Th2 subset that produces IL-4, IL-5, IL-9 and IL-13, cytokines involved in humoral immunity, allergy and response to helminth infections. IL-1β, IL-6, IL-23 and transforming growth factor beta (TGFβ) drive differentiation into Th17 subset that produces IL-17, IL-21 and IL-22, involved in neutrophilic inflammation, response to bacterial and fungal infections, as well as autoimmunity. Other Th subsets include regulatory T cell subset (Treg) that produces the anti-inflammatory cytokine IL-10, follicular helper T cell subset (Tfh) that produces IL-21, and Th9 subset that produces IL-9 (14,22,23).

Immature B cells first express low affinity IgM, and mature naïve B cells also express IgD. Within LN follicles, naïve B cells recognise antigen via surface immunoglobulins (B cell receptors), and Tfh cells at the T-B border provide co-stimulatory signals for B cell activation. This interaction results in the formation of germinal centres, and isotype class switching of B cells where gene rearrangement enables switching of the constant region (Fc) of immunoglobulin heavy chain, leading to mature B cells switching their immunoglobulin production to high affinity IgG, IgA or IgE, depending on the stimulatory cytokines involved. During this B cell maturation, somatic hypermutation and affinity maturation further refine antigen specificity, and antibody-producing plasma cells as well as long-term memory B cells are formed in the germinal centre (3,14). IgG consists of several subclasses, and is involved in pathogen opsonisation and complement fixation, whilst antigen-IgG immune complex (IC) is involved in a number of autoimmune diseases. IgA is involved in mucosal defences, and IgE is associated with allergy and responses to helminths (24).

Lymphocytes stay transiently in the LN in search of antigen. Experiments using adoptive transfer of T cells showed peripheral LN residence time of 12 hours for $CD4^+$ T cells with the time reduced in $MHCII^{-/-}$ recipient mice, and 21 hours for $CD8^+$ T cells with the time unaffected in $MHCI^{-/-}$ recipient mice (25). Lymphocytes egress via efferent lymphatics back into the circulation, guided by sphingosine-1-phosphate (S1P) gradients in lymphatics (26).

1.2.2. Role of innate immune cells and stromal cells in LNs

In peripheral tissues, antigen such as bacteria can be phagocytosed by DCs; activated DCs then upregulate CCR7 expression, and migrate via lymphatics into the draining LN (dLN), guided by CCL19 and CCL21 produced by lymphatic vessels (11,27). Peripheral antigen draining via afferent lymphatics into the SCS can be captured by LN-resident DCs that present the antigen to T cells (28). Antigen can also be captured by specialised $CD169^{+}CD11b^{+}$ macrophages that line the floor of the SCS, limiting the systemic spread of pathogens beyond the dLN (29).

Within the LN paracortex, resident DCs are positioned near HEVs to facilitate encounters with incoming T cells (30), and FRCs form conduits providing a structural network along which T cells can move and interact with DCs (21). FRCs themselves can also directly present antigen to T cells (31). Therefore, the LN paracortex / interfollicular areas are sites of T cell activation; innate cells such as DCs capture and process antigen for presentation on MHC molecules to T cells, influencing T cell differentiation and the immune response to the antigen. Macrophages resident in T cell zones have also been identified that function to efferocytose apoptotic T cells (32).

Within LN follicles, B cell activation by antigen encounter with Tfh co-stimulation results in the formation of germinal centres, with B cells maturing into antibody-producing plasma cells and long-term memory B cells (14). Antigen from peripheral tissue draining via afferent lymphatic vessels into the SCS can be captured by SCS macrophages and transferred to follicular B cells, leading to B cell maturation (33,34). Within the follicle, FDCs act as long-term stores of antigen, in the form of antigen-antibody IC, to facilitate germinal centre B cell responses (35). The anatomical structure and cellular organisation of a LN is summarised in Figure 1.2.

Whilst DCs and macrophages are traditionally considered professional antigen presenting cells, and play important roles in the generation of B and T cell responses in LNs as described above, it is now recognised that other innate immune cells also play a role in shaping the adaptive immune response. Neutrophils, traditionally considered the archetypal circulating innate effector cell type that are recruited from blood to inflammatory tissues for pathogen killing, are capable of expressing MHCII and co-stimulatory molecules for antigen presentation and interaction with T cells (36). The recently characterised ILCs reside within tissues including mucosal barrier sites, responding rapidly (hence innate-like) to local inflammatory stimuli by producing cytokines; some ILC subsets, including ILC2s and ILC3s, have also been shown to be capable of expressing MHCII (37). Neutrophils (38), ILC2s and ILC3s (39) are found within LNs, placing them in locations where they can potentially interact

with lymphocytes and other LN-resident immune and stromal cells to influence the adaptive immune response (Figure 1.2).

During my research I investigated the influence of innate immune cells on adaptive immunity, and specifically focussed on studying the dynamic behaviour of two innate immune cell types within LNs, neutrophils and ILCs (ILC2s in particular). These cell types will be described in more detail below.

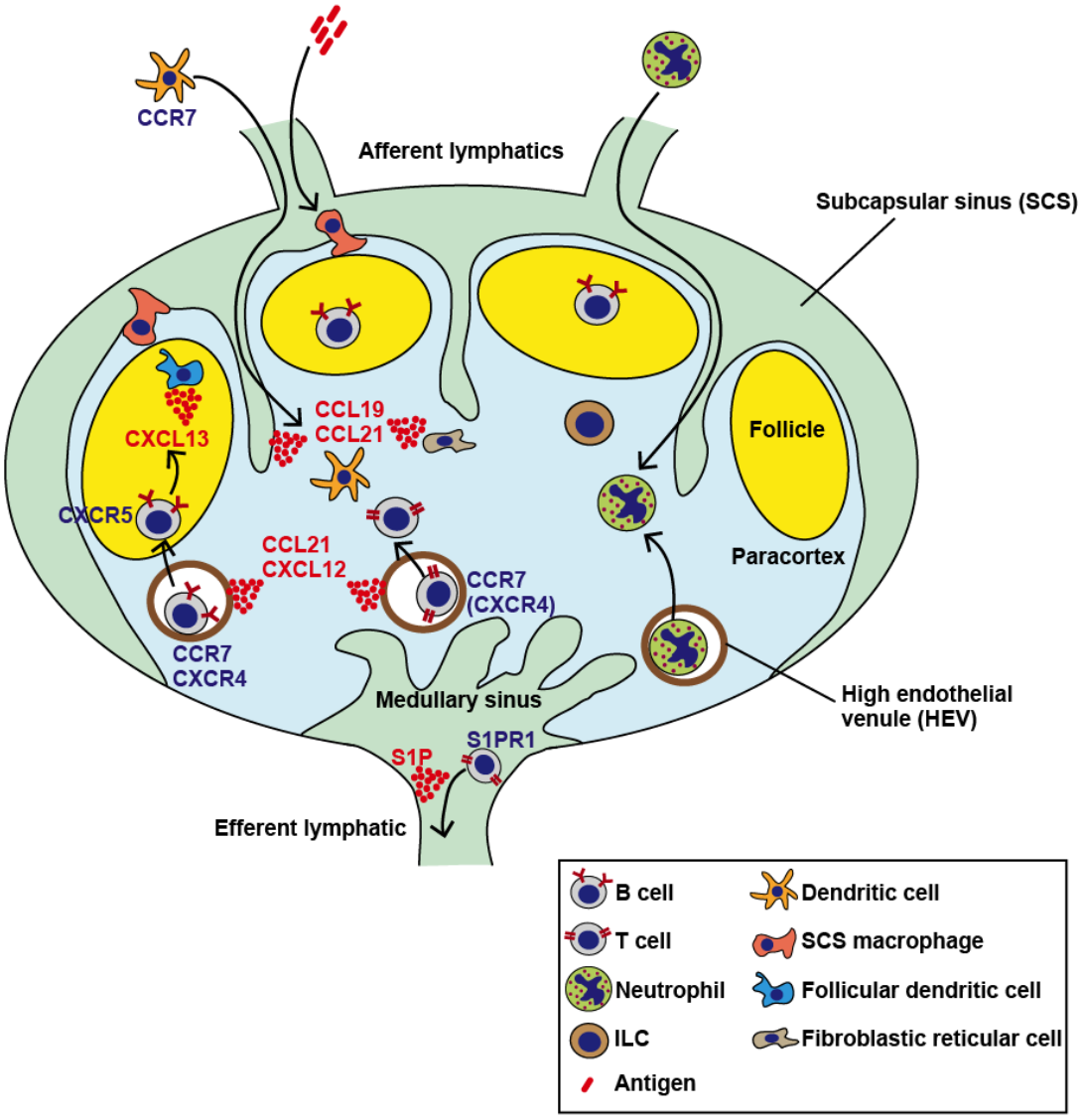

Figure 1.2. Structure of LN. B and T cells enter via HEVs to reside in follicles and paracortex, respectively. Antigen enters via afferent lymphatics, captured by DCs or SCS macrophages. Migrated DCs reside near HEVs to interact with T cells. Lymphocytes re-enter circulation via efferent lymphatics. Cell migration is guided by chemokines (in red) from endothelial and stromal cells and chemokine receptors (in blue) on immune cells.

Neutrophils have been shown to migrate to LNs in inflammation, and ILCs have also been shown to be present in LNs.

1.3. Neutrophils: overview

Neutrophils are a key early effector of the innate immune response. They are efficient phagocytes that are rapidly recruited to sites of infection or tissue injury. The cytoplasm of neutrophils, also known as polymorphonuclear leukocytes (PMNs) due to their distinct nuclear morphology, is filled with primary (azurophilic), secondary (specific) and tertiary (gelatinase) granules, containing pro-inflammatory proteins (40). Neutrophils can be primed by cytokines such as tumour necrosis factor alpha (TNFα), and a second signal such as the bacterial peptide N-formyl-methionyl-leucyl-phenylalanine (fMLP) then fully activates primed neutrophils (41), leading to processes including the generation of reactive oxygen species (ROS) via nicotinamide adenine dinucleotide phosphate (NADPH) oxidase activation, phagocytosis of pathogens, degranulation of cytotoxic proteins, and release of neutrophil extracellular traps (NETs).

These processes enable efficient killing of pathogens, but can also result in collateral tissue damage, as evident in a number of chronic respiratory and systemic diseases where persistent neutrophilic inflammation is an important feature (42). In addition to their functions in innate immunity, neutrophils are also increasingly recognised to play important roles in shaping the adaptive immune response, via processes such as antigen presentation, production of cytokines, and interactions with other immune cells, as described in more detail below.

1.4. Neutrophil life cycle

Granulopoiesis occurs in the BM, where haematopoietic stem cells differentiate into common myeloid progenitors, then granulocyte-monocyte progenitors, then myeloblasts, the first granulocyte-committed stage. Myeloblasts differentiate into promyelocytes then myelocytes, which terminally differentiate through metamyelocytes, band cells and segmented cells into mature neutrophils, with the nuclei gradually reshaping to their polymorphonuclear appearance in these latter stages (43). Neutrophils are produced in response to granulocyte colony-stimulating factor (G-CSF) and other signals including granulocyte-macrophage colony-stimulating factor (GM-CSF) and IL-6 (44,45).

Mature neutrophils are released from the BM into the total intravascular granulocyte pool, consisting of the freely circulating and marginated pools. The marginated pool consists mainly of neutrophils in the liver and spleen, and these neutrophils can be readily remobilised into the freely circulating pool, for example during exercise (46). In mice, neutrophils have also been shown to marginate in the capillaries of the lungs at baseline, with intravascular crawling mediated by CD11b, positioning these neutrophils to respond rapidly to systemic pathogens (47). However, this is not the case in humans, where injection of radiolabelled autologous neutrophils showed pulmonary margination of GM-CSF-primed neutrophils, but minimal pulmonary retention of unprimed neutrophils (48).

In humans, neutrophils are the most abundant circulating leukocytes, comprising 50-70% of blood leukocytes, whilst in mice neutrophils comprise 10-25% of blood leukocytes (49). Neutrophil trafficking between the BM and blood is regulated by BM stromal CXCL chemokine and neutrophil surface CXCR signalling, with release from BM mediated by upregulation of CXCL1/2-CXCR2 and downregulation of CXCL12-CXCR4. Aged murine neutrophils upregulate CXCR4, leading to their return back to the BM for destruction (50–53), although circulating neutrophils are also cleared by the liver and spleen in equal proportions (54).

CXCR4 inhibition by plerixafor (55) results in increased circulating neutrophils due to increased demargination of lung neutrophils and decreased neutrophil return to BM, whereas G-CSF results in increased circulating neutrophils by increasing BM neutrophil release (52). In WHIM (warts, hypogammaglobulinaemia, immunodeficiency and myelokathexis) syndrome, gain-of-function mutations in CXCR4 result in blood neutropenia due to increased neutrophil retention in BM (56). Both plerixafor and G-CSF are used clinically in the management of patients with blood neutropenia. IL-6, a pleiotropic cytokine involved in autoimmune and inflammatory disorders, can also influence neutrophil return to the BM, as demonstrated by impaired trafficking of neutrophils to BM in healthy human volunteers treated with the anti-IL-6 receptor antibody tocilizumab (57). Neutrophil release from and return to BM follows a circadian rhythm and influences haematopoietic stem cell release from the BM (53,58).

Neutrophils have traditionally been considered terminally differentiated cells with a short half-life in peripheral blood. Green fluorescent protein (GFP)-positive neutrophils isolated from BM and transferred intravenously into wild type recipient mice showed a half-life of 8 hours in the circulation (59). *In vivo* and *ex vivo* radiolabelling studies showed estimated neutrophil circulatory half-lives of approximately 10 hours in mice and 18 hours in humans (60–63), although estimates were variable, which might in part be due to differences in study

methodologies, such as the radiolabelling of whole blood or isolated neutrophils, and the different durations of labelling (64). One study using long-term $^{2}H_2O$ labelling *in vivo* showed much longer estimates in murine and human neutrophils, with respective circulatory half-lives of 12.5 hours and 3.8 days, and lifespans of 0.75 days and 5.4 days (65), but this might be due to an assumption of a large blood neutrophil pool to BM neutrophil precursor pool ratio (63).

1.4.1. Influence of microbiota on neutrophil trafficking

The microbiota is increasingly recognised to exert influence on immune responses, and has been shown to affect neutrophil kinetics. Laboratory mice, maintained in specific pathogen free conditions, showed significant changes in immune cell populations when co-housed with pet store mice, including increased numbers of splenic myeloid cells, with peripheral blood mononuclear cell gene expression profiles more closely resembling that of adult humans (66). The microbiota has been shown to promote ageing of circulating neutrophils, as demonstrated by CXCR4 expression, with lower numbers of aged neutrophils in the circulation of antibiotic-treated or germ free mice (67). In neonatal mice, maternal antibiotic treatment resulted in reduced number of gut bacteria, reduced numbers of blood and BM neutrophils, reduced number of BM granulocyte-monocyte progenitors, and reduced plasma G-CSF level. The effect of the microbiota on neutrophil numbers was shown to be via IL-17 produced by ILC3 (Section 1.13.1) in the gut (68). In zebrafish, conventionally raised animals had higher numbers of neutrophils at baseline, with higher speed of movement and increased recruitment to tailfin injury compared to germ free animals, suggesting a role of the microbiota in neutrophil trafficking at baseline and in inflammation (69).

1.4.2. Neutrophil survival in local tissues

Agents such as GM-CSF and lipopolysaccharide (LPS) delay apoptosis of neutrophils cultured *in vitro* (70); such signals are likely to prolong survival of neutrophils recruited to inflammatory tissues *in vivo*. In a *Staphylococcus aureus* skin wound model, BM neutrophils were mobilised into the circulation, and c-kit^{+} BM progenitor cells were recruited into the wound where they proliferated and differentiated into mature neutrophils; depletion of these progenitor cells reduced overall survival from infection (71). In humans, circulating and alveolar neutrophils isolated from patients with acute respiratory distress syndrome showed prolonged survival when cultured *ex vivo* compared to circulating neutrophils from healthy volunteers (72).

1.5. Neutrophil surface receptors

Neutrophils express a wide range of cell surface receptors that enable them to recognise and respond to diverse infectious and inflammatory stimuli. These include pattern recognition receptors (PRRs) that bind to molecular structures on pathogens and to products of cellular damage, Fc receptors that bind to the Fc region of immunoglobulin, cytokine receptors that bind to pro- and anti-inflammatory cytokines, G-protein coupled receptors (GPCRs) including receptors for bacterial components, chemokines and chemoattractants, and adhesion molecules that bind to ligands involved in leukocyte migration (73). These receptors allow neutrophils to function efficiently as early responders to inflammatory signals, and are described further below.

1.5.1. Neutrophil surface receptors: PRRs

PRRs are innate immune receptors that recognise and bind to molecular structures conserved across microbial species known as pathogen-associated molecular patterns (PAMPs), and to fragments released by damaged cells known as damage-associated molecular patterns (DAMPs). Neutrophils express multiple classes of PRRs, enabling them to respond rapidly to infectious and inflammatory challenges.

Toll-like receptors (TLRs) are a major class of PRRs that bind to a range of extracellular and intracellular PAMPs from microbes: TLR1/2 to bacterial lipopeptide, TLR3 to double stranded RNA, TLR4 to bacterial LPS, TLR5 to bacterial flagellin, TLR7/8 to single stranded RNA, and TLR9 to CpG DNA motifs (74). Neutrophils express most TLRs, except TLR3 for human neutrophils (75) and TLR5 for mouse neutrophils (76); TLR7 and TLR9 are intracellular receptors located on the endoplasmic reticulum. TLRs signal via myeloid differentiation primary response 88 (MyD88) to activate the transcription factor nuclear factor-kappa B (NF-κB), leading to transcription of pro-inflammatory cytokines (2).

Neutrophils also express other PRRs. C-type lectin receptors (CLRs), such as dectin-1 and dectin-2, bind to fungal glucans and activate the NF-κB pathway. NOD-like receptors (NLRs) expressed on neutrophils include NOD2, which responds to cytoplasmic bacterial degradation products, and NLRP3, which forms part of the NLRP3 inflammasome constructed in response to signals of cellular damage including urate, potassium efflux, and extracellular adenosine triphosphate (ATP). RIG-like receptors (RLRs), such as RIG-1, respond to viral double stranded RNA (2,73).

1.5.2. Neutrophil surface receptors: Fc gamma receptors

Neutrophils express a number of surface receptors for the Fc portion of IgG (Fc gamma receptors, FcγRs) that recognise antibody-coated pathogens, leading to neutrophil activation and phagocytosis of pathogens; FcγRs also bind to antigen-antibody IC, leading to neutrophil activation, which may contribute to autoimmunity (77). There are a number of activating FcγRs containing or associated with an immunoreceptor tyrosine-based activation motif (ITAM), and a single inhibitory FcγRIIb containing an immunoreceptor tyrosine-based inhibitory motif (ITIM). The ratio of IgG binding to the activating receptors and the inhibitory receptor, known as the A/I ratio, determines the overall response of the immune cell (78).

Murine neutrophils express activating FcγRIII and FcγRIV and inhibitory FcγRIIb, whereas human neutrophils express activating FcγRIIA (CD32A) and FcγRIIIB (CD16B), with inhibitory FcγRIIB (CD32B) expressed only on a subset of neutrophils (79). The ratio of FcγRIIA to FcγRIIB, and consequently the degree of activation by IgG, has been shown to vary amongst healthy human neutrophils (80). In patients with rheumatoid arthritis, treatment with infliximab (anti-TNFα monoclonal antibody) induced an increase in neutrophil FcγRIIB expression and a corresponding reduction in FcγRIIA expression (81).

1.5.3. Neutrophil surface receptors: GPCRs and cytokine receptors

A number of GPCRs are present on the neutrophil surface, where upon ligand binding the Gα inhibitory subunit dissociates from the Gβγ heterodimer, and signalling through the Gβγ heterodimer leads to intracellular calcium release and activation of cellular pathways. GPCRs include formyl peptide receptors that recognise bacterial peptides; receptors for chemoattractants such as leukotriene B_4 (LTB_4), platelet activating factor (PAF), and complement C5a; and chemokine receptors, such as CXCR2, the receptor for IL-8 in humans, and for IL-8 homologues CXCL1 (KC) and CXCL2 (macrophage inflammatory protein-2, MIP-2) in mice.

Neutrophils also express a range of cytokine receptors, including type I cytokine receptors such as IL-6R and GM-CSFR, type II cytokine receptors such as IL-10R, IL-1R family such as IL-18R, and TNFR family such as TNFR1 and TNFR2, enabling neutrophils to respond to a wide variety of cytokines (73). Figure 1.3 summarises the surface receptors found on neutrophils.

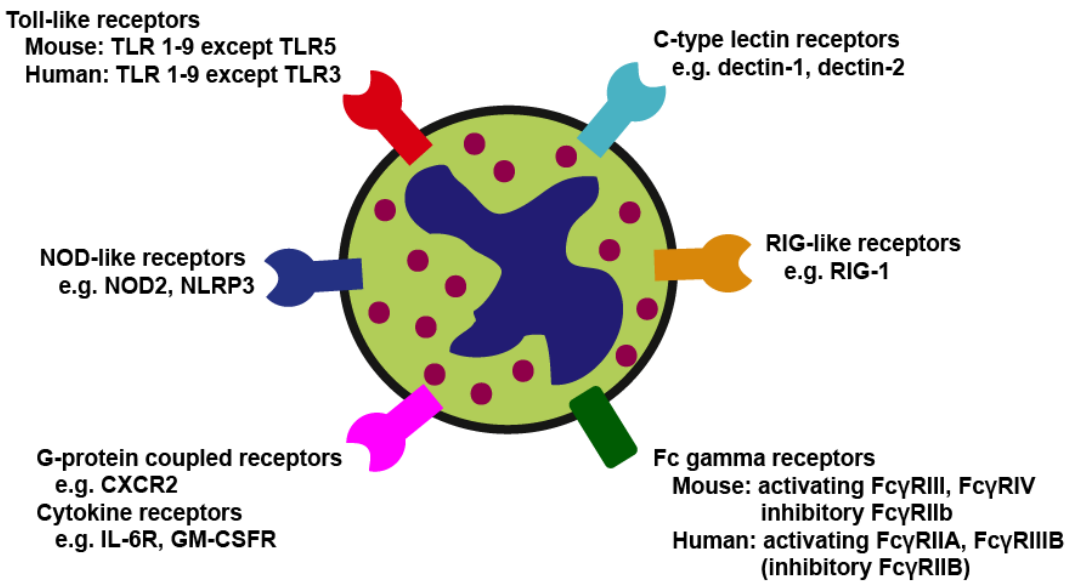

Figure 1.3. Neutrophil surface receptors. Diagram illustrating surface receptors expressed on neutrophils. PRRs enable rapid response to stimuli by recognition of PAMPs and DAMPs; these receptors include TLRs, CLRs, NLRs and RLRs. GPCRs and cytokine receptors respond to signals that result in neutrophil recruitment and activation. FcγRs bind to antibody-coated pathogens and antigen-antibody immune complex, and are involved in pathogen killing and in autoimmunity.

1.5.4. Surface markers for identification of neutrophils

Although neutrophils have a distinctive microscopic nuclear morphology, surface immunological markers are required for the study and identification of murine and human neutrophils. In mice, lymphocyte antigen 6 complex locus G (Ly6G) is selectively expressed on neutrophils, and recognised by the 1A8 clone of anti-Ly6G antibody. Myeloid differentiation antigen-1 (Gr-1) consists of Ly6G and Ly6C (expressed on neutrophils and monocytes), and the RB6-8C5 clone of anti-Gr-1 antibody recognises both Ly6G and Ly6C, with neutrophils being Gr-1-high and monocytes Gr-1-intermediate (82). Ly6G has been shown in one study to inhibit neutrophil migration towards chemoattractants in a β2-integrin (CD18)-dependent manner, similar to the function of the human Ly6G homologue CD177 (83). However, with the Catchup Ly6G-tdTomato reporter, homozygous animals were Ly6G-deficient but showed normal neutrophil function *in vitro* and *in vivo* (84). CD11b, which complexes with CD18 as an integrin involved in neutrophil migration, is expressed on myeloid cells (85); although not specific, CD11b is often used as an additional marker to Ly6G to identify murine neutrophils.

There are no specific cell surface markers for human neutrophils. Common markers used to identify human neutrophils include CD15 (Lewis X), involved in neutrophil migration and phagocytosis; CD16 (FcγRIIIB), highly expressed on human neutrophils; and CD66b, an activation marker. CD11b is highly expressed but, as with murine neutrophils, is also expressed by other myeloid cells (86,87).

1.6. Neutrophil effector functions

Neutrophils are considered the classical early effector cells of the innate immune system, responding rapidly to inflammatory and infectious stimuli, and killing pathogens by mechanisms including ROS generation, phagocytosis, degranulation of cytotoxic proteins and NET production. The processes of ROS generation and NET production involve activation of the NADPH oxidase complex in a two-step process of neutrophil priming followed by activation.

The NADPH oxidase complex includes the membrane subunits $gp91^{phox}$ and $p22^{phox}$ that form the catalytic core, and the cytosolic subunits $p40^{phox}$, $p47^{phox}$ and $p67^{phox}$. Exposure to a variety of agents, such as TNFα, GM-CSF, PAF, IL-8 and LPS, results in neutrophil priming, where the $p47^{phox}$ subunit is partially phosphorylated, and the $gp91^{phox}$ and $p22^{phox}$ heterodimer, contained within secretory vesicles, is transported to the cell membrane via vesicle exocytosis. A second activating agent, such as fMLP, stimulates phosphorylation and membrane translocation of the cytosolic subunits as well as translocation of Rac2, leading to full assembly of the NADPH oxidase complex. NADPH oxidase activation is required for ROS generation; on the cell membrane this results in extracellular ROS release for killing larger extracellular pathogens, whilst for phagocytosed pathogens activated NADPH oxidase on the phagolysosome results in ROS release within the phagolysosome and intracellular killing (88,89).

The process of priming results in changes such as shape change, exocytosis of integrins contained in secretory vesicles, and delayed apoptosis *in vitro*, and the phenotype of the primed neutrophil can differ according to the priming agent (41,90,91). Primed neutrophils show enhanced responses when activated, including degranulation, ROS production, and NET production. One previous study examining the metabolome of neutrophils by nuclear magnetic resonance spectroscopy did not find differences in the metabolic profile of control, TNFα-treated or LPS-treated human neutrophils (92). Neutrophils have also been shown to deprime, *in vitro* and *in vivo* (48,93).

Neutrophil granules are formed sequentially during different stages of myelopoiesis, and are packed with contents that can be readily released by degranulation, including cytotoxic and antimicrobial proteins for microbial killing, and proteases against extracellular matrix proteins to guide neutrophils that have transmigrated across the endothelium through the tissues to local inflammatory sites. Primary or azurophilic granules are peroxidase-positive and are formed early, containing antimicrobial proteins such as myeloperoxidase, defensins and bactericidal / permeability-increasing protein, and serine proteases such as proteinase-3, elastase and cathepsin G. Secondary or specific granules contain predominantly antimicrobial proteins, including lactoferrin (an iron-binding antimicrobial protein) and neutrophil gelatinase-associated lipocalin (NGAL), but also the collagenase matrix metalloproteinase 8 (MMP8). Tertiary or gelatinase granules contain the gelatinase MMP9 for extracellular matrix degradation. Some antimicrobial proteins, such as lysozyme, are present in multiple types of granules. There are also secretory vesicles containing membrane proteins such as Mac-1 and formyl peptide receptors, allowing rapid upregulation of these proteins on the cell surface upon stimulation to facilitate neutrophil migration and effector function (94,95).

NETs have recently been described as structures consisting of DNA, structural proteins such as histones and antimicrobial proteins such as myeloperoxidase and neutrophil elastase (96). NETs are released from activated neutrophils in a NADPH oxidase-dependent manner, potentially capable of trapping and killing pathogens. NET production has been shown to occur selectively for pathogens such as fungal hyphae that are too large to be phagocytosed, with the CLR dectin-1 regulating between phagocytosis and NET release (97). NETs, however, have also been implicated in autoimmune diseases, for example by transferring pathogenic myeloperoxidase to DCs in vasculitis (98).

1.7. Neutrophil recruitment to inflamed tissue

In order for neutrophils to perform the above effector functions, circulating neutrophils are recruited to inflammatory tissue sites in an orchestrated manner, and the mechanisms in this neutrophil recruitment cascade have been well described. Chemoattractants, such as fMLP, C5a and CXCL1 / IL-8, are produced by endothelial cells and by tissue resident cells such as macrophages upon stimulation by local inflammatory signals (99); neutrophils, with surface receptors for these chemoattractants (Section 1.5.3), are guided from the circulation towards tissue sites of inflammation.

A number of adhesion molecules are present on the neutrophil surface to facilitate neutrophil recruitment and migration across the endothelium. Selectins are involved in the initial step of neutrophil rolling on the endothelial surface, with L-selectin (CD62L) and P-selectin glycosylated ligand-1 (PSGL-1, CD162) on the neutrophil surface being shed as they bind to endothelial selectins, and physical tethers being formed on the neutrophils to stabilise the rolling process (100).

Neutrophil rolling is then followed by adhesion, crawling and subsequent transmigration across the endothelium and pericyte layer towards the interstitium. These steps involve integrins, glycoprotein heterodimers on the surface of neutrophils, such as LFA-1, a CD11a / CD18 or αLβ2 heterodimer; macrophage-1 antigen (Mac-1), a CD11b / CD18 or αMβ2 heterodimer, also known as complement receptor 3; and very late antigen-4 (VLA-4), an α4β1 heterodimer. Mac-1 is expressed mainly on myeloid cells, with neutrophils showing high levels of expression at baseline, whereas LFA-1 and VLA-4 are also expressed on other leukocytes. Neutrophil integrins bind to endothelial cell adhesion molecules, including ICAMs, junctional adhesion molecules (JAMs) and vascular cell adhesion molecules (VCAMs) (40,73).

At the tissue level, intradermally transferred neutrophils have been found to migrate towards local laser-induced sterile injury in several phases, with small numbers of scouting neutrophils migrating towards the injury initially, followed by amplified neutrophil recruitment or swarming, then persistence of neutrophil swarm at the injury site (101). LTB_4 and integrins are required in the chemotaxis and swarming of transmigrated neutrophils towards inflammatory tissues, as demonstrated in laser-induced injury and *Pseudomonas aeruginosa* bacterial infection (102).

Zebrafish models of inflammation have also shown other tissue signals to be involved. Neutrophil recruitment to *P. aeruginosa* infection required additional tissue damage signals, such as phospholipase A2, which initiates arachidonic acid metabolism and production of eicosanoids, including leukotrienes (103). Local tissue generation of hydrogen peroxide promoted neutrophil recruitment to wounds but not to bacterial infections (104,105). Interstitial extracellular matrix components can also play a role; for instance, extracellular matrix heparan sulphate proteoglycans have been shown to bind to zebrafish CXCL8 homologue to form tissue chemokine gradients, guiding neutrophil migration to the source of chemotactic signal (106).

1.8. Fate of neutrophils recruited to inflamed tissue

It is now recognised that, in addition to their role in the early innate immune response, neutrophils also play important roles in shaping adaptive immunity. Whilst neutrophils undergo *in situ* apoptosis and efferocytosis by macrophages at inflamed sites (107), and can be lost in secretions such as pus and sputum, there is accumulating evidence that cell death is not the sole fate of neutrophils recruited to inflammatory tissues (Figure 1.4). In rats, *in situ* apoptosis and efferocytosis by tissue macrophages only accounted for the fate of one-fifth of infiltrating neutrophils following IC-induced experimental glomerulonephritis (108). In zebrafish, some of the neutrophils recruited following tailfin injury were observed by microscopy to migrate away from the injury site (109); these reverse-migrated neutrophils exhibited normal migration, ROS production and phagocytic capacity (110). Although mathematical modelling suggested reverse migration to be a stochastic event in zebrafish (111), murine studies showed neutrophil reverse migration to occur via the transendothelial route back into the circulation or via lymphatics to the dLN, both with functional consequences (112–114).

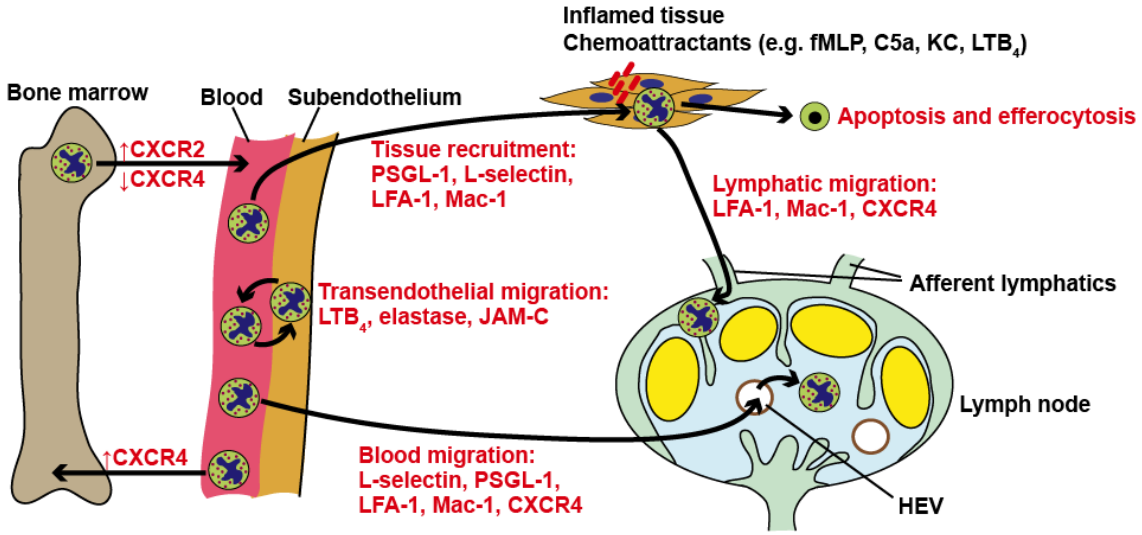

Figure 1.4. Neutrophil trafficking and migration following inflammatory stimulus. Neutrophil trafficking to and from BM is regulated by expression of CXCR2 and CXCR4. Local inflammation results in recruitment of circulating neutrophils, and some undergo apoptosis and efferocytosis. Neutrophils in the subendothelium can migrate back into the circulation to disseminate inflammation systemically. Neutrophils can also migrate to the LN via blood or lymphatic vessels.

1.8.1. Reverse migration of neutrophils into blood vessels

In vitro, human neutrophils that have reverse-migrated across an endothelial cell layer showed a different phenotype to blood and tissue neutrophils, with high expression of ICAM-1 (CD54), low expression of CXCR1 (receptor for IL-8), and prolonged survival. Blood from healthy volunteers and from patients with rheumatoid arthritis showed 0.25% and 1% of neutrophils with this phenotype, respectively (115). In a mouse model of local cremaster muscle ischaemia-reperfusion injury, tissue LTB_4 promoted neutrophil elastase-dependent loss of JAM-C at endothelial cell junctions, leading to the reverse transendothelial migration of ICAM-1^{High} neutrophils from the subendothelial layer back into the blood vessel lumen, which then served to disseminate local inflammation to distant organs including the lungs, heart and liver (112,116). Similar findings have also been observed in pancreatitis, where ICAM-1^{High}CXCR1^{Low} reverse-migrated neutrophils were associated with acute lung injury in both mice and humans (117).

On the other hand, in a murine model of sterile liver injury, neutrophils were found to migrate into sites of injury and contribute to tissue repair by phagocytosis of cellular debris from tissue damage; this was followed by reverse migration of neutrophils from tissues into blood vessels to the lungs without causing lung injury and then, by upregulating CXCR4, to the BM where they became apoptotic (118). Whilst some differences in neutrophil migration have been shown in studies, including different adhesion molecules and cytokines involved, these are thought to be stimulus-specific rather than organ-specific effects (40).

1.8.2. Reverse migration of neutrophils into lymphatics

Whilst reverse transendothelial migration may contribute to systemic spread of local inflammation, reverse migration of neutrophils from inflamed tissues into lymphatic vessels enables neutrophils to traffick to dLN and interact with LN-resident cells to modulate the adaptive immune response. In mice, intradermal Bacillus Calmette-Guérin (BCG) immunisation to the ear led to early antigen capture by neutrophils which migrated into lymphatics in a CD11b / ICAM-1-dependent manner, with confocal microscopy of tissue explants showing neutrophils in the lymphatic vessel lumen (119,120). Neutrophils have also been observed by intravital imaging to migrate within lymphatic vessels following peripheral *S. aureus* challenge (114). In a complete Freund's adjuvant (CFA)-induced model of cremasteric inflammation, TNFα produced by local tissues stimulated CCR7-dependent neutrophil migration from tissue into lymphatic vessels and Mac-1 / ICAM-1-dependent neutrophil crawling within the lymphatic vessel lumen (121). TNFα and Mac-1 / ICAM-1 have also been shown to be required for neutrophil adhesion onto and transmigration across

human lymphatic endothelial layers, and chemokines such as CXCL2, CXCL5 and CXCL8 produced by the luminal side of lymphatic endothelial cell layer promoted neutrophil transmigration *in vitro* (120).

Following ovalbumin (OVA) intradermal immunisation in sheep, examination of the draining lymphatic fluid showed that the majority of cells responsible for the early wave (6 hours) of lymphatic antigen trafficking were neutrophils, with a later wave (after 24 hours) of trafficking by DCs (122). In mice, immunisation with OVA with prior sensitisation resulted in a transient wave of neutrophils carrying OVA to dLN, with the peak of neutrophil influx at 6 hours post immunisation, returning to baseline by 12 hours post immunisation (123,124).

Neutrophil lymphatic trafficking may be dependent on the nature of the inflammatory stimulus. Local sterile injury to the ear by needle scratching resulted in neutrophil recruitment to the injury, but no subsequent neutrophil migration to the dLN (114). Following intradermal immunisation with Vaccinia virus, most of the Vaccinia-positive cells in the dLN 4 hours post immunisation were macrophages and DCs, with only 7% being neutrophils (125). Interestingly, Vaccinia-loaded neutrophils were also found to traffick to BM, inducing a $CD8^+$ T cell response that was attenuated in CCR1-deficient mice (126). In rhesus macaques, at 24 hours following adjuvant-human immunodeficiency virus (HIV) immunisation, antigen-carrying cells in the dLN consisted of a mixture of myeloid cells, including neutrophils, monocytes and DCs, with varying proportions depending on the type of adjuvant used (127). Another study showed neutrophil recruitment to dLN 6 hours following skin infection with *S. aureus* but not herpes simplex virus (128).

1.8.3. Neutrophil entry into LNs via lymphatic and blood vessels

As well as lymphatic migration to dLN, neutrophils can also enter the dLN via blood vessels following local inflammatory challenges. *In vivo* studies using intravital imaging and local *S. aureus* challenges demonstrated that neutrophils arrived in the dLN via lymphatic vessels, with neutrophils carrying bacteria from the periphery to the SCS (114), or via blood across HEVs with neutrophils migrating in the dLN towards the SCS to phagocytose bacteria arriving from the periphery via afferent lymphatics, therefore containing the bacteria within the dLN and limiting systemic spread of infection (129,130). OVA immunisation to the footpad also led to neutrophil recruitment into dLN via lymphatics or HEVs, in mice that received prior OVA / CFA immunisation (123,131).

Whilst most studies showed neutrophil recruitment to LN peaking early within several hours following administration of an inflammatory stimulus, one study showed that neutrophil

number in dLN peaked at 12 hours and returned back to baseline by 24 hours following peripheral stimulus with inactivated *S. aureus*, but neutrophil number in dLN remained persistently elevated for up to 7 days following peripheral infection with live *S. aureus* (129). The latter, however, might represent continued neutrophil recruitment into dLN with ongoing skin infection. Another study using hen egg lysozyme (HEL) with adjuvant immunisation showed an initial wave of neutrophil recruitment to the dLN peaking within 1 hour, followed by a second wave of neutrophil recruitment from 3 days post immunisation (113).

Experiments using blocking antibodies or inhibitors have shown that some of the mechanisms for trafficking of inflammatory neutrophils into LNs are similar to that described for lymphocyte trafficking into LNs (Section 1.2.1) and to that of neutrophil recruitment to inflamed tissues (Section 1.7). Following local *S. aureus* or OVA immunisation, L-selectin, PSGL-1 and PNAd, involved in leukocyte rolling on endothelium and HEVs, were used by neutrophils migrating into dLNs from blood, whereas CXCR4, LFA-1 and Mac-1, involved in lymphocyte transmigration across HEVs and / or neutrophil transendothelial migration, were used by neutrophils migrating into dLNs from both blood and lymphatic routes (114,130,131).

In a tumour model of sterile inflammation induced by photodynamic therapy, IL-17 produced by dLN Th17 cells drove IL-1β production, leading to neutrophil migration into dLN via HEVs involving L-selectin / PNAd and CXCL2 / CXCR2 interactions (132). IL-1β produced by macrophages has also been shown to promote neutrophil recruitment to dLN following local *P. aeruginosa* infection, with clodronate macrophage depletion reducing neutrophil recruitment, and IL-1β co-localising with SCS macrophages by confocal microscopy (29).

Studies on the role of CCR7, required for DC lymphatic migration to LN (11), in neutrophil migration have yielded conflicting results. Neutrophils contain intracellular stores of CCR7, and although at baseline neutrophils only showed low levels of cell surface CCR7 expression that did not increase following stimulation with agents such as GM-CSF, stimulated neutrophils showed increased migration towards CCL19 / CCL21 *in vitro*, and neutrophil migration to dLN following peripheral CFA stimulation was impaired in CCR7-deficient mice (131,133). Other studies have shown, however, that CCR7 was not required for neutrophil migration via lymphatics to dLN following skin Staphylococcal challenge, with the process of neutrophil migration remaining intact in CCR7-deficient mice, in mice receiving adoptive transfer of CCR7-deficient BM cells, and in photoconvertible CCR7-deficient mice (114). Similarly, neutrophil migration via HEVs into dLN following skin Staphylococcal challenge has been shown to be independent of CCR7 (130).

Interestingly, whilst S1P produced by lymphatic endothelial cells of the medullary sinuses led to the egress of lymphocytes, expressing S1P receptor 1 (S1PR1), from LN back into the circulation (26), IC stimulation in neutrophils led to upregulation of S1PR4 and increased neutrophil lymphatic and blood migration into dLN, a process that was inhibited by the S1PR agonist fingolimod that resulted in receptor internalisation and degradation (131).

Therefore, in response to a variety of peripheral tissue microbial and inflammatory stimuli, neutrophils can migrate to dLN, either capturing peripheral antigen then migrating via lymphatic vessels draining into the LN, or migrating via blood vessels across HEVs into the LN where antigen is encountered.

1.9. Function of neutrophils within LNs

Neutrophils that are recruited to dLNs following peripheral inflammatory stimuli have been shown to migrate to the SCS, where SCS macrophages are located to capture draining antigen, and to the paracortex, where T cells and DCs and located (113,119,123), placing recruited neutrophils in positions to interact with these LN immune cells and contribute to the adaptive immune response.

1.9.1. Survival of neutrophils within LNs

Neutrophils recruited to non-lymphoid inflammatory tissues may show prolonged survival in response to local pro-survival signals (71,72). Whilst the residence time of neutrophils recruited to LNs has not been fully characterised, one study showed that, both at baseline and 8 hours following Staphylococcal challenge to the ear, the majority of neutrophils recruited to the ear were alive, but the majority of neutrophils in the dLN were apoptotic, as identified by positive Annexin V staining (114). Apoptotic neutrophils were shown *in vitro* to increase production of pro-inflammatory cytokines such as IL-1β and IL-6 by microbe-infected macrophages, although production of anti-inflammatory IL-10 was also increased (134). Apoptotic cells generated DAMPs leading to activation of DCs and subsequent antigen cross-presentation to $CD8^+$ T cells (135). $CX3CR1^+$ macrophages within T cell paracortical areas of the LN efferocytosed apoptotic cells, but these macrophages did not activate antigen-specific $CD4^+$ T cells when co-cultured *in vitro* (32).

Aged neutrophils have been described as showing low L-selectin expression and high CXCR4 expression; both L-selectin and CXCR4 are involved in neutrophil migration into LNs (131). Aged neutrophils showed an activated phenotype with higher CD11b expression and

NET formation (67), and enhanced recruitment to and increased phagocytic capacity in peripheral tissues following systemic LPS inflammation (136). Aged neutrophils have also been identified in the lungs where they could potentially contribute to the development of fibrotic interstitial lung disease (137). Similar processes may occur with LN neutrophils, which may be apoptotic or aged but nevertheless exert effector functions and modulate other immune cells (138). However, a recent study has shown in contrast that only a small proportion of LN neutrophils were Annexin V positive (139).

1.9.2. Neutrophils and SCS macrophages: response to microbes

SCS macrophages, identified as $CD169^{+}CD11b^{+}F4/80^{-}$ cells that line the floor of the SCS (140), capture antigen draining in from afferent lymphatics and limit the spread of pathogens beyond the dLN, as evidenced by experiments showing that clodronate macrophage depletion increased the systemic spread of footpad viral and bacterial infections (29,33). Pathogens such as *S. aureus* draining into the SCS can stimulate neutrophil recruitment via HEVs into the LN, with neutrophils migrating into the SCS to phagocytose the bacteria (129). Anti-PNAd antibody blockade of neutrophil recruitment worsened LN and systemic spread of infection above the effects of clodronate macrophage depletion alone, suggesting that neutrophils as well as SCS macrophages play a role in the control of spread of peripheral pathogens beyond the dLN (130).

Following skin infection with the intracellular parasite *Toxoplasma gondii*, neutrophils were recruited to the dLN and formed swarms in two stages, with an initial stage of pioneer neutrophils arriving, followed by a second stage of larger swarms; neutrophil recruitment was reduced in MyD88-deficient mice, where TLR signalling is impaired. These neutrophil swarms were observed to disrupt the SCS macrophage network (141).

Local infection with modified Vaccinia Ankara virus induced inflammasome activation in dLN SCS macrophages, as demonstrated by ASC speck formation using intravital imaging, followed by SCS macrophage pyroptosis and extracellular release of ASC specks, leading to IL-1R-dependent recruitment of innate cells including neutrophils, monocytes and natural killer (NK) cells to the dLN (142). SCS macrophage IL-1β has also been shown to drive neutrophil recruitment to dLN following bacterial infection with *P. aeruginosa* (29). In a CpG (TLR9 agonist)-induced inflammation model, however, SCS macrophage disruption required DCs not neutrophils, as shown using antibody neutrophil depletion and conditional MyD88 deletion (143).

Together, these studies demonstrate that viral, bacterial and parasitic peripheral microbial infections can stimulate recruitment of neutrophils to the dLN, where they work in concert with SCS macrophages to generate an inflammatory response and limit the spread of pathogens beyond the dLN.

1.9.3. Neutrophils and DCs: antigen presentation

Neutrophils can interact with DCs, which are considered professional antigen presenting cells that capture and process antigen for presentation and cross-presentation to $CD4^+$ and $CD8^+$ T cells in LNs, respectively. Upon antigen encounter, activated DCs upregulate expression of MHCII for loading of processed antigen, CCR7 for trafficking into dLN, and co-stimulatory molecules such as CD40, CD80 and CD86 required for T cell activation. *In vitro* human cell co-cultures showed that DC maturation was induced by *Mycobacterium tuberculosis*-infected and GM-CSF-stimulated neutrophils, with contact-dependent upregulation of CD83, MHCII, CD40, CD80 and CD86 expression on DCs (144,145). The formation of clusters of DCs and activated neutrophils was dependent on interactions between DC-specific intercellular adhesion molecule-3 grabbing non-integrin (DC-SIGN, CD209) and Mac-1, as demonstrated by immunoprecipitation and by confocal imaging of co-cultured cells and colonic biopsies from patients with Crohn's disease (146). Neutrophils also produced CCL3, CCL19 and CCL20 to promote DC recruitment to tissues (147–149).

Murine models of lung inflammation have shown that neutrophils promote DC maturation in non-lymphoid organs *in vivo*. Following *Aspergillus fumigatus* fungal lung infection, neutrophils promoted lung DC maturation including expression of CD40, CD86 and MHCII, and migration of DCs to mediastinal LN (150). In a model of lung transplantation with prolonged donor organ cold ischaemic time, recipient neutrophils recruited to the airways interacted with donor lung DCs with a short mean contact time of 6.8 minutes, with occasional prolonged interactions observed by intravital imaging *in vivo*, whilst degranulation and TNFα production by donor airway neutrophils drove production of the Th1 cytokine IL-12 by recipient BM-derived DCs *ex vivo*; anti-Ly6G neutrophil depletion *in vivo* reduced IFNγ production by donor lung T cells (151). In a murine model of neutrophilic airway inflammation induced by house dust mite and LPS, neutrophil cytoplasts, being enucleated neutrophils post NET release, were found in the lungs and mediastinal LN, and in *ex vivo* co-culture inflammatory airway neutrophil cytoplasts stimulated lung DCs which, in turn, stimulated IL-17 and IL-13 production by $CD4^+$ T cells (152). Another study using intranasal house dust mite challenge, however, showed that anti-Ly6G neutrophil depletion resulted in enhanced delivery of OVA antigen by DCs from airway to mediastinal LN (153).

Neutrophils stimulated with bacteria and fungi *in vitro* activated DCs, with increase in IL-2 production, reduction in IL-10 production, and phagocytosis of antigen-containing neutrophils, subsequently leading to enhanced antigen presentation and cross-presentation to $CD4^+$ and $CD8^+$ T cells (144,154,155). However, within LNs, *ex vivo* imaging of dLN following HEL / CFA immunisation showed only brief neutrophil-DC contacts of 1 to 3 minutes in duration within the first 2 hours post immunisation. At later time points of 6 to 10 hours post immunisation, the number and duration of subsequent DC-T cell contacts were enhanced by neutrophil depletion, despite no further neutrophil-DC contacts observed. This resulted in an enhanced $CD4^+$ T cell response with IL-2 and IFNγ production, an effect independent of NADPH oxidase (113). *In vivo* studies showed that neutrophils reduced the activation (as measured by CD86 and MHCII expression), antigen uptake and CCR7 expression (and therefore migration) of DCs, via release of extracellular myeloperoxidase; neutrophil-mediated DC suppression consequently reduced $CD4^+$ T cell activation, including reduced proliferation and IFNγ production, in the dLN, as demonstrated in infectious / inflammatory models with *Leishmania major*, delayed skin hypersensitivity and OVA autoimmune arthritis (156,157).

BCG-infected DCs produced neutrophil chemoattractants including IL-6, CXCL1 and CXCL2, and induced neutrophil production of IL-10, an effect dependent on CD11b-mediated cellular contact and the MyD88 pathway, downregulating Th17 response (158). Co-culture of human monocyte-derived DCs with apoptotic neutrophils resulted in higher DC expression of CD83 and MHCII, indicating activation, but lower DC expression of co-stimulatory molecules and lower ability of DCs to stimulate T cells in a mixed lymphocyte reaction (159).

Overall, the above studies have shown evidence of both activation and suppression of DCs by neutrophils in a contact-dependent manner, although some of these experiments were *in vitro* or in non-lymphoid organs, and therefore may not truly reflect the effects of neutrophils on DC functions, including antigen presentation, in LNs *in vivo*.

1.9.4. Neutrophils: direct antigen presentation

In addition to interactions with DCs, neutrophils themselves can also show phenotypic features of antigen presenting cells. There are conflicting reports on whether neutrophils can express surface molecules involved in antigen presentation, including MHCII, and the co-stimulatory molecules CD40, CD80 and CD86.

Although human peripheral blood neutrophils did not express surface MHCII at baseline when examined by flow cytometry (160,161), MHCII expression could be induced under

various inflammatory conditions *in vitro*. Neutrophil expression of MHCII as well as CD80 / CD86 was induced by culturing with GM-CSF and IFNγ, with variability amongst donors, and expression enhanced by extracellular acidification (162–164). Another study showed induction of MHCII expression by ageing neutrophils for 20 hours in culture (160). Antibody crosslinking of CD11b in whole blood was sufficient to upregulate these molecules on neutrophils (165). Neutrophils have also been shown to acquire MHCII from macrophages *in vitro* (166) and from B cells *in vivo* (137).

Neutrophils isolated from thioglycollate-induced peritoneal exudate cells expressed MHCII, but at lower levels compared to isolated macrophages (167). In a murine model of chronic colitis, increased expression of MHCII and CD86 was observed in colonic neutrophils, compared to mesenteric LN and splenic neutrophils (168). Synovial (joint) fluid neutrophils from patients with rheumatoid arthritis, an autoimmune disease involving neutrophilic inflammation, showed higher MHCII expression by Western blotting compared to blood neutrophils from healthy volunteers and rheumatoid arthritis patients (160). In human visceral Leishmaniasis, low-density neutrophils have been identified in blood with higher MHCII, CD80 and CD86 expression (169). Blood neutrophils from patients with allergy, when stimulated with GM-CSF, IFNγ and IL-3 *in vitro*, showed delayed apoptosis, increased uptake and processing of allergen, and upregulation of MHCII expression (170). Blood neutrophils from patients with sepsis, however, did not show any increase in MHCII expression, despite increased CD40 and CD86 expression (171).

With regards to neutrophils within LNs *in vivo*, murine neutrophils recruited to the dLN following peripheral stimulation with *S. aureus* upregulated expression of MHCII and the co-stimulatory molecules CD80 and CD86, compared to neutrophils from other sites such as blood and spleen (114). However, 6 hours following peripheral OVA stimulation, the majority of OVA-containing cells were neutrophils negative for MHCII expression (123). In rhesus macaques, 24 hours following peripheral HIV immunisation with adjuvant, monocytes and DCs showed higher expression of MHCII and CD80 than neutrophils within the dLN (127).

Interestingly, neutrophils have been reported to show a hybrid phenotype, expressing surface markers of both neutrophils and activated DCs. Murine Gr-1^{High} BM granulocytes, after *in vitro* culture with GM-CSF for 6-8 days, showed large oval nuclei with dendritic morphology, and were positive for the neutrophil marker Ly6G, the DC marker CD11c, and antigen presentation molecules including MHCII, CD80 and CD86. These hybrids retained phagocytic and NET capacities in response to bacterial and fungal infections, and were present *in vivo* in skin and dLN following skin inflammation (172–175).

Human $CD15^+$ cells isolated from peripheral blood mononuclear cell fractions of patients with infections or haematological malignancies and cultured with GM-CSF, TNFα and IL-4 for 9 days expressed CD15, CD66b (neutrophil markers), CD1c, CD11c (DC markers), MHCII and co-stimulatory molecules (176). $CD66b^+$ synovial fluid neutrophils from rheumatoid arthritis patients expressed CD14, CD64, CD83 and MHCII (177). In human lung cancer tissues, subsets of $CD15^+CD66b^+CD11b^+$ neutrophils with rounded nuclear morphology expressed markers associated with antigen presenting cells, including MHCII (HLA-DR), CD14, CD206, CD86 and CCR7, but negative for other markers such as CD209 (DC-SIGN), CD163, CD83, CD1c and CCR6; these hybrids originated from immature BM neutrophil progenitors, and produced more TNFα and IL-12 post LPS stimulation *ex vivo* (178).

1.9.5. Neutrophils and T cells: adaptive immunity

The studies discussed above show that neutrophils interact with DCs to influence antigen presentation, or directly present antigens via MHC to T cells, thereby affecting the adaptive immune response. *In vitro*, neutrophils isolated from thioglycollate-induced peritoneal exudate cells have been shown to present OVA via MHCII to OVA-specific $CD4^+$ T cells in a contact-dependent manner, leading to T cell activation as demonstrated by proliferation and production of cytokines including IL-2 and IL-17 (167,179). Lamina propria neutrophils from mice with chronic colitis increased $CD4^+$ T cell proliferation when co-cultured (168). In rhesus macaques, neutrophils from dLN 24 hours following peripheral HIV immunisation were able to present antigen to and stimulate proliferation of $CD4^+$ T cells *ex vivo*, although not as effectively as monocytes or myeloid DCs (127,161).

In vitro, co-cultures of human neutrophils with T cells have shown variable results. Neutrophils from healthy volunteers, when stimulated with GM-CSF and IFNγ, upregulated MHCII, but studies have not consistently shown antigen-specific T cell proliferation (162,163). Neutrophils from patients with allergy, when stimulated with allergen, GM-CSF, IFNγ and IL-3, increased T cell proliferation, but less effectively than monocytes (170). Neutrophils from Cytomegalovirus (CMV)- and Influenza-positive volunteers stimulated antigen-specific proliferation of autologous $CD4^+$ T cells, but less effectively than DCs and monocytes; neutrophil MHCII upregulation required the presence of antigen and antigen-specific memory T cells, as stimulation with TLR7/8 ligand was not sufficient (161). Blood neutrophils from patients with visceral Leishmaniasis showed higher MHCII and programmed death ligand 1 (PD-L1) expression, but exerted no effects on T cell proliferation (169).

OVA-pulsed neutrophils could also cross-present antigen via MHCI to murine and human $CD8^+$ T cell, leading to antigen-specific OTI $CD8^+$ T cell activation, including cell proliferation

and production of IL-2, TNFα and IFNγ, shown in co-cultures *in vitro* and when pulsed neutrophils were transferred *in vivo* (180–182). Blood and tumour-associated neutrophils from colorectal cancer patients enhanced $CD8^+$ T cell activation *in vitro* as evidenced by CD69 expression and IFNγ production, and tumour-infiltrating neutrophils co-localised with $CD8^+$ T cells, which was associated with improved overall survival (183). Murine neutrophil-DC hybrids, as described above, could also present and cross-present antigen to $CD4^+$ and $CD8^+$ T cells *in vitro* (172–175). Human neutrophil-DC hybrids isolated from lung cancer tissues, when exposed to antigen in the form of IC (therefore crosslinking FcγR) *in vitro*, could cross-present antigen to antigen-specific $CD8^+$ T cells (178). Neutrophils produce a range of cytokines that can contribute to the activation of tissue effector T cells (149). Following influenza infection, neutrophils have been shown to secrete trails of CXCL12 to guide $CD8^+$ T cell recruitment in the trachea (184).

Murine studies using *in vivo* neutrophil depletion have shown conflicting results with regards to the effects of neutrophils on LN T cell responses (Table 1.1). Following *S. aureus* peripheral stimulus, anti-Ly6G neutrophil depletion led to reduced $CD4^+$ and $CD8^+$ T cell numbers (129) and proliferation in the dLN (114); neutrophils arriving via HEVs interacted with $CD4^+$ T cells, but the majority of interactions were transient (64% lasting less than 1 minute) and none prolonged (129). However, in a herpes simplex virus skin infection model, antigen-specific $CD4^+$ and $CD8^+$ T cell responses in the dLN, as measured by proliferation of adoptively transferred labelled T cells, were unaffected by anti-Ly6G neutrophil depletion (128). Furthermore, following HEL / CFA immunisation, $CD4^+$ T cell activation, as measured by IL-2 and IFNγ production, was increased by neutrophil depletion with either anti-Ly6G or anti-Gr-1, independent of NADPH oxidase (113).

Peripheral OVA stimulation in mice with prior immunisation led to increased $CD4^+$ T cell activation and proliferation in the dLN, effects that were abrogated with NIMP-R14 antibody neutrophil depletion; however, in the same study, neutrophils isolated from OVA-stimulated dLN also resulted in inhibition of OTII (OVA-specific) $CD4^+$ T cell proliferation *in vitro*, in a mechanism involving PD-L1 (124). In humans, subsets of $CD62L^{Low}$ neutrophils have been found in blood following intravenous LPS challenge and severe injury, and these neutrophils suppressed T cell proliferation *ex vivo* in a Mac-1-dependent mechanism (185). Neutrophils with suppressive effects are a recently described neutrophil subset that forms part of a group of cells termed myeloid derived suppressor cells. These suppressive neutrophils may account for the inhibitory rather than stimulatory effects on T cell responses in some of the above studies, with mechanisms of suppression including arginase secretion and ROS production (86).

1.9.6. Neutrophils and B cells: adaptive immunity

Neutrophils have been shown to influence B cell responses in lymphoid and non-lymphoid tissues. Co-cultures of peripheral blood neutrophils and autologous B cells from rhesus macaques following viral infection resulted in B cell activation and immunoglobulin class switching, as evidenced by increased activation-induced cytidine deaminase (AID) and Ki67 (proliferation marker), and decreased CD27, IgM and IgD (186). In human tonsil and small bowel mucosal associated lymphoid tissue (MALT), elastase$^+$ and CD15$^+$ cells co-stained for the B cell activating factor a proliferation inducing ligand (APRIL) (187). In the human spleen, within the marginal zone (a site for T-independent B cell responses to antigens such as LPS), a subset of B-helper neutrophils have been described that enhanced marginal zone B cell antibody production (IgM, IgA and IgG) in *ex vivo* co-culture; these B-helper neutrophils showed higher MHCII and CD86 expression, and produced cytokines involved in B cell development and activation, including B cell activating factor (BAFF), APRIL and IL-21 (188). These findings, however, have not been replicated in a second, independent study (189).

Other studies have demonstrated inhibitory effects on B cells. In a murine model of lupus, confocal examination showed that splenic neutrophils preferentially co-localised with T cells at disease onset but with B cells in established disease; anti-Ly6G neutrophil depletion at disease onset, but not during established disease, increased splenic germinal centre B cells and Tfh cells, and enhanced autoimmunity (190). Sublingual immunisation with bacterial antigen resulted in serum and mucosal IgA responses in neutrophil-depleted but not wild type mice (191). Following intranasal house dust mite allergen challenge, serum levels of house dust mite-specific IgE and IgG were higher in anti-Ly6G neutrophil-depleted mice compared to control mice (153). In the pulmonary capillaries, neutrophils have been observed to interact with B cells with a mean interaction time of 4.5 minutes, with CD18 required for this interaction, leading to neutrophils acquiring MHCII molecules from B cells. B cell depletion led to reduced apoptosis and interstitial infiltration of neutrophils in the lungs, resulting in pulmonary fibrosis, suggesting bidirectional crosstalk between neutrophils and B cells (137).

Within LNs, *in vivo* studies have also shown inconsistent results on the effects of neutrophils on B cell responses (Table 1.1). Following HEL / CFA immunisation, depletion of the initial wave of neutrophil recruitment led to increased IgG production by B cells, as well as increased CD4$^+$ T cell activation (113). Following *S. aureus* infection, neutrophils migrated via both lymphatics and HEVs into LNs; anti-Ly6G neutrophil depletion led to increased dLN B cell numbers and TGFβ-dependent production of IgM and IgG, but reduced dLN CD4$^+$ and

$CD8^+$ T cell numbers in one study (129), whilst in another study neutrophil depletion resulted in reduced proliferation of B cells, $CD4^+$ T cells and $CD8^+$ T cells in the dLN (114). As with T cell interactions, neutrophil-B cell interactions were mainly transient (54% lasting less than 1 minute), but some (17%) of the observed interactions were over 30 minutes in duration (129).

In a model of emergency granulopoiesis in neutropenic lysozyme-diphtheria toxin mice, CFA immunisation did not lead to early neutrophil recruitment, but instead a late wave of neutrophil recruitment to dLN 7 days post immunisation, with increases in neutrophil BAFF production, IL-17^+ T cells, $B220^+$ B cells, and $CD138^+$ plasma cells (192).

Reference	**Stimulus**	**Neutrophil depletion**	**Neutrophil LN entry**	**Effect on T cell response**	**Effect on B cell response**
Yang *et al*. 2010 (113)	HEL + adjuvant	Anti-Ly6G Anti-Gr-1	Lymphatics	↑$CD4^+$ activation	↑IgG
Hampton *et al*. 2015 (114)	*S. aureus*	Anti-Ly6G	Lymphatics	↓$CD4^+$ and $CD8^+$ proliferation	↓Proliferation
Kamenyeva *et al*. 2015 (129)	*S. aureus*	Anti-Ly6G	HEVs	↓$CD4^+$ and $CD8^+$ cell numbers	↑Plasma cells, ↑IgM, ↑IgG
Hor *et al*. 2017 (128)	Herpes simplex virus	Anti-Ly6G	Not tested *in vivo*	No difference $CD4^+$ or $CD8^+$	Not tested

Table 1.1. Neutrophil and adaptive lymphocytes *in vivo*. Summary of studies using antibody neutrophil depletion to examine effect on LN T and B cell responses *in vivo*. Anti-Ly6G (clone 1A8) recognises only Ly6G, whereas anti-Gr-1 (clone RB6-8C5) recognises Ly6G and Ly6C.

Therefore, in response to a variety of microbial and sterile inflammatory stimuli, neutrophils are capable of interacting with other LN immune cells to influence innate and adaptive immune responses (Figure 1.5). Although some of the studies described were *in vitro* or in non-lymphoid organs, nevertheless they contribute to the emerging concept that neutrophils have a diverse range of immune functions beyond the traditional role of early innate pathogen defence.

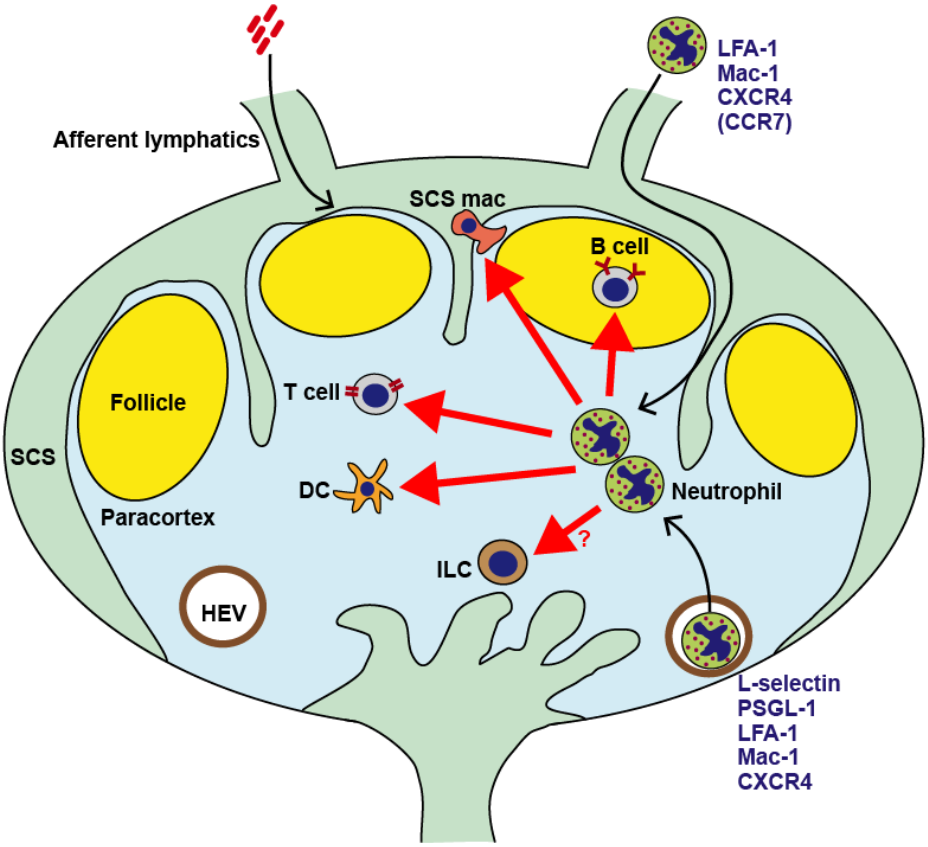

Figure 1.5. Function of LN neutrophils in inflammation. Following inflammatory stimuli, neutrophils can migrate into LN via lymphatic vessels and HEVs, guided by a number of molecules expressed on neutrophils (in blue). Within the LN, neutrophils have been shown to interact with B cells, T cells, DCs and SCS macrophages to influence innate and adaptive responses.

1.9.7. Neutrophil subsets

The studies described above demonstrate the diversity of neutrophils in phenotype and function. Aged neutrophils showed CXCR4 expression and an activated phenotype (136), with their presence driven by the microbiota (67); they have also been shown to contribute to the development of lung fibrosis (137). ICAM-1^{High} neutrophils have been shown to reverse migrate across the endothelium and contribute to systemic dissemination of local inflammation (116), and have been found in the circulation of patients with rheumatoid arthritis (115). Neutrophil-DC hybrids have been shown to express surface molecules associated with DCs and with antigen presentation (172–175). B-helper neutrophils have been described in the human spleen (188). Neutrophils expressing vascular endothelial

growth factor receptor have been shown to be recruited from the circulation to tissues and promote angiogenesis (193). Neutrophils categorised by their CD16 expression, CD62L expression and degree of nuclear hypersegmentation showed differential responses to *S. aureus ex vivo* (194).

Following laboratory density gradient separation of leukocytes (Section 3.4), neutrophils are found in the lower granulocyte layer, but low-density neutrophils have also been found within the upper peripheral mononuclear cell layer. These low-density neutrophils consist of both mature and immature neutrophils, and have been identified in a number of diseases, showing pro-inflammatory effects in autoimmune disorders but suppressive effects (as neutrophil myeloid derived suppressor cells) in cancer, although pro-inflammatory neutrophils have also been described in the context of cancer (195,196).

This phenotypic variation has led to recent proposals of the concept of neutrophil subsets, in which neutrophils can be categorised into distinct subgroups with characteristic cell surface markers and different functions. Whilst there is good evidence that neutrophils are functionally more diverse compared to the classical view of neutrophils being short-lived terminally differentiated cells with the main function of pathogen killing, it is unclear whether neutrophils consist of true subsets, or neutrophils consist of a heterogeneous group of innate immune cells with functional plasticity driven by different tissue environments and different infectious and inflammatory stimuli. Neutrophils that migrate to LNs following inflammation can influence other LN immune cells in a number of ways as described above, but similarly it is unclear whether this represents a distinct LN-specific neutrophil subset or this reflects the heterogeneity of neutrophils.

1.10. Neutrophils in inflammatory diseases

The multiple roles of neutrophils in immune responses are reflected by their involvement in a number of inflammatory as well as infectious diseases. For example, deficiency in subunits of NADPH oxidase results in chronic granulomatous disease, where defective phagocyte ROS production leads not only to recurrent bacterial and fungal infections, but also to granuloma formation and inflammatory complications such as colitis (197). Neutrophils are involved in lupus and vasculitis syndromes, through mechanisms such as NETosis and release of autoantigens including myeloperoxidase, activation of DCs influencing T cell responses, and secretion of cytokines such as BAFF that sustains autoreactive B cells (198). Neutrophils have been shown to infiltrate tumours and can exert both pro-inflammatory and anti-inflammatory effects on cancer growth (183,199). The crosstalk between neutrophils

and other immune cells may also contribute to the immunopathology of acute and chronic rejection in solid organ transplants, with neutrophil infiltration observed in allografts with rejection (200).

Neutrophilic inflammation is a major feature of chronic obstructive pulmonary disease, with neutrophil release of elastase and other granule proteins driving persistent inflammation and tissue damage most commonly seen as a result of tobacco smoking (201). In asthma, usually considered a Th2-driven airways disease with eosinophilic inflammation being a feature (202), a proportion of patients have predominantly neutrophilic airway inflammation. Neutrophils have been shown to stimulate alveolar macrophage IL-1β production and NLRP3 inflammasome activation in mice with respiratory viral infections, common triggers for exacerbations of airways diseases (203). Other respiratory diseases, such as bronchiectasis, interstitial lung disease and acute respiratory distress syndrome, are also associated with pathological neutrophilic inflammation (42).

Many autoimmune disorders are associated with antigen-antibody IC, which can activate neutrophils directly by Fc receptor crosslinking or indirectly by complement fixation and complement receptor binding. IC can be soluble or insoluble depending on the antibody to antigen ratio, with insoluble IC having a higher antibody to antigen ratio (204). *In vitro*, soluble IC stimulated degranulation and ROS secretion in GM-CSF-primed but not unprimed neutrophils, whilst insoluble IC stimulated degranulation and intracellular ROS generation in both unprimed and primed neutrophils (205).

In rheumatoid arthritis, the synovial fluid of inflamed joints contains IC that stimulates neutrophils, by mechanisms such as neutrophil C5aR activation leading to LTB_4 release enhancing further neutrophil recruitment, and engagement of neutrophil FcγRIII leading to IL-1β release driving the inflammatory process (206). A lower copy number of the *FCGR3B* gene correlates with lower neutrophil surface expression of FcγRIIIB and lower neutrophil uptake of IC *in vitro*; low *FCGR3B* copy number has also been associated with systemic lupus erythematosus, a disease characterised by IC deposition, in Caucasian but not in Chinese populations (207). In a model of lung injury triggered by MHCI antibody administration, FcγR-deficient mice were protected from lung injury, which was restored by transfer of wild type neutrophils, demonstrating the role of neutrophil FcγR in lung inflammation (208).

Although neutrophils have been shown to be involved in many inflammatory diseases, and pharmacological manipulation of the trafficking, tissue recruitment and effector functions of neutrophils may represent attractive therapeutic strategies, to date there are few specific

treatments available that target the processes of neutrophilic inflammation. The role of neutrophils in the resolution phase of inflammation is not as well studied, and understanding the basic immunological mechanisms in the resolution of inflammation may also provide therapeutic targets for the treatment of chronic inflammatory diseases (209).

1.11. Neutrophils in tissues at baseline

Whilst neutrophils are considered circulating leukocytes that are recruited to sites of infection or tissue injury, there is evidence that neutrophils are also present in tissues at baseline without inflammatory stimuli. Imaging of the non-inflamed ear dermis of lysozyme M (LysM)-GFP mice, in which neutrophils show high GFP fluorescence, demonstrated the presence of extravascular neutrophils crawling at a mean speed of 3 μm/min (101). Lethal irradiation of LysM-GFP mice resulted in neutrophils disappearing from tissues with half-lives of 2 days in the spleen and 6 days in the lungs, although the study did not distinguish between intravascular and extravascular neutrophils (59).

A recent study demonstrated, using parabiosis, that circulating neutrophils migrated into multiple tissues at baseline, with neutrophils being largely extravascular in BM, spleen and intestine, but largely intravascular in liver and lungs; neutrophils in the intestine were phagocytosed by macrophages and influenced IL-23 production and consequently granulopoiesis, whereas neutrophils in the lungs influenced circadian transcription of genes involved in cell survival, migration and carcinogenesis (210).

Examination of published studies of neutrophil recruitment to dLN following infectious and inflammatory stimuli shows, in their control conditions, the presence of small numbers of neutrophils at baseline within peripheral LNs (114,157). Intravital imaging of the popliteal LN showed motile neutrophils at baseline, with significant increase in neutrophil recruitment following local infection (130). In healthy aged mice, lymphoid organs including spleen and LNs contained increased numbers of neutrophils compared to young mice; however, aged mice also showed increased systemic inflammation with increased plasma IL-6 and TNFα, and splenic and LN neutrophils from these mice showed an activated phenotype, including nuclear hyper-segmentation, increased survival, increased CD11b expression and increased ICAM-1 expression (211).

In sheep, lymphatic fluid draining from the periphery contained neutrophils as well as DCs and monocytes in the absence of inflammatory stimuli, suggesting lymphatic trafficking of neutrophils into LNs at baseline (122). In uninfected Rhesus macaques, neutrophils were

present in inguinal LNs, with higher expression of CCR7 and BAFF compared to blood neutrophils, although in the study neutrophils were defined as $CD66^+$ and eosinophils were not excluded (186).

1.12. Neutrophils: summary and unanswered questions

The studies described above demonstrate the varied role of neutrophils in modulating innate and adaptive immune responses. Circulating neutrophils are rapidly recruited to peripheral sites of infection or tissue injury, with neutrophil migration across endothelium and within tissues guided by chemoattractants and adhesion molecules. A wide range of surface receptors allow neutrophils to respond to many different pathological stimuli, exerting their effector functions including phagocytosis, ROS generation, degranulation of cytotoxic substances and NET release, ultimately resulting in the disposal of pathogens. Whilst some of these neutrophils undergo *in situ* apoptosis, it is now recognised that neutrophils can be recruited to LNs, the sites of adaptive immune responses.

Following inflammatory and infectious challenges, neutrophils have been shown to migrate into dLNs, either carrying antigen via lymphatic vessels into dLNs, or entering dLNs via HEVs where antigen draining from the periphery is encountered. Within LNs, neutrophils are capable of interacting with other LN immune cells including SCS macrophages, DCs, T cells and B cells, influencing innate and adaptive immune responses, and contributing to antigen presentation indirectly by interacting with DCs or directly by acting as antigen presenting cells. However, studies have shown conflicting results on the effects of neutrophils on other immune cells, with some showing stimulatory effects and others showing inhibitory effects; it is unclear whether this is due to differences in study conditions, stimulus-specific neutrophil responses, or tissue site-specific neutrophil effects.

Under homeostatic conditions, neutrophils have been shown to be present in a number of tissues, including lungs, intestine and skin, in addition to their presence in the circulation. There is also some evidence of the presence of neutrophils in LNs at baseline, but to date there have not been detailed studies on the anatomical location, interactions with other immune cells, or the potential function of neutrophils within LNs at baseline. Understanding the role of neutrophils in innate and adaptive immune responses, in homeostatic and inflammatory conditions, is important in the development of neutrophil-targeted therapies in inflammatory diseases.

1.13. ILCs: overview

ILCs have recently been characterised as a group of innate immune cells with diverse functions in regulating the initiation and resolution of inflammation. Derived from common lymphoid progenitors that also give rise to adaptive lymphocytes, ILCs differ from B and T lymphocytes in that they lack antigen-specific receptors generated by somatic gene rearrangement. ILCs are found in lower frequencies compared to neutrophils and adaptive lymphocytes in the circulation, but are instead present and enriched at mucosal barrier sites such as skin, lungs and intestine, where a variety of epithelial- and mononuclear phagocyte-derived signals such as cytokines, chemokines and lipid mediators produced upon microbial stimuli and tissue damage trigger cytokine production by ILCs to influence innate and adaptive immune responses (6,212).

The original subsets of ILCs identified were NK cells and lymphoid tissue inducer (LTi) cells. Subsequently further subsets have been identified, and ILCs are now classified into groups 1, 2 and 3, showing analogous expression patterns of transcription factors and effector cytokines to Th1, Th2 and Th17 cells respectively (213); regulatory ILCs have also been described (214). These subsets have been characterised in both murine and human systems, and have been associated with several inflammatory diseases such as inflammatory bowel disease, asthma and psoriasis (215).

1.13.1. Classification of ILCs

ILCs are identified by a lack of lineage markers for other cell types including myeloid cells, B cells and T cells (although a subset of ILC3s are $CD4^+$), and positive expression of surface markers such as IL-7Rα (CD127), IL-2Rα (CD25), common gamma chain (γc, CD132, or IL-2Rγ) and in mice Thy1 (CD90) (6,215). The three groups of ILCs can be considered innate counterparts to T helper cell subsets, and classified based on their patterns of transcription factor expression and cytokine production (Figure 1.6).

Group 1 ILCs (ILC1s) express T-bet, a T-box transcription factor expressed by Th1 cells; in response to the tissue signals IL-12 and IL-15 produced by myeloid and epithelial cells in intracellular infections such as those caused by viruses, ILC1s secrete IFNγ and TNFα to mediate type 1 immunity. This group also includes T-bet negative NK cells, which require eomesodermin (eomes) for development (216), and mediate killing of infected cells and tumour cells by producing cytolytic agents including granzymes and perforins as well as IFNγ, therefore showing similar functions to cytotoxic $CD8^+$ T cells.

Group 2 ILCs (ILC2s) express the transcription factors GATA binding protein 3 (GATA3) and retinoic acid receptor-related orphan receptor alpha (RORα), although their expression is not limited to ILC2s. Following tissue damage, epithelial cells produce so-called alarmins, including IL-25, IL-33 and thymic stromal lymphopoietin (TSLP), which act as tissue signals that stimulate ILC2s to secrete the type 2 cytokines IL-4, IL-5, IL-9 and IL-13, mediating responses to extracellular parasitic infections as well as allergic diseases (217). ILC2s are involved in tissue repair via the production of amphiregulin, the ligand for epidermal growth factor receptor (218). ILC2s also regulate epithelial cells in a feedback circuit, where ILC2-derived IL-13 promotes hyperplasia of epithelial tuft cells which in turn produce IL-25 to stimulate ILC2s (219).

Group 3 ILCs (ILC3s) express retinoic acid receptor-related orphan receptor gamma T (RORγt) and aryl hydrocarbon receptor (AHR). They respond to myeloid cell-derived IL-1β, IL-6 and IL-23 by producing IL-17, IL-22, GM-CSF and lymphotoxin, promoting processes such as release of antimicrobial peptides from epithelial cells and tissue neutrophil recruitment to facilitate defence against extracellular bacterial and fungal infections. In mice, one subset consists of ILC3s negative for CCR6 and positive for T-bet, with some expressing the natural cytotoxicity receptor (NCR) NKp46 (NKp44 in humans). Another subset consists of CCR6-positive LTi cells that produce lymphotoxin, with some expressing CD4. $CCR6^-$ ILC3s are located at mucosal sites such as skin and intestinal lamina propria, whilst $CCR6^+$ LTi cells are located within lymphoid tissues such as LNs and Peyer's patches (5,6,212,213).

1.13.2. Development of ILCs

Both innate and adaptive lymphocytes are derived from common lymphoid progenitors, found in the fetal liver and adult bone marrow. Expression of several transcription factors, including inhibitor of DNA binding 2 (Id2), nuclear factor interleukin-3 related (NFIL3), thymocyte selection-associated high mobility group box (Tox) and GATA3, are associated with the differentiation of common lymphoid progenitors into ILCs, although some of these transcription factors are not restricted to ILCs. Id2 suppresses E-protein transcription factors such as E2A that are required for B and T lymphocyte development, and therefore upregulation of Id2 promotes differentiation into ILC subsets. A recent study demonstrated using a murine Id2-RFP reporter that Id2 was expressed in all ILC subsets (including NK cells, ILC1s, ILC2s and ILC3s), and that $Id2^+$ ILC precursors gave rise to all ILC subsets (220).

Downstream of common lymphoid progenitors, common helper ILC precursors that express promyelocytic leukaemia zinc finger (PLZF) give rise to ILC1s, ILC2s and $CCR6^-$ ILC3s,

whilst NK cells arise from NK precursors, and LTi cells arise from α4β7 integrin-positive precursors (221,222). In addition, IL-7Rα^{+} lymphoid-primed multipotent progenitors have been shown to differentiate into T cells and ILC2s independent of common lymphoid progenitors, acting as a major source of neonatal ILC2s that in the lungs can persist into adulthood (223). In humans, CD117 (c-kit)-positive ILC progenitors that can differentiate into all ILC subsets are present in peripheral blood as well as lungs and tonsillar (lymphoid) tissues (216). Development from committed ILC precursors into subsets is guided by transcription factors including T-bet, GATA3, RORα, RORγt and AHR (222) (Figure 1.7). A recent study reported the generation of a five-colour polychromic reporter mouse for transcription factors Id2, GATA3, Bcl11b, RORα and RORγt, facilitating investigation into the processes of ILC development (224).

There is plasticity between the ILC subsets. In the presence of IL-12, ILC3s have been shown to downregulate RORγt expression and upregulate T-bet expression to change into an IFNγ-producing ILC1 phenotype (225). IL-1β stimulated human ILC2s to express T-bet and produce IFNγ in the presence of IL-12 *ex vivo*, thus becoming ILC1-like cells (226); this plasticity was lost in ILC2s from patients with IL-12R deficiency (227), and could be reversed with IL-4 *ex vivo* (228). In response to IL-1β and IL-23, ILC2s showed reduced GATA3 and increased RORγt, converting into IL-17-producing ILC3-like cells (229). A subset of regulatory ILCs has also been described in the gut that expressed transcription factors distinct from other ILCs and inhibited ILC1 and ILC3 activity via IL-10 secretion (214).

The recombination-activating genes RAG1 and RAG2 are expressed in B and T adaptive lymphocytes and are essential in the VDJ gene rearrangement of antigen receptors. RAG-deficient mice therefore do not develop adaptive lymphocytes (230), whilst ILC populations remain intact as they do not express antigen-specific receptors. On the other hand, mice deficient in both RAG and common gamma chain lack adaptive lymphocytes and ILCs, with lymphoid tissue development also affected due to a lack of LTi cells. These mouse models that make use of differences in development between innate and adaptive lymphocytes have been used in experimental studies of ILCs (231).

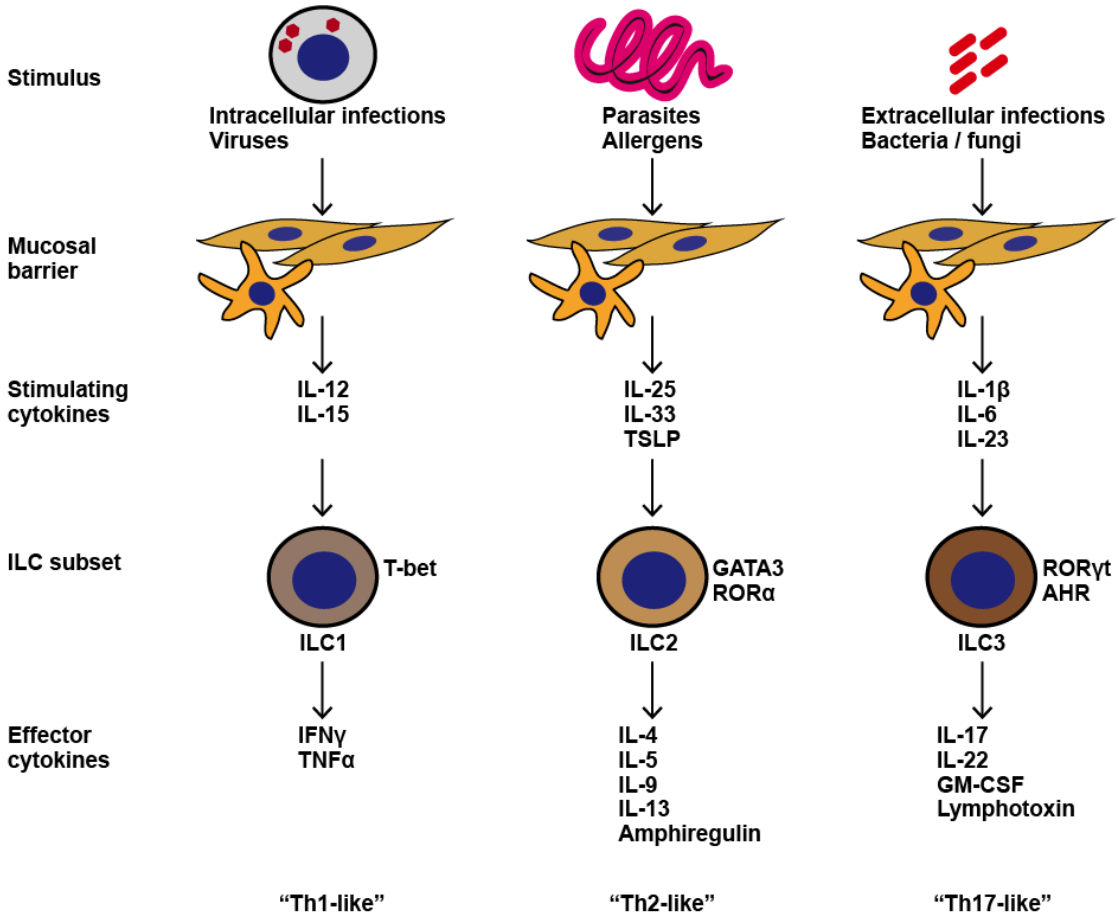

Figure 1.6. Classification of ILCs. ILCs are caterogised into three subsets. In response to certain types of stimuli, epithelial and immune cells at mucosal barrier sites produce cytokines that activate ILCs, which express transcription factors and produce cytokines in patterns analogous to Th cell subsets.

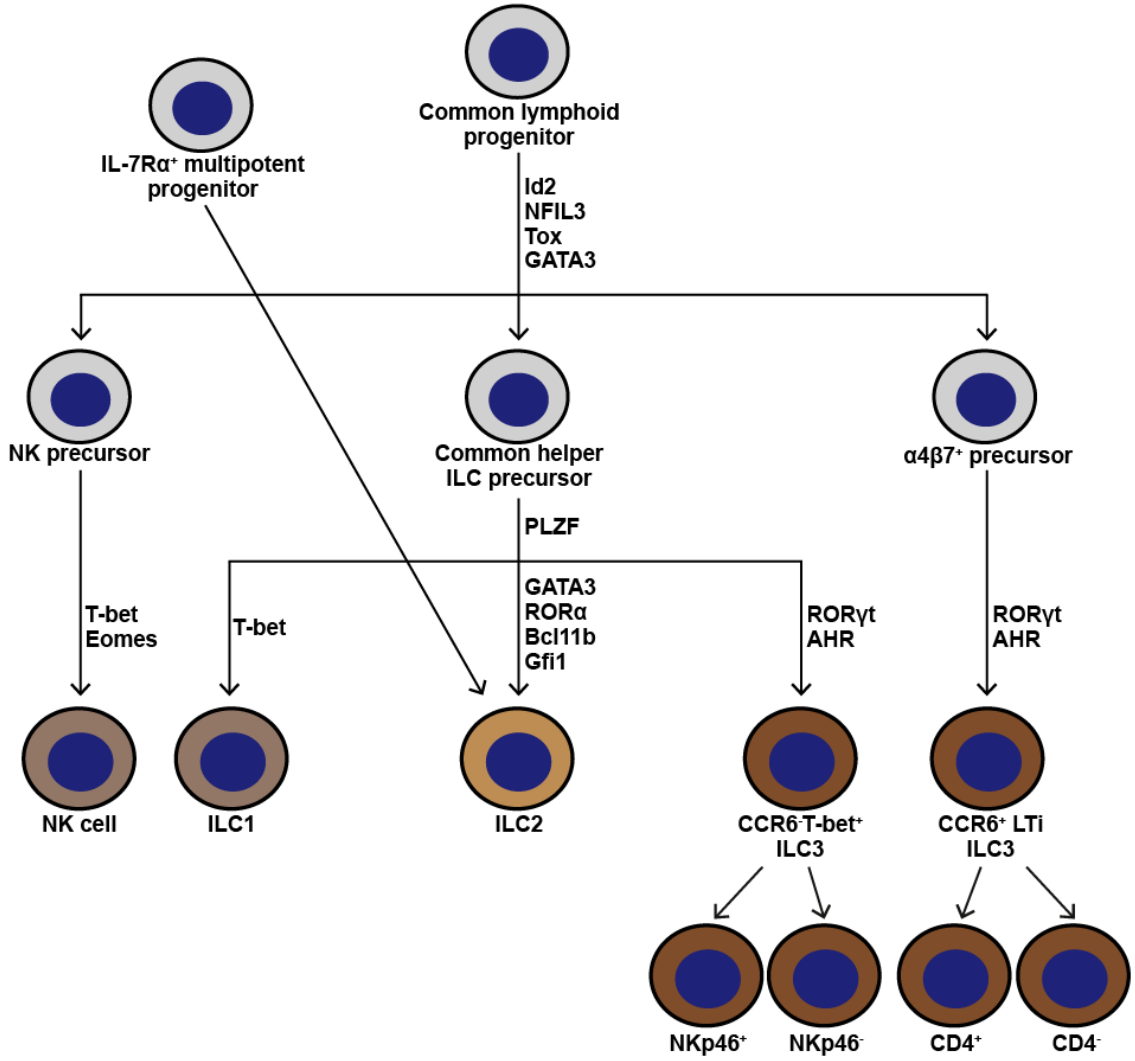

Figure 1.7. Development of ILCs. Common lymphoid progenitors differentiate into ILCs, instead of B and T cells, upon expression of several transcription factors. Development into ILC subsets is further guided by different transcription factors for each group. In addition, ILC2s can be derived from multipotent progenitors independent of common lymphoid progenitors.

1.14. Characteristics of ILC2s

Whilst ILC subsets share common gene transcripts, such as *Il7r* and *Cxcr6*, and some subsets are not easily distinguishable, ILC2s appear to be a group with higher number of gene transcripts distinct from other ILC subsets (232). Recent murine and human studies have provided evidence of the role of ILC2s in the generation of Th2 responses, despite their relatively low cell numbers compared to other type 2 effector immune cells. During the

second part of my research project, I focussed on the behaviour of ILC2s in homeostasis and inflammation, and will therefore consider them in more detail.

The existence of ILC2s was first suggested in studies investigating the effects of IL-25, which is structurally related to IL-17, showing a population of cells that were not B cells, T cells or myeloid cells but produced type 2 cytokines (233,234). Several studies were then published in 2010 characterising this novel population in tissues at rest and following type 2 inflammatory stimuli; these cells were initially named natural helper cells, innate helper type 2 cells or nuocytes (235–237), and subsequently renamed ILC2s when a consensus was agreed on the nomenclature for ILCs (213).

As well as expressing markers seen in other ILC subsets, including IL-7Rα (CD127), IL-2Rα (CD25), common gamma chain (CD132), Thy1 (CD90), c-kit (CD117) and in humans CCR6, ILC2s express markers including ST2 (IL-33R subunit), IL-17RB (IL-25R), inducible T cell costimulator (ICOS), killer-cell lectin like receptor G1 (KLRG1) and chemoattractant receptor-homologous molecule expressed on Th2 cells (CRTH2) (215,238,239). Some of these markers show variable expression depending on the stimuli present, as demonstrated in a study comparing IL-33- and house dust mite-induced lung inflammation (240). ILC2s from different tissues have been shown to exhibit distinct transcriptional profiles, such as IL-18R1-expressing ILC2s in the skin, with cytokine production independent of the microbiota, suggesting the existence of ILC2 subsets that respond to tissue-specific signals (241).

The transcription factors GATA3, RORα, Bcl11b and Gfi1 are required for ILC2 development (242,243). Whilst GATA3 is expressed during development of other ILC subsets, mature ILC2s maintain high expression of GATA3 that is important for their function, with TSLP shown to increase GATA3 expression and type 2 cytokine production by human ILC2s *in vitro* (244). Although RORα is also expressed by ILC3s, RORα-deficient mice lacked ILC2s but still contained RORγt^{+} ILC3s, and RORα deficiency resulted in failure to mount pulmonary inflammation to allergen (245) and failure to expel intestinal worms (246). In Bcl11b-deficient mice, ILC2s were absent even following stimulation, whilst ILC3 numbers in the gut were increased (247). ICAM-1 is also required for ILC2 development and function, with ICAM-1-deficient mice showing reduced BM and tissue ILC2 numbers, and reduced ILC2 cytokine production following IL-33 stimulation or allergen challenge with the fungus *Alternaria alternata* (248).

ILC2s are early effectors in helminth- and allergen-induced inflammation and produce type 2 cytokines, including significant amounts of IL-5 and IL-13, as well as IL-4 and IL-9. ILC2s are involved in tissue repair via the secretion of amphiregulin (218,249). Cultured ILC2s have

also been shown to produce other cytokines, including the immunosuppressive cytokine IL-10, the pleiotropic cytokine IL-6, and GM-CSF which exerts a range of effects including granulopoiesis and neutrophil priming (237).

1.15. Distribution and trafficking of ILC2s

ILC2s have been identified in a variety of non-lymphoid and lymphoid tissues. Using an IL-4 reporter, ILC2s (IL-4$^+$ cells with negative lineage markers including CD3, siglec-F, CD11b, CD49b and IgE) have been shown to be present at rest in tissues, with highest numbers in mesenteric LN, spleen, liver and BM, and also in lung and peritoneum (236). ILC2 numbers increased following IL-25 stimulation, IL-33 stimulation or *Nippostrongylus brasiliensis* helminth infection (which results in release of epithelial IL-25, IL-33 and TSLP); as they are the main IL-13-producing cell population, IL-13 reporter mice have also been used to identify ILC2s (237). ILC2s are present in adipose tissues, originally identified as lineage$^-$ and c-kit$^+$Sca-1$^+$ cells within murine and human mesenteric fat-associated lymphoid clusters (FALCs) that produced IL-5 and IL-13 (235). In the skin, dermal ILC2s constitutively produce IL-13 at baseline (250).

In long-term parabiosis experiments, the majority of ILC1s, ILC2s and ILC3s, but not NK cells, remained host-derived in tissues including small intestine lamina propria, lung and mesenteric LN, demonstrating that they were predominantly tissue-resident cells. Following *N. brasiliensis* helminth infection, local tissue-resident ILC2s proliferated and were responsible for the early expansion of ILC2s at the infection site. At a later time point, however, donor-derived inflammatory ILC2s recruited from the systemic circulation also partially contributed to the expansion of ILC2 population post infection (10). Intravenously transferred ILC2s have been shown, by non-invasive *in vivo* imaging, to migrate to the lungs of mice 24 to 30 hours following IL-33 or CXCL16 (ligand for CXCR6) nasal challenge (251).

Intranasal administration of *A. alternata*, which induces allergic airway inflammation, increased serum IL-33 and trafficking of ILC2 progenitors out of BM; conversely, IL-33 deficiency resulted in BM accumulation of ILC2 progenitors with higher CXCR4 expression (252). The resultant increase in ILC2 recruitment to the lungs following *Alternaria* challenge was dependent on the β2 integrin CD18 (253). The migration of BM ILC2s to the small intestine involved expression of CCR9 and α4β7 integrin on ILC2s, and, unlike ILC3 migration, was independent of retinoic acid (254).

Complement activation is involved in ILC2 recruitment, with one study showing that the increase in lung ILC2 numbers following house dust mite challenge was impaired in mice deficient in C3a, an anaphylatoxin that also acts as a neutrophil chemoattractant (255). ILC2s express CRTH2, the receptor for prostaglandin D_2, and intranasal administration of prostaglandin D_2 resulted in ILC2 recruitment to the lungs (256). Human ILC2s have been shown to produce prostaglandin D_2 upon stimulation *in vitro* (257), suggesting that ILC2s may themselves contribute to cellular recruitment in an autocrine manner.

A subset of ILC2s, expressing IL-25R and KLRG1 but not ST2, has been described as inflammatory ILC2s that has been shown to develop either into $ST2^+$ ILC2s following IL-25 stimulation or *N. brasiliensis* infection, or into IL-17-producing (ILC3-like) cells following TGFβ / IL-6 stimulation or *Candida albicans* infection. Whilst local tissue natural ILC2s respond to IL-33, inflammatory ILC2s respond to IL-25 (258). Adoptive transfer experiments showed that inflammatory ILC2s were derived from small intestinal ILC2s, and upon stimulation they migrated via lymphatics into the circulation and to distant organs including the lungs, dependent on S1P, contributing to defence against *N. brasiliensis* infection and subsequent tissue repair via amphiregulin production (259).

Therefore, whilst ILC2s are tissue-resident cells that undergo local renewal and expansion at baseline and following inflammatory challenges, they are also recruited from BM and the gut to distant organs following stimulation, a pattern similar to that of T cells which are activated within LNs then migrate to local tissues to exert effector functions (260).

1.15.1. ILCs in lymphoid tissues

The development of secondary lymphoid organs, including LNs and Peyer's patches, requires LTi ILC3s. Mice that lacked LTi cells, such as Id2-deficient and RORγt-deficient mice, failed to develop these secondary lymphoid organs (39). All three ILC subsets have been identified in adult lymphoid tissues, with differences in composition shown between mucosal-draining LNs (mesenteric and mediastinal LNs) and peripheral-draining LNs (inguinal and brachial LNs), including higher numbers of all ILCs subsets in mesenteric LN, with a larger proportion of ILC3s in mesenteric and mediastinal LNs.

ILC2s and ILC3s have been shown to be located within interfollicular zones of mesenteric LN. Using the photoconvertible *Kaede* mice, in which cells photoconvert from green to red fluorescence following exposure to violet light, ILC2s ($IL\text{-}7R\alpha^+Sca\text{-}1^+$) and ILC3s ($IL\text{-}7R\alpha^+CCR6^+$) have both been shown to traffick from the small intestine to mesenteric LN.

Whilst CCR7 was involved in the trafficking of ILC3s to mesenteric LN, this was not the case for ILC2s, as CCR7-deficient mice had normal numbers of mesenteric LN ILC2s (261,262).

1.16. ILC2s in Th2 responses

In type 2 immune responses, inflammatory signals from helminths and allergens at mucosal barrier sites activate a number of immune cell types, including DCs, basophils and ILC2s, leading to activation of Th2 cells and subsequent effector functions in defence against parasitic infections and in allergic inflammatory responses. Basophils produce IL-4, the cytokine that drives Th2 cell differentiation. DCs upregulate transcription factors interferon regulatory factor 4 (IRF4) and Krüppel-like factor 4 (KLF4), and the co-stimulatory molecule OX40 ligand (OX40L), leading to Th2 cell stimulation. Th2 cells produce the type 2 cytokines IL-4, IL-5, IL-9 and IL-13, which exert a number of effects, such as B cell class-switching to IgE production, eosinophil recruitment, mast cell recruitment, macrophage polarisation, goblet cell hyperplasia / mucus secretion, and smooth muscle contraction (263).

ILC2s are critical early effectors in the initiation of Th2 responses. *In vitro*, ILC2s promoted Th2 differentiation and inhibited Th1 differentiation in a contact-dependent manner (264). Being tissue-resident cells with surface expression of receptors such as ST2 (IL-33R) and IL-17RB (IL-25R), ILC2s can respond rapidly to the epithelial cell-derived alarmins IL-25, IL-33 and TSLP, and produce type 2 cytokines. IL-33, in particular, is a key mediator of ILC2 responses in organs such as the lungs, whilst other cytokines may play more important roles in other organs, such as IL-25 in the gut and TSLP in the skin (219,265).

Lung inflammation induced by the protease allergen papain required ILC2s, as ILC2-deficient mice showed impaired eosinophil, neutrophil, DC and $CD4^+$ T cell recruitment, reduced IL-5 and IL-13 production, reduced IgE levels, and lower mucus production. ILC2s were the main source of IL-5 and IL-13 early (day 2) following papain stimulation, with $CD4^+$ T cells becoming the dominant source only at a later time point (266). In ozone-induced nasal inflammation, eosinophil recruitment was abrogated in *Rag2*$^{-/-}$*Il2rg*$^{-/-}$ mice that lacked ILCs, T cells and B cells, but intact in *Rag2*$^{-/-}$ mice that lacked T and B cells but had normal ILC2s (267). Following house dust mite challenge, however, immune cell recruitment to the lungs consisted initially of neutrophils, then eosinophils and $CD4^+$ T cells, prior to arrival of ILC2s (268); this may represent stimulus-specific differences in ILC2 dynamics. *In vitro*, IL-10, TGFβ and dexamethasone inhibited type 2 cytokine production by human blood ILC2s (269).

ILC2s work in conjunction with other immune and stromal cells in generating type 2 responses. In a transgenic murine model with increased numbers of mast cells, *Heligmosomoides polygyrus* helminth infection resulted in early increased IL-33 production by mast cells and subsequently increased ILC2 numbers, leading to increased worm expulsion (270). In a vitamin D analogue-induced skin inflammation model of type 2-driven atopic dermatitis, basophils were the major IL-4 producing cell type required for ILC2 recruitment, ILC2 proliferation and induction of skin inflammation (271). ILC2s themselves have been demonstrated to contribute to T cell activation via IL-4 *in vitro* (272). Another study using papain-induced lung inflammation, however, showed that IL-4 is not essential in generating type 2 responses (266).

Transfer experiments demonstrated that ILC2s and $CD4^+$ T cells worked synergistically in stimulating type 2 responses, including airway eosinophilia and IL-13 production, following ovalbumin-induced inflammation (272,273). IL-13 produced by ILC2s promoted a number of processes in the local tissues and dLN, such as CCL17 production by $IRF4^+$ DCs leading to pulmonary recruitment of memory Th2 cells expressing CCR4 (receptor for CCL17) following papain-induced inflammation (243), activation of alveolar macrophages involved in killing of *N. brasiliensis* larvae (274), and migration of $CD40^+$ DCs to and differentiation of Th2 cells in the mediastinal dLN following papain stimulation (266). *In vitro*, recombinant IL-13 reduced production of IL-6 and TNF by BM-derived mast cells (250).

ILC2s can also promote early immunoglobulin production by B cells. ILC2s promoted B cell IgM production via IL-5 in co-culture, and adoptive transfer experiments demonstrated that ILC2s promoted antigen-specific IgM production following inhaled antigen challenge independent of T cells (275). ILC2s from FALCs produced cytokines including IL-5 and IL-6, and stimulated B1 cell proliferation and IgA production in *ex vivo* co-culture (235). Therefore, ILC2s function as a network with other innate and adaptive immune cells to generate the early response to type 2 inflammatory stimuli.

1.16.1. ILCs and antigen presentation

Like neutrophils, ILCs are capable of antigen presentation. ILC2s have been shown, by flow cytometry and microarray, to express MHCII at baseline (233,237), with higher MHCII expression on ILC2s from lymphoid tissue than those from non-lymphoid tissue. Murine ILC2s can process and present antigen *in vitro* via MHCII, and human ILC2s can also present antigen to T cells. In ILC2 and OTII T cell co-cultures, addition of OVA peptide led to an MHCII-dependent increase in T cell proliferation. *In vivo*, ILC2s increased antigen-specific T cell responses to OVA peptide, whilst MHCII-deficient ILC2s showed impaired

ability to mediate *N. brasiliensis* worm expulsion (264,276). C3a did not affect antigen uptake or processing but increased peptide uploading onto MHCII *in vitro*, and C3a-deficient ILC2s showed reduced ability to activate antigen-specific $CD4^+$ T cells *in vitro* and *in vivo* (255).

ILC2s can contribute to T cell activation via expression of co-stimulatory molecules (277). *In vitro*, ILC2s expressed CD80 and CD86, and in ILC2 and OTII T cell co-culture, OVA peptide-induced T cell proliferation was reduced by antibody blockade of CD80 and CD86 (276). In response to IL-33 stimulation, ILC2s upregulated surface expression of OX40L, which was required for tissue expansion of Th2 and Treg cells, and for type 2 immune response to allergen and to *N. brasiliensis* infection (278). Murine lung ILC2s and human peripheral blood ILC2s express both the co-stimulatory molecule ICOS and its ligand ICOS-ligand (ICOS-L), and ICOS-deficient ILC2s showed impaired ability to stimulate eosinophilic inflammation and airway hyperreactivity in adoptive transfer experiments (279).

As well as presenting peptide antigen, ILC2s can present lipid antigen to T cells. Human skin ILC2s express CD1a, which is expressed on other antigen presenting cells in the skin for presentation of endogenous and exogenous lipids; ILC2s pulsed with house dust mite or bacterial components produced endogenous lipid ligands for CD1a-mediated presentation to co-cultured T cells, as evidenced by increased T cell secretion of IFNγ, IL-22 and IL-13 (280).

ILC3s have also been shown to express MHCII and present antigen *in vitro*, leading to negative regulation of $CD4^+$ T cell responses, as the generation of MHCII-deficient ILC3s resulted in increased $CD4^+$ T cell response to commensal bacteria, an effect that was reversed by antibiotic administration (281). *In vivo*, mice with MHCII-deficient ILC3s showed increased follicular helper T cell numbers and increased IgA production in an IL-4-dependent manner (282).

1.16.2. Crosstalk between ILC2s and neutrophils

Whilst ILC3s mediate neutrophilic inflammation via production of cytokines, including IL-17 (283) and GM-CSF, which promote granulopoiesis, neutrophil priming and neutrophil survival, there is also some evidence of interaction between ILC2s and neutrophils. GM-CSF is produced by murine tissue ILC2s (232,237). In human ILC2s, *in vitro* overexpression of GATA3 led to increased expression of IL-5, IL-13 and GM-CSF following stimulation with IL-2, IL-33 and TSLP (244). ILC2s, like other ILC subsets, demonstrate plasticity in their transcription factor expression and cytokine production, including upregulation of RORγt and

IL-17 production, therefore promoting neutrophilic inflammation (229). IL-33 stimulation resulted in production of IL-17 by lung $ST2^+$ ILC2s that also produced IL-5 and IL-13, in a process dependent on AHR but independent of RORγt (284). In a murine model of traumatic injury, increased blood and lung IL-33 led to increased IL-5 production by ILC2s as well as neutrophils; the upregulation of neutrophil IL-5 expression was dependent on ILC2s, and amplified the type 2 response (285).

ILC2s have been shown to promote the immunosuppressive effects of neutrophils. In a lymphocytic choriomeningitis virus (LCMV) hepatitis model, IL-33 treatment increased neutrophil recruitment and reduced T cell numbers and liver injury, with *in vitro* experiments demonstrating the mechanism of this anti-inflammatory neutrophil effect to be via ILC2-derived IL-13 stimulation of neutrophils, leading to STAT6-mediated production of arginase-1 by neutrophils (286). Furthermore, neutrophils have recently been shown to suppress ILC2s. In an intranasal house dust mite challenge model, anti-Ly6G neutrophil depletion resulted in increased ILC2 production of IL-5 and IL-13 in bronchoalveolar lavage fluid, with the lack of negative feedback by neutrophils to the IL-23 / IL-17 / G-CSF axis leading to increased G-CSF, which promoted Th2 cytokine production. Human blood ILC2s also showed increased IL-5 and IL-13 expression following G-CSF stimulation *in vitro* (153). These studies suggest that there is bi-directional crosstalk between ILC2s and neutrophils, although both stimulatory and inhibitory effects have been demonstrated.

1.17. ILC2s and inflammatory diseases

ILC2s have been implicated to contribute to the pathogenesis of a number of respiratory and systemic inflammatory diseases.

1.17.1. ILC2s and respiratory diseases

Studies have demonstrated the role of ILC2s in respiratory tract diseases (287). In patients with severe asthma, ILC2 numbers have been shown to be increased in sputum and blood; although the absolute numbers of $CD4^+$ Th2 cells were higher, ILC2s were major producers of IL-5 and IL-13, with *in vitro* cytokine production reduced by dexamethasone (288,289). Biological therapies targeting parts of this pathway have been developed, such as the anti-IL-5 antibody mepolizumab used successfully for asthma (263,290). ILC2s have been found, localised in eosinophil-rich areas, in nasal polyps from patients with chronic rhinosinusitis (228), and ILC2s showed plasticity in producing IL-17 *ex vivo* (291).

In chronic obstructive pulmonary disease, where persistent inflammation results most commonly from tobacco smoking, there is Th1 predominance, and ILC2s show plasticity towards an ILC1 phenotype. Influenza virus and respiratory syncytial virus, common viral triggers for disease exacerbations, downregulated lung ILC GATA3 expression leading to an ILC1 phenotype (292), and cigarette smoke exposure in mice led to decreased ST2 expression on ILC2s (293). ILC2s have also been shown to be involved in airway repair. Following influenza infection, anti-CD90.2 ILC depletion resulted in impaired murine airway remodelling, which was restored by adoptive transfer of lung ILC2s or by administration of amphiregulin (218). Bronchoalveolar lavage fluid from patients with idiopathic pulmonary fibrosis contained higher numbers of ILC2s compared to controls, suggesting a pathogenic role (294).

1.17.2. ILC2s and other diseases

Human and murine white adipose tissue contains ILC2s, with their numbers reduced in obesity. ILC2s have been shown in mice to play a role in the IL-33-dependent beiging of adipose tissue, which limits obesity (295). Higher numbers of ILC2s and basophils have been found in proximity to each other in skin biopsies from atopic dermatitis patients (271). Increased ILC2s have been shown by confocal microscopy in healing human skin wounds, and in mice ILC2 depletion resulted in delayed skin wound healing (296). In rheumatoid arthritis, IL-9 production was shown to be from lineage-positive cells in active disease, but from ILC2s in disease remission, and ILC2-derived IL-9 promoted resolution of arthritis by stimulating Treg cells (297).

In a murine model of sepsis with caecal ligation and puncture, ILC2 numbers were increased in the small bowel lamina propria, and plasma IL-33 was increased in this model as well as in patients with sepsis (298). In common variable immune deficiency, a disorder of impaired antibody production associated with recurrent infections and autoimmunity, lower numbers of peripheral blood ILC2s have been found, with reduced expansion and impaired MHCII expression upon *ex vivo* stimulation (299).

Some studies, however, have suggested redundancy of ILCs *in vivo*. In a group of severe combined immunodeficiency patients that have received stem cell transplants, persistent ILC deficiency was observed but without clear association with disease (300). In mice, ILC2s were present in kidneys at baseline, but ILC2 depletion did not alter the severity of experimental ischaemia-reperfusion renal injury (301). NCR^+ ILC3s were shown to be involved in the control of gut infection with *Citrobacter rodentium*, a Gram-negative organism

that generates a strong Th17 response, in RAG-deficient mice lacking adaptive lymphocytes, but ILC3s were redundant in the infection response in immunocompetent mice (302).

1.17.3. ILC2s and helminth infections

Helminth infections trigger type 2 immune responses involving a number of immune cells, including activation of ILC2s by epithelial alarmins released following mucosal barrier damage. Infection with the rodent nematode (roundworm) parasite *N. brasiliensis* is commonly used as a model of type 2 inflammation of the lungs and gut, and is therefore used in a number of studies of ILC2s.

In the life cycle of *N. brasiliensis* (Figure 1.8), eggs present in soil hatch into L1 worms or larvae, moulting twice into L2 then L3 larvae. L3 larvae infect mice by penetrating the skin, and within hours enter blood vessels to migrate into the lung parenchyma, where they mature into L4 larvae and cause acute lung injury and haemorrhage, 2 to 3 days following initial infection. The larvae then migrate into the airways, and are coughed up and swallowed into the gut, reaching the small bowel about 4 days post infection. The L4 larvae mature into adults and lay eggs in the gut, inducing a strong Th2 response. In rats, adult worms can continue to lay eggs, whilst in mice the Th2 response leads to worm expulsion about 10 days post infection (249). Worm expulsion from the gut is dependent on IL-13 signalling via STAT6 (303), and ILC2s are important in providing type 2 cytokines for worm expulsion, as ILC2 depletion has been shown to result in increased worm burden and reduction in Th2 cells (276). The airway remodelling following infection can subsequently lead to emphysema in the lungs (249,304).

Another model of type 2 inflammation used for studying ILC2s is infection with *Schistosoma mansoni*, a human trematode (flatworm) parasite that causes significant disease worldwide. In their natural life cycle, *S. mansoni* eggs hatch in free water and infect snails, an intermediate host, from which they are released as cercariae. The cercariae infect humans by penetrating the skin, and migrate into the hepatic portal venous system where they mature into adult worms, which migrate into the mesenteric veins and lay eggs (305). When administered to mice, *S. mansoni* eggs induced a strong Th2 inflammatory response and granuloma formation; killed eggs and soluble egg antigen also generated the same immune response (306). Mice challenged with *S. mansoni* showed increased lung and mediastinal LN ILC2s, which induced collagen deposition and granuloma formation in an IL-13-dependent manner (294).

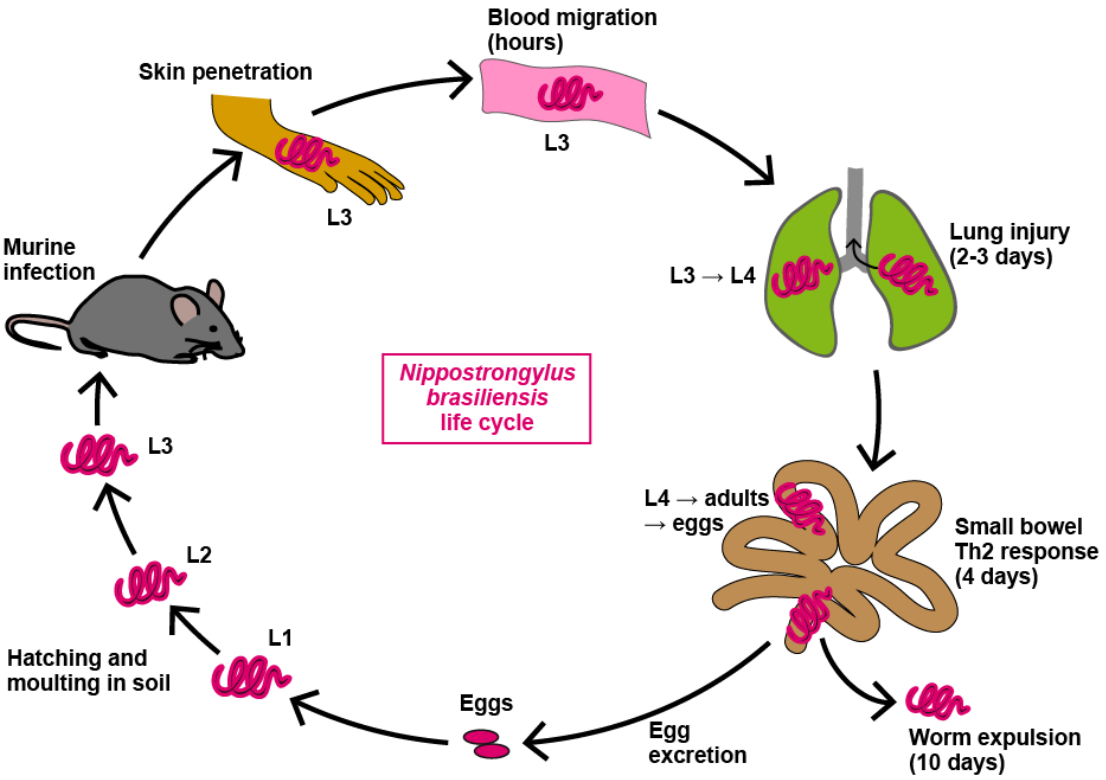

Figure 1.8. Life cycle of *N. brasiliensis*. Summary of the life cycle of *N. brasiliensis*. Eggs hatch and moult in soil into L3 larvae which penetrate murine skin and enter blood vessels within hours of infection to migrate to the lungs. L3 larvae mature into L4 larvae, causing acute lung injury and haemorrhage 2 to 3 days post infection. L4 larvae are coughed up and swallowed, reaching the small bowel 4 days post infection. In the gut L4 larvae mature into adults and lay eggs, inducing a strong Th2 response that in mice leads to worm expulsion about 10 days post infection.

1.18. Dynamic behaviour of ILCs *in vivo*

To date there have been few studies investigating the dynamic behaviour of ILCs *in vivo*, in part due to the difficulties in achieving stable live imaging of tissues such as the lungs and gut, affected by ventilation and peristalsis respectively. ILC2s were visualised in one study by intravital imaging in the ear skin, as CXCR6-GFP cells in mixed bone marrow chimeras, showing similar mean speed to migratory dermal DCs, and slower mean speed but similar meandering index compared to T cells. ILC2s showed brief interactions (not quantified in the study) with mast cells, but were not seen to interact with macrophages or DCs (250).

In another study, using a model where lungs were explanted, sectioned, stained with antibodies then imaged *ex vivo*, ILC2s (visualised as IL-13-GFP cells) were observed to increase in numbers around airways and large blood vessels following IL-33 stimulation, showing amoeboid movements with speed (median approximately 3 μm/min) and distance higher than that of $CD4^+$ T cells. CCR8 antibody blockade reduced ILC2 movement, suggesting a role of this chemokine receptor in ILC2 migration. Chemical inhibition of collagen fibre cross-linking increased the speed and distance of movement of ILC2s, and reduced eosinophil recruitment, suggesting possible ILC2 interaction with the extracellular matrix (307).

In the gut, intravital imaging of ILC3s, identified as GFP^+ cells in RAG-deficient IL-23R-GFP mice, demonstrated trafficking of ILC3s in and out of cryptopatches (structures containing ILC3s and DCs), with cells mobilising out of cryptopatches following induction of colitis in a GM-CSF-dependent manner, although ILC3s within the cryptopatches demonstrated little motility (308).

1.18.1. Reporter mice for identifying ILCs *in vivo*

To date a number of mouse models have been used in the identification of ILCs. Fluorescent reporters for type 2 cytokines have been used to identify ILC2s, although other cells such as Th2 cells also produce type 2 cytokines and therefore these reporter mice would be expected to have limited specificity as ILC2 reporters for *in vivo* studies. The 4get mouse, with GFP fluorescence on cells expressing IL-4, was originally generated for the investigation of Th2 responses. In contrast to knock-out mouse models, the 4get reporter is a knock-in model, with IL-4 activity remaining intact (309). Whilst 4get mice have subsequently been used to characterise ILC2s, GFP expression is not limited to ILC2s, and one study using genetic tracking of cytokine production was unable to show significant IL-4 secretion by ILC2s at baseline and following stimulation *in vivo* despite their GFP fluorescence in the reporter mice (236).

IL-5 and IL-13 reporter mice have been used to identify ILC2s, which are major but not exclusive producers of these cytokines. The IL-5 reporter Red5, with tdTomato and Cre recombinase linked to the *Il5* gene, has been used to show the constitutive expression of IL-5 by ILC2s in peripheral tissues, with the majority of fluorescent cells showing phenotypic markers of ILC2s (310). IL-13 reporters linked to GFP (237) and to YFP / Cre recombinase (YetCre-13) (236) have also been used to characterise ILC2s. These reporters could, however, under-estimate ILC2 numbers, as not all ILC2s were positive at baseline (241).

Cre-containing cytokine reporters have been crossed with Rosa26-stop flox-YFP mice to achieve stable expression of the reporter in the target cells and their progenies; these fate mapping reporter mice are useful in the *in vivo* tracing of cell lineage (231,236,310). Fluorescent cytokine reporters, such as IL-22 and IL-23, have been used for the identification of ILC3s, with similar limitations to cytokine reporters for ILC2s (231).

Reporter mice for ILC-associated transcription factors may represent an alternative strategy in the *in vivo* identification of ILCs. A recent study proposed the identification of ILC2s as lineage-negative GATA3-positive cells (311); however, GATA3 is expressed by other ILCs and T cells, and therefore GATA3-GFP reporter mice would have limited use as an ILC2-specific reporter (231). RORγt-GFP reporter mice have been used in the study of ILC3s (312), but similarly the expression of RORγt is not limited to ILC3s. A multi-colour reporter has recently been generated including fluorescent markers for Id2, RORα and RORγt (224), which may help address the issue of cell specificity in the *in vivo* study of ILCs.

1.19. ILCs: summary and unanswered questions

ILCs are of lymphoid origin but lack antigen-specific receptors, and respond to stimuli by producing cytokines in an analogous fashion to Th cell subsets. Whilst low in frequency, ILCs are present in a number of lymphoid and non-lymphoid tissues, and are involved in the initiation and resolution of inflammation. ILC2s provide the early response to allergens and helminths, responding to epithelial damage signals by producing cytokines including IL-5 and IL-13 to promote type 2 immune responses. ILC2s have been shown to express MHCII for antigen presentation to $CD4^+$ T cells, and there is also some evidence of crosstalk between ILC2s and neutrophils.

Although there is evidence of crosstalk between ILCs and other immune cells, much focus has been on their role as cytokine producers, with few studies to date investigating the *in vivo* dynamic behaviour of ILCs in tissues. ILCs are present in LNs, but there are little data on their behaviour in LNs *in vivo*, such as their trafficking patterns, their interactions with other LN immune cells, and whether similar processes occur in LNs compared to tissue sites of inflammation. As ILC2s have been implicated in inflammatory diseases such as asthma, understanding the *in vivo* dynamics of ILC2s within the network of cells that constitute type 2 immunity can potentially aid the future development of ILC2-targeted therapies for these disorders.

1.20. Intravital two-photon imaging

Intravital two-photon or multiphoton microscopy has recently become a useful tool for the study of immune cell behaviour *in vivo*, allowing live animal imaging of cellular interactions within tissues that are otherwise difficult to model *in vitro*. The physical principles of two-photon excitation are illustrated in the Jablonski diagram (313).

In two-photon excitation, the simultaneous absorption of two photons, both spatially and temporally, enables fluorophore excitation at much longer, infrared-range wavelengths, but with emission spectra identical to that from single-photon excitation. As the simultaneous absorption of two photons is a rare event, the laser beam is spatially focussed and delivered in extremely short pulses in the femtosecond range to generate enough two-photon excitation events of fluorophores for imaging, and specialist lasers such as tuneable titanium sapphire (Ti:sapphire) lasers are used to achieve this. These properties result in less scattering and less out-of-focus absorption, and therefore lead to deeper tissue penetration and reduced photo-damage, enabling intravital imaging over prolonged periods of time (314). In second harmonic generation (SHG), two-photon excitation results in emission at half of the excitation wavelength without any loss of energy (vibrational relaxation) and without the need for fluorophore excitation (313); this is commonly employed in acquiring signals from tissue collagen fibres during imaging without the need for fluorophore binding.

A wide variety of tissues have now been examined using intravital imaging, including LN (315,316), ear skin (317), lung (318) and bone (319). *In vivo* studies of LNs have significantly advanced understanding of immune cell interactions. The popliteal LN in particular has often been the LN of choice for imaging studies (320), as it is relatively easy to access and immobilise surgically compared to other LNs, it is small in size allowing for imaging of different microanatomical regions concurrently, and it serves as the main lymphatic drainage from the footpad making it a convenient model for investigating cellular and antigen trafficking (316).

The principles of single-photon excitation, two-photon excitation and second harmonic generation are summarised in Figure 1.9.

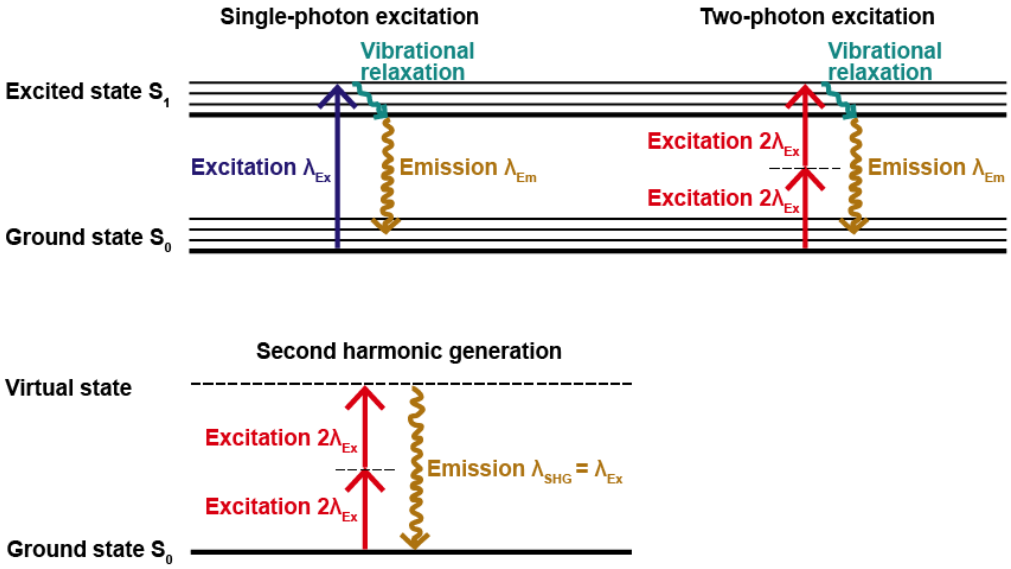

Figure 1.9. Principles of two-photon excitation. Jablonski diagram showing the principles of single-photon excitation, two-photon excitation and second harmonic generation. Excitation of a single photon from ground (S_0) to excited (S_1) state results in photon emission with wavelength (λ_{Em}) longer than the excitation wavelength (λ_{Ex}) due to some energy loss (vibrational relaxation) following excitation; the difference in wavelengths is known as Stokes shift. In two-photon excitation, the simultaneous excitation of two photons allows excitation at much longer wavelengths but with the same λ_{Em} as single-photon excitation. In second harmonic generation, two-photon excitation to a virtual state results in emission without energy loss, enabling signal generation from tissues such as collagen without fluorophore binding.

1.21. Summary

The immune system consists of a complex network of innate and adaptive immune cells working together to respond to infectious and inflammatory challenges. Innate immune cells are activated rapidly and form the early host defence, performing functions such as pathogen killing, cytokine production, and antigen presentation to T cells to activate adaptive immunity. Whilst DCs and macrophages are traditionally considered professional antigen presenting cells, other innate cells can also present antigen. Neutrophils are the archetypal innate effector cell type exhibiting effective mechanisms for pathogen killing, and ILCs are a recently characterised group of innate cells that are efficient at cytokine production, with ILC2s producing type 2 cytokines; both neutrophils and ILC2s can also express MHCII and present antigen to influence adaptive immunity. LNs are organs packed with immune cells

that encounter incoming antigen from peripheral tissues and from the circulation, and are thus ideal sites for immune cellular interactions and antigen presentation.

Neutrophils have been shown to migrate to LNs following inflammatory stimuli, influencing adaptive immunity by interacting with other LN immune cells and by direct antigen presentation. However, *in vitro* and *in vivo* studies have shown conflicting results on the effects of neutrophils on the overall immune response, and it is unclear whether this represents stimulus-specific or tissue-specific differences. There is limited evidence of the presence of neutrophils in tissues at baseline, but detailed studies are lacking on the anatomical location, *in vivo* dynamic behaviour and potential function of neutrophils within LNs in the homeostatic state. ILC2s have mainly been considered tissue-resident effector cells that influence adaptive immunity via cytokine production, and few studies have investigated the *in vivo* behaviour of ILC2s. Although ILCs are present in LNs, little data exist on the dynamics and cellular interactions of LN ILC2s.

Intravital two-photon microscopy allows the examination of cellular behaviour and interaction in live animals, and is a powerful tool for investigating innate immune cell behaviour in LNs. Both neutrophils and ILC2s have been associated with a number of inflammatory diseases, and understanding the dynamic behaviour of these cells at baseline and in inflammation provides important mechanistic knowledge potentially leading to strategies for therapeutic modulation of inflammatory disorders.

Chapter 2. Hypotheses and aims

2.1. Overall aim

Innate immune cells respond rapidly to pathogenic stimuli to provide the early host response to infection and tissue injury, and they can also influence adaptive immune responses. LNs are specialised secondary lymphoid organs where immune cells are concentrated and arranged in a specific anatomical distribution, and are sites for potential interactions between innate and adaptive immune cells. Neutrophils have been shown to migrate to LNs following inflammatory stimuli to influence other immune cells, but whether this occurs in physiological conditions is less clear. ILCs are tissue-resident cells that shape immune responses via cytokine production, but to date few studies have investigated their *in vivo* dynamic behaviour and interactions with other immune cells in lymphoid and non-lymphoid organs.

Therefore the overall aim of my project is to study the dynamic behaviour of innate immune cells within lymphoid organs, focussing in particular on neutrophils and ILC2s, using methods including intravital two-photon microscopy.

2.2. Hypothesis and aims: neutrophil dynamic behaviour

2.2.1. Hypothesis

Neutrophils traffick tonically into LNs under homeostatic conditions, with the potential to influence the adaptive immune response by interacting with other LN immune cells and by delivering systemic antigen to LNs.

2.2.2. Aims

- Identify and quantify neutrophils in LNs from unstimulated mice and from human organ donors
- Examine the anatomical location of neutrophils within LNs, and interactions between neutrophils and other LN immune cells
- Quantify the dynamic behaviour of LN neutrophils at baseline *in vivo*
- Investigate the route and mechanism of trafficking of neutrophils from the circulation into LNs at baseline and following inflammation
- Characterise the phenotype of LN neutrophils, including their expression of MHCII

- Investigate the potential function of LN neutrophils, such as the delivery of circulating antigen to LNs

2.3. Hypothesis and aims: ILC dynamic behaviour

2.3.1. Hypothesis

ILC2s are present in lymphoid organs in homeostasis and in inflammation, and their dynamic behaviour changes in response to type 2 inflammatory stimuli, with the potential to increase the spatial distribution of type 2 cytokines.

2.3.2. Aims

- Examine ILC2s in lymphoid organs, including Peyer's patches and popliteal LNs, using different experimental helminth models of type 2 inflammation
- Quantify and compare the dynamic behaviour of ILC2s *in vivo* at baseline and following type 2 inflammatory stimuli in Peyer's patches and popliteal LNs
- Investigate whether ILC2s and T cells engage in prolonged interactions *in vivo*
- Quantify the dynamic behaviour of ILC2s *in vivo* in small bowel mucosa
- Examine the use of a novel triple reporter mouse for simultaneous intravital imaging of ILC subsets

Chapter 3. Methods

3.1. Mice

C57BL/6 mice were purchased from Charles River Laboratories UK. LysM-GFP mice (321) were a gift from Professor Sussan Nourshargh (Queen Mary University London) and used as neutrophil reporter mice. Ubiquitin-GFP mice (322) were obtained from Jackson Laboratories and used for isolation of cell type of interest for adoptive transfer. CD11c-yellow fluorescent protein (YFP) mice (323) were originally obtained from Rockefeller University and used as DC reporter mice. CD2-GFP/IL-13-tomato mice were obtained from Dr Andrew McKenzie (Laboratory of Molecular Biology, Cambridge) and used as reporter mice for ILC2s ($CD2^{-}IL\text{-}13^{+}$) (237) and T cells ($CD2^{+}$). Id2-blue fluorescent protein (BFP)/Rora-teal/Rorc-katushka mice were novel triple reporter mice obtained from Dr Andrew McKenzie (224) for investigating its use in the simultaneous imaging of multiple cell subsets including ILC2s, ILC3s, DCs and T cells.

Mice were bred in facilities at the University of Cambridge or Laboratory of Molecular Biology, and were maintained in specific pathogen free conditions. All experimental procedures were approved in accordance with the Animals (Scientific Procedures) Act 1986 UK.

3.2. Murine unstimulated LN analysis

For the quantification of neutrophils in unstimulated LNs, young female mice aged 8 to 10 weeks were used, avoiding the risk of skin injury and subsequent neutrophil recruitment to LNs in male mice that may fight when co-housed. Anti-CD45 antibody (1 µg in 100 µl PBS per mouse) was injected intravenously via the tail vein immediately (within 1 minute) prior to euthanasia to label all circulating leukocytes within the vasculature, enabling intravascular and extravascular neutrophils to be distinguished by flow cytometry (324). Inguinal, popliteal, mesenteric, mediastinal and axillary LNs, as well as spleen, BM and blood for comparison, were harvested following euthanasia and kept on ice then promptly processed.

For flow cytometry, LNs were mechanically dissociated by mashing through 70 µm cell strainers into single cell suspensions in phosphate-buffered saline (PBS) with 1% fetal calf serum (FCS). Spleen and BM were similarly dissociated with additional red cell lysis at room temperature. Chemical tissue digestion methods were avoided in order to preserve tissue

neutrophils and minimise *ex vivo* neutrophil activation. For confocal microscopy, harvested LNs were fixed and frozen sections generated and stained.

3.3. Murine neutrophil isolation and adoptive transfer

For neutrophil isolation, BM from the femurs of each donor mouse was flushed using PBS with 2 mM EDTA and 0.5% heat-inactivated normal mouse serum (NMS, Southern Biotech) and gently strained through a 70 µm cell strainer. Red cell lysis was performed with ammonium chloride-based lysis buffer for 2 minutes at room temperature, and then cells washed. During later experiments I omitted the red cell lysis step to reduce neutrophil *ex vivo* time and inadvertent activation, and this did not result in any reduction in purity of isolation. BM neutrophils were isolated by magnetic negative selection using MACS Mouse Neutrophil Isolation Kit as per manufacturer's instructions (Miltenyi Biotec).

Cell yield was calculated manually using a haemocytometer. Cell purity was determined by generating cytospin slides and identifying mature and immature neutrophils counting a minimum of 200 cells by microscopy, and / or by flow cytometry identifying viable (using Live/dead stain) neutrophils as $Ly6G^{+}CD11b^{+}$ cells for C57BL/6 or ubiquitin-GFP donors or as $LysM^{High}Ly6G^{+}$ cells for LysM-GFP donors.

Following isolation, GFP^{+} neutrophils were promptly transferred by intravenous tail vein injection into C57BL/6 recipients, with 2×10^{6} neutrophils in a volume of 100 to 200 µl PBS transferred per recipient mouse. For PNAd blocking experiments, mice were given one intraperitoneal injection of anti-PNAd (200 µg) 4 to 6 hours prior to neutrophil transfer, and a second injection of the same dose 1 hour prior to intravital imaging.

With the LysM-GFP mice (321), although LysM is expressed by other myeloid cells, GFP-bright neutrophils were distinguishable from GFP-intermediate monocytes and macrophages during intravital imaging by their morphology as well as fluorescence intensity, and for adoptive transfer neutrophils were isolated *ex vivo* prior to transfer to further improve the neutrophil purity of GFP^{+} cells. With the ubiquitin-GFP mice, all cells are positive for GFP, and therefore neutrophil isolation *ex vivo* was required prior to neutrophil adoptive transfer.

3.4. Human LN analysis and neutrophil isolation

All human blood and tissue samples were anonymised prior to being used in experiments. Ethical approval was obtained from the East of England Research Ethics Committee (references 12/EE/0446 and 15/EE/0152), and experiments were performed in accordance with the Declaration of Helsinki. Intact whole human LNs and sections of spleen were surgically removed by the clinical transplant team from deceased organ transplant donors and kept on ice for transport to the laboratory. In some cases peripheral blood was also taken at the time of donation. Similar to the processing of murine LNs, human LNs were mechanically dissociated by mashing through 70 μm cell strainer into single cell suspensions for flow cytometry, or fixed and frozen for sectioning for confocal microscopy.

For *ex vivo* neutrophil stimulation experiments, peripheral blood was drawn from healthy volunteers and transferred into tubes containing citrate as anticoagulant. Autologous platelet-poor plasma was generated, and red blood cells separated by sedimentation with 6% dextran for 30 minutes at room temperature. The leukocyte-rich layer was resuspended in autologous plasma, and discontinuous (42% and 51%) plasma-Percoll (Fisher Scientific) gradients under-layered for centrifugation. Peripheral blood mononuclear cells from the top (plasma/42%) interface were removed. Neutrophils were harvested from the lower (42%/51%) interface and washed three times, first with autologous plasma, then with PBS without calcium chloride and magnesium chloride (Sigma), then with PBS with calcium chloride and magnesium chloride (Sigma) (325).

Cell yield was calculated manually using a haemocytometer, and neutrophil purity assessed by generating cytospin slides and counting a minimum of 200 cells by microscopy, where neutrophils, eosinophils, peripheral blood mononuclear cells and red blood cells were distinguished by their different morphologies.

3.5. Neutrophil stimulation

IC was generated by incubating A647-conjugated whole OVA (Molecular Probes) with polyclonal rabbit anti-OVA (Sigma-Aldrich) in a 1:10 ratio for 1 hour at 37°C. *Streptococcus pneumoniae* (serotype 14) was opsonised with 10% NMS for 30 minutes at 37°C. For *ex vivo* stimulation, isolated human peripheral blood neutrophils or murine BM neutrophils were resuspended at 5 million cells per ml in Iscove's Modified Dulbecco's Media (IMDM), and incubated with PBS control, ATP (1 mM, Sigma-Aldrich), LPS (*Escherichia coli* O111:B4, 1 μg/ml, Sigma-Aldrich), *S. pneumoniae* (unopsonised or opsonised, neutrophil to bacteria ratio 1:23) or OVAIC (5 μg/ml OVA) for 1 hour at 37°C in a Thermomixer at 300 rpm,

following which stimulation was quenched and cells washed with cold PBS for staining for flow cytometry.

For reverse-transcriptase polymerase chain reaction (RT-PCR), murine BM neutrophils were stimulated with PBS control, OVA or OVAIC for 2 hours at 37°C, and mRNA expression of genes for MHCII and co-stimulatory molecules quantified using primers for *H2-Aa*, *H2-Ab1*, *Cd80*, *Cd86* and *Cd40*. For co-culture experiments, OVA- or OVAIC-stimulated murine BM neutrophils were incubated with OTII $CD4^+$ T cells in a 2:1 ratio for 48 hours prior to staining for flow cytometry to assess T cell activation.

For *in vivo* stimulation with systemic IC, OVAIC was generated *in vitro* as described above. OVA or OVAIC (5 µg OVA per mouse) was made up to a volume of 200 µl with PBS and injected intravenously via the tail vein into LysM-GFP mice, followed 1 hour later by popliteal LN intravital imaging or LN harvest for flow cytometry. For generation of local IC *in vivo*, rabbit anti-B-phycoerythrin (PE) antibody (2 mg, Rockland) was administered by intraperitoneal injection one day prior to imaging, and PE (15 µg, Invitrogen) administered by subcutaneous footpad (hock) injection at the start of the surgical preparation for intravital imaging, with PEIC forming in the imaged popliteal dLN (326).

3.6. Antibodies

Antibodies were purchased from BioLegend, eBioscience, R&D or Thermo Fisher for staining for flow cytometry, confocal microscopy or intravital microscopy. Anti-mouse and anti-human antibodies used in experiments are listed in Tables 3.1 and 3.2, respectively. For biotinylated primary antibodies, fluorophore-conjugated streptavidin was used for secondary staining.

Antibody	Clone	Conjugated fluorophore
B220	RA3-6B2	Pacific Blue, BV605, A647
CCR7	4B12	A488, PerCP.Cy5.5
CD11b	M1/70	Pacific Blue, FITC, BV605, PerCP.Cy5.5, APC
CD11c	N418	A488, PE.Cy7, A700
CD169	3D6.112	A647
CD25	PC61	PerCP.Cy5.5
CD3	OKT3	BV510, BV605, PE, A647
CD45	30-F11	BUV395, eFluor450
CD69	H1.2F3	BV785
CD8	53-6.7	BV785, PE.Cy7
CXCR4	2B11	PE
F4/80	BM8	FITC, eFluor660
FcεR1	MAR-1	PE.Cy7
GFP	Rabbit polyclonal	A488
Gr-1	RB6-8C5	Pacific Blue, PE.Cy7, A700
ICOS	C398.4A	PerCP.Cy5.5
IL-7Rα	A7R34	Biotin
KLRG1	3F12F2	PerCP.eFluor710
Live/dead	-	Aqua, A780
Ly6G	1A8	Pacific Blue, A647, A700, BV785
LYVE-1	223322	PE
MHCII	M5/114.15.2	Pacific Blue, BV650, A700
NK1.1	PK136	BUV395, PE.Cy7
PNAd	MECA-79	Biotin
Siglec-F	E50-2440	A647
Streptavidin	-	BV421, APC, A647
Ter119	Ly-76	PE.Cy7

Table 3.1. List of anti-mouse antibodies used.

Antibody	Clone	Conjugated fluorophore
CCR7	3D12	FITC, PE
CD11b	M1/70	BV421, Pacific Blue, BV605
CD15	HI98	eF450, FITC, BV650, A700
CD16	3G8	Pacific Blue, BV650, APC.eFluor780
CXCR4	12G5	FITC, PE
HLA-DR	L243	PB, PerCP.eFluor710
Live/dead	-	Aqua
LYVE-1	537028	APC
PNAd	MECA-79	PE

Table 3.2. List of anti-human antibodies used.

3.7. Flow cytometry

Single cell suspensions of isolated cells or organs (processed as described above) were given Fc block with 0.5% NMS for 20 minutes on ice prior to staining. Antibodies were used at 1:200 and cells were stained for 45 minutes on ice, then washed and stained with Live/dead stain at 1:333 for 15 minutes at room temperature. For antibody mixtures containing anti-CCR7, staining was instead performed for 30 minutes at room temperature, with Live/dead stain added in the last 15 minutes, in order to maximise staining of CCR7 which exhibits receptor recycling. After staining, cells were washed with cold PBS, and either fixed and kept on ice until analysis, or resuspended in PBS and analysed immediately to preserve GFP fluorescence on live cells. Data were acquired using LSRFortessa flow cytometer and FACSDiva software (BD Biosciences).

3.8. Confocal microscopy

Harvested LNs were fixed in 1% paraformaldehyde (PFA) overnight at 4°C, dehydrated in 30% sucrose for 8 to 10 hours at 4°C, and frozen in optimum cutting temperature (OCT) compound (VWR). Frozen LNs were cut to 30 to 50 µm sections in a cryotome. For staining, sections were first immersed in blocking buffer containing 0.1 M TRIS, 1% bovine serum albumin (Reagent diluent, R&D), 1% NMS and 0.3% Triton X-100 (Sigma-Aldrich) for 1 hour at room temperature to reduce non-specific antibody binding, then stained with

antibodies in blocking buffer overnight at 4°C in a humidified chamber. Antibodies were used at 1:50 for anti-Ly6G and 1:100 for others. Rabbit polyclonal anti-GFP-A488 was used to augment GFP fluorescence in fixed tissue sections. Slides were washed three times with PBS, and when primary biotin-conjugated antibody was used further staining with secondary streptavidin antibodies was performed for 30 minutes at room temperature in a humidified chamber. After further PBS washes microscopy coverslips were mounted with Vectashield mounting medium (Vector).

Confocal images were acquired using a Leica TCS SP8 microscope and 40x oil immersion objective, with optical sections under 2 μm, and the tiling function used in some cases to generate images of whole LN sections. With the use of commercially available antibodies with large Stokes shifts (the difference between excitation and emission wavelengths), such as the Brilliant Violet antibodies, tissue sections could be stained with five or six fluorophore-conjugated antibodies simultaneously for confocal imaging with four excitation laser lines, which in our set up were 405 nm, 488 nm, 561 nm and 633 nm lasers. This technique enabled multiple cell types to be imaged and analysed by standard confocal microscopy (327) .

3.8.1. Confocal quantification of neutrophil number and location

For each LN, 50 μm sections were generated, with five sections stained and tiled confocal images of whole sections taken. Neutrophils, with bright LysM-GFP fluorescence, were manually counted, and the average cell number in a 50-μm section multiplied by the total number of sections to calculate the number of neutrophils in the whole LN. The location of each neutrophil was determined manually to be within interstitium, within $PNAd^+$ HEVs or within $LYVE\text{-}1^+$ lymphatic vessels; if the neutrophil was partially within a vessel it was classified as within the vessel.

3.9. Helminth models for imaging ILC2s

Both *N. brasiliensis* larvae and *S. mansoni* eggs were provided by Dr Andrew McKenzie (Laboratory of Molecular Biology, Cambridge). For the *N. brasiliensis* model, live L3 *N. brasiliensis* larvae were injected subcutaneously into each mouse (300 to 500 live larvae in 200 μl PBS per mouse) on day 0. Intravital imaging of Peyer's patch and small bowel was performed on day 5, with confirmation of the presence of larvae in the small bowel by visual inspection of the bowel lumen after imaging. For the *S. mansoni* model, *S. mansoni* eggs were inactivated by UV irradiation and injected subcutaneously into the left hind footpad

(5000 eggs in 25 µl PBS per mouse), with PBS injected into the right hind footpad as control on day 0, and intravital imaging of both popliteal LNs performed on day 1 following footpad immunisation.

3.10. Intravital microscopy

Popliteal LNs and Peyer's patches were surgically exposed in anaesthetised mice. For some experiments, a combination of single- and two-photon excitation was used.

3.10.1. Surgical preparation

Each mouse was anaesthetised using inhaled isoflurane at approximately 2% for induction and 1-2% for maintenance via a vaporiser and driven through oxygen at a flow rate of 1 L/min. In some experiments, vessels were visualised by intravenous tail vein injection of Qtracker655 (10 to 20 µl, Life Technologies) to label blood vessels and subcutaneous hind footpad (hock) injection of anti-LYVE-1-PE antibody (5 µl) to label lymphatic vessels. In other experiments, the SCS was outlined by subcutaneous hind footpad (hock) injection of anti-CD169-A647 antibody (5 µl) to label SCS macrophages. Hair was removed from the skin of the imaged area (knee for popliteal LN, abdomen for small bowel) by shaving and application of depilatory cream.

The mouse was kept warm on an electric heat pad during the surgical dissection. For popliteal LN imaging, the mouse was placed prone and one leg secured into position on a custom-made imaging stage. Under a dissecting microscope, a skin window was made in the popliteal fossa; the popliteal LN, located lateral to the popliteal vein, was exposed by careful dissection of overlying structures whilst minimising bleeding. The exposed LN was kept moist with warm PBS, and a cover slip placed above to create a water seal (Figure 3.1). The mouse was then transferred to the imaging box, and popliteal LN imaging performed with the temperature in the imaging box maintained at 36°C.

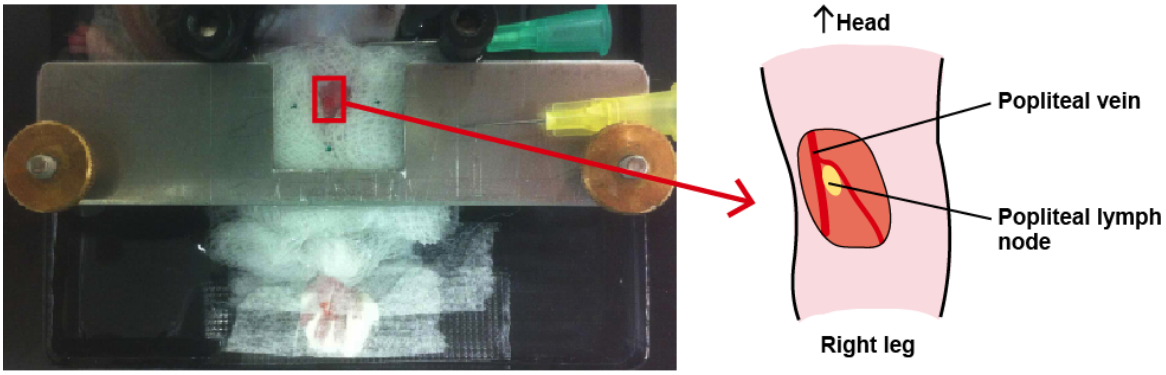

Figure 3.1. Intravital popliteal LN imaging. Photograph showing the setup for popliteal LN imaging with the mouse on a customised stage and the popliteal LN surgically exposed and secured under a cover slip. The anatomical landmarks used to identify the popliteal LN are shown in the diagram on the right.

For small bowel imaging, a small midline incision was made in the upper abdomen and the peritoneum was opened. The mouse was placed laterally on the imaging stage. A loop of small bowel containing Peyer's patch was carefully externalised to minimise trauma, kept moist with warm PBS and cover slip placed above to create a water seal. The mouse was then transferred to the imaging box for imaging of Peyer's patch and small bowel at 36°C throughout. With this set up the small bowel wall could be imaged without trauma from surgical incision of the small bowel.

3.10.2. Image acquisition

Two-photon imaging was performed with a Chameleon Vision-S tuneable (excitation wavelength range 690 nm to 1050 nm) Ti:Sapphire multiphoton laser attached to a Leica TCS SP8 microscope on a stabilising platform which minimised movement artefacts during imaging. A 25x water dipping objective was used, with optical sections 2 µm and one Z stack imaged every 40 seconds to acquire data for generation of time-lapse movies. For experiments investigating neutrophil trafficking, two doses of anti-PNAd blocking antibody were administered prior to imaging as detailed above (Section 3.3). Focal laser damage was achieved by two-photon excitation of a confined area of the LN at 860 nm and 90% laser power for 1 to 2 minutes, with subsequent autofluorescence of the damaged area confirming local tissue injury whilst allowing easy visualisation of neutrophil recruitment towards local laser damage.

For two-photon excitation at around 920 nm, the microscope detectors were set to fixed wavelengths to detect the following: GFP, 500/15 nm; YFP, 530/11 nm; collagen second harmonic generation, 460/50 nm; PE, 585/40 nm; Qtracker655, 675/55 nm. For experiments involving A647 or equivalent fluorophores, which would not be excited at the 920 nm wavelength, I used sequential excitation within each time frame, with two-photon excitation at 920 nm for GFP, collagen second harmonic generation, PE and Qtracker655, followed by single-photon excitation at 633 nm for A647; PE could also be excited with single-photon laser at 561 nm instead.

3.10.3. CD2/IL-13 double reporter imaging

The optimal two-photon excitation wavelengths for GFP and tomato are different, being around 920 nm for GFP and 1050 nm for tomato (328). For the intravital imaging of the CD2-GFP/IL-13-tomato double reporter mouse using two-photon excitation, this would have required sequential excitation and signal acquisition with repeated re-tuning of the multiphoton laser, which in our microscope equipment setup would result in significant delay. Instead, for intravital imaging I used simultaneous single-photon excitation with 488 nm (for GFP) and 561 nm (for tomato) excitation lasers. Although this had the potential disadvantages of less tissue penetration and more photo-bleaching, in reality I was able to obtain images of sufficient Z depth, for durations long enough for quantitative analysis of cellular dynamics without suffering significant photo-bleaching.

3.10.4. Id2/Rora/Rorc triple reporter imaging

The imaging strategy of the Id2/Rora/Rorc triple reporter, with the fluorophores BFP, teal and katushka respectively, required careful consideration. Teal was not a bright fluorophore, but a two-photon excitation wavelength of 920 nm resulted in adequate emission of teal, as well as collagen by second harmonic generation. BFP, however, required a shorter two-photon excitation wavelength, at which the signal from teal was significantly masked by macrophage autofluorescence. There was also overlap in the emission spectra of BFP and teal. Katushka required two-photon excitation wavelength at approximately 1100 nm, longer than the limit of our tuneable laser (314).

To avoid these issues, I used a strategy of sequential single- and two-photon excitation, and in combination with specific detector ranges I was able to achieve minimal signal overlap between fluorophores. This strategy also allowed for an additional fifth channel, either A647 detection with single-photon excitation (for example SCS macrophage labelling using anti-CD169-A647 antibody), or Qtracker655 detection with two-photon excitation (for labelling of

blood vessels). For consistency I used the same settings for all four- or five-channel imaging experiments with the triple reporter mouse (Table 3.3).

Fluorophore	Excitation (wavelength)	Detector range
Teal	Two-photon (920 nm)	500-550 nm
Collagen second harmonic generation	Two-photon (920 nm)	435-485 nm
Qtracker *	Two-photon (920 nm)	648-702 nm
BFP	Single-photon (405 nm)	410-485 nm
Katushka	Single-photon (516 nm)	565-630 nm
A647 *	Single-photon (633 nm)	650-750 nm

Table 3.3. Excitation and detection strategy for the imaging of triple reporter tissues. Microscope settings for sequential two-photon and single-photon imaging of multiple fluorophores. * Either Qtracker or A647 (not both) was acquired in combination with teal, collagen, BFP and katushka, resulting in five-colour images.

3.11. Image processing and data analysis

Intravital movies and confocal images were processed using Imaris software version 7.4 (Bitplane) and Fiji Image J (NIH). Non-specific background noise was filtered using the Gaussian filter function. For some confocal images the 'co-localisation' function was used to render surfaces with co-expression of two fluorophores. For intravital movies, cells were tracked using the 'surfaces' function, and cell tracks were visually checked and artefactual tracks manually corrected. Dynamic parameters including mean speed, maximum speed, track straightness, cell volume and cell surface area were generated for analysis. Time-lapse movies were recorded at 10 frames per second (fps), or at slower rates for some movies for clarity of presentation. *In vivo* cellular interactions were quantified by examining time-lapse movies and manually determining the durations of interactions.

For the data from the Id2/Rora/Rorc triple reporter, surfaces were generated for each of the $Id2^+$, $Rora^+$ and $Rorc^+$ cell populations, and dual- or triple-positive cells were manually identified and assigned new surfaces, including $Id2^+Rora^+$, $Id2^+Rora^+Rorc^+$ and $Rora^+Rorc^+$ cells.

Flow cytometry data were processed using FlowJo software version 10.0.8. Data were analysed using GraphPad Prism version 6. Statistical analysis was performed using unpaired t-tests or one-way ANOVA with Holm-Sidak correction for between-group multiple comparisons. $p < 0.05$ was considered to be statistically significant. All graphs are shown as mean ± SEM unless otherwise indicated.

Chapter 4. The role of lymph node neutrophils in homeostasis

4.1. Background

Neutrophils are traditionally considered early effectors of innate immunity, being circulating leukocytes with short half-lives that are rapidly recruited to inflamed tissues, responding to pathogenic stimuli by expressing multiple surface receptors that recognise PAMPs, DAMPs and antigen-antibody IC. In addition, neutrophils are increasingly recognised to exert influence on innate and adaptive immunity. Following local inflammatory or infectious stimuli, neutrophils can migrate to dLNs via both blood and lymphatic vessels, with the mechanism of entry involving molecules such as PNAd, CXCR4 and CD11b; neutrophils have also been shown to carry peripheral bacterial antigen via lymphatics to LNs (114,130,131). Within the LN, neutrophils can interact with other immune cells following inflammatory and infectious stimuli, such as with SCS macrophages to limit systemic pathogen spread, with DCs to influence antigen presentation, and with B and T lymphocytes to influence adaptive immunity directly, although studies have shown inconsistent results on the overall effects of these interactions on the adaptive immune response. Neutrophils themselves can present antigen to $CD4^+$ T cells via MHCII *in vitro* (161,167), and cross-present antigen to $CD8^+$ T cells via MHCI *in vivo* (181).

Beyond their roles in inflammation, the presence of neutrophils has also been demonstrated in a number of non-lymphoid tissues at baseline (210). Whilst there is limited evidence of neutrophils being present in LNs at baseline, there have not been detailed *in vivo* studies characterising the anatomical location, trafficking, cellular interactions and potential function of LN neutrophils in homeostatic conditions. Such data would provide evidence of broader functional remits of neutrophils in immune homeostasis, beyond their classical function of pathogen killing, and advance knowledge on the biological processes underlying many chronic inflammatory diseases where persistent neutrophilic inflammation is a feature.

Therefore I addressed the question of whether neutrophils traffick tonically into LNs under homeostatic conditions, expanding their routine patrol territory beyond the circulation, with the potential to influence adaptive immunity. For this I used techniques including confocal and intravital two-photon microscopy to examine the number and location of LN neutrophils at baseline, *in vivo* dynamics and interactions with other LN immune cells, the route and mechanism of trafficking into LNs, and the phenotype and potential function of neutrophils in LNs, such as delivery of systemic antigen to LNs.

4.2. Choice of reporter mouse and neutrophil isolation method

For studying LN neutrophils in homeostasis, I first used wild type (WT) C57BL/6 mice and identified neutrophils as $Ly6G^{+}CD11b^{+}$, using the neutrophil-specific 1A8 clone of anti-Ly6G antibody. Although neutrophils showed high Ly6G expression by flow cytometry, when used for confocal microscopy anti-Ly6G gave a weak signal and showed non-specific background staining, requiring co-staining with anti-CD11b for neutrophil identification. A transgenic reporter mouse with fluorescent neutrophils was also required for intravital imaging. For imaging studies, I therefore used the LysM-GFP mouse, commonly used as a neutrophil reporter (321). Examination of LysM-GFP tissues showed that whilst F4/80 macrophages were GFP-intermediate, the majority of GFP-high cells were $Ly6G^{+}CD11b^{+}$ neutrophils (Figure 4.1A,B); by microscopy these cells were also distinguishable by their differences in nuclear morphology and intensity of GFP fluorescence.

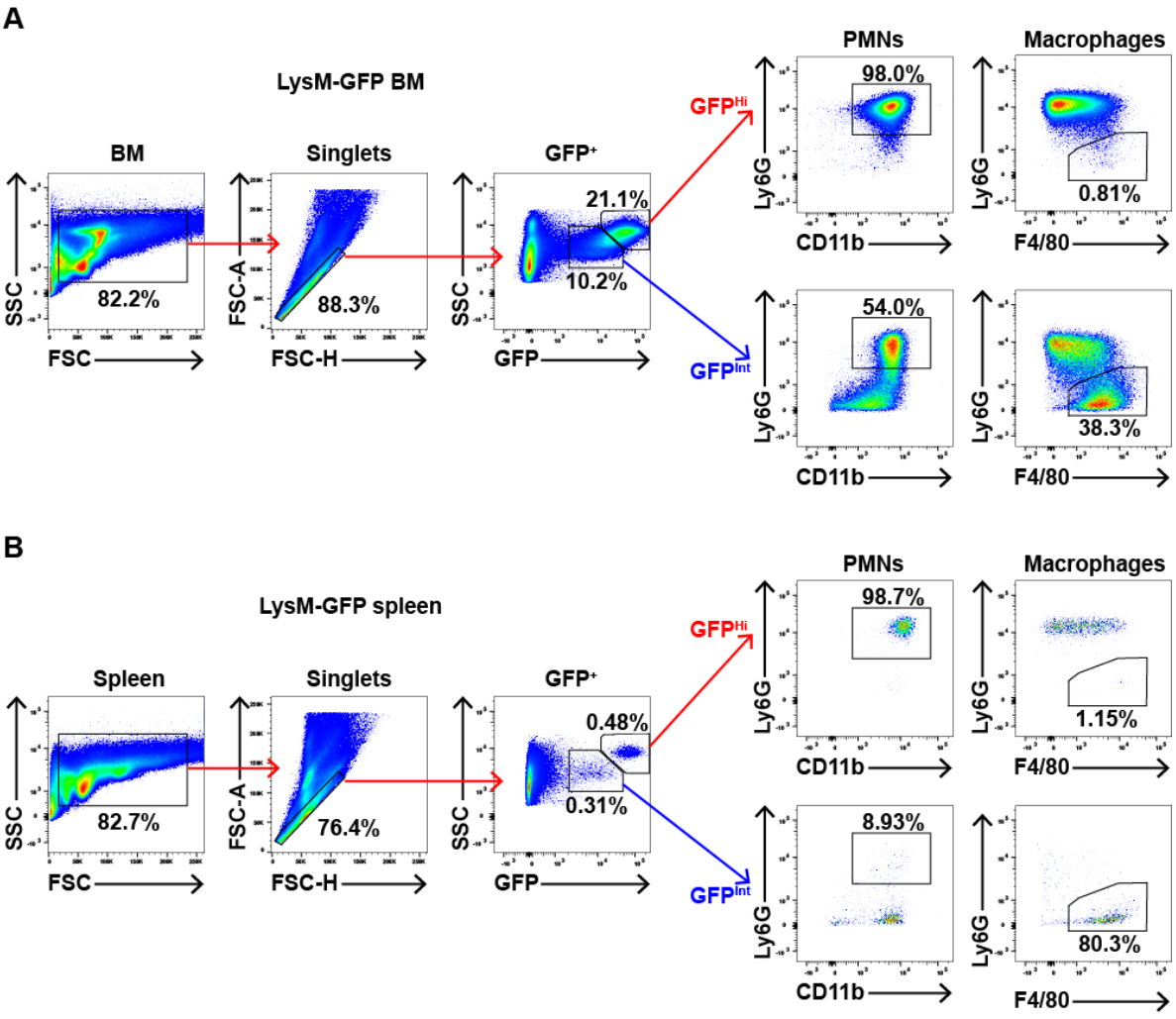

Figure 4.1. Specificity of LysM-GFP mouse for neutrophils in tissues. Flow cytometry plots showing proportions of neutrophils ($Ly6G^{+}CD11b^{+}$) and macrophages ($Ly6G^{-}F4/80^{+}$) in

GFP-high (GFP^{Hi}) and GFP-intermediate (GFP^{Int}) cell populations in (A) BM and (B) spleen of an unstimulated LysM-GFP mouse.

I established a method for murine neutrophil isolation, in order to assess neutrophil trafficking *in vivo* and to characterise the effects of inflammatory stimuli *ex vivo*. I made attempts to isolate murine neutrophils from peripheral blood, drawn via inferior vena caval or cardiac puncture, using magnetic negative selection, but cell yield was consistently low with a maximum of 400,000 neutrophils per mouse, insufficient for adoptive transfer for *in vivo* imaging. Murine BM neutrophils have been shown to be functionally similar to peripheral blood neutrophils, in degranulation and reactive oxygen species generation (329), and cell yields from BM isolation are much higher compared to that from peripheral blood (330). Therefore, for my experiments I proceeded to neutrophil isolation from BM.

Neutrophils were isolated from BM of donor mice using red cell lysis and magnetic bead negative selection, with an average yield of 7.1×10^6 neutrophils per mouse. Assessment of purity by light microscopy showed average of 80.2% morphologically mature neutrophils (with characteristic ring-shaped nuclei) and 14.7% immature neutrophils (Figure 4.2A). By comparison, isolation of human neutrophils from peripheral blood using red cell sedimentation and plasma-Percoll gradients (325,331) yielded an average purity of 95% neutrophils, with contaminants being eosinophils (3%), lymphocytes and red blood cells (Figure 4.2B).

By flow cytometry, for murine BM neutrophil isolation the average viability was 97.1%, and purity ($Ly6G^+CD11b^+$) was 92.9% (Figure 4.2C). When LysM-GFP BM was used, the purity was improved with an average of 96.8% of GFP^+ cells being $Ly6G^+$ (Figure 4.2D). In later murine neutrophil isolations, the red cell lysis step was omitted, reducing *ex vivo* exposure time without affecting purity post isolation.

The process of isolation did not result in inadvertent neutrophil activation, as demonstrated by the ability of isolated neutrophils to upregulate CD11b upon *ex vivo* OVAIC stimulation (Figure 4.2E). Therefore, neutrophils isolated from BM of WT unstimulated C57BL/6 and LysM-GFP mice were used for subsequent *ex vivo* stimulation, confocal microscopy and *in vivo* intravital imaging experiments.

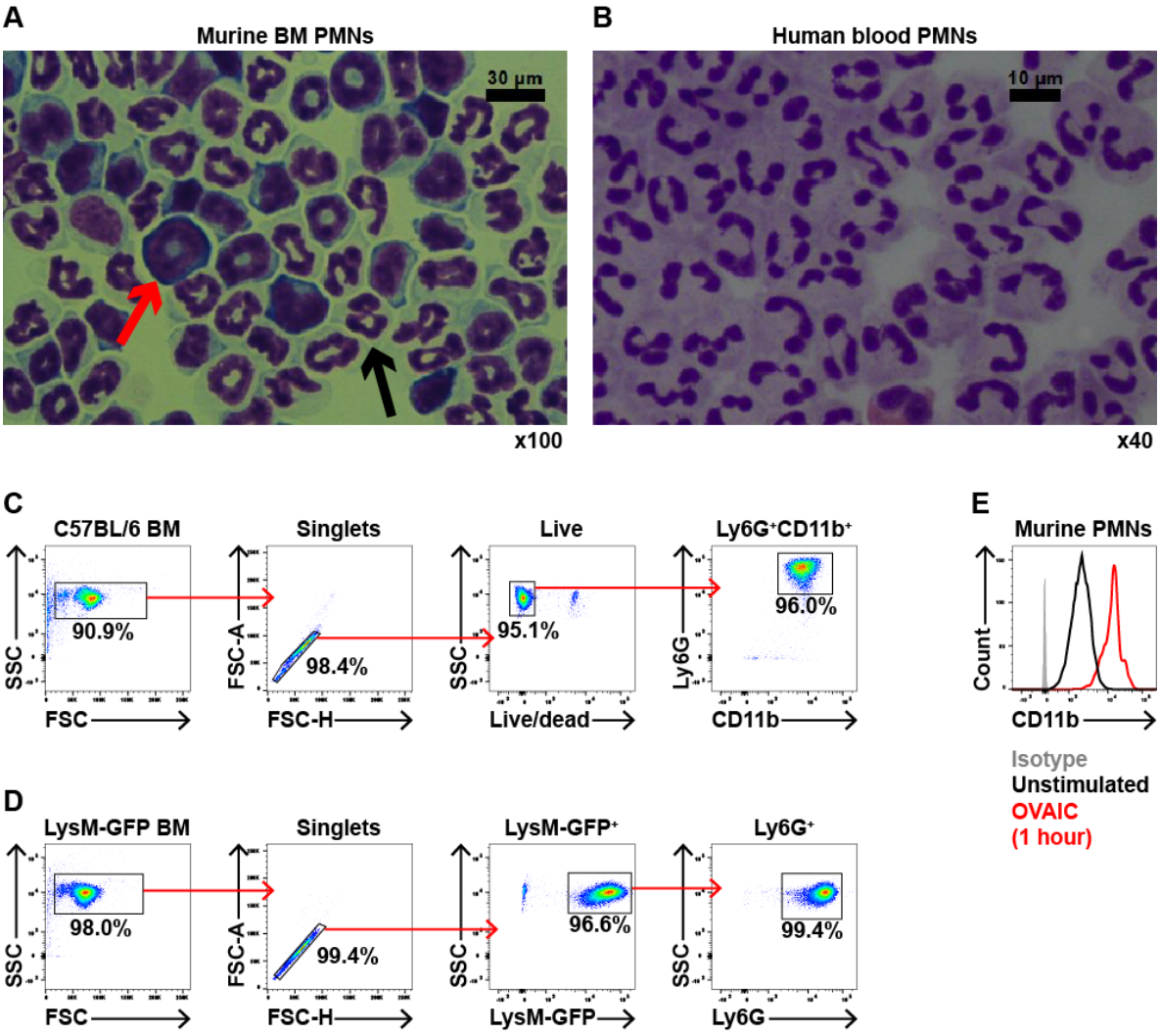

Figure 4.2. Neutrophil purity and activation status *ex vivo* following isolation. (A) Light microscopy image of murine BM neutrophils post isolation, with examples of immature (red arrow) and mature (black arrow) neutrophils; original magnification x100. (B) Light microscopy image of human peripheral blood neutrophils post isolation; original magnification x40. (C) Representative flow cytometry plots showing neutrophil purity post isolation from BM of C57BL/6 mouse. (D) Representative flow cytometry plots showing neutrophil purity post isolation from BM of LysM-GFP mouse. (E) Neutrophil activation as measured by CD11b expression of unstimulated and OVAIC-stimulated murine neutrophils post isolation.

4.3. Presence of neutrophils in unstimulated LNs

Firstly, I examined whether neutrophils were present in LNs under unstimulated, homeostatic conditions. I harvested wild type murine LNs from a number of anatomical sites including inguinal, popliteal, mesenteric, mediastinal and axillary LNs, using young (aged 8 to 10 weeks) female mice to avoid any confounding from skin injuries in male mice which are more

prone to fighting when co-housed. In all sampled LNs, small populations of live $Ly6G^{+}CD11b^{+}$ neutrophils were observed (Figure 4.3A,B), with the popliteal LN containing the fewest absolute number of cells due to its small size (Figure 4.3C). Circulating leukocytes were labelled with intravenous administration of CD45 antibody immediately prior to organ harvest; the majority of LN neutrophils were negative for anti-CD45, showing they were within tissues and not simply circulating within LN blood vessels (Figure 4.3D,E).

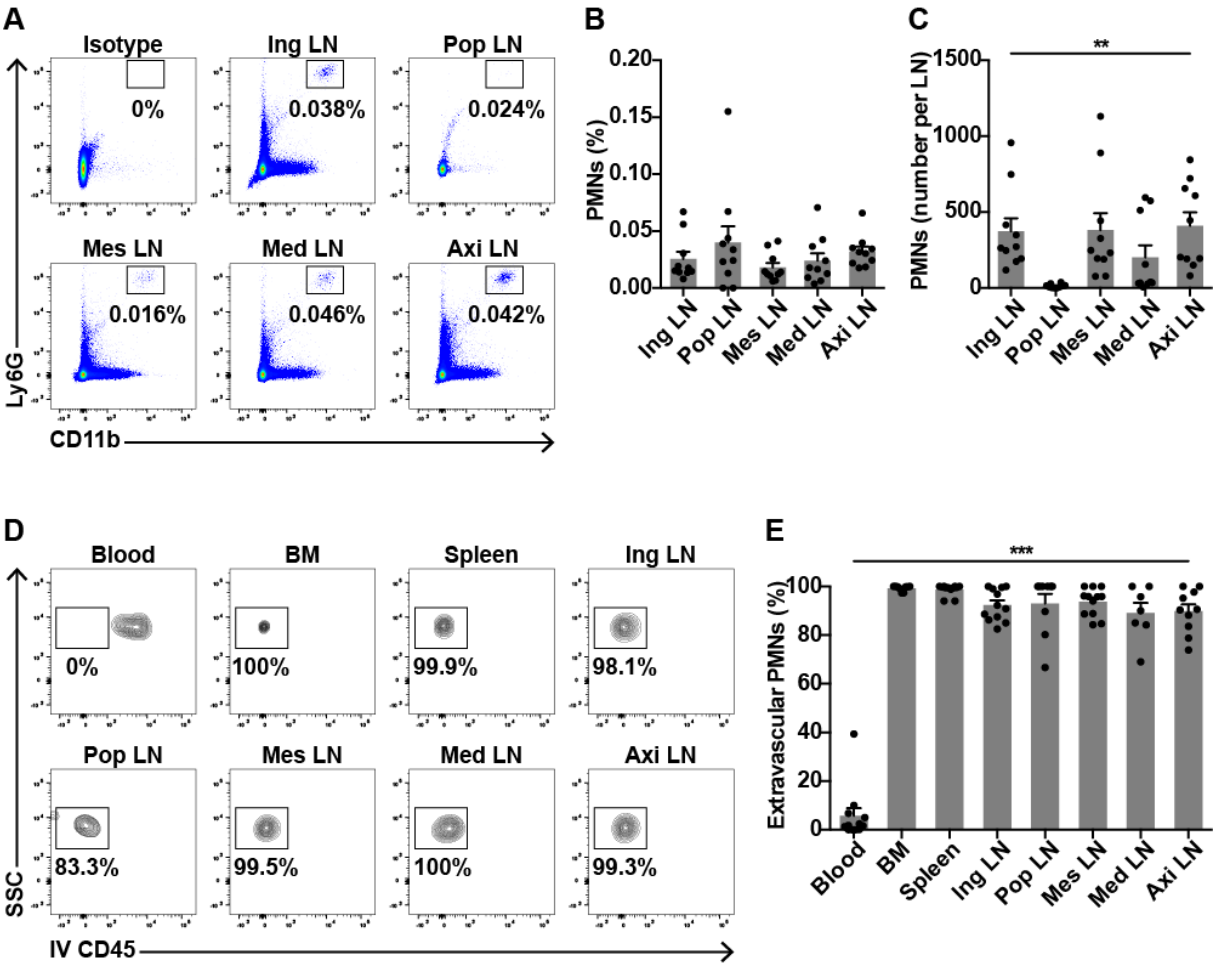

Figure 4.3. Neutrophils in unstimulated LNs as quantified by flow cytometry. (A-C) Flow cytometry quantification of neutrophil numbers in inguinal (ing), popliteal (pop), mesenteric (mes), mediastinal (med) and axillary (axi) LNs from unstimulated wild type mice, with (A) representative plots of neutrophils, (B) neutrophil numbers as % live cells, and (C) absolute neutrophil numbers per LN; $^{**}p < 0.01$ across groups. Data from 10 mice in 7 experiments. (D-E) Extravascular neutrophils quantified as % negative for intravenously injected anti-CD45, with (D) representative flow cytometry plots, and (E) quantification of extravascular neutrophils; $^{***}p < 0.001$ across groups. Data from 12 mice in 9 experiments.

Confocal microscopy of LN sections also showed neutrophils within LNs, distributed mainly in the periphery, and in the interfollicular and interlobar areas (Figure 4.4A). Confocal quantification showed that the true neutrophil numbers within LNs were over ten-fold higher than estimates by flow cytometry (Figure 4.4B). Mechanical dissociation for flow cytometry has been shown to underestimate tissue cell numbers in other organs (332). Together, these indicate the presence of neutrophils in unstimulated LNs under homeostatic conditions.

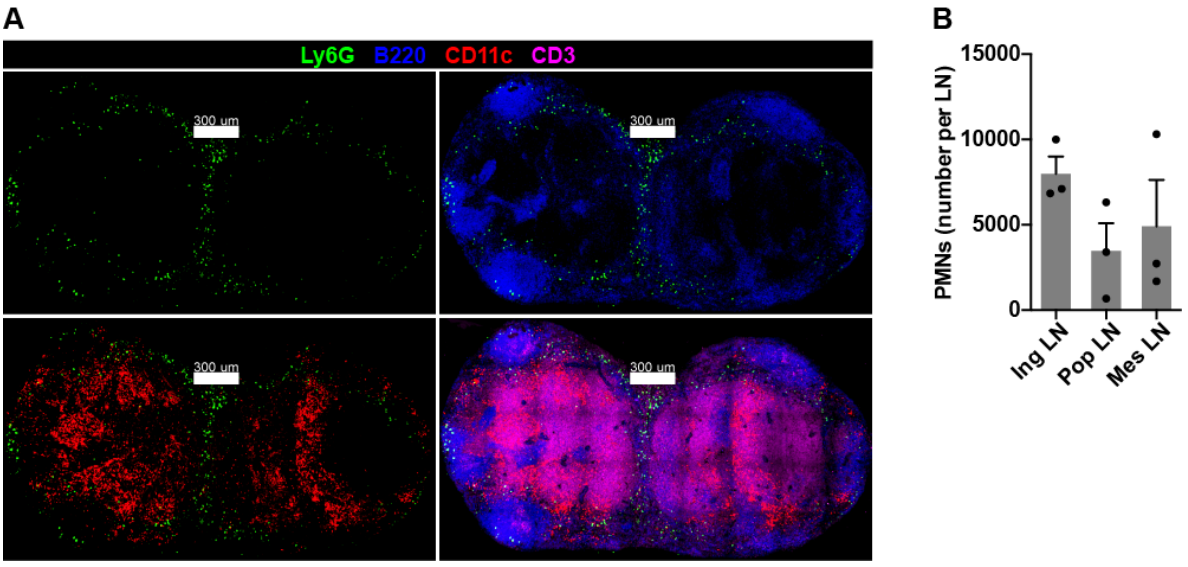

Figure 4.4. Neutrophils in unstimulated LNs as quantified by confocal microscopy. (A) Confocal image of whole inguinal LN section from unstimulated C56BL/6 mouse; scale bar 300 μm, Z stack 5 μm. (B) Confocal quantification of neutrophil numbers from unstimulated LNs. Data from 3 mice.

4.4. Location and dynamic behaviour of neutrophils within LNs

I next asked the question of whether LN neutrophils were present in blood and lymphatic vessels supplying the LN, or within the LN parenchyma. I examined the anatomical location of neutrophils by confocal microscopy of unstimulated LysM-GFP (neutrophils as GFP^+; Figure 4.5A) and C57BL/6 (neutrophils as $Ly6G^+CD11b^+$; Figure 4.5B) LNs. A small proportion of neutrophils were within HEVs and lymphatic vessels, labelled by PNAd and LYVE-1 respectively, but the majority (75-82%) of neutrophils were located within the LN interstitium, as quantified in LNs from different sites (Figure 4.5C). The presence of neutrophils within the lumen of both HEVs and lymphatic vessels suggests that they may traffick into LNs from both blood and peripheral tissues. Staining of WT C57BL/6 LN with anti-GFP antibody did not show non-specific background staining (Figure 4.6A), enabling the

use of anti-GFP to improve confocal detection of LysM. LN neutrophils were rarely found in B cell follicles, but were located predominantly in interfollicular zones and the floor of the SCS, in close proximity to T cells (Figure 4.7A), SCS macrophages (Figure 4.7B) and DCs (Figure 4.7C), placing them in positions for potential interactions with these LN immune cells.

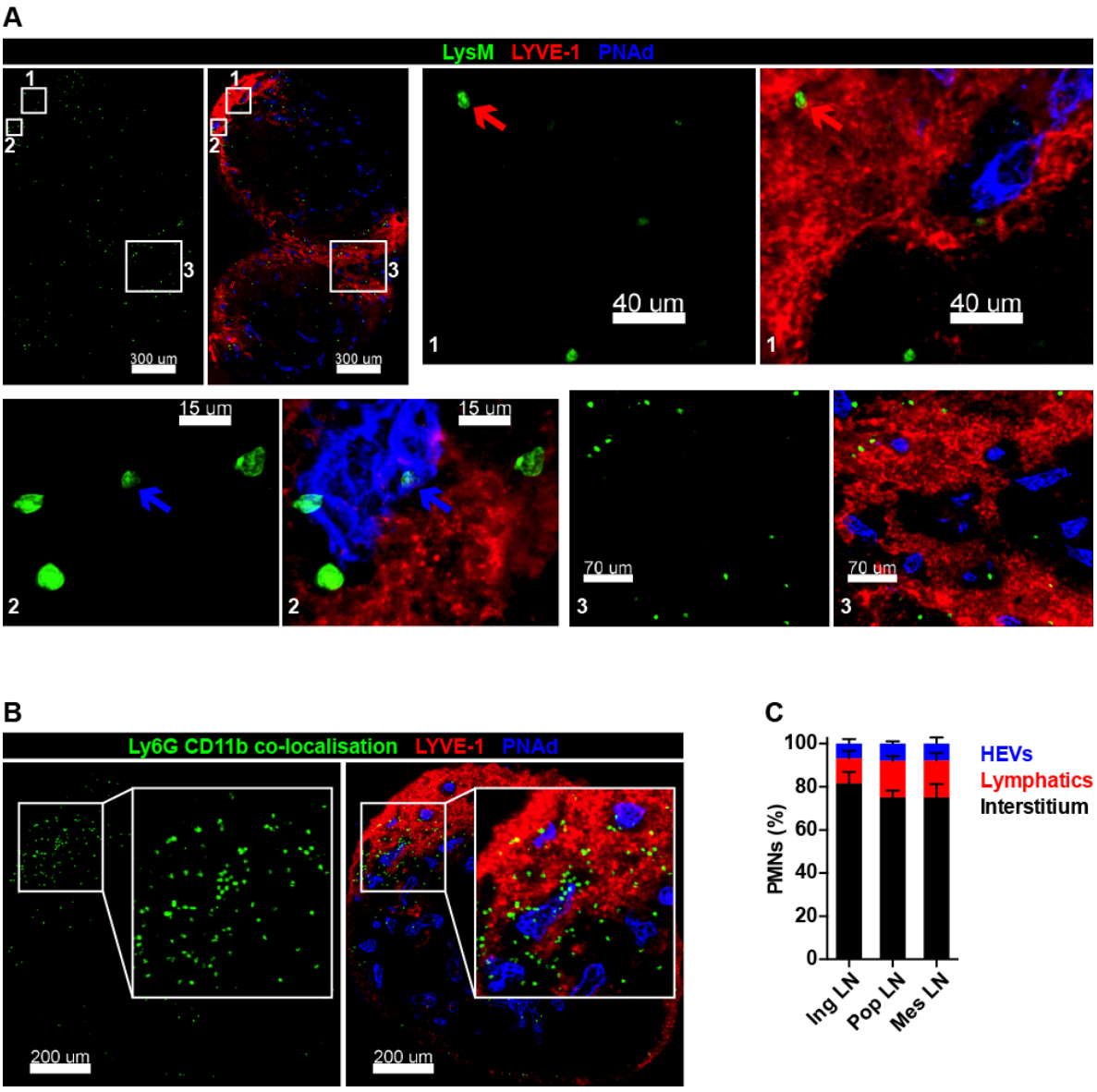

Figure 4.5. Location of LN neutrophils in relation to lymphatic and blood vessels. (A) Confocal image of inguinal LN from unstimulated LysM-GFP mouse, scale bar 300 μm, Z stack 10 μm; 3 boxed areas magnified, with red arrow showing a neutrophil within lymphatic vessel, and blue arrow a neutrophil within HEV. (B) Confocal image of popliteal LN from unstimulated C57BL/6 mouse showing neutrophils ($Ly6G^+CD11b^+$); scale bar 200 μm, Z stack 15 μm. (C) Confocal quantification of neutrophil location in relation to vessels within LNs. Data from 3 mice.

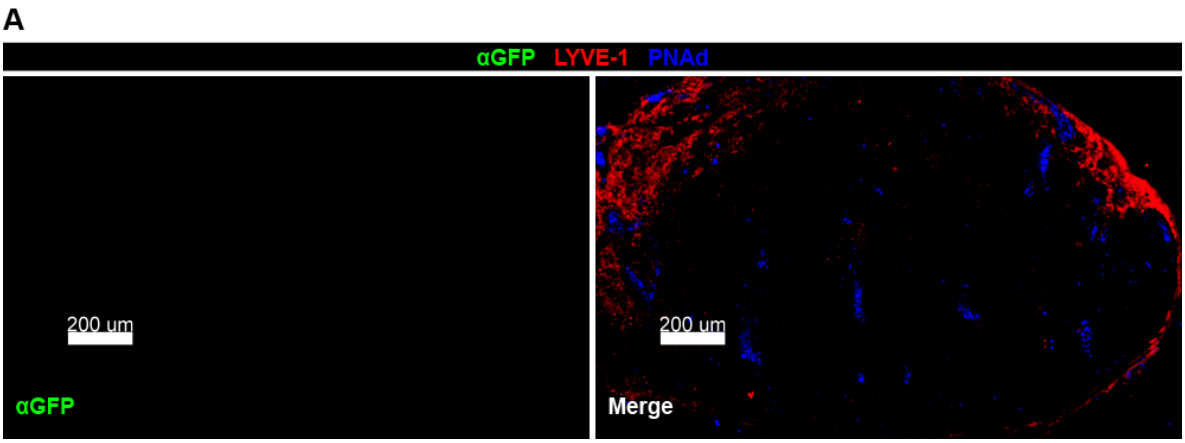

Figure 4.6. Absence of background non-specific staining with anti-GFP antibody. (A) Confocal image of mesenteric LN from WT C57BL/6 mouse stained with anti-GFP; scale bar 200 μm, Z stack 15 μm.

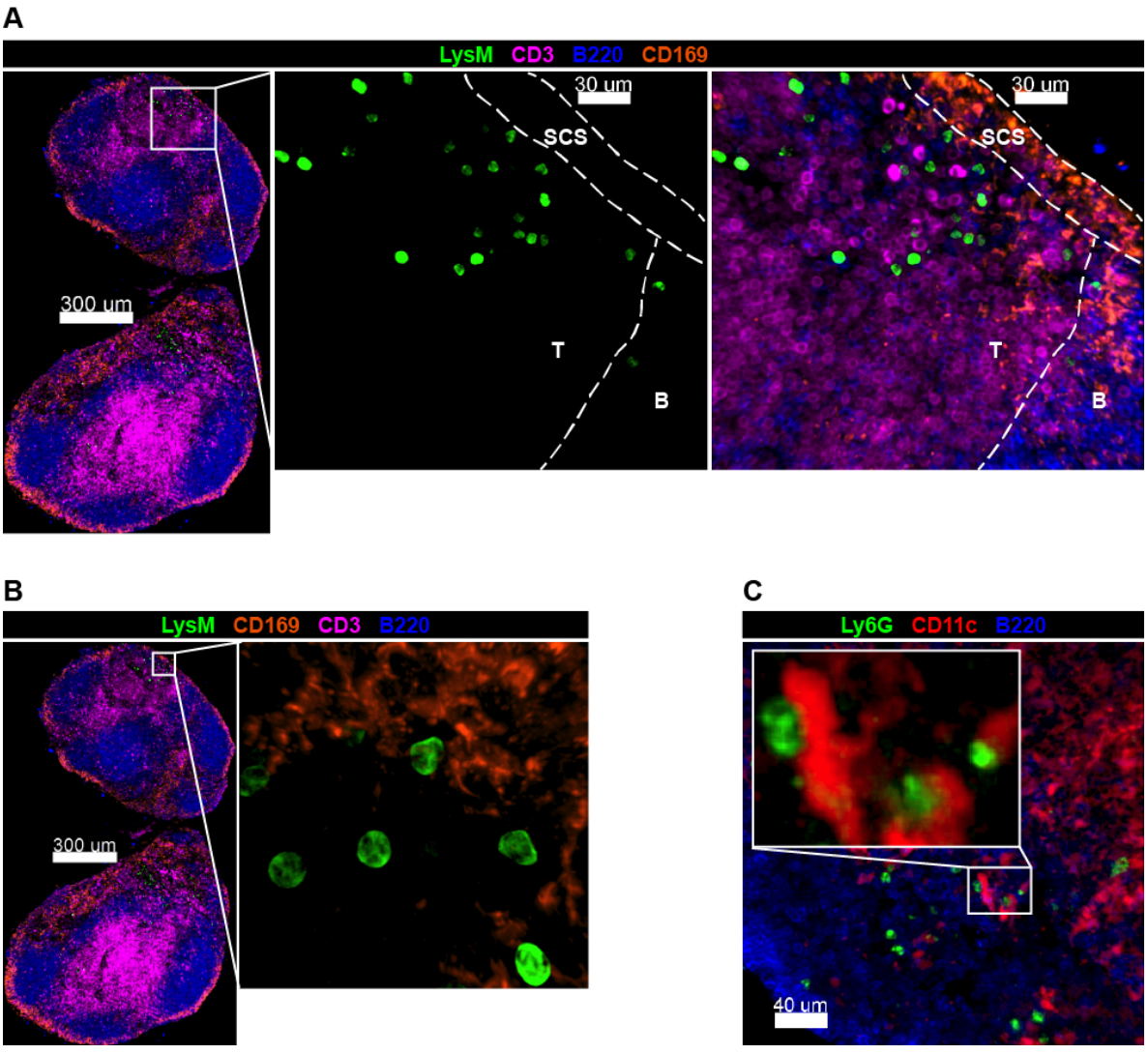

Figure 4.7. Anatomical location of neutrophils within LNs. (A) Confocal image of inguinal LN, scale bar 300 μm, Z stack 20 μm; magnified area annotated to show anatomical location of neutrophils in relation to B cell ($B220^+$) and T cell ($CD3^+$) areas. (B) Confocal image of inguinal LN, scale bar 300 μm, Z stack 20 μm; inset showing neutrophils in proximity to $CD169^+$ SCS macrophages. (C) Confocal image of inguinal LN, scale bar 40 μm, Z stack 11 μm; inset showing neutrophil co-localisation with $CD11c^+$ DCs.

The behaviour of LN neutrophils was examined *in vivo* by intravital two-photon imaging of popliteal LNs of LysM-GFP mice without prior infectious or inflammatory challenge. LN neutrophils were motile and showed random crawling (Figure 4.8A) at a mean speed of 5.8 μm/min (Figure 4.8B), similar to that of lymphocytes within LNs (28,333).

4.5. Trafficking of circulating neutrophils into LNs

Given the presence of neutrophils in HEVs, I sought to determine whether neutrophils tonically traffick into LNs from the circulation. GFP^+ neutrophils were isolated from donor BM and transferred intravenously into C56BL/6 mice, and recipient LNs were subsequently examined by intravital imaging. At 24 hours post transfer, neutrophils were present in the SCS and cortex of LNs (Figure 4.8C) crawling at a mean speed of 6.5 μm/min (Figure 4.8D), similar to that of native neutrophils.

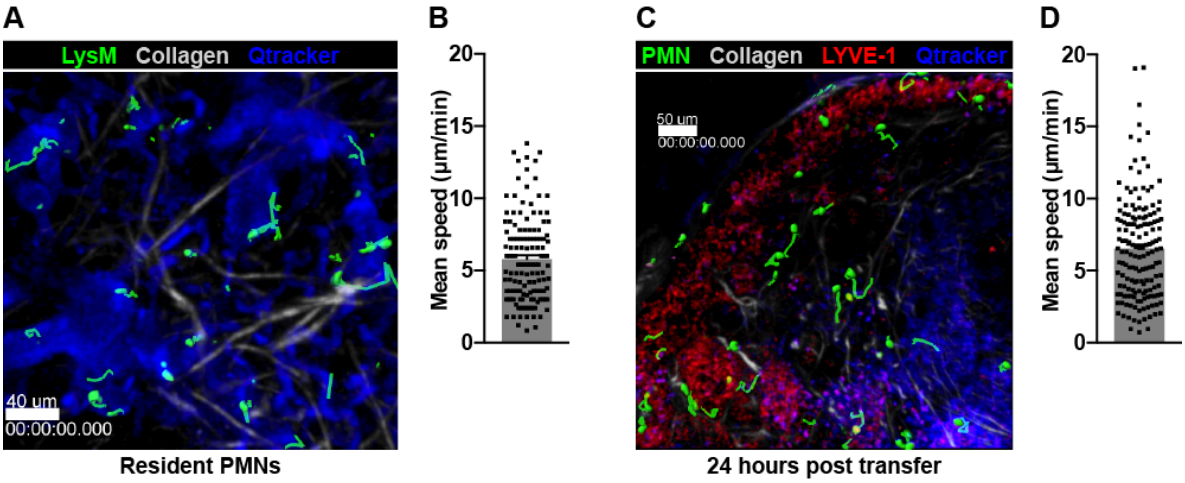

Figure 4.8. Dynamic behaviour of native and transferred neutrophils in LNs *in vivo*. (A) Intravital two-photon image of unstimulated LysM-GFP popliteal LN, movements shown in green tracks; scale bar 40 μm, Z stack 60 μm. (B) Mean speed of neutrophil movement

within LN; pooled data from 4 movies, with each dot representing one cell track. (C) Intravital image of C57BL/6 popliteal LN 24 hours following intravenous transfer of LysM-GFP neutrophils, movements shown in green tracks; scale bar 50 μm, Z stack 80 μm. (D) Mean speed of transferred neutrophil movement within LN; pooled data from 3 movies, with each dot representing one cell track.

Surprisingly, given the dogma that neutrophils are short-lived cells, at 4 to 5 days post intravenous transfer motile GFP$^+$ cells were still observed within LNs (Figure 4.9A); confocal microscopy of LNs 7 days post transfer confirmed these GFP$^+$ cells were still present, and co-staining with Gr-1 showed they were intact neutrophils rather than efferocytosed neutrophils fragments (Figure 4.9B). Although these neutrophils were isolated from BM and may therefore be less mature, these data challenge the current dogma that neutrophils exiting the BM only survive for a matter of hours.

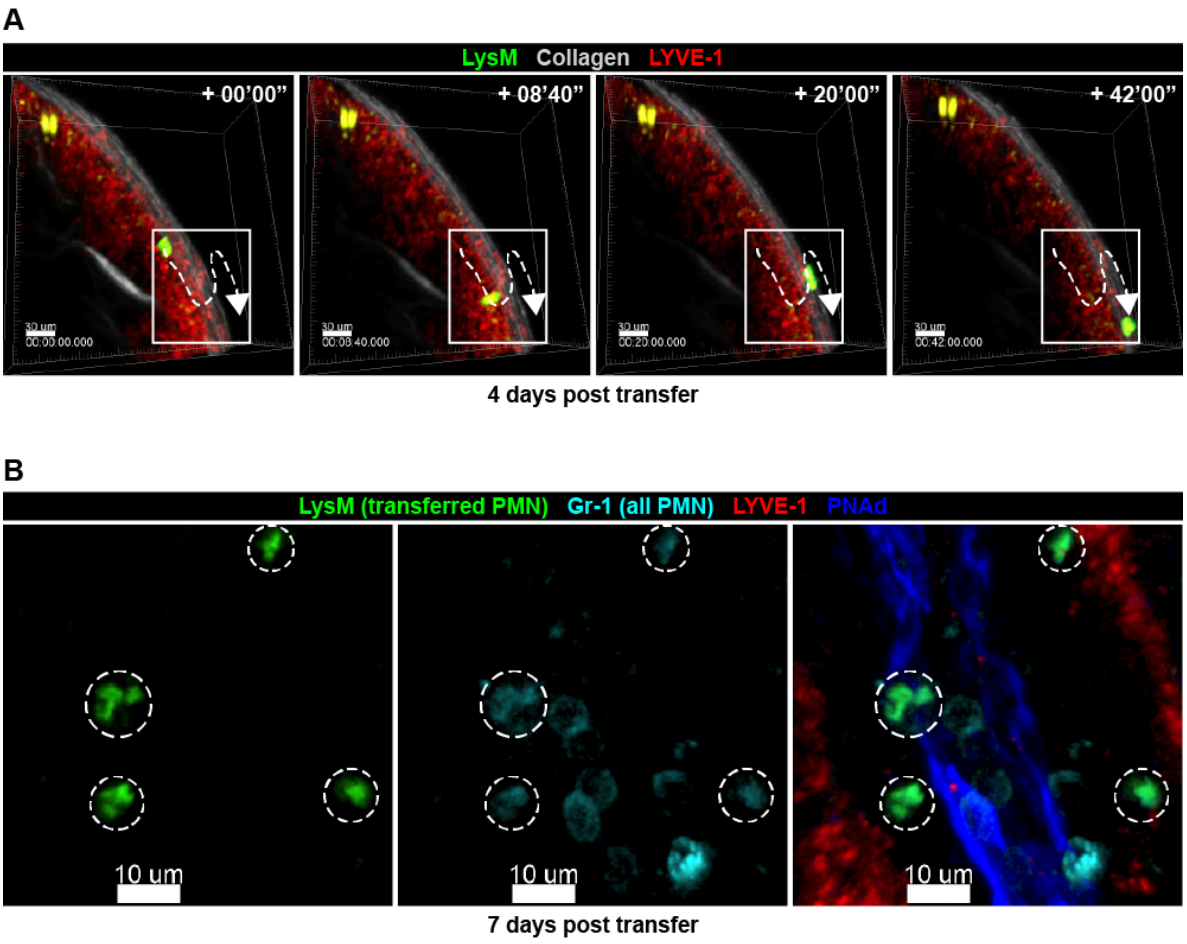

Figure 4.9. Presence of transferred neutrophils in LNs. (A) Intravital image of popliteal LN of C57BL/6 mouse 4 days following intravenous LysM-GFP neutrophil transfer, cell

movement in white dotted track; scale bar 30 μm, Z stack 80 μm. (B) Confocal image of mesenteric LN of C57BL/6 mouse 7 days following intravenous LysM-GFP neutrophil transfer stained with anti-Gr-1, showing transferred ($LysM^{+}Gr\text{-}1^{+}$) and native ($LysM^{-}Gr\text{-}1^{+}$) neutrophils; scale bar 10 μm, Z stack 18 μm.

Using *in vivo* administrations of subcutaneous anti-LYVE-1 and intravenous Qtracker to label lymphatic and blood vessels respectively, intravenously transferred neutrophils were observed by intravital imaging to traffick into LNs via both lymphatic vessels (Figure 4.10A) and HEVs (Figure 4.10B), with GFP^{+} cells seen to emerge from labelled vessels. Within the LN, some of these neutrophils were observed to crawl along collagen fibres, visible via second harmonic generation, over prolonged periods (Figure 4.11A).

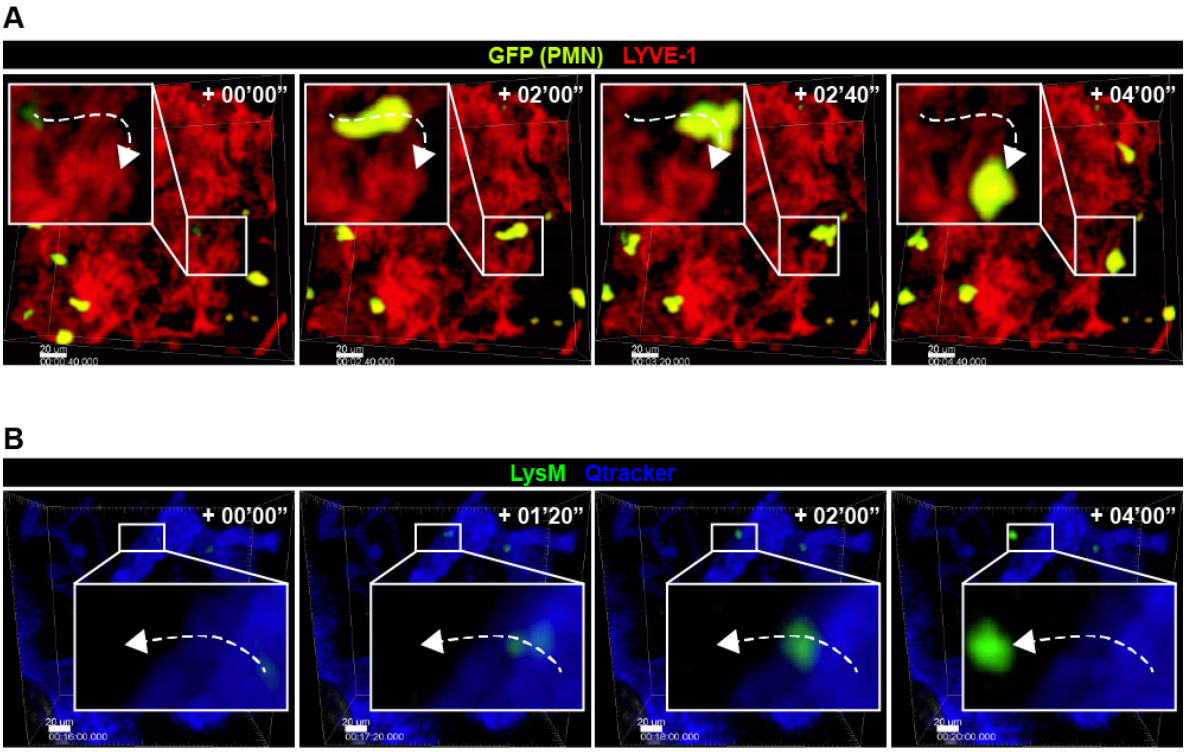

Figure 4.10. Trafficking of circulating neutrophils into LNs *in vivo*. (A) Example by intravital imaging of intravenously transferred neutrophil trafficking from lymphatic vessel into popliteal LN, cell track in dotted white line; scale bar 20 μm, Z stack 60 μm. (B) Example by intravital imaging of intravenously transferred neutrophil trafficking from HEV into popliteal LN, cell track in dotted white line; scale bar 20 μm, Z stack 90 μm.

A

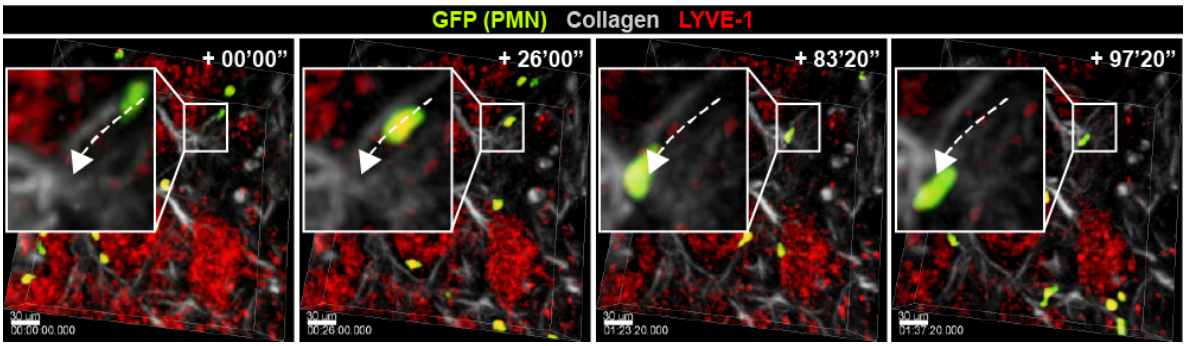

Figure 4.11. Movement of neutrophils along collagen fibres within LNs *in vivo*. (A) Example by intravital imaging of transferred neutrophil crawling along collagen fibre within the popliteal LN, cell track in dotted white line; scale bar 30 μm, Z stack 80 μm.

4.6. Presence of neutrophils in human LNs

Compared to murine neutrophils, human neutrophils are the most abundant white cell type in blood and have longer circulating half-lives (60–63,65,334). I therefore investigated whether neutrophils were also present in human LNs. Whole intact inguinal, mesenteric and thoracic LNs were obtained from human organ donors and mechanically disaggregated for immediate assessment by flow cytometry. The characteristics of the organ donors are summarised in Table 4.1 below, with a mean age of 52 years (range 10 to 78 years), 64% being male, and the majority of donors having suffered fatal intracranial injury.

Small populations of neutrophils, identified as live $CD15^+CD16^+$ cells by flow cytometry, were identified in all LNs studied (Figure 4.12A). The relative neutrophil numbers in human LNs from different sites were not statistically different (Figure 4.12B), but higher compared to those in murine LNs. Confocal imaging of LN sections using CD15 as a neutrophil marker confirmed that these cells were located mainly within the LN interstitium, near $LYVE\text{-}1^+$ lymphatic vessels (Figure 4.12C) and $PNAd^+$ HEVs (Figure 4.12D). Therefore, similar to murine LNs, human LNs also contained neutrophils that were mostly located within the LN tissue.

Age	Sex	Donor	Cause of death	Known infections	Co-morbidities
69	F	DBD	Intracranial haemorrhage	None	Hypercholesterolaemia
71	M	DBD	Intracranial haemorrhage	None	Hypertension, ischaemic heart disease, asthma
63	M	DCD	Intracranial haemorrhage	None	High alcohol intake
30	M	DBD	Cerebral oedema	Cerebral abscess	Diabetes
76	M	DBD	Intracranial haemorrhage	None	None
77	M	DCD	Subdural haematoma post RTC	Fever of unknown source	Diabetes, peripheral vascular disease, hypertension, depression
27	F	DBD	RTC	None	None
23	M	DCD	Hypoxic brain injury post RTC	None	None
10	F	DBD	Glioma with intracranial hypertension	None	Crohn's disease
22	M	DCD	Cardiac arrest post heroin overdose	Possible aspiration pneumonia	None
64	M	DCD	Acute respiratory distress syndrome	Bacteraemia	Diabetes
59	M	DCD	Hypoxic brain injury	None	None
78	F	DBD	Intracranial haemorrhage	None	Hypertension
52	F	DBD	Intracranial haemorrhage	Lobar pneumonia	Psoriasis

Table 4.1. Summary of human organ donor characteristics. Data from 13 spleen, 2 blood, 5 inguinal LN, 9 mesenteric LN and 11 thoracic LN samples from a total of 14 donors. Age in years. M, male; F, female; DBD, donation after brainstem death; DCD, donation after circulatory death; RTC, road traffic collision.

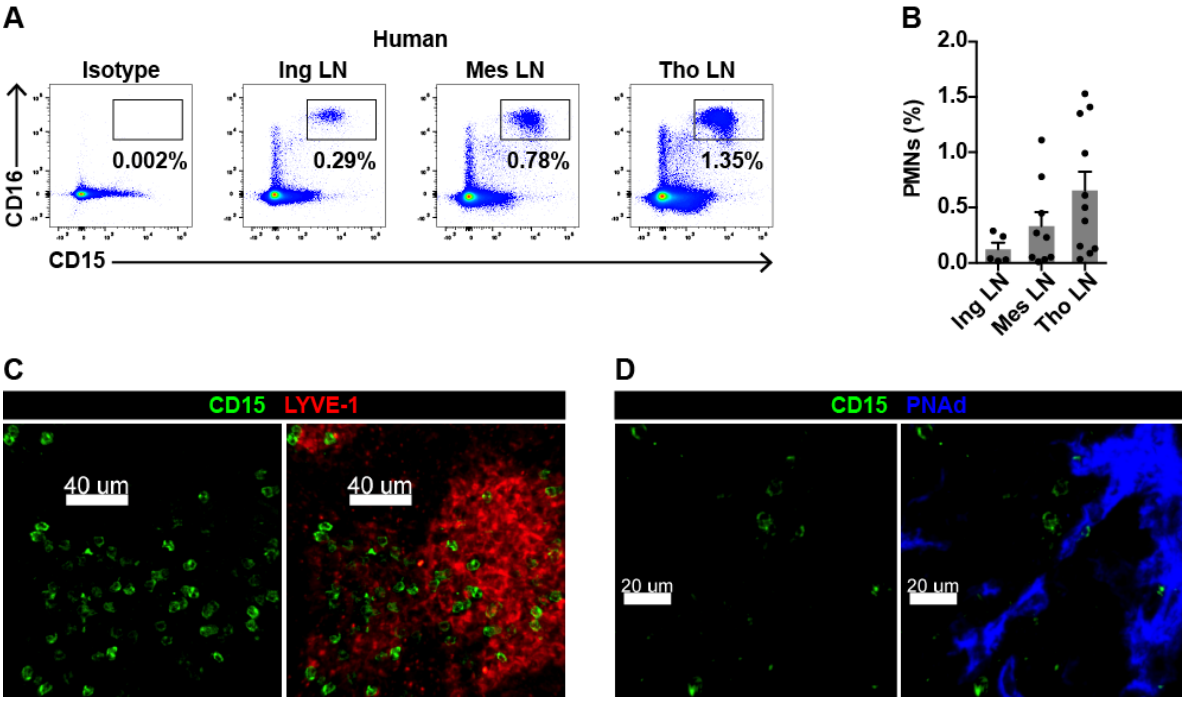

Figure 4.12. Presence of neutrophils in human LNs. (A-B) Flow cytometry quantification of neutrophils in human inguinal (ing), mesenteric (mes) and thoracic (tho) LNs with (A) representative plots and (B) neutrophil numbers as % live cells. Data for from 5 inguinal LN, 9 mesenteric LN and 11 thoracic LN samples from a total of 14 human organ donors. (C) Confocal image of mesenteric LN showing neutrophils ($CD15^+$) near lymphatic vessels; scale bar 40 μm, Z stack 12 μm. (D) Confocal image of thoracic LN showing neutrophils near HEVs; scale bar 20 μm, Z stack 18 μm.

4.7. Mechanism of neutrophil entry into LNs

Neutrophils have been shown to be recruited to LNs following *S. aureus* challenge via HEVs in a L-selectin / PNAd-dependent manner (130). I established a laser damage model of local sterile inflammation, which resulted in immediate neutrophil recruitment, and observed a reduction in neutrophil recruitment in mice given systemic anti-PNAd blockade prior to imaging (Figure 4.13A). Quantification of the mean number of neutrophils recruited per field of view showed a significant but incomplete reduction (13.2 control *vs* 4.8 anti-PNAd, $^{**}p < 0.01$) follow laser damage. There was also a trend towards reduction in neutrophil recruitment at baseline (5.4 control *vs* 1.7 anti-PNAd) (Figure 4.13B). These data showed that circulating neutrophils trafficked into LNs via both blood and lymphatic vessels in homeostasis and during sterile inflammation, in a process partially dependent on PNAd.

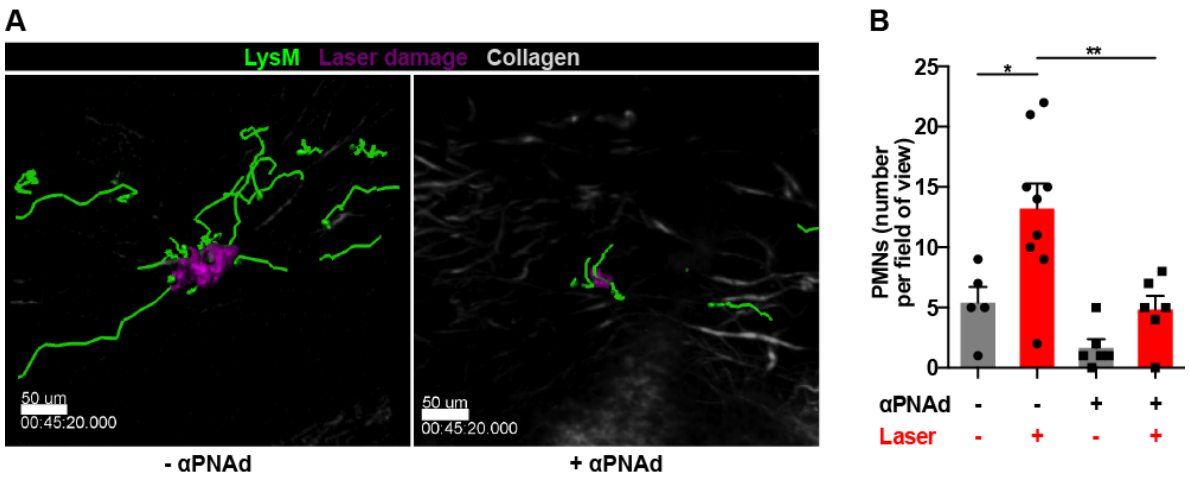

Figure 4.13. Effect of PNAd blockade on neutrophil trafficking into LN. (A) Intravital images of transferred neutrophils showing recruitment (green cell tracks) following local laser damage, without PNAd blockade (left panel) and with PNAd blockade (right panel); scale bar 50 μm, Z stack 70 μm. (B) Quantification of neutrophil numbers per field of view, before (grey bars) and after (red bars) laser damage; *$p < 0.05$ control *vs* laser, **$p < 0.01$ laser *vs* laser + anti-PNAd. Each dot represents one movie, with 5-9 movies from 3 independent experiments for each condition.

CD11b / Mac-1 and CXCR4 have been shown to be involved in neutrophil recruitment to LNs, via lymphatics following *S. auerus* challenge (114), and via both lymphatics and HEVs following OVA challenge in OVA/CFA-sensitised mice (131). I therefore examined the baseline surface expression of CD11b and CXCR4 on neutrophils from LNs, spleen, blood and (in mice) BM. Neutrophil CD11b expression did not differ between these tissues in humans (Figure 4.14A,B) or unchallenged mice (Figure 4.14C,D). CXCR4 was expressed in some human LN neutrophils, but this was not statistically different from blood neutrophils (Figure 4.15A,B). In unchallenged mice, CXCR4 expression on LN neutrophils from several sites was significantly higher compared to that on blood neutrophils (Figure 4.15C,D).

Previous studies have shown CCR7 to be involved in neutrophil migration to LNs following peripheral CFA stimulation (131,133), but not following peripheral *S. aureus* challenge (114,130). I examined neutrophil surface CCR7 expression in murine and human LNs, but I was unable to demonstrate CCR7 expression on blood or LN neutrophils at baseline. This could, however, have been due to receptor internalisation following ligand binding during entry into LNs resulting in lack of surface expression on LN neutrophils.

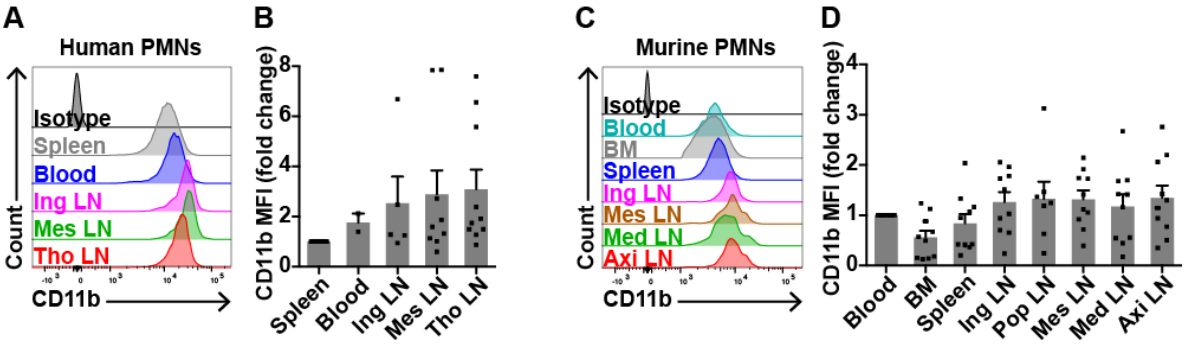

Figure 4.14. CD11b expression on human and murine LN neutrophils. (A-B) CD11b expression on human spleen, blood and LN neutrophils with (A) representative plots and (B) quantification of CD11b MFI on neutrophils. Data from 13 spleen, 2 blood, 5 inguinal LN, 9 mesenteric LN and 11 thoracic LN samples from a total of 14 donors. (C-D) CD11b expression on murine blood, BM, spleen and LN neutrophils from unstimulated mice with (C) representative plots and (D) quantification of CD11b MFI on neutrophils. Data from 6 unstimulated mice in 5 experiments.

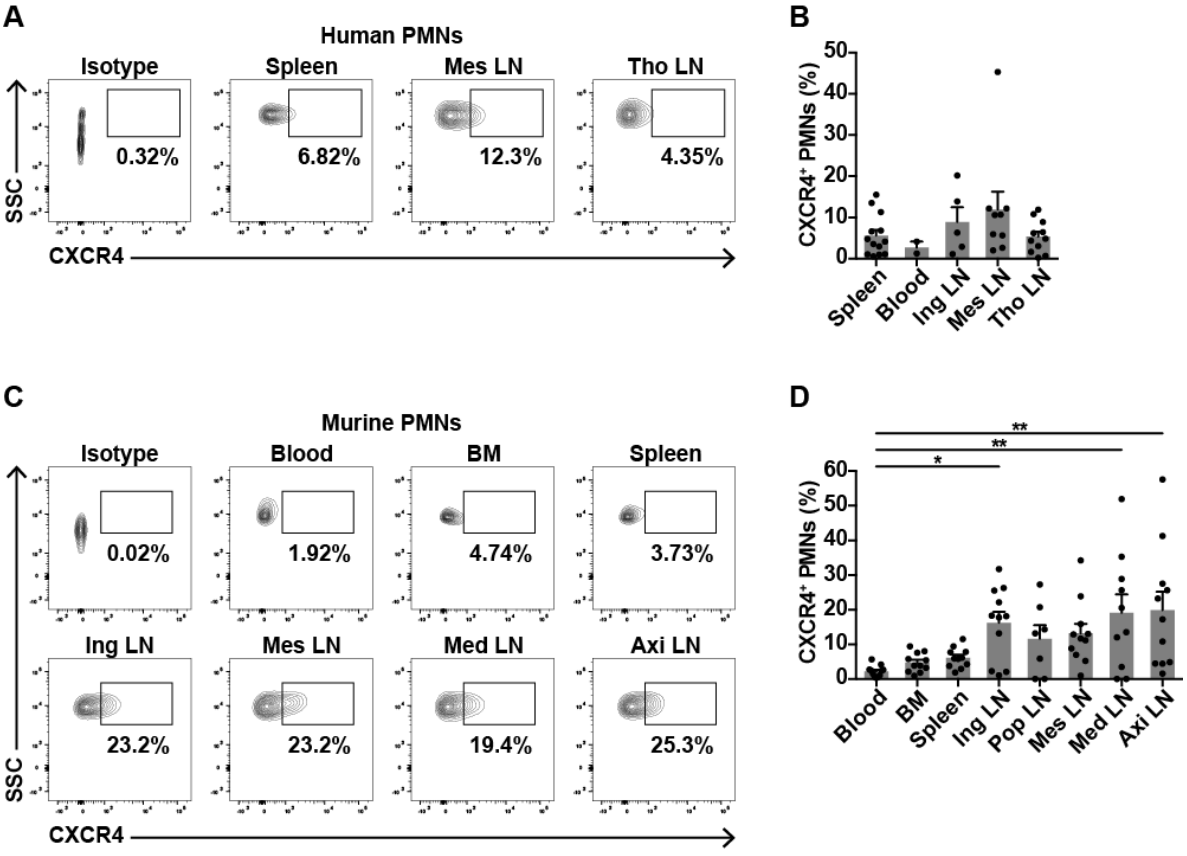

Figure 4.15. CXCR4 expression on human and murine LN neutrophils. (A-B) CXCR4 expression on human LN neutrophils with (A) representative plots and (B) quantification of % CXCR4-high neutrophils. Data from 13 spleen, 2 blood, 5 inguinal LN, 9 mesenteric LN and

11 thoracic LN samples from a total of 14 donors. (C-D) CXCR4 expression on murine blood, BM, spleen and LN neutrophils from unstimulated mice with (C) representative plots and (D) quantification of % CXCR4-high neutrophils; *$p < 0.05$, **$p < 0.01$ *vs* blood. Data from 6 unstimulated mice in 5 experiments.

4.8. Neutrophil phenotype

Having quantified the presence of neutrophils in LNs from unstimulated mice and humans, and examined their route and mechanism of trafficking into LNs at baseline and following inflammation, I next investigated the potential function of these LN neutrophils. As stimulated neutrophils have previously been shown to upregulate MHCII expression and present antigen to $CD4^+$ T cells (167), I examined MHCII expression on LN neutrophils at baseline.

4.8.1. Neutrophil MHCII expression in LNs and following *ex vivo* stimulation

Neutrophils from human LNs expressed variable levels of MHCII, with up to 50% MHC^+ neutrophils in some donors (Figure 4.16A,B). Neutrophils from unchallenged murine LNs showed significantly higher levels of surface MHCII expression compared to blood neutrophils (Figure 4.16C,D). These data showed that LN neutrophils expressed MHCII in the homeostatic state and could, therefore, potentially be capable of antigen presentation to $CD4^+$ T cells.

To characterise the stimuli that induced neutrophil MHCII expression, human blood neutrophils were isolated and challenged *ex vivo* with a variety of immunologically relevant stimuli, including ATP (a DAMP), LPS (a TLR4 agonist from Gram-negative bacteria), heat-killed *S. pneumoniae* (a TLR2 agonist and Gram-positive bacteria), opsonised heat-killed *S. pneumoniae* (TLR2 agonist and FcγR crosslinking), and OVAIC (IgG IC, FcγR crosslinking). To avoid cell death from longer durations of stimulation, isolated neutrophils were stimulated *ex vivo* for 1 hour, resulting in minimal cell death (Figure 4.17A), significant upregulation of CD11b with OVAIC indicating neutrophil activation (Figure 4.17B,C), and high phagocytic rates of opsonised bacteria and OVAIC (Figure 4.17D,E). OVAIC stimulation resulted in significant upregulation of MHCII expression on human neutrophils (Figure 4.17F,G).

Isolated murine BM neutrophils were also incubated *ex vivo* for 1 hour with the same stimuli. This resulted in reduced survival of cells stimulated with opsonised *S. pneumoniae* (90.8%) compared to unstimulated cells (Figure 4.18A). Compared to human blood neutrophils, opsonised *S. pneumoniae* and OVAIC stimulation resulted in neutrophil activation, as

evidenced by significant upregulation of CD11b (Figure 4.18B,C), despite opsonised *S. pneumoniae* not being well phagocytosed (Figure 4.18D,E). There was no increase in surface MHCII expression with any stimuli after 1 hour of *ex vivo* stimulation (Figure 4.18F,G). Extending the incubation period to 2 hours, OVAIC stimulation resulted in the upregulation in mRNA expression of the MHCII gene (*H2-Aa*, *H2-Ab1*), as well as the co-stimulatory molecules *Cd80*, *Cd86* and *Cd40* (Figure 4.19A). Therefore, these *ex vivo* stimulation experiments demonstrated that OVAIC activated both human blood and murine BM neutrophils, resulting in increased neutrophil expression of MHCII as well as the co-stimulatory molecules CD80, CD86 and CD40.

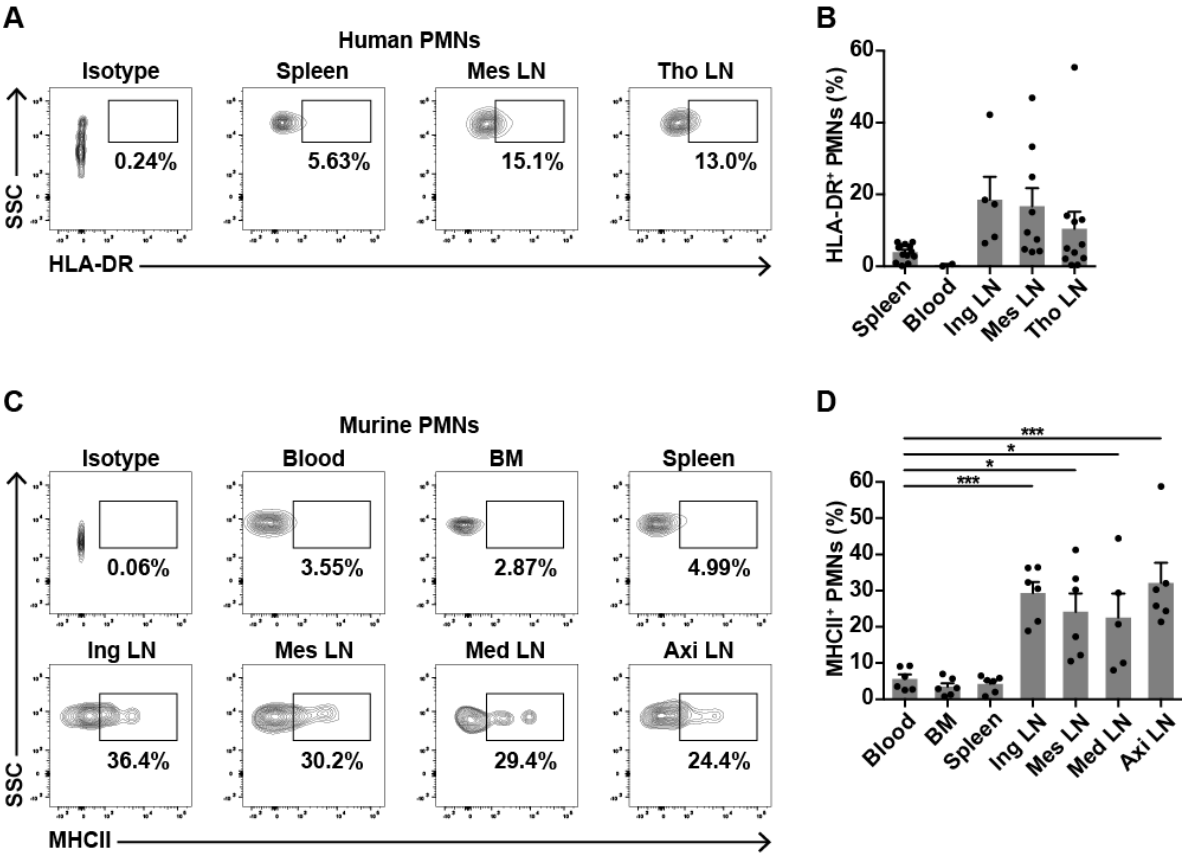

Figure 4.16. MHCII expression on human and murine LN neutrophils. (A-B) MHCII expression on human LN neutrophils with (A) representative plots and (B) quantification of % MHCII-high neutrophils. Data from 13 spleen, 2 blood, 5 inguinal LN, 9 mesenteric LN and 11 thoracic LN samples from a total of 14 donors. (C-D) MHCII expression on murine blood, BM, spleen and LN neutrophils from unstimulated mice with (C) representative plots and (D) quantification of % MHCII-high neutrophils; *$p < 0.05$, ***$p < 0.001$ *vs* blood. Data from 6 unstimulated mice in 5 experiments.

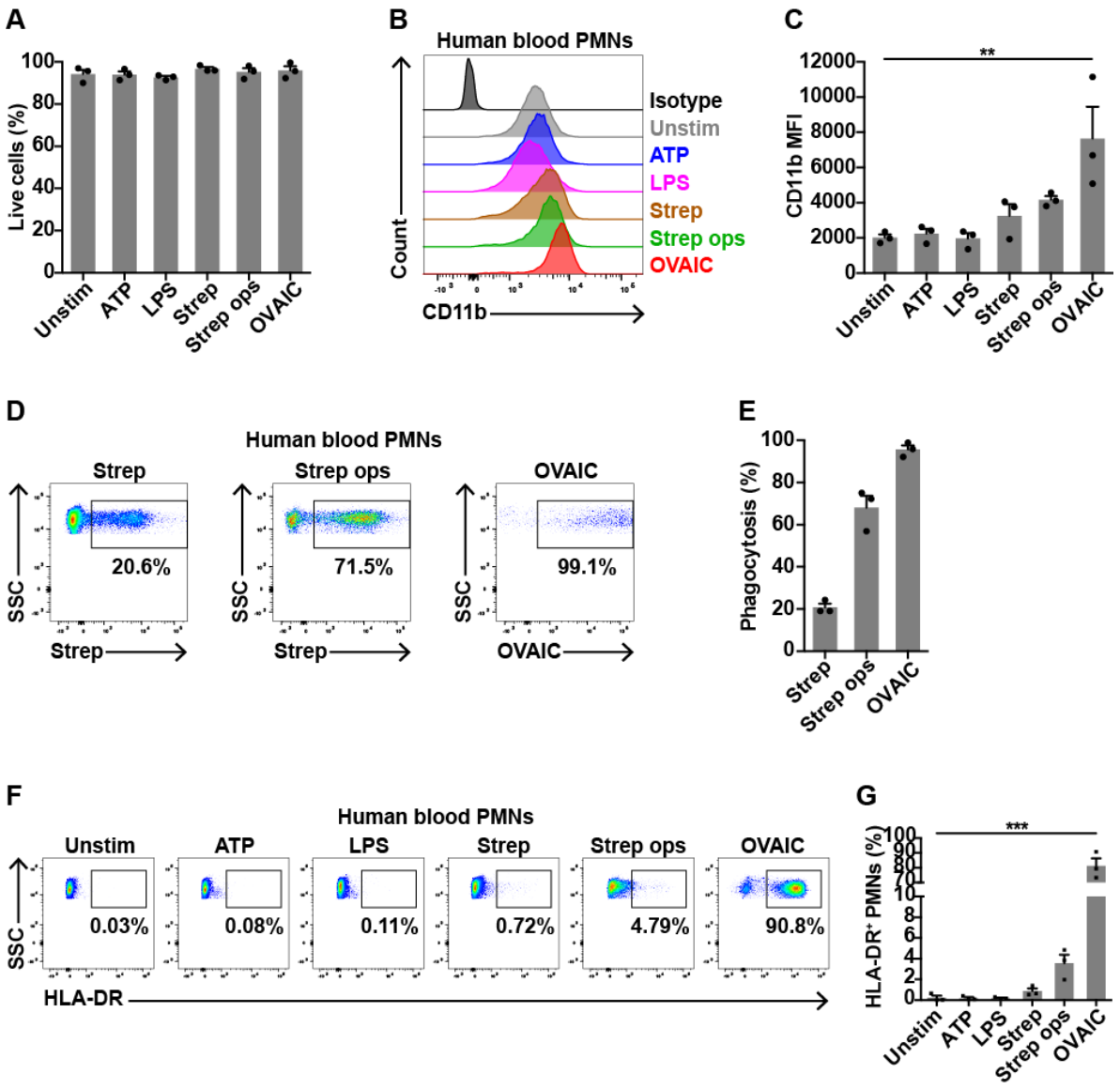

Figure 4.17. MHCII surface expression on human blood neutrophils following stimulation *ex vivo*. Human blood neutrophils were isolated and stimulated *ex vivo* for 1 hour with ATP, LPS, unopsonised *S. pneumoniae* (Strep), opsonised *S. pneumoniae* (Strep ops) or OVAIC, followed by surface staining for flow cytometry. (A) Cell survival as % live neutrophils post stimulation. (B-C) Neutrophil activation as measured by CD11b expression, with (B) representative plots and (C) quantification of CD11b MFI; $^{**}p < 0.01$ OVAIC *vs* unstimulated. (D-E) Neutrophil phagocytosis of Strep, Strep ops and OVAIC, with (D) representative plots and (E) quantification of % phagocytosis. (F-G) Neutrophil MHCII expression post stimulation, with (F) representative plots and (G) quantification of % MHCII-high neutrophils; $^{***}p < 0.001$ OVAIC *vs* unstimulated. Data from 3 donors in 3 experiments performed in triplicate.

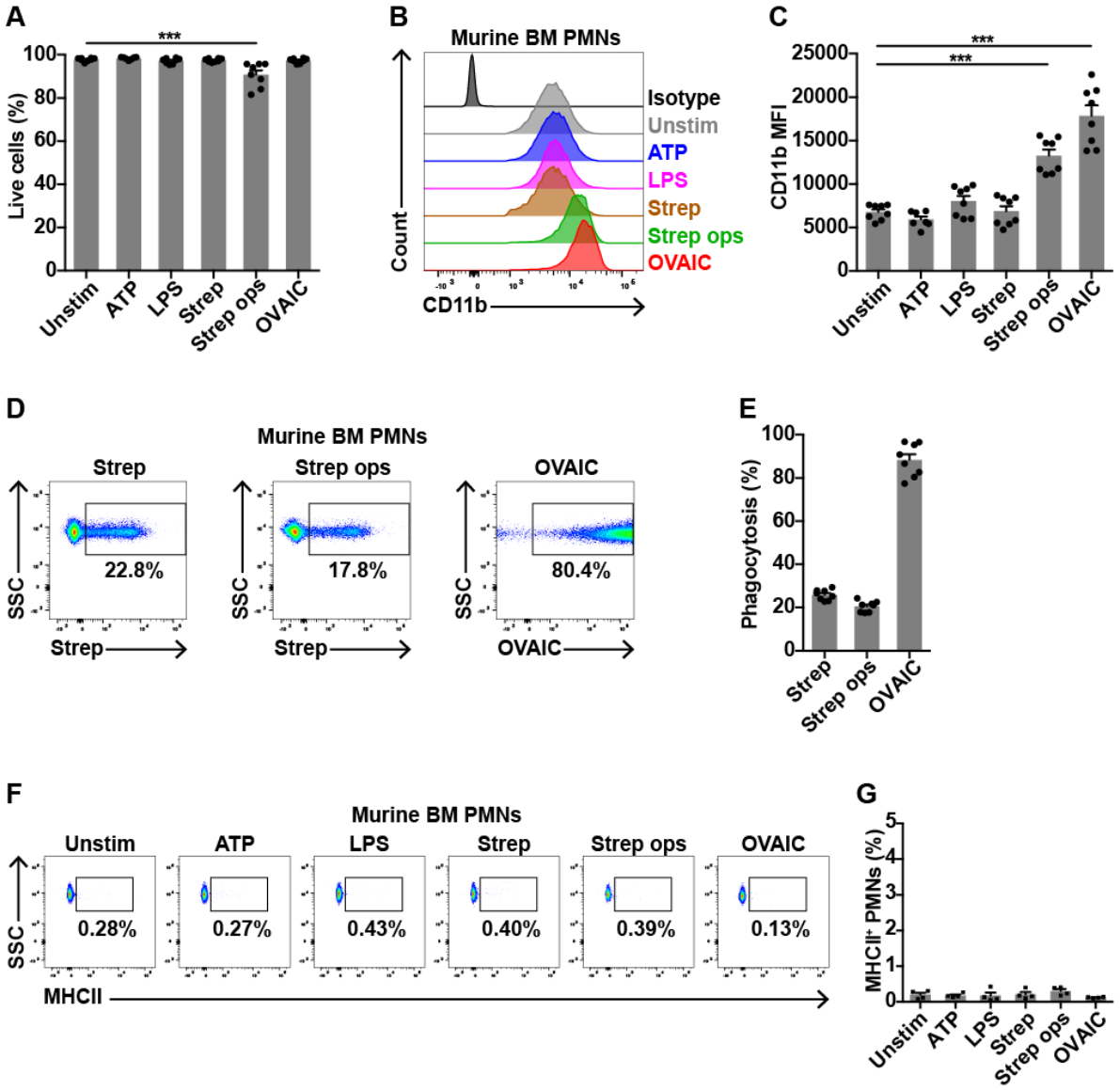

Figure 4.18. MHCII surface expression on murine BM neutrophils following stimulation *ex vivo*. Murine BM neutrophils were isolated and stimulated *ex vivo* for 1 hour with ATP, LPS, unopsonised *S. pneumoniae* (Strep), opsonised *S. pneumoniae* (Strep ops) or OVAIC, followed by surface staining for flow cytometry. (A) Cell survival as % live neutrophils post stimulation; ***$p < 0.001$ Strep ops *vs* unstimulated. (B-C) Neutrophil activation as measured by CD11b expression, with (B) representative plots and (C) quantification of CD11b MFI; ***$p < 0.001$ Strep ops / OVAIC *vs* unstimulated. (D-E) Neutrophil phagocytosis of Strep, Strep ops and OVAIC, with (D) representative plots and (E) quantification of % phagocytosis. (F-G) Neutrophil MHCII expression post stimulation, with (F) representative plots and (G) quantification of % MHCII-high neutrophils. Data from 8 mice in 2 independent experiments.

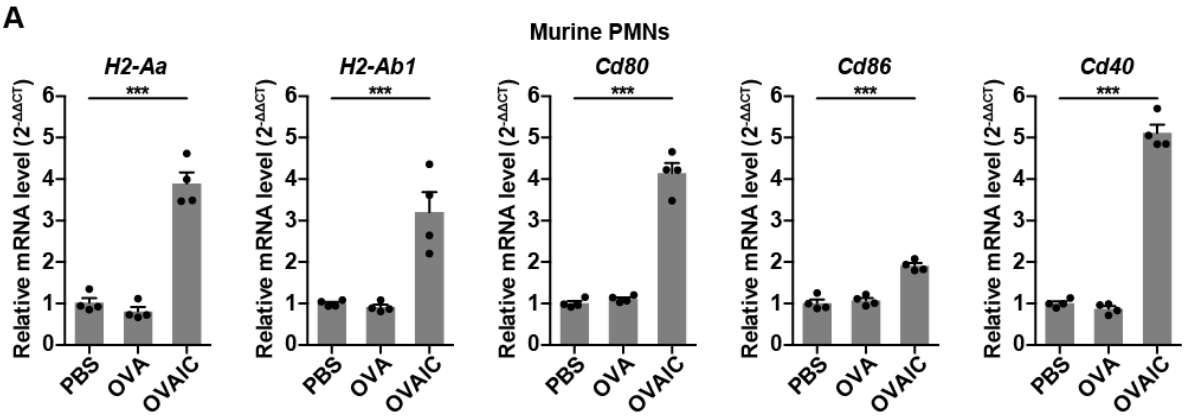

Figure 4.19. mRNA expression of MHCII and co-stimulatory molecules in murine BM neutrophils following stimulation *ex vivo*. (A) *H2-Aa*, *H2-Ab1*, *Cd80*, *Cd86* and *Cd40* mRNA expression, relative to *Gapdh* ($2^{-\Delta\Delta CT}$), in isolated murine BM neutrophils by RT-PCR following 2 hours of *ex vivo* stimulation with OVA or OVAIC; ***$p < 0.001$ OVAIC *vs* PBS. 1 of 2 experiments shown, each dot representing a triplicate.

4.8.2. Neutrophil CXCR4 and CCR7 expression following *ex vivo* stimulation

As murine LN neutrophils expressed higher CXCR4 as well as MHCII compared to neutrophils in other tissues at baseline, and OVAIC stimulates neutrophil MHCII expression *ex vivo*, I next investigated whether OVAIC increased CXCR4 expression on neutrophils. *Ex vivo* stimulation with OVAIC did not increase surface CXCR4 expression in human or murine neutrophils. In murine neutrophils, however, CXCR4 expression was increased following stimulation with unopsonised but not opsonised *S. pneumoniae*, potentially suggesting an inhibitory effect of FcγR crosslinking on the response to TLR2 stimulation (Figure 4.20A-D).

I also examined the expression of CCR7 on neutrophils following *ex vivo* stimulation. Although I did not find any CCR7 expression on human or murine LN neutrophils at baseline, *ex vivo* stimulation with OVAIC resulted in significant upregulation of surface CCR7 in both human and murine neutrophils (Figure 4.21A-D), suggesting a potential mechanism through which neutrophils traffick to LNs following IC stimulation.

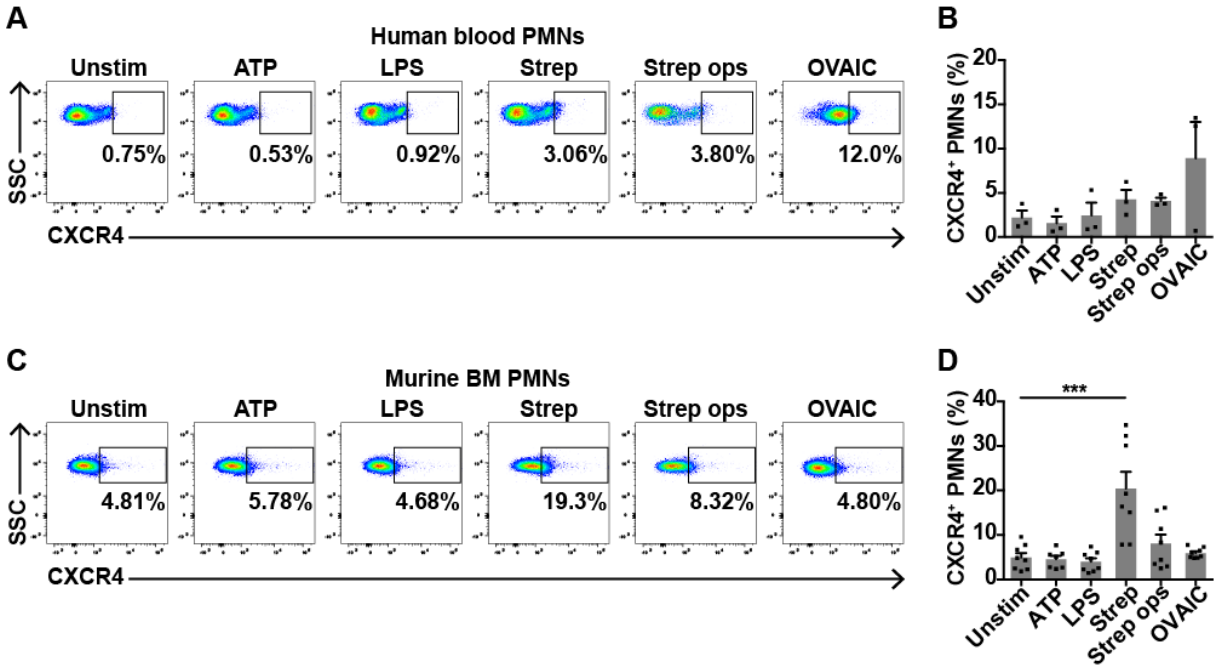

Figure 4.20. CXCR4 surface expression on human and murine neutrophils following stimulation *ex vivo*. Neutrophils were isolated and stimulated *ex vivo* followed by surface staining for flow cytometry. (A-B) Human blood neutrophil CXCR4 expression, with (A) representative plots and (B) quantification of % CXCR4-high neutrophils. Data from 3 donors in 3 experiments performed in triplicate. (C-D) Murine BM neutrophil CXCR4 expression, with (A) representative plots and (B) quantification of % CXCR4-high neutrophils; ***p < 0.001 Strep *vs* unstim. Data from 8 mice in 2 independent experiments.

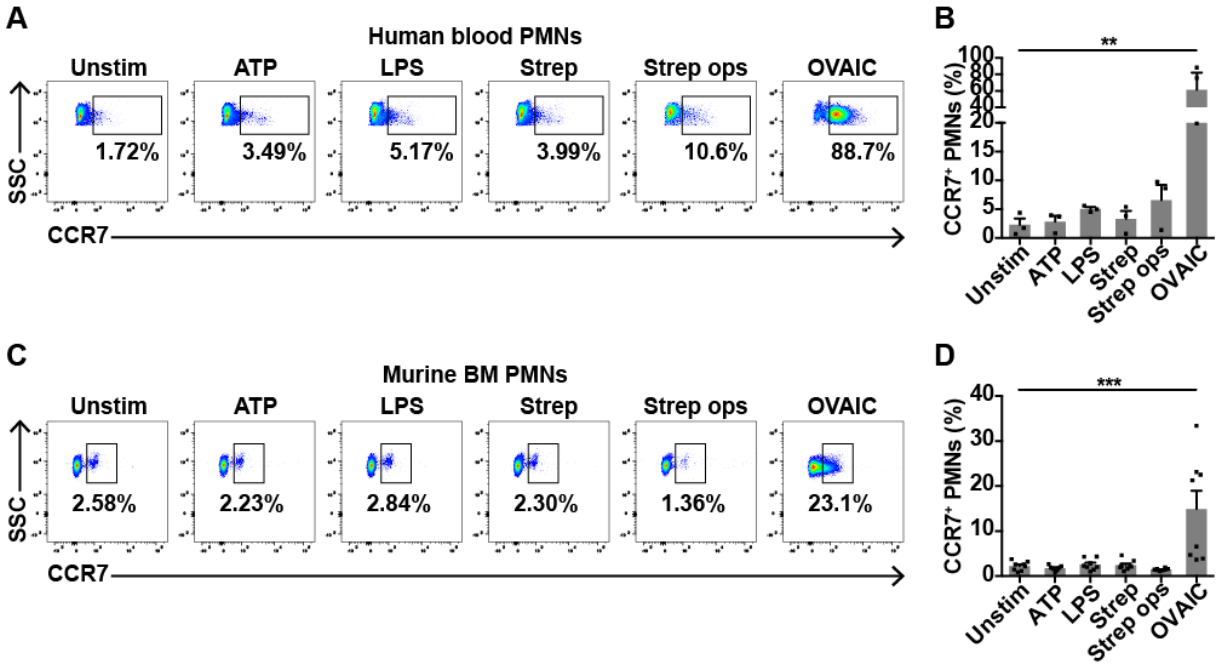

Figure 4.21. CCR7 surface expression on human and murine neutrophils following stimulation *ex vivo*. Neutrophils were isolated and stimulated *ex vivo* followed by surface staining for flow cytometry. (A-B) Human blood neutrophil CCR7 expression, with (A) representative plots and (B) quantification of % CCR7-high neutrophils; $^{**}p < 0.01$ OVAIC *vs* unstim. Data from 3 donors in 3 experiments performed in triplicate. (C-D) Murine BM neutrophil CCR7 expression, with (A) representative plots and (B) quantification of % CCR7-high neutrophils; $^{***}p < 0.001$ OVAIC *vs* unstim. Data from 8 mice in 2 experiments.

4.9. Effect of IC neutrophil stimulation on T cell activation in *ex vivo* co-culture

To investigate the functional outcome of IC stimulation of neutrophils, murine BM neutrophils were isolated and stimulated with OVAIC *ex vivo*, and co-cultured with $CD4^+$ T cells isolated from the spleen of OTII (OVA-specific) mice (335). OVAIC-stimulated neutrophils increased T cell activation in co-culture, as evidenced by increased surface T cell expression of the activation markers CD25 (Figure 4.22A,B) and CD69 (Figure 4.22C,D). Together, these data suggest that IC stimulated neutrophil MHCII expression, and IC-stimulated neutrophils led to increased $CD4^+$ T cell activation *ex vivo*, potentially via antigen presentation.

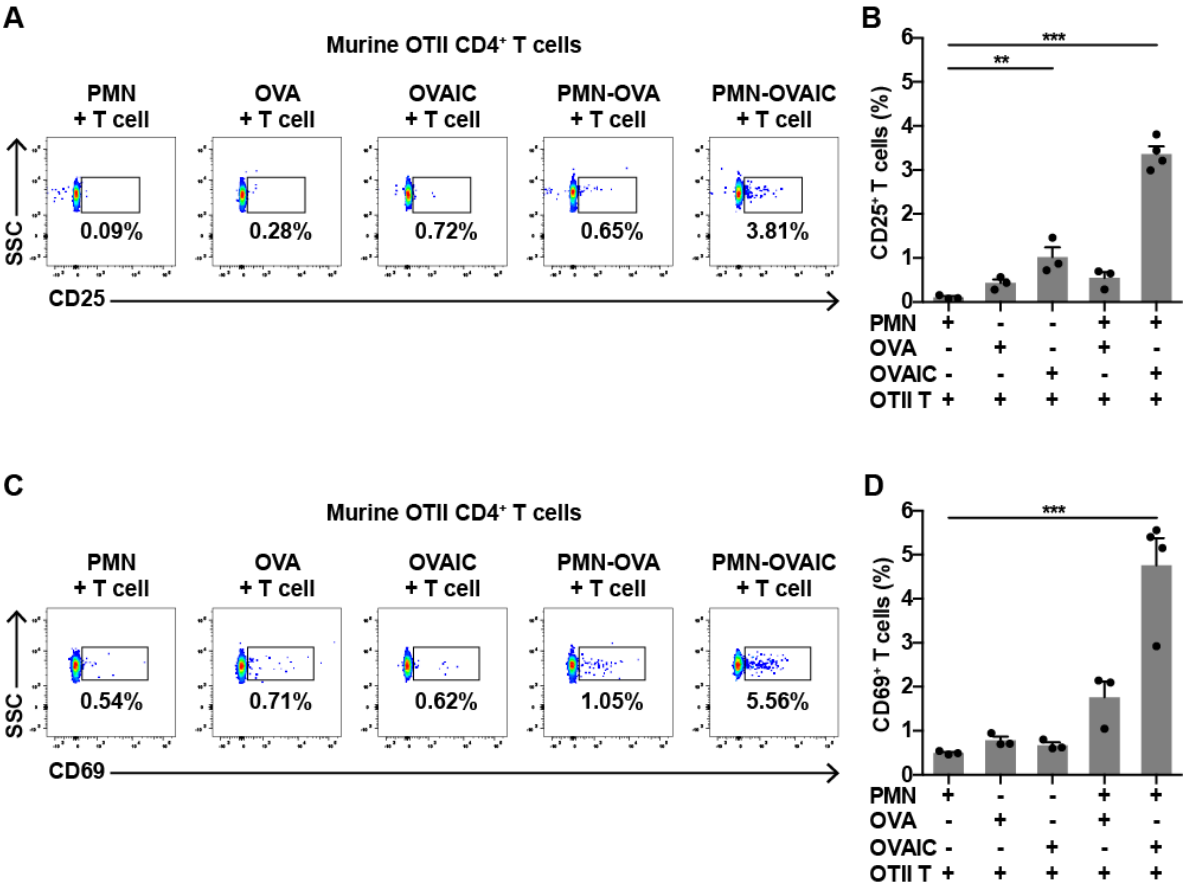

Figure 4.22. Effects of OVAIC neutrophil stimulation on T cell activation *ex vivo*. Expression of (A-B) CD25 and (C-D) CD69 on OTII $CD4^+$ T cells following co-culture for 48 hours with OVA- or OVAIC-stimulated neutrophils or controls, with representative plots and quantification shown; $^{**}p < 0.01$, $^{***}p < 0.001$ *vs* PMN + OTII T control. Data from 1 of 2 experiments shown.

4.10. Uptake of systemic and local IC by neutrophils and early migration to LNs

I next examined the effects of systemic and local IC administration on neutrophil dynamics *in vivo*. OVAIC was formed *in vitro*, and administered intravenously into LysM-GFP mice, followed by examination of the LNs 1 to 2 hours post administration. By intravital imaging, OVAIC-positive neutrophils were identified crawling in the popliteal LN (Figure 4.23A). By flow cytometry, neutrophils containing OVAIC, but not OVA alone, were observed in the inguinal, mesenteric and axillary LNs as well as the spleen (Figure 4.23B).

IC was also generated locally *in vivo* by administration of intraperitoneal anti-PE antibody followed by subcutaneous footpad injection of PE and imaging of the draining popliteal LN. PEIC generation in the LN resulted in rapid recruitment of neutrophils (Figure 4.24A,B), with some of these neutrophils being PEIC-positive (Figure 4.24C). These data demonstrated that exposure to systemic and local IC promoted neutrophil trafficking into peripheral LNs, suggesting a role of neutrophils in the early delivery of antigen to LNs.

4.10.1. Neutrophil interactions with other LN immune cells *in vivo*

Following local PEIC generation *in vivo*, intravital imaging of the popliteal LN showed that neutrophils were recruited to the SCS, where SCS macrophages phagocytose PEIC, and to the LN cortex, where cells such as DCs reside (Figure 4.25A). Neutrophils in the SCS moved at a slower speed than neutrophils in the LN cortex following PEIC stimulation (Figure 4.25B,C). In the SCS, neutrophils were seen to interact with PEIC-positive SCS macrophages (Figure 4.25D). In the LN cortex, neutrophils were observed to interact with $CD11c^+$ DCs at baseline (Figure 4.26A). Although interactions were short in duration, there was an increase in the proportion of interactions of over 2 minutes following PEIC stimulation (Figure 4.26B,C). Of note, confocal examination of LNs from unstimulated CD11c-YFP mice also demonstrated evidence of neutrophil-DC interactions in the unstimulated state (Figure 4.26D).

Overall these experiments showed that neutrophils trafficked to LNs and interacted with other LN immune cells such as SCS macrophages and DCs, potentially shaping the immune response under homeostatic conditions and following inflammatory stimuli such as IC challenge.

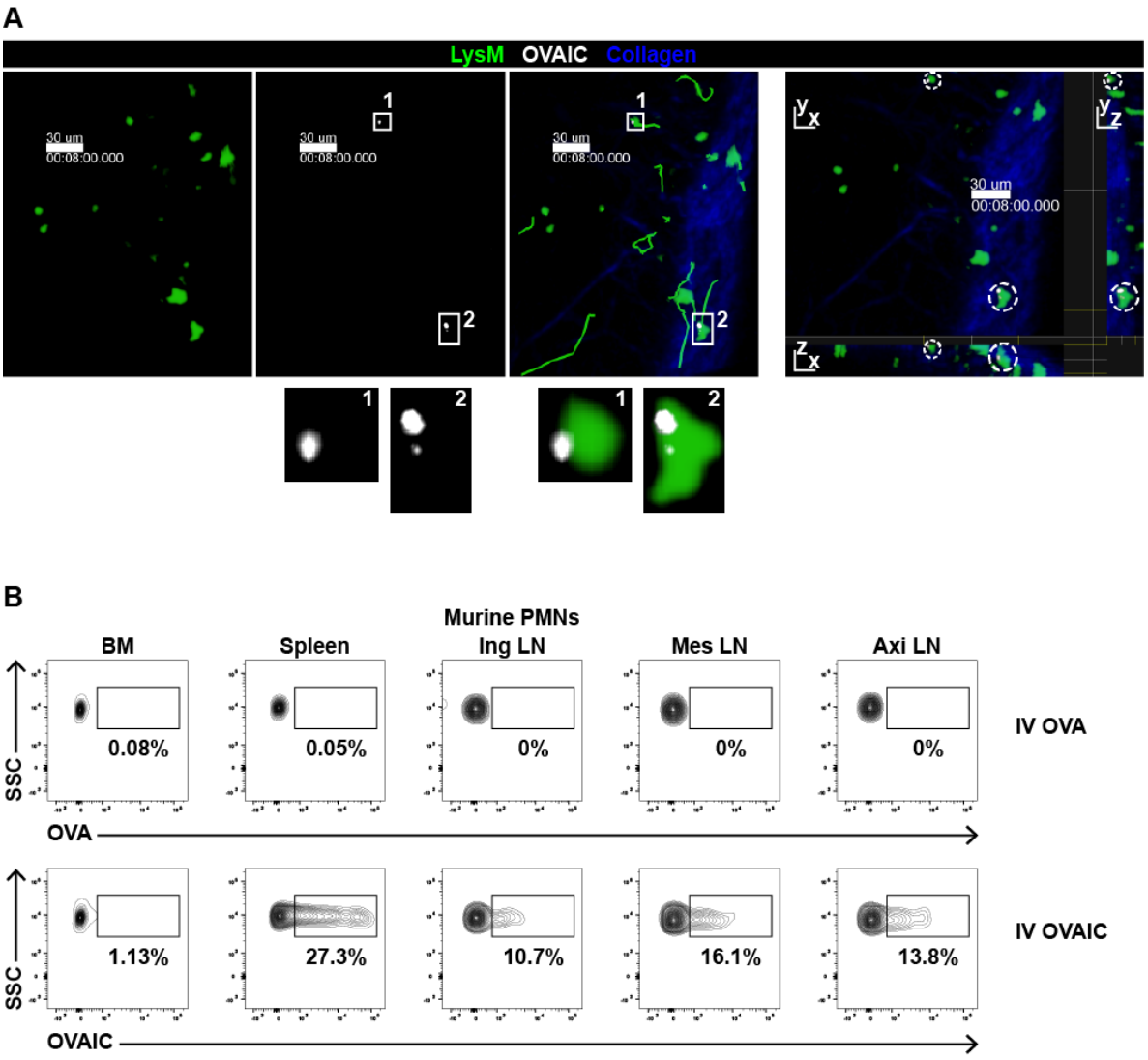

Figure 4.23. Uptake of systemic IC by neutrophils and early migration to LNs *in vivo*. (A) Intravital image of popliteal LN of LysM-GFP mouse 2 hours following intravenous OVAIC administration; neutrophil tracks in green, right panel showing image in 3 planes, insets and boxes / dotted circles showing OVAIC^{+} neutrophils. Scale bar 30 μm, Z stack 40 μm. (B) Flow cytometry plots of BM, spleen and LN neutrophils 1 hour following intravenous OVA or OVAIC administration to LysM-GFP mouse.

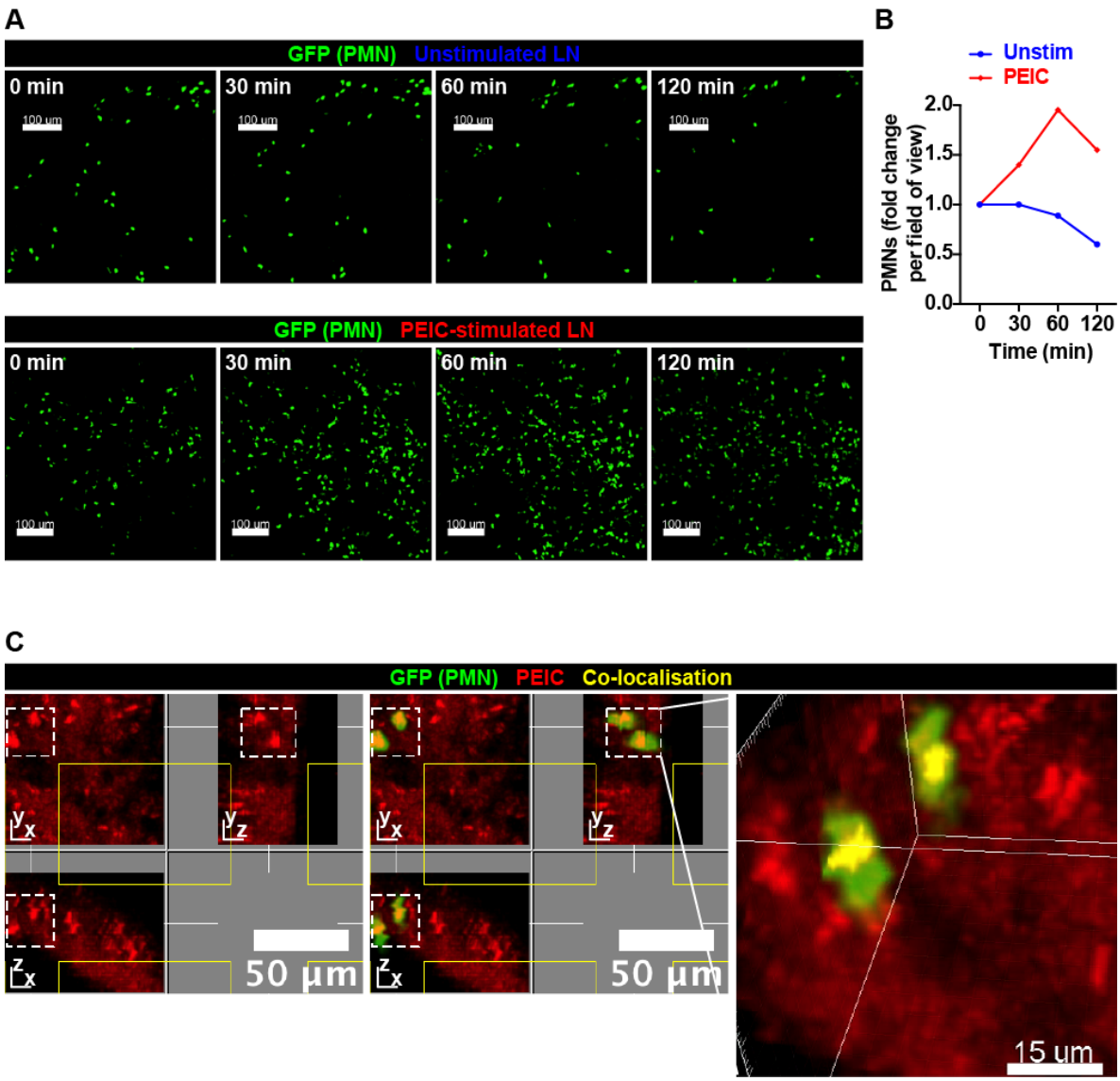

Figure 4.24. Early neutrophil recruitment to LNs following local IC stimulation *in vivo*. (A) Intravital images of popliteal LNs unstimulated and following local PEIC stimulation; scale bar 100 µm, Z stack 80 µm. (B) Quantification of early neutrophil recruitment as fold change from baseline of cells per field of view. (C) Neutrophils containing phagocytosed PEIC moving within popliteal LN; left panels showing image in three planes and PEIC-positive neutrophils in dotted white boxes, right panel showing neutrophils at higher magnification. Scale bar 50 µm / 15 µm, Z stack 60 µm.

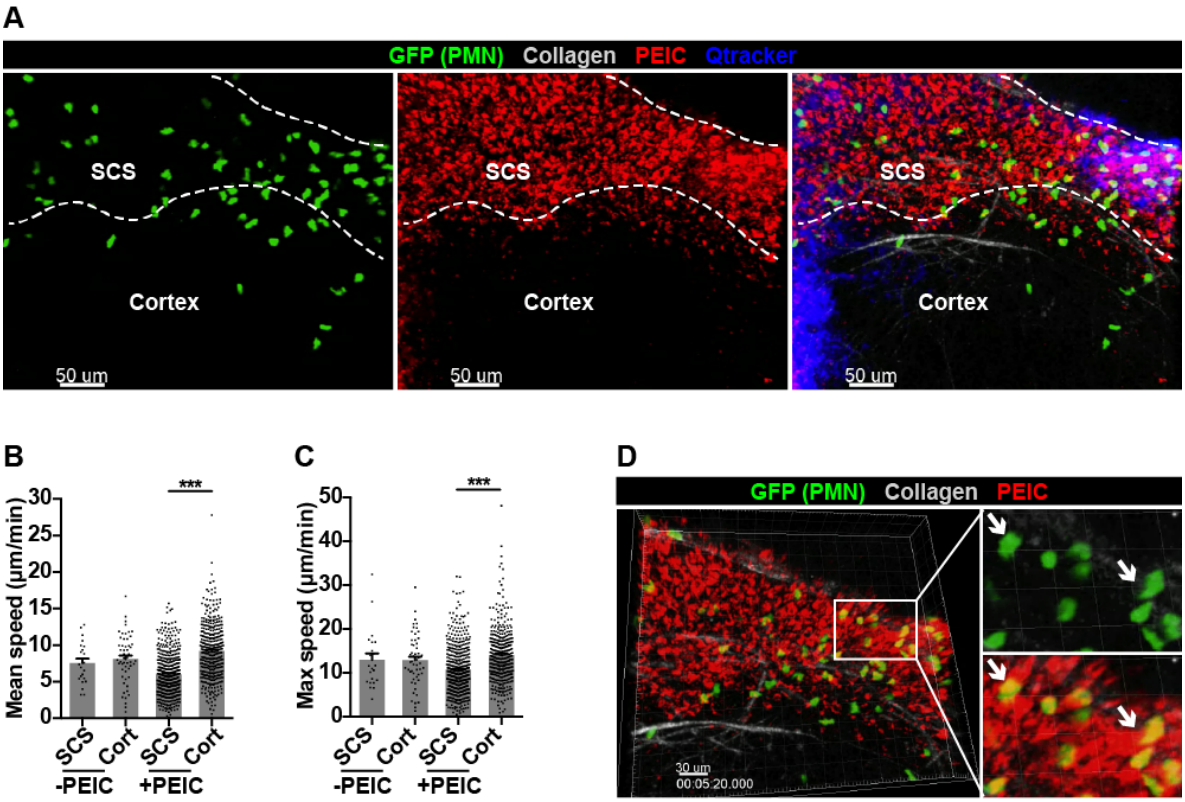

Figure 4.25. Neutrophil dynamics and interactions with SCS macrophages following IC stimulation *in vivo*. (A) Anatomical location of neutrophils in popliteal LN by intravital two-photon imaging following local PEIC stimulation *in vivo*; scale bar 50 µm, Z stack 40 µm. (B-C) Mean and maximum speeds of neutrophil movement in SCS and cortex with and without PEIC treatment; ***$p < 0.001$ SCS *vs* cortical neutrophils. Pooled data from 3 independent experiments, with each dot representing one cell track. (D) Intravital examples of interactions (white arrows) between GFP^+ neutrophils and $PEIC^+$ SCS macrophages following IC stimulation; scale bar 30 µm, Z stack 40 µm.

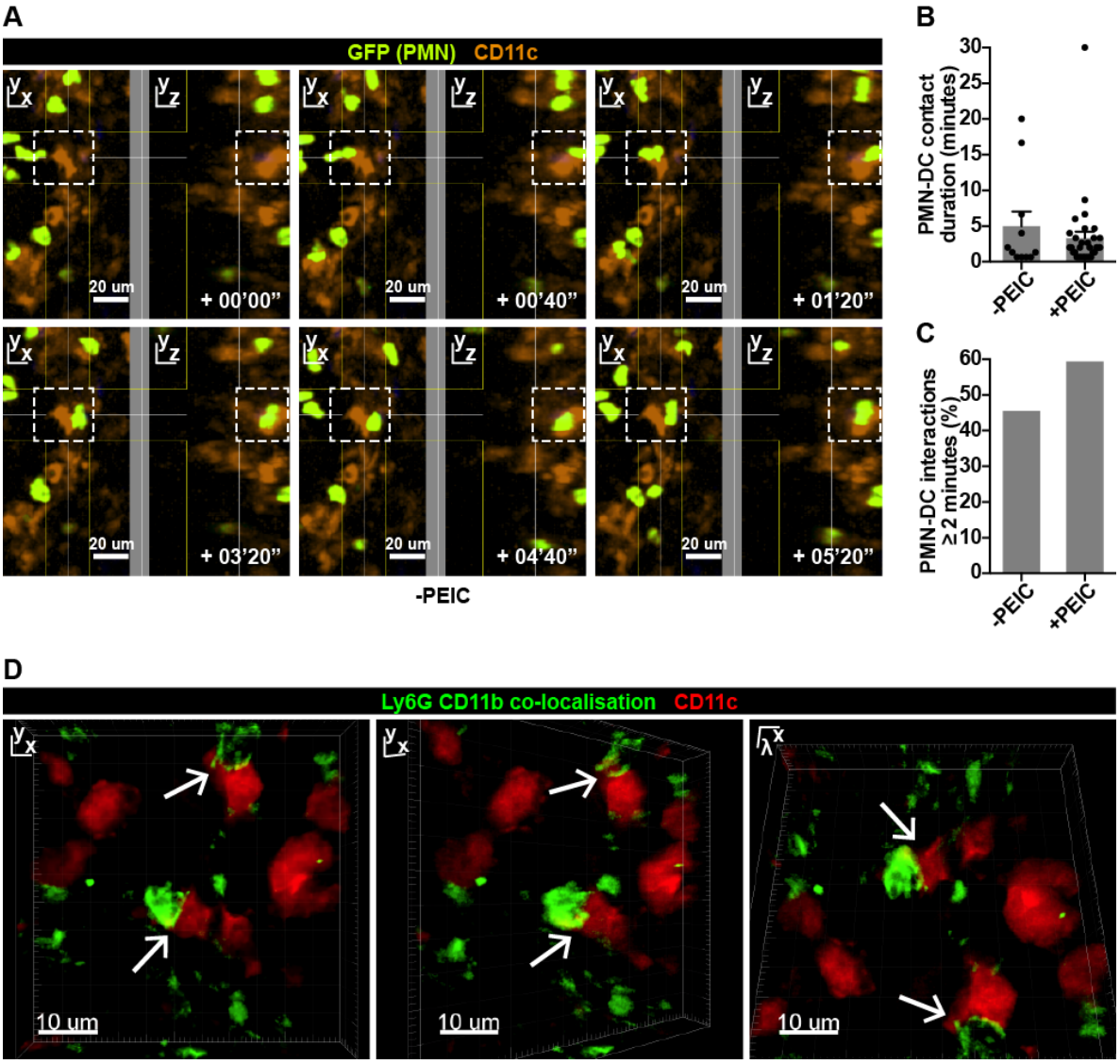

Figure 4.26. Neutrophil interactions with DCs *in vivo*. (A) Intravital image of popliteal LN showing *in vivo* example of interaction (dotted white boxes) between GFP$^+$ neutrophil and CD11c$^+$ DC at baseline; image shown in two planes, scale bar 20 μm, Z stack 80 μm. (B-C) Quantification of (B) duration of neutrophil-DC contact time in minutes and (C) % of neutrophil-DC interactions lasting ≥ 2 minutes; pooled data from 2 independent experiments, with each dot representing one interaction. (D) Confocal image of inguinal LN from unstimulated CD11c-YFP mouse showing PMN-DC interactions (white arrows), with image shown in three different rotations; scale bar 10 μm, Z stack 7 μm.

4.11. Summary of results

The results above demonstrated, using flow cytometry and confocal microscopy, that neutrophils were present in unstimulated murine LNs draining the skin, lungs and gut, with confocal microscopy showing the numbers of LN neutrophils to be much higher compared to quantification by flow cytometry. The majority of neutrophils were located in LN interstitium outside of blood and lymphatic vessels, as demonstrated by labelling of intravenous leukocytes and by quantification using confocal microscopy. Within the LN, neutrophils were located peripherally, in interfollicular areas near the floor of the SCS, enabling them to interact with other immune cells in the LN including T cells, DCs and SCS macrophages.

Intravital two-photon imaging showed motile neutrophils in LNs at baseline exhibiting random crawling, with mean speeds similar to that of LN lymphocytes. Intravenously transferred neutrophils trafficked from the circulation into LNs via both blood and lymphatic vessels at baseline; mechanistically, neutrophil trafficking at baseline and following laser damage was partially dependent on PNAd, and neutrophils from unstimulated LNs showed higher CXCR4 expression compared to blood neutrophils. Examination of LNs from human organ donors also demonstrated the presence of neutrophils within the LN interstitium near blood and lymphatic vessels, in a similar distribution to that of murine LN neutrophils.

Both human and murine LN neutrophils expressed MHCII at baseline. *Ex vivo* stimulation experiments showed that IC upregulated expression of neutrophil MHCII and co-stimulatory molecules including CD80, CD86 and CD40, whilst *S. pneumoniae* but not IC upregulated expression of murine neutrophil CXCR4. IC-stimulated neutrophils increased antigen-specific $CD4^+$ T cell activation, as measured by T cell expression of CD25 and CD69, in co-culture. *In vivo*, intravenous administration of systemic IC resulted in early antigen delivery by neutrophils from the circulation into peripheral LNs, and generation of local IC resulted in early neutrophil recruitment to LNs. Neutrophils were capable of interacting with other LN immune cells, such as SCS macrophages and DCs, including neutrophil-DC interactions at baseline, potentially influencing adaptive immunity in homeostasis and following inflammatory challenges.

4.12. Discussion

Overall, I demonstrated that neutrophils trafficked tonically into LNs under homeostatic conditions, showing a distinct phenotype with higher MHCII expression compared to blood

neutrophils, and potentially influencing adaptive immunity by early delivery of systemic antigen to LNs.

4.12.1. Presence of neutrophils in unstimulated murine LNs

Whilst neutrophils have been considered circulating leukocytes that are recruited to tissue sites of inflammation where they exert their effector functions and then undergo local apoptosis and efferocytosis, there is increasing evidence that they have more diverse roles in addition to pathogen killing. This includes migration into dLNs following local inflammatory or infectious challenges to influence other LN innate and adaptive immune cells. Careful examination of data presented in previous studies as control comparators to the stimulation under investigation also shows the presence of neutrophils in LNs at baseline (114,130), suggesting potential functions of neutrophils in homeostasis as well as in inflammation.

Aged mice showed increased numbers of neutrophils with an activated phenotype in lymphoid organs compared to young mice, although systemic inflammation was also increased in these animals (211). One study using parabiosis showed that circulating neutrophils migrated into multiple tissues in homeostasis, with neutrophils being largely extravascular in BM, spleen and intestine, but largely intravascular in liver and lungs (210). Another study using a cremasteric inflammation model showed that following PBS stimulation the majority of neutrophils in the dLN were in the stroma, with the proportion of neutrophils in lymphatic vessels increased following CFA stimulation (121).

My results provide detailed characterisation of neutrophils in LNs in homeostatic conditions, using flow cytometry to quantify $Ly6G^+CD11b^+$ neutrophils in unstimulated LNs draining multiple mucosal and peripheral sites. Compared to confocal microscopy, mechanical dissociation of tissues for flow cytometry was shown in a previous study to underestimate tissue memory $CD8^+$ T cell numbers to varying degrees in different organs, with 70-fold difference in the lungs, 13-fold difference in the small bowel, and 1.2-fold difference in LN; the degree of underestimation was also affected by the cell phenotype and by the anatomical location within each organ (332). Therefore I used confocal microscopy to quantify LN neutrophils, showing much higher true cell numbers of over 10-fold difference compared to flow cytometry estimates. Whilst this difference in LN neutrophil estimate was higher compared to previous estimate for LN T cells, as flow cytometry quantification was affected by the phenotype and anatomical location within T cells (332), the difference in cell type could also have an effect.

In addition, confocal microscopy allowed detailed examination of the anatomical location of neutrophils within LNs in relation to blood and lymphatic vessels and other immune cells. With intravenous anti-CD45 leukocyte labelling for flow cytometry and with confocal quantification, I confirmed that the majority of LN neutrophils were within the interstitium, in proximity to, but outside of, blood ($PNAd^+$) and lymphatic ($LYVE\text{-}1^+$) vessels. Therefore these neutrophils were not simply circulating leukocytes transiting within vessels.

To ensure the results accurately reflected LNs in unstimulated conditions, for neutrophil quantification I used young female mice aged 8 to 10 weeks (to avoid potential effects of ageing) with minimal handling prior to organ harvest, avoiding males which are more prone to skin injury (which may lead to neutrophil recruitment to dLNs) from fighting when co-housed. Intravital imaging showed motile neutrophils exhibiting random crawling within LNs at baseline, with mean speed similar to that of LN lymphocytes. Although intravital imaging experiments involved surgical exposure of the popliteal LN, the number of neutrophils did not increase during the period of imaging, suggesting their presence in the LNs was not simply as a result of neutrophil recruitment induced by tissue damage from the imaging procedure.

4.12.2. Presence of neutrophils in human LNs

There are differences in neutrophil biology and kinetics between mice and humans; for example, neutrophils comprise a higher proportion of circulating leukocytes in humans compared to mice (49). I confirmed that the presence of neutrophils in LNs was not a finding limited to mice, demonstrating the presence of neutrophils in human LNs, by flow cytometry showing populations of $CD15^+CD16^+$ cells in LNs from different sites, and by confocal microscopy showing neutrophils in LN interstitium near blood and lymphatic vessels, in a similar anatomical location to that observed in murine LN neutrophils. The proportion of neutrophils is higher in human compared to murine LNs, which may reflect neutrophils as a higher proportion of circulating leukocytes in humans, or that LN neutrophil dynamics are affected by the differences in the microbiome of humans and laboratory mice.

Although human LNs were obtained from deceased organ donors who might arguably have had a degree of systemic inflammation or in a few cases infection, the majority of donors did not have any specific infectious or inflammatory insult in the tissue territories drained by the LNs studied. Furthermore, this represented a valuable opportunity to examine whole human LNs from different body sites as close to the baseline state as possible, as it would otherwise be unethical to remove whole LNs from healthy volunteers. These results therefore provided evidence of the presence of neutrophils in both human and murine LNs at baseline.

4.12.3. Adoptive transfer model for investigating neutrophil trafficking

Following local inflammatory or infectious challenges, neutrophils have been shown to migrate into dLNs via both HEVs (129–131) and lymphatics (114,131), with neutrophils migrating via lymphatics capable of carrying bacteria from the periphery into the SCS (114). However, the baseline migration of neutrophils into LNs *in vivo* has not been studied in detail. To address this, I isolated GFP^+ BM neutrophils for adoptive transfer into wild type mice that were subsequently imaged, with neutrophils isolated by negative magnetic selection, and good purity of neutrophils achieved. Neutrophils were transferred promptly following isolation to minimise *ex vivo* exposure and inadvertent activation. At 24 hours post intravenous transfer, neutrophils were observed to be crawling within the LN interstitium at similar speeds to native neutrophils, demonstrating that circulating neutrophils traffick into LNs under homeostatic conditions.

The observation by microscopy that LN neutrophils were present up to 7 days post intravenous transfer challenges the current dogma that neutrophils are short-lived circulatory leukocytes. One caveat to this conclusion is that for adoptive transfer, neutrophils were isolated from the BM, which provides much higher cell yields compared to blood but contains some immature cells. Previous studies showed isolated BM neutrophils to be functionally mature (329), and when transferred intravenously into wild type mice BM neutrophils showed a short half-life of 8 hours in the circulation (59). Nevertheless, in my experiments a small proportion of isolated BM neutrophils were immature, and these might have contributed to the long-lived neutrophils observed in LNs several days post transfer.

In vivo and *ex vivo* labelling studies have shown variable estimates of circulating neutrophil half-life partly due to different study methodologies, such as labelling of whole blood or isolated neutrophils, and different labelling protocols (60–65,334). Further studies will be required to investigate the true lifespan of neutrophils within LNs, and to address whether neutrophils that traffick into LNs encounter pro-survival signals or cellular interactions that prolong their survival within LNs compared to circulating neutrophils. A recent study showed that neutrophils were detectable in efferent lymphatic fluid, and that S1PR blockade resulted in increased neutrophil as well as lymphocyte numbers within LNs, suggesting that, like lymphocytes, neutrophils that traffick into LNs can egress back into the circulation (139).

4.12.4. Mechanism of neutrophil trafficking into LNs

Using intravital imaging I generated *in vivo* evidence that neutrophils trafficked into LNs via both blood and lymphatic vessels at baseline. L-selectin / PNAd has been shown in other

studies to be involved in lymphocyte entry into LNs (18), and in neutrophil trafficking into LNs via HEVs post inflammation (130,131,139). I used PNAd antibody blockade to inhibit trafficking via HEVs, which led to an incomplete reduction of neutrophil trafficking, both at baseline and following laser damage, but I did not simultaneously inhibit neutrophil trafficking via lymphatics to examine whether neutrophil trafficking into LNs would be reduced further. It is therefore possible that the PNAd blockade was incomplete, or that there was also neutrophil trafficking in a PNAd-independent manner via lymphatics. In keeping with the latter, I did observe neutrophils within the lumen of lymphatic vessels in LN sections, and neutrophils emerging from LYVE-1^+ vessels during intravital imaging experiments.

Whilst circulating neutrophils might be expected to be capable of relatively rapid migration across HEVs into LNs, the migration via lymphatics into LNs would imply that circulating neutrophils traffick into peripheral non-lymphoid tissues then migrate via lymphatics to LNs at baseline. This would be consistent with previous reports showing that in mice neutrophils were present in non-lymphoid tissues at baseline (210), and in sheep lymphatic fluid draining from periphery without inflammatory stimuli contained neutrophils as well as DCs and monocytes, suggesting lymphatic migration of neutrophils from peripheral tissues to LNs (122). It would be interesting to expand on these findings by quantifying the relative contributions of neutrophil migration via blood or lymphatic routes, at baseline and following different infectious and sterile inflammatory stimuli.

CD11b and CXCR4 have been shown to be involved in neutrophil trafficking via HEVs and lymphatics following sterile and infectious stimuli (114,131). CD11b, part of the Mac-1 integrin heterodimer, is highly expressed on neutrophils and shows upregulation in expression on activated neutrophils, as I demonstrated on neutrophils activated by OVAIC *ex vivo*. The processes of neutrophil transmigration across endothelium towards inflamed tissues and neutrophil trafficking into LNs post inflammation have both been shown to involve CD11b. I therefore examined the expression of CD11b on murine and human LN neutrophils at baseline, but did not find differences in CD11b expression between LN and blood neutrophils. An antibody clone against the activation epitope of human CD11b exists, which may be useful in examining the activation status of CD11b / Mac-1 on neutrophils.

CXCR4 is involved in neutrophil trafficking in and out of BM. The release of neutrophils from BM involves downregulation of neutrophil CXCR4. Aged murine neutrophils upregulate CXCR4 leading to their return to the BM for destruction (50,53,54). Following *S. aureus* peripheral stimulus, the majority of neutrophils recruited to dLNs were apoptotic (38,114); *in vitro*, apoptotic neutrophils increased macrophage production of both pro-inflammatory and anti-inflammatory cytokines (134). In addition to its upregulation on aged neutrophils,

CXCR4 has also been shown as one of the mechanisms of neutrophil migration to LN post inflammation (38,131).

I examined for CXCR4 expression on murine and human LN neutrophils at baseline. In humans, LN and splenic neutrophils from some organ donors expressed CXCR4, but overall this was not statistically different compared to expression on blood neutrophils. In mice, unstimulated LN neutrophils from several sites expressed higher levels of CXCR4 compared to blood neutrophils, demonstrating the possibility that CXCR4 is involved in neutrophil trafficking into LNs at baseline as well as following inflammation. I did not perform Annexin V staining to determine directly whether LN neutrophils were live but apoptotic and thus showing higher CXCR4 expression; however, intravital imaging of transferred and native neutrophils showed motile neutrophils with high GFP fluorescence, and confocal microscopy of unstimulated LN sections showed neutrophils with their typical polymorphonuclear nuclei, not apoptotic nuclei.

Previous studies have investigated the role of CCR7 in neutrophil migration to LNs, as CCR7 is also required for the migration of DCs from the periphery via lymphatic vessels to the dLN, in which the corresponding ligands CCL19 and CCL21 are expressed (11). Although neutrophils contain intracellular stores of CCR7, and neutrophil migration to LNs following peripheral CFA stimulation has been shown to involve CCR7 (131,133), other studies have shown using several experimental models that CCR7 was not required for neutrophil migration via either lymphatic or blood vessels to dLNs following skin *S. aureus* challenge (114,130). I examined neutrophil surface CCR7 expression in murine and human LNs, but I was unable to demonstrate significant CCR7 expression on blood or LN neutrophils at baseline. This could be because CCR7 is not required for neutrophil entry into LNs at baseline, or because CCR7 undergoes receptor internalisation following ligand binding during entry into LNs resulting in lack of surface expression or staining on LN neutrophils, and that intracellular staining is required to detect neutrophil CCR7 expression.

Within LNs, neutrophils were observed to be present for prolonged periods during intravital imaging, with some crawling along collagen fibres. Other studies have shown evidence of crosstalk between neutrophils and the local tissue environment. Airway neutrophils from patients with viral respiratory tract infections expressed the collagen receptor leukocyte-associated immunoglobulin-like receptor-1 (LAIR-1), with LAIR-1 ligation leading to reduced NET formation *ex vivo* (336), and LAIR-1-deficient mice showing enhanced airway neutrophil recruitment (337). Whilst neutrophils can release cytotoxic proteins and cause stromal cell damage and tissue inflammation (338), the respiratory burst from activated neutrophils has

also been implicated in the generation of local tissue hypoxia leading to resolution of inflammation (339).

In summary, I have provided *in vivo* evidence by intravital imaging of the trafficking of neutrophils via both blood and lymphatic vessels into LNs in homeostatic conditions. The process of neutrophil trafficking involved PNAd, as antibody blockade of PNAd partially impaired the migration of neutrophils into LNs at baseline and following local sterile inflammation. Murine LN neutrophils showed higher expression of CXCR4 compared to blood neutrophils at baseline, suggesting another potential mechanism of neutrophil entry into LNs in homeostatic conditions. CD11b and CCR7, shown in other studies to be involved in neutrophil trafficking following peripheral inflammatory stimuli, did not show upregulation on LN neutrophils at baseline. Within LNs, some neutrophils were observed to crawl along collagen fibres, potentially enabling them to interact with the extracellular matrix.

4.12.5. Neutrophil MHCII expression at baseline

Previous studies have shown that whilst blood neutrophils did not express surface MHCII at baseline (160,161), inflammatory stimuli were capable of inducing neutrophil expression of MHCII, CD80 and CD86, leading to antigen presentation and T cell activation *in vitro* (162–164,167,340), and *in vivo* neutrophils recruited to dLNs following peripheral *S. aureus* challenge upregulated MHCII, CD80 and CD86 (114). Neutrophils can also influence antigen presentation via interactions with DCs, and neutrophil-DC hybrids with a mixed phenotype including expression of the machinery required for antigen presentation have been reported in the literature (172–174). However, whether neutrophils in tissues express MHCII at baseline is unclear.

I demonstrated, by confocal imaging of unstimulated LN sections, that neutrophils were located peripherally in interfollicular areas of LNs, ideally positioned for T cell interactions including antigen presentation via MHCII to activate $CD4^+$ T cells. I examined for MHCII expression on LN neutrophils by flow cytometry, and found that a proportion of both human and murine LN neutrophils showed MHCII expression at baseline, demonstrating the potential for antigen presentation.

Therefore, I have shown that neutrophils present within human and murine LNs in homeostatic conditions exhibited a distinct phenotype, with expression of CXCR4 as a potential mechanism through which neutrophils tonically traffick into LNs at baseline, and expression of MHCII potentially enabling antigen presentation within LNs.

4.12.6. Neutrophils and antigen presentation

Ex vivo, I tested a number of inflammatory stimuli, showing that IC stimulation of neutrophils led to increased expression of CD11b indicating activation, and marked increase in the expression of MHCII, enabling antigen presentation; OVAIC-stimulated neutrophils increased antigen-specific OTII $CD4^+$ T cell activation in co-culture experiments. These results are consistent with those of other studies showing the ability of antigen-stimulated neutrophils to present antigen via MHCII to activate $CD4^+$ T cells *in vitro* (161,167).

IC stimulation led to increased surface expression of CCR7 on neutrophils, which may represent a mechanism for the migration of neutrophils into LNs following IC stimulation. On the other hand, I did not find surface CCR7 expression on LN neutrophils at baseline. This may be due to CCR7 not being required for basal neutrophil migration into LNs without IC stimulation, or that CCR7 receptor internalisation occurs following basal neutrophil entry into LNs whilst neutrophils stimulated with IC *ex vivo* are fixed and stained before receptor internalisation occurs. Whilst IC stimulation *ex vivo* led to increased neutrophil expression of MHCII, CD11b and CCR7, it is unclear which signals drive MHCII expression on neutrophils in LNs at baseline in the absence of IC stimulation.

In vivo, I demonstrated that neutrophils were capable of the early delivery of circulating IC to LNs, with IC-positive neutrophils observed crawling in peripheral LNs within one to two hours of intravenous IC administration. I did not determine directly whether IC-positive neutrophils process and present IC to antigen-specific $CD4^+$ T cells in LNs *in vivo*. However, the data on baseline LN neutrophil MHCII expression, neutrophil MHCII upregulation and $CD4^+$ T cell activation following IC stimulation *ex vivo*, and location of neutrophils in T cell areas of unstimulated LNs all provided supportive evidence that circulating IgG-opsonised antigen may be sampled by neutrophils for delivery to LNs and direct presentation to $CD4^+$ T cells, thus positively influencing adaptive immunity.

Other studies examining the effects of neutrophils on LN T cell responses following peripheral inflammatory stimuli have shown conflicting results, with *in vivo* antibody depletion of circulating neutrophils leading to reduced LN T cell numbers following *S. aureus* challenge (114,129), increased LN $CD4^+$ T cell activation following HEL stimulation (113), and no difference in LN T cell response following Herpes simplex virus challenge (128). Similarly, *in vivo* neutrophil depletion in two different studies both using *S. aureus* as the inflammatory challenge led to increased LN B cell response in one study and decreased LN B cell response in another (114,129). Further intravital imaging studies are required to investigate directly, within LNs *in vivo*, whether neutrophils present antigen to T cells, the nature of the

interactions between neutrophils and T cells, and whether these interactions stimulate or inhibit B and T cell responses.

4.12.7. Neutrophil interactions with other LN immune cells

Following generation of IC locally within the popliteal LN, I showed that intravenously transferred neutrophils were rapidly recruited to the LN, and were present in both the LN cortex and the SCS, suggesting that similar to the unstimulated state neutrophils traffick via blood and lymphatic vessels into LNs in inflammation. Neutrophils in the SCS moved slower than neutrophils in the cortex, supporting the finding of neutrophils interacting with SCS macrophages following local IC stimulation. Whilst most of the PEIC was taken up by SCS macrophages, some PEIC was also taken up by neutrophils, showing that neutrophils are capable of IC uptake both locally from within LNs and systemically from the circulation for delivery to LNs. Other studies have also shown crosstalk between neutrophils and SCS macrophages following inflammatory stimuli; for example, neutrophil swarms have been shown to disrupt SCS macrophages (141), and SCS macrophage-derived IL-1β may drive neutrophil recruitment to LNs (29).

In the LN cortex, I observed *in vivo* interactions between neutrophils and DCs, both at baseline and following local IC stimulation, although the interactions were mostly short in duration. Other imaging studies have shown similar durations of interactions between neutrophils and DCs following inflammatory stimuli, in the lungs *in vivo* (151) and in LNs *ex vivo* (113). My results provide additional novel intravital imaging data on *in vivo* interactions between neutrophils and DCs within LNs at baseline. In terms of subsequent effects on T cell responses, previous studies have shown evidence of neutrophils activating DCs and enhancing antigen presentation *in vitro* (144,154) but inhibiting DCs *in vivo* (156,157). The effect of neutrophil-DC interactions, in the absence of prior inflammatory stimuli, on $CD4^+$ and $CD8^+$ T cell responses in LNs is currently unclear.

4.12.8. Significance of findings

Neutrophils are traditionally considered circulating leukocytes that are recruited to tissues following infectious and inflammatory stimuli, being terminally differentiated leukocytes with short circulatory half-lives that act as early innate effector cells with functions such as phagocytosis, release of antimicrobial proteins and generation of NETs. More recently, neutrophils have been shown to have more diverse roles, including migration into LNs following local inflammatory stimuli to influence other innate and adaptive immune cells, for example by MHCII expression and antigen presentation. This is of relevance in human

inflammatory diseases, for example in rheumatoid arthritis where synovial fluid neutrophils have been shown to express higher MHCII (160), and in human visceral Leishmaniasis where blood neutrophils have been shown to express higher MHCII and co-stimulatory molecules (169). During homeostatic conditions, however, it is unclear whether neutrophils have functional roles in lymphoid organs. Limited data exist on the presence of neutrophils in non-lymphoid tissues in mice (210), but there are no studies characterising in detail the number and anatomical location of LN neutrophils under homeostatic conditions, and there are no studies examining at baseline the presence and function of neutrophils in human LNs.

I have provided novel data, using flow cytometry and confocal microscopy as complimentary methods, showing that neutrophils were present in murine and human LNs at different body sites in the absence of prior inflammatory stimuli. The majority of neutrophils were within LN interstitium and localised peripherally in interfollicular zones, sites of T cell activation. I provided direct *in vivo* evidence that neutrophils trafficked into LNs via blood and lymphatic vessels at baseline, partially dependent on PNAd, and that neutrophils formed interactions with DCs in LNs at baseline. LN neutrophils had a distinct phenotype, with higher expression of MHCII and CXCR4. *Ex vivo*, IC stimulation resulted in upregulation of MHCII and co-stimulatory molecules leading to T cell activation. *In vivo*, neutrophils were capable of carrying systemic IC into peripheral LNs.

The above data are in support of a novel role of neutrophils in homeostatic immune surveillance, whereby under homeostatic conditions neutrophils traffick tonically into murine and human LNs, extending their routine patrol beyond the circulation. Neutrophils are capable of sampling circulating IgG-opsonised antigen for delivery to peripheral lymph nodes, with the potential for subsequent antigen presentation and influence on adaptive immune responses. Consistent with this, LN neutrophils show a distinct phenotype with higher MHCII expression, and form interactions with DCs within LNs at baseline. These data suggest neutrophils have broader, under-appreciated functions in homeostasis and immune surveillance, in addition to their classical roles as innate effector cells in inflammation.

Whilst neutrophils are critical in innate host defence, persistent neutrophilic inflammation can also lead to tissue damage, as is the case in many chronic inflammatory diseases, such as chronic obstructive pulmonary disease, bronchiectasis and rheumatoid arthritis. To date there are few neutrophil-targeted therapies for managing these inflammatory disorders. Understanding the diverse role of neutrophils in homeostasis, and their basal dynamic behaviour in LNs, sites for interactions between innate and adaptive immune cells, will contribute to the scientific knowledge required in the future development of such therapies.

4.12.9. Future work

The above results could be complemented by a number of additional experiments. Whilst I observed the presence of neutrophils within LNs several days following intravenous transfer, further experiments are required to determine the lifespan of neutrophils in LNs. One approach could involve intravenous adoptive transfer of fluorescent neutrophils followed by harvest of LNs at different time points for flow cytometry and confocal quantification of neutrophil numbers and calculation of neutrophil half life. Local inflammatory stimuli, such as LPS, could be administered and their effect on LN neutrophil lifespan examined. Another approach could involve radiolabelling isolated neutrophils, for example with the radioisotope indium-111 chelated to tropolone, for intravenous transfer and measuring gamma radioactivity of whole LNs harvested at different time points. I have previously used radiolabelled autologous neutrophils to investigate human whole body neutrophil trafficking in healthy volunteers (57,341), and could potentially adapt this approach with the use of gamma probe counters to quantify radioactivity non-invasively over time in human volunteers, providing novel *in vivo* data on homeostatic neutrophil LN trafficking in humans.

For the examination of neutrophil trafficking into LNs, I used PNAd antibody blockade to inhibit trafficking via HEVs. Further reduction in neutrophil trafficking could be demonstrated by concomitant blockade of lymphatic trafficking, for example by antibody blockade of ICAM-1, expressed on lymphatic endothelium and shown to be involved in neutrophil lymphatic trafficking (121), comparing the relative contribution of blood and lymphatic routes of neutrophil entry into LNs at baseline and following sterile or infectious stimuli, such as laser-induced damage, IC stimulation, and bacterial stimulation. In terms of the mechanism of neutrophil entry into LNs under homeostatic conditions, examining the role of CXCR4, CD11b and CCR7 would be reasonable, given their involvement in neutrophil trafficking into LNs following inflammatory stimuli (114,131). Potentially, one could block each of these molecules and investigate whether this leads to a reduction in neutrophil numbers within LNs. For example, CXCR4, expressed on LN neutrophils at baseline as shown in the data above, could be blocked using the CXCR4 inhibitor plerixafor (also known as AMD3100) (55). CD11b and CCR7 could be inhibited by using neutrophils from CD11b-deficient (342) or CCR7-deficient (343) mice for adoptive transfer, or by using antibody blockade, although systemic CCR7 blockade would also affect trafficking of DCs and lymphocytes.

I showed that IC stimulation resulted in upregulation of MHCII and co-stimulatory molecules *ex vivo*, and neutrophils were capable of carrying systemic IC into LNs. Direct *in vivo* examination of whether these antigen-carrying neutrophils process and present antigen to T cells in LNs would add to these results; for example, fluorescent neutrophils could be

adoptively transferred to OTII mice then intravital imaging of LNs performed following systemic IC administration to observe for interactions between IC-positive neutrophils and antigen-specific T cells within LNs, and the role of MHCII examined by quantifying neutrophil-T cell interactions following transfer of wild type or MHCII-deficient neutrophils. In addition to the capacity for carrying IC, an IgG-opsonised sterile antigen, into LNs, I could examine whether neutrophils carry other IgG-opsonised pathogenic antigen, such as opsonised bacteria, from the circulation into LNs and if so whether this leads to subsequent interactions with T cells. I could also examine by intravital imaging whether neutrophils transfer systemic antigen to other LN immune cells, such as DCs and SCS macrophages, to influence adaptive immune responses indirectly.

Whilst I observed neutrophil interactions with DCs at baseline, the effect of these interactions on adaptive immune responses is unclear. This could be investigated by using antibodies to block neutrophil trafficking into LNs then examining levels of LN T cell activation. I could examine whether neutrophil-DC interactions result in trogocytosis and neutrophil acquisition of MHCII. Further intravital imaging could be performed to observe for interactions *in vivo* between neutrophils and other LN immune cells at baseline, for example by adoptively transferring fluorescent neutrophils to T- and B-cell reporter mice and performing intravital imaging of LNs. The concept of neutrophils trafficking into LNs to contribute to immune surveillance in homeostasis could be explored further, using techniques such as single cell sequencing or mass cytometry (344) to characterise the phenotype of LN neutrophils more broadly. This would enable the examination of the expression profiles of cytokines and co-stimulatory molecules that may reveal further information on the potential functions of neutrophils within LNs, such as antigen presentation to T cells, antigen transfer to other LN innate immune cells, or interaction with B cells. It would be of interest to examine whether these interactions occurring at baseline encourages immune tolerance, for example by examining the effects of blocking neutrophil trafficking in autoimmune disease models.

In summary, the above findings of neutrophils tonically trafficking into LNs with the potential to influence adaptive immunity could be expanded upon, including quantification of the lifespan of neutrophils within LNs, investigation of the route and mechanism of neutrophil trafficking into LNs, examination of the occurrence and nature of neutrophil interactions with other LN innate and adaptive immune cells at baseline and their functional significance, as well as investigation of the *in vivo* effects of systemic antigen delivery to LNs by neutrophils.

Chapter 5. The behaviour of ILC2s in homeostasis and inflammation

5.1. Background

ILCs are a recently characterised group of cells present at mucosal barrier sites such as the lungs, skin and intestine, responding rapidly to local tissue signals of infection and tissue damage. ILC2s express transcription factors such as GATA3 (242,244) and RORα (245,246), and are critical early effectors of type 2 immunity; in response to the tissue alarmins IL-25, IL-33 and TSLP produced in helminth- and allergen-induced inflammation, ILC2s are the main early source of cytokines including IL-5 and IL-13. ILC2s have been identified in a number of lymphoid and non-lymphoid tissues at baseline (236), and following inflammatory stimuli tissue ILC2 numbers increase as a result of local expansion as well as recruitment from BM and gut (10,259,345). There is evidence of interactions between ILC2s and other immune cells, including mast cells and basophils promoting ILC2 recruitment, ILC2s activating DCs, Th2 cells and B cells, and ILC2s interacting with neutrophils, although both stimulatory and inhibitory effects on neutrophils have been demonstrated. ILC2s can also express MHCII (237) and co-stimulatory molecules, process and present antigen *in vitro*, and contribute to T cell responses *in vivo*.

The interactions between ILC2s and other immune cells have been considered to be mainly via cytokine production, and few studies have examined the *in vivo* dynamic behaviour of tissue ILC2s. Intravital imaging of the ear skin showed ILC2s moving at similar speed to migratory DCs and interacting with mast cells (250). *Ex vivo* imaging of sectioned lung explants showed ILC2s moving at higher speed compared to T cells post IL-33 stimulation (307). Whilst ILC2s are present in LNs, to date there are little data on the *in vivo* dynamics of LN ILC2s. ILC2s have been associated with inflammatory disorders such as asthma (346), and understanding their dynamic behaviour would add to knowledge on the role of ILC2s in type 2 inflammation and potentially lead to future development of ILC2-targeted therapies.

Therefore I addressed the question of whether ILC2s exhibit different dynamic behaviour in homeostasis and in inflammation. Using two different helminth models of type 2 inflammation, I examined ILC2s in Peyer's patch and popliteal LN to quantify their *in vivo* dynamics at baseline and following type 2 inflammatory stimuli, and to examine for cellular interactions. For comparison I examined the behaviour of ILC2s in small bowel mucosa. I also investigated the use of a novel triple reporter mouse for simultaneous imaging of different ILC and other immune cell subsets.

5.2. CD2/IL-13 double reporter mouse for imaging ILC2s

For imaging ILC2s *in vivo*, I used a CD2-GFP/IL-13-tomato double reporter mouse, in which ILC2s were identified as $CD2^{-}IL\text{-}13^{+}$ cells, whereas Th2 cells were $CD2^{+}IL\text{-}13^{+}$. Previous studies demonstrated that the majority of IL-13-producing cells in the mesenteric LN 5 days following *N. brasiliensis* infection were ILC2s (237). I made attempts at intravital imaging of mesenteric LN, but this was difficult to achieve, as the process of surgical exposure of the LN caused significant trauma and bleeding to tissues, rendering live imaging problematic.

Instead, Peyer's patches and popliteal LNs were imaged, using *N. brasiliensis* infection and *S. mansoni* immunisation respectively as experimental models of type 2 inflammation. By flow cytometry, both tissues had very few $IL\text{-}13^{+}$ cells at baseline, but these were all ILC2s, being positive for IL-7Rα (all ILCs) and ICOS (ILC2s), and negative for CD2 (T cells), Siglec-F (eosinophils), and lineage markers CD8, CD5 (T cells), CD19 (B cells), NK1.1 (NKT cells), CD11b (myeloid cells), CD11c (dendritic cells), Gr1 (neutrophils), FcεR1 (basophils), and Ter119 (red blood cells) (Figure 5.1A,B). Therefore the CD2/IL-13 reporter provides a model for studying ILC2s *in vivo*, with $CD2^{+}$ T cells acting as *in vivo* controls. However, gating in reverse showed that of the $Lin^{-}SiglecF^{-}IL\text{-}7R\alpha^{+}ICOS^{+}$ cells in the popliteal LN, 40% were $IL\text{-}13^{+}$, illustrating the caveat that not every ILC2 is visualised with this reporter mouse.

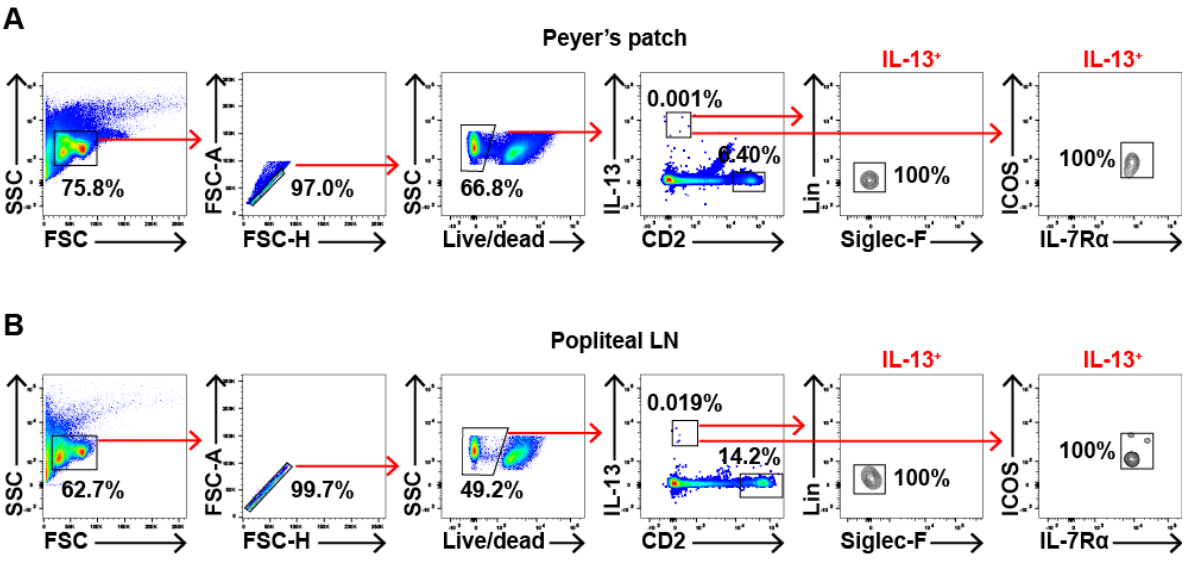

Figure 5.1. Specificity of $IL\text{-}13^{+}$ cells for ILC2s in the CD2/IL-13 reporter. Flow cytometry plots showing proportions of ILC2s ($Lin^{-}Siglec\text{-}F^{-}$, $IL\text{-}7R\alpha^{+}ICOS^{+}$) in $CD2^{-}IL\text{-}13^{+}$ cell populations in (A) Peyer's patch and (B) popliteal LN of a CD2/IL-13 reporter mouse.

5.3. *N. brasiliensis* infection model

In *N. brasiliensis* infection (Section 1.17.3), L3 larvae infect mice by penetrating the skin, and migrate via blood vessels into the lungs, where they mature into L4 larvae and cause acute lung injury. The larvae are coughed up and swallowed, reaching the small bowel where they mature into egg-laying adults, which induce a strong Th2 response leading to worm expulsion (249,303). This is a commonly used model of type 2 inflammation of the lungs and gut, and therefore I used this model to investigate the behaviour of ILC2s *in vivo*. Confocal microscopy of lung tissue harvested following *N. brasiliensis* infection showed the presence of ILC2s, being IL-13-high cells that were negative for CD2 and siglec-F; ILC2s were mostly located near clusters of T cells ($CD2^+$) and eosinophils (siglec-F^+) within the lung (Figure 5.2A,B), and in the mediastinal LN ILC2s were mostly in T cell zones although some were also in B cell areas (Figure 5.3A).

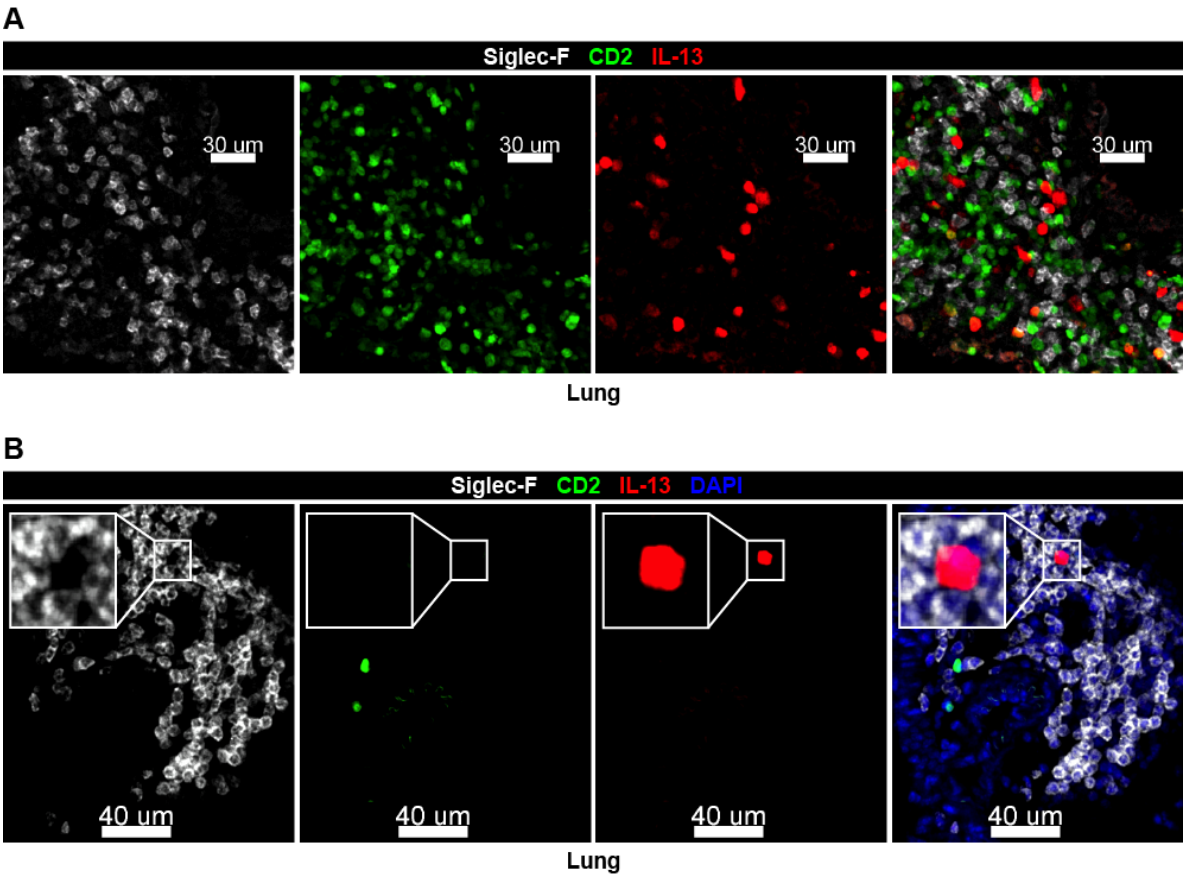

Figure 5.2. ILC2s in lungs following *N. brasiliensis* infection. (A) Confocal image of the lung of CD2/IL-13 mouse 3 days post *N. brasiliensis* infection, showing IL-13^+ ILC2s; scale bar 30 μm, Z 2 μm. (B) Confocal image of ILC2 in the lung post *N. brasiliensis* infection; scale bar 40 μm, Z 2 μm.

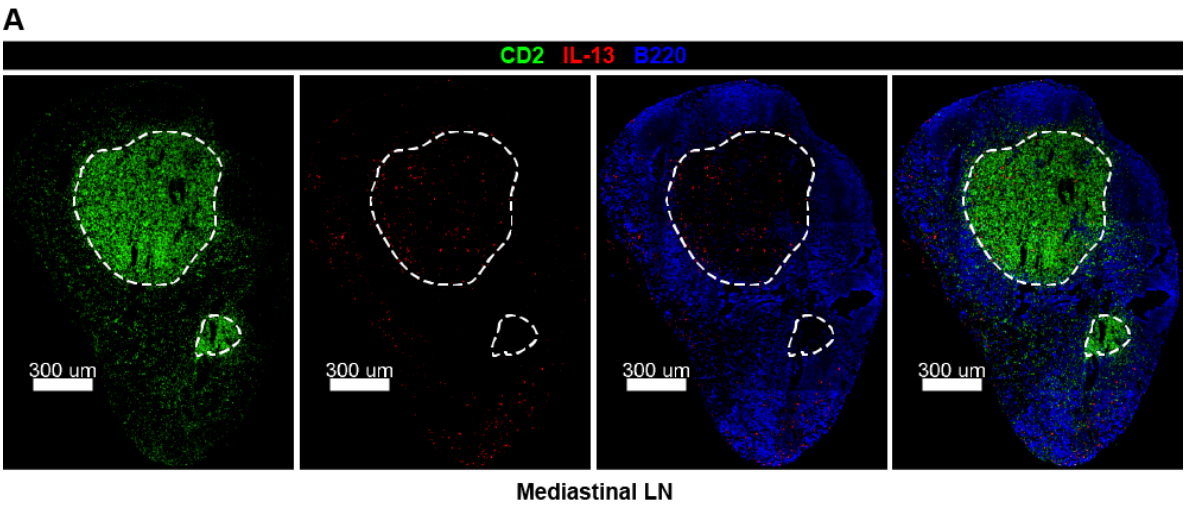

Figure 5.3. ILC2s in mediastinal LN following *N. brasiliensis* infection. (A) Confocal image of whole mediastinal LN following *N. brasiliensis* infection showing location of IL-13$^+$ ILC2s in relation to T cell areas (white dotted lines); scale bar 300 μm, Z 2 μm.

5.3.1. ILC2s in Peyer's patch following *N. brasiliensis* infection

From the lungs, *N. brasiliensis* larvae migrate into the gut where they mature, with adult worms seen in the small bowel from about 4 days post infection. Intravital examination of Peyer's patches, lymphoid aggregates on the wall of the small bowel, showed that whilst some IL-13$^+$ cells were present at baseline, the number increased from 5 days following infection, persisting to 9 days post infection, when worm expulsion is expected to occur (Figure 5.4A,B).

Similar to the lungs, most IL-13$^+$ cells were located in T cell areas. At 5 days post infection, an early time point following the arrival of *N. brasiliensis* into the small bowel, these IL-13$^+$ cells were CD2$^-$, confirming their identity as ILC2s (Figure 5.4C). At this early time point, Th2 cells (CD2$^+$IL-13$^+$) were not present, suggesting that ILC2s instead were important early sentinel effector cells following type 2 inflammatory challenge.

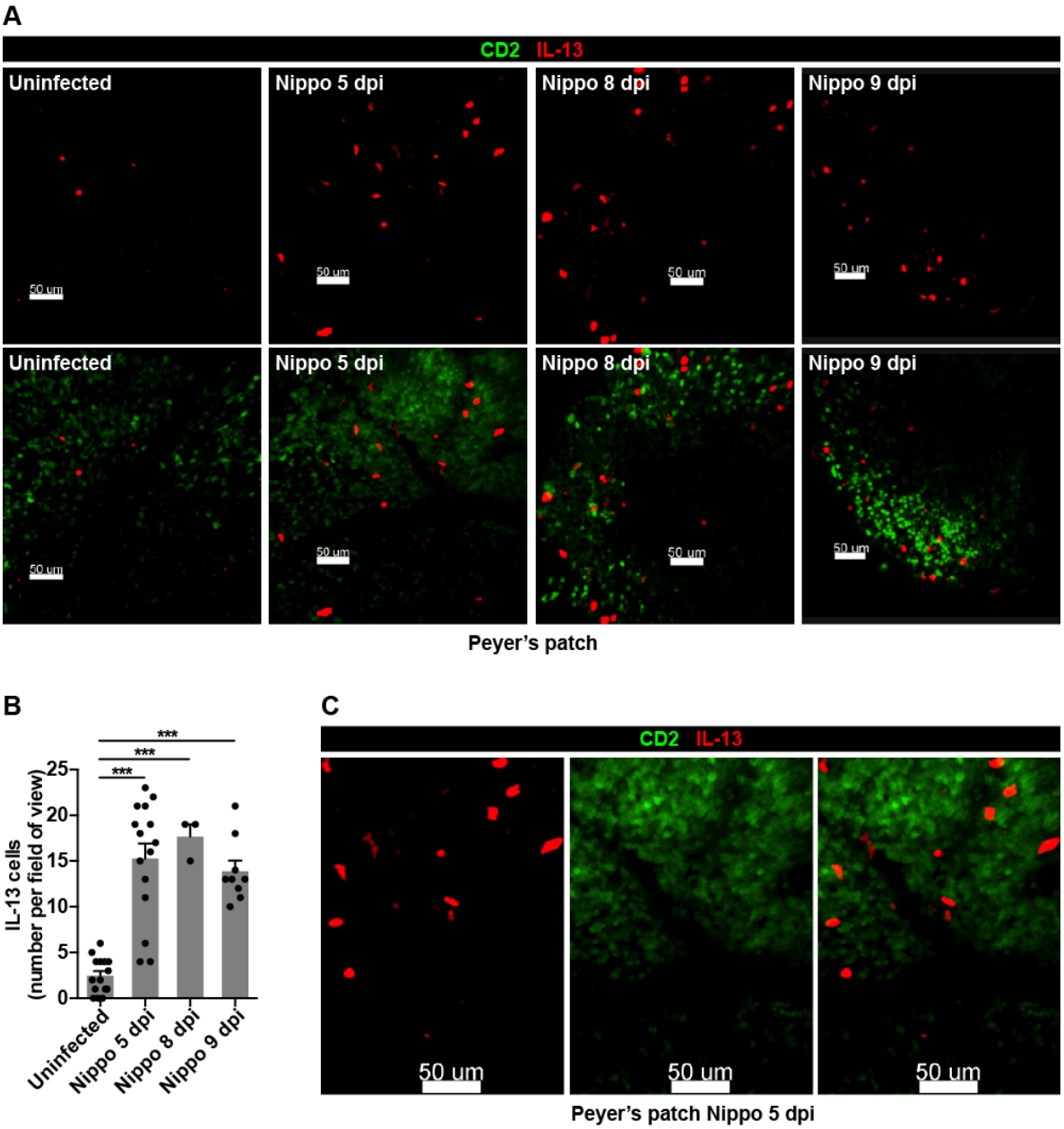

Figure 5.4. ILC2s in Peyer's patch following *N. brasiliensis* infection. (A) Intravital images of IL-13$^+$ ILC2s in Peyer's patch in CD2/IL-13 mice uninfected, and 5, 8 and 9 days post infection (dpi) with *N. brasiliensis* (Nippo); scale bar 50 μm, Z stack 40 μm. (B) Quantification of ILC2 numbers per field of view; ***$p < 0.001$ *vs* uninfected. Pooled data from 1-5 movies from 1-3 mice for each time point, with each dot representing one field of view. (C) Intravital image of IL-13$^+$ ILC2s in Peyer's patch 5 dpi; scale bar 50 μm, Z stack 40 μm.

5.4. Dynamic behaviour of ILC2s in Peyer's patch

I then examined the *in vivo* dynamic behaviour of ILC2s in the Peyer's patch at baseline and 5 days post *N. brasiliensis* infection. In uninfected Peyer's patch, ILC2s and T cells moved at similar speed and with similar directionality. Following *N. brasiliensis* infection, T cells did not show any increase in speed of movement, although the directionality of movement increased compared to that of uninfected T cells. ILC2s, in contrast, moved at significantly greater speed and with increased directionality, compared to T cells as well as to uninfected ILC2s (Figure 5.5A-C). ILC2s also increased in size post infection, showing significantly higher cell surface area and cell volume (Figure 5.6A-C). No cell divisions were observed during the acquisition of intravital movies. Therefore, these data showed that ILC2s increased in size and moved at faster speed following *N. brasiliensis* infection.

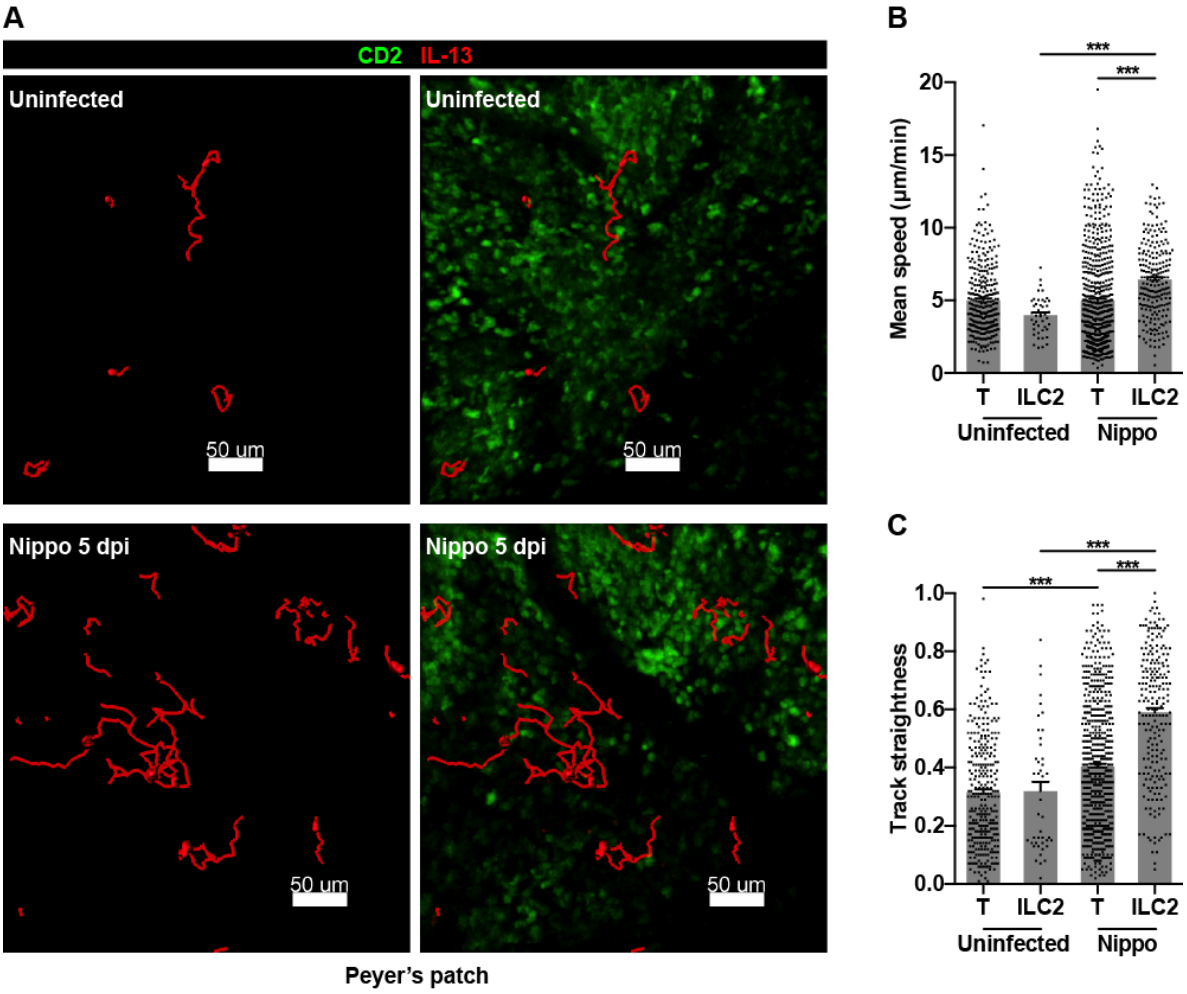

Figure 5.5. Dynamic behaviour of ILC2s in Peyer's patch. (A) Intravital images of IL-13^{+} ILC2s in CD2/IL-13 Peyer's patch, uninfected and 5 dpi, cell tracks in red; scale bar 50 μm, Z stack 48 μm. (B-C) Quantification of (B) mean speed and (C) track straightness (measure of

directionality) of Peyer's patch T cells and ILC2s, uninfected and 5 dpi; ***$p < 0.001$. Pooled data from 6-9 movies from 3 mice per condition, with each dot representing one cell track.

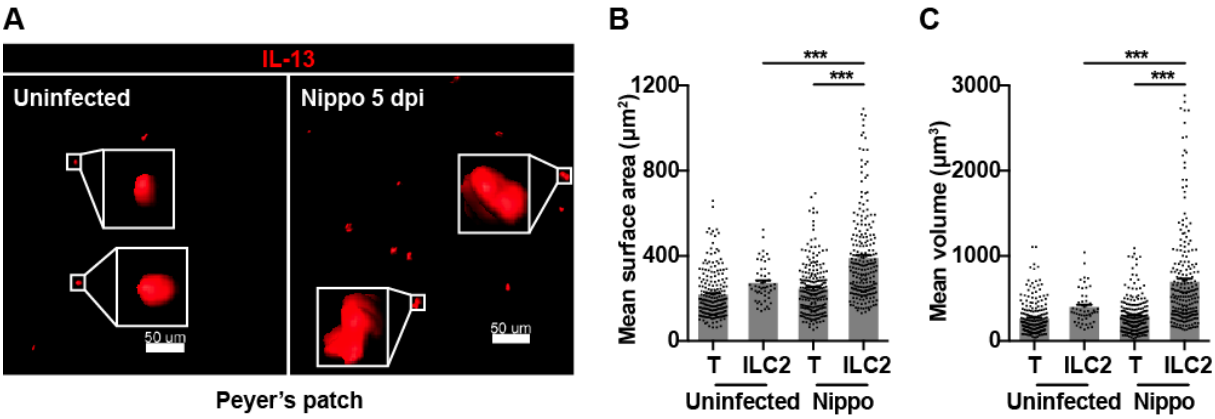

Figure 5.6. Cell size of ILC2s in Peyer's patch. (A) Intravital images of IL-13$^+$ ILC2s in Peyer's patch, uninfected and 5 dpi; scale bar 50 µm, Z stack 48 µm, insets (white boxes) at same scale. (B-C) Quantification of (B) mean cell surface area and (C) mean cell volume of T cells and ILC2s, uninfected and 5 dpi; ***$p < 0.001$. Pooled data from 6-9 movies from 3 mice per condition, with each dot representing one cell track.

5.4.1. Interactions between ILC2s and T cells in Peyer's patch

In uninfected mice, rare incidences of interactions between ILC2s and T cells were observed (Figure 5.7A), although the majority of ILC2s moved within the Peyer's patch without interacting with T cells. Following *N. brasiliensis* infection, there were no incidences of interactions seen between ILC2s and T cells in any of the intravital movies acquired.

Overall, *in vivo* imaging of ILC2s and T cells in Peyer's patch showed that, early following *N. brasiliensis* infection, ILC2s increased in size and moved with increased speed and directionality, without interacting with T cells, suggesting a role of ILC2s in distributing cytokines early in the Th2 response.

A

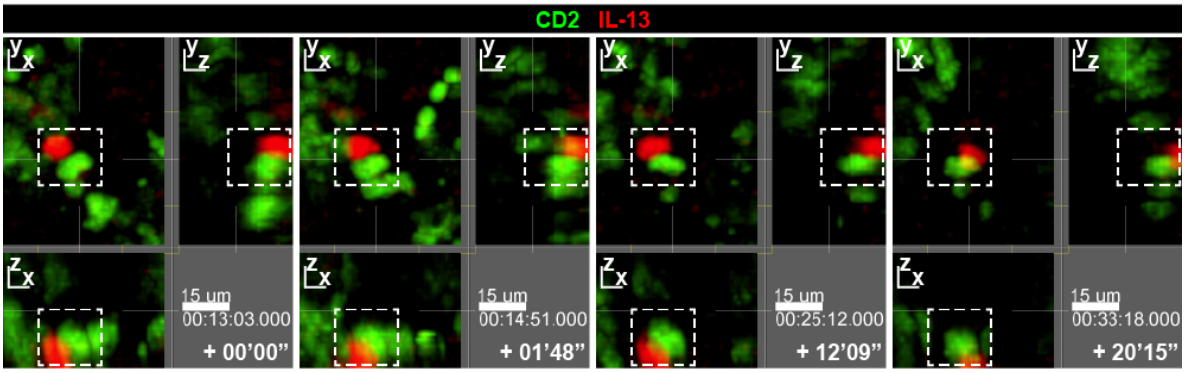

Uninfected Peyer's patch

Figure 5.7. Interaction between ILC2 and T cell in Peyer's patch. (A) Intravital image showing interaction between IL-13$^+$ ILC2 and CD2$^+$ T cell (dotted white boxes) in an uninfected Peyer's patch, image shown in three planes; scale bar 15 μm, Z stack 36 μm.

5.5. Dynamic behaviour of ILC2s in small bowel following *N. brasiliensis* infection

Next I examined the presence and behaviour of IL13$^+$ ILC2s in the wall of the small bowel at baseline and following *N. brasiliensis* infection. There were very few IL13$^+$ ILC2s present in the small bowel wall in uninfected mice, and the number of IL13$^+$ ILC2s significantly increased 5 days post *N. brasiliensis* infection (Figure 5.8A,B). ILC2s were located in the mucosa, where T cells were also present; similar to the Peyer's patch, at this early time point the IL-13$^+$ cells present in the small bowel were CD2$^-$IL-13$^+$ ILC2s rather than CD2$^+$IL-13$^+$ Th2 cells (Figure 5.8C).

In uninfected mice, there were too few ILC2s in the small bowel wall to examine their *in vivo* behaviour by intravital imaging. Following *N. brasiliensis* infection, ILC2s were observed to crawl along the small bowel wall (Figure 5.9A); in keeping with findings in the Peyer's patch, ILC2s in the small bowel moved at higher speed and with greater directionality compared to T cells (Figure 5.9B,C). There was, however, no difference in mean cell surface area or mean cell volume between ILC2s and T cells (Figure 5.9D,E).

Whilst there were no observed interactions between ILC2s and T cells in the Peyer's patch following *N. brasiliensis* infection, in the small bowel wall ILC2s were observed to interact with T cells, with an example of a prolonged 40-minute interaction shown in Figure 5.10A.

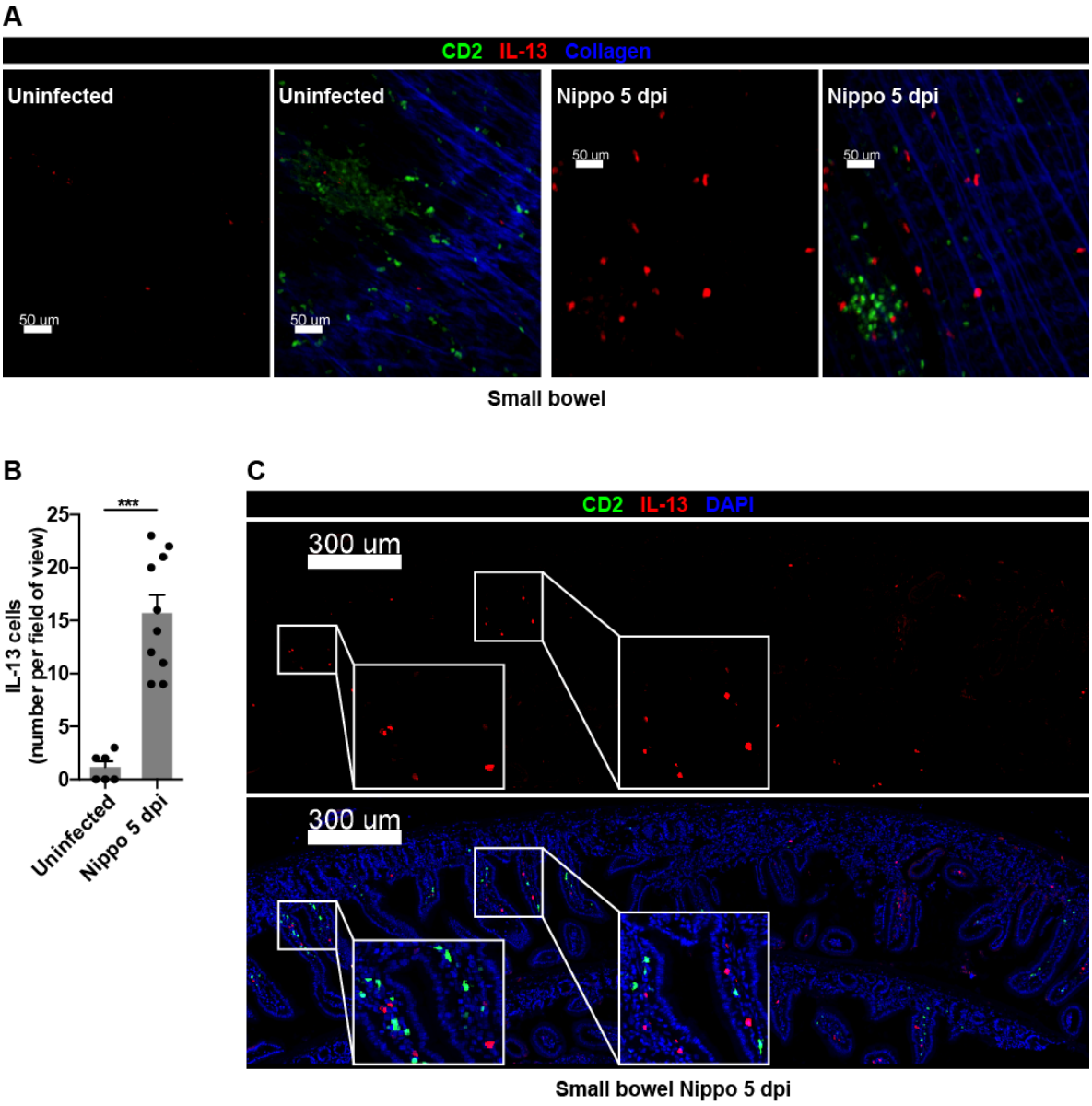

Figure 5.8. ILC2s in small bowel following *N. brasiliensis* infection. (A) Intravital image of IL-13^{+} ILC2s in small bowel, uninfected and 5 dpi; scale bar 50 μm, Z stack 16-30 μm. (B) Quantification of ILC2 numbers per field of view; ***$p < 0.001$. Pooled data from 4 movies from 1-3 mice for each condition, with each dot representing one field of view. (C) Confocal image of IL-13^{+} ILC2s in the small bowel 5 dpi; scale bar 300 μm, Z 2 μm.

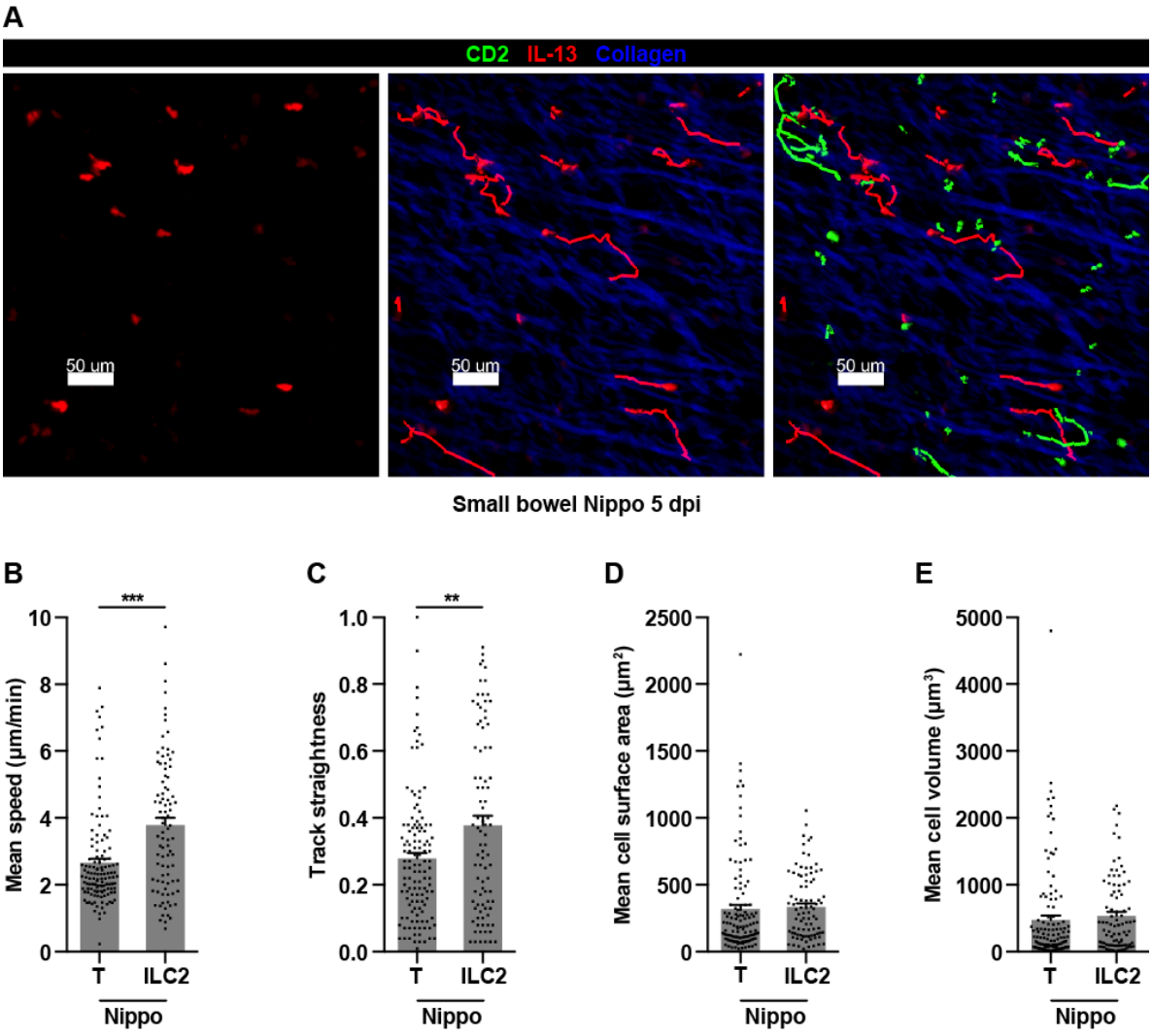

Figure 5.9. Dynamic behaviour of ILC2s in small bowel. (A) Intravital image of small bowel 5 dpi, with $CD2^+$ T cell tracks in green and $IL\text{-}13^+$ ILC2 cell tracks in red; scale bar 50 µm, Z stack 30 µm. (B-E) quantification of (B) mean speed, (C) track straightness, (D) mean cell surface area and (E) mean cell volume of T cells and ILC2s 5 dpi; $^{**}p < 0.01$, $^{***}p < 0.001$. Pooled data from 3 movies, with each dot representing one cell track.

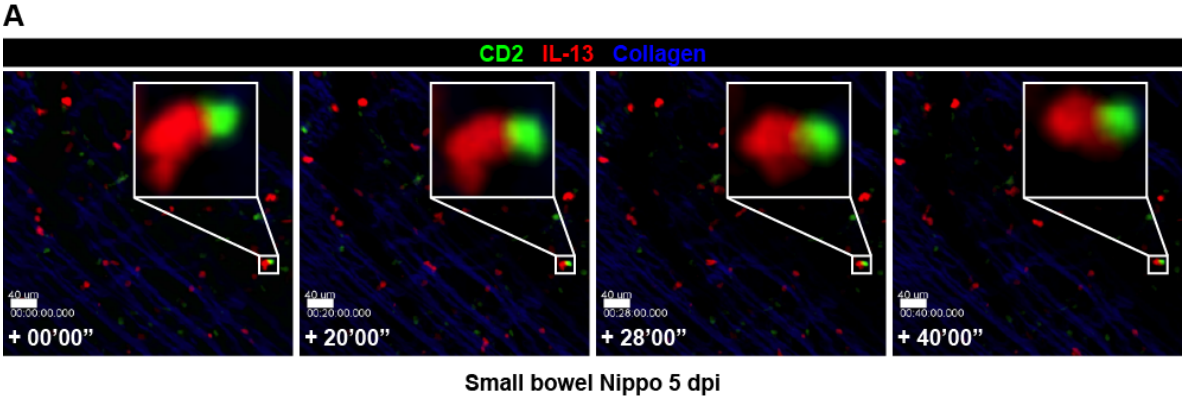

Figure 5.10. Interaction between ILC2 and T cell in small bowel. (A) Intravital image of small bowel 5 dpi showing interaction between IL-13$^+$ ILC2 and CD2$^+$ T cell (white box); scale bar 40 μm, *Z* stack 26 μm.

Therefore, early following *N. brasiliensis* infection in the gut, ILC2s were recruited into Peyer's patches and the small bowel wall, crawling at greater speed and with greater directionality compared to T cells. In the Peyer's patch, ILC2s increased in cell size and were not observed to interact with T cells; in the small bowel wall, ILC2s did not increase in size, but interactions were observed between ILC2s and T cells. Together, these data demonstrated changes in the dynamic behaviour of ILC2s early following *N. brasiliensis* infection, with differences in the Peyer's patch and small bowel wall suggestive of ILC2s having different roles in the early response to type 2 inflammatory stimuli.

5.6. *S. mansoni* immunisation model

To complement the data on the dynamic behaviour of ILC2s in the Peyer's patch and small bowel following *N. brasiliensis* infection, I next used a different model of Th2 inflammation to study ILC2 behaviour *in vivo*. *S. mansoni* is a parasite that causes significant disease in humans worldwide, and *S. mansoni* eggs can induce strong Th2 response in mice, with ILC2s shown to be involved in this response (294,305,306). I therefore used *S. mansoni* eggs as an experimental model to investigate the behaviour of ILC2s.

CD2/IL-13 mice were subcutaneously injected with UV-killed *S. mansoni* eggs into the left footpad and PBS into the right footpad, followed by intravital imaging of the draining popliteal LNs day 1 post immunisation. This experimental setup had the advantage of having *S. mansoni*-immunised and control popliteal LNs within the same animals.

5.6.1. ILC2s in popliteal LN following footpad *S. mansoni* immunisation

At the early time point of day 1 following immunisation, the IL-13$^+$ cells present in the popliteal LN were ILC2s not Th2 cells, as they were CD2$^-$ (Figure 5.11A). This was consistent with the flow cytometry data in Figure 5.1B. Similar to the data from the Peyer's patch, ILC2s were mostly located near T cell areas within popliteal LNs, and ILC2 cell numbers were higher following *S. mansoni* immunisation compared to control (Figure 5.11A,B).

Preliminary analysis to date showed that, following *S. mansoni* immunisation, popliteal LN ILC2s moved at a higher mean speed compared to T cells (Figure 5.11C), but there was no difference in the directionality of movement (Figure 5.11D), or in cell size (Figure 5.11E). This was therefore supportive of the data on the dynamic behaviour of ILC2s in the gut, although more data are required to draw conclusions on the changes in dynamic behaviour of ILC2s in the popliteal LN following *S. mansoni* immunisation.

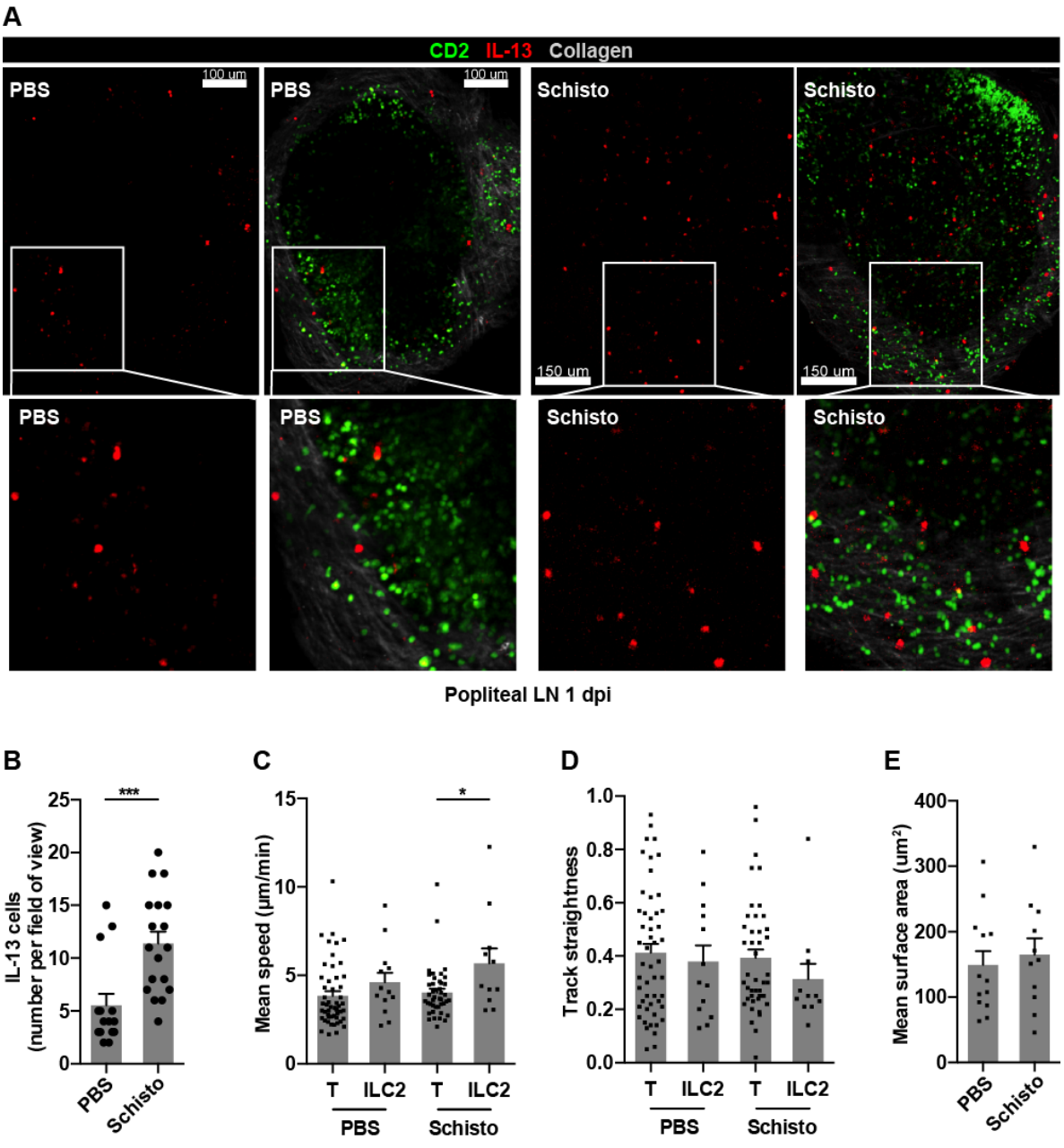

Figure 5.11. Dynamic behaviour of ILC2s in popliteal LN following PBS or *S. mansoni* immunisation. (A) Intravital images showing IL-13^{+} ILC2s in popliteal LN 1 day post immunisation (dpi) with PBS or *S. mansoni* (Schisto) by subcutaneous footpad injections; PBS, scale bar 100 μm, Z stack 40 μm; Schisto, scale bar 150 μm, Z stack 70 μm. (B)

Quantification of ILC2 numbers per field of view; ***$p < 0.001$. Pooled data from 5-6 movies from 4 mice for each condition, with each dot representing one field of view. (C-D) Quantification of (C) mean speed and (D) track straightness of popliteal LN T cells and ILC2s, 1 dpi; *$p < 0.05$. Data from 1 movie for each condition. (E) Quantification of mean cell surface area of popliteal LN ILC2s, 1 dpi. Data from 1 movie for each condition.

5.7. Id2/Rora/Rorc triple reporter mouse for imaging ILCs

The CD2/IL-13 reporter mouse provided a useful tool for studying ILC2s *in vivo*; however, one potential limitation was that only IL-13$^+$ ILC2s were visualised, and this might not represent the whole ILC2 population, especially at baseline when IL-13 production might be lower. To address this, I investigated the use of a novel Id2-BFP/Rora-teal/Rorc-katushka triple reporter mouse to examine ILC subsets (224).

Id2 is a transcription factor required for the differentiation of all ILC subsets from common lymphoid progenitors (6,220,347); it is also expressed by DCs (348). RORα, encoded by *Rora*, is required for ILC2 development. RORγt, encoded by *Rorc*, is expressed by ILC3s but not ILC2s (232,245). Therefore, with this triple reporter, ILC2s would be expected to be Id2$^+$Rora$^+$ (Figure 5.12A population 2), and ILC3s Id2$^+$Rora$^+$Rorc$^+$ (Figure 5.12A population 3), providing a means of simultaneously studying different ILC subsets, with other cells, such as Id2$^+$ cells (largely DCs, Figure 5.12A population 1), Rora$^+$ and Rora$^+$Rorc$^+$ cells (T cells), acting as control cells within the same *in vivo* environment.

Popliteal LN (PBS- and *S. mansoni*-immunised), Peyer's patch and small bowel from the triple reporter were harvested, and tissues mechanically dissociated for flow cytometry. The markers CD3 (T cells), IL-7Rα (ILCs, provided a negative T cell marker also present) and KLRG1 (ILC2s) were used to identify ILC2s as IL-7Rα$^+$KLRG1$^+$, and ILC3s as CD3$^-$IL-7Rα$^+$; these were applied to the Id2$^+$ populations as negative control. The proportions of Id2$^+$Rora$^+$ cells that were ILC2s in the PBS-immunised popliteal LN (14.7%), *S. mansoni*-immunised popliteal LN (35.8%) and Peyer's patch (38.0%) were lower than expected, and some Id2$^+$Rora$^+$ cells were T cells. A higher proportion in the small bowel lamina propria (72.8%) was ILC2s. The purity of the Id2$^+$Rora$^+$Rorc$^+$ populations was better, with higher proportions in the PBS-immunised popliteal LN (63.0%) and *S. mansoni*-immunised popliteal LN (69.2%) being ILC3s, and the majority in the Peyer's patch (95.6%) and small bowel lamina propria (99.1%) being ILC3s (Figure 5.12B-E).

Therefore, the Id2/Rora/Rorc triple reporter had limitations in its use as a tool for examining ILCs, with variable proportions of Id2$^+$Rora$^+$ cells being ILC2s in different tissues, but a higher proportion of Id2$^+$Rora$^+$Rorc$^+$ cells being ILC3s, especially in the gut where the triple reporter mouse could potentially be used for simultaneous ILC2 and ILC3 imaging.

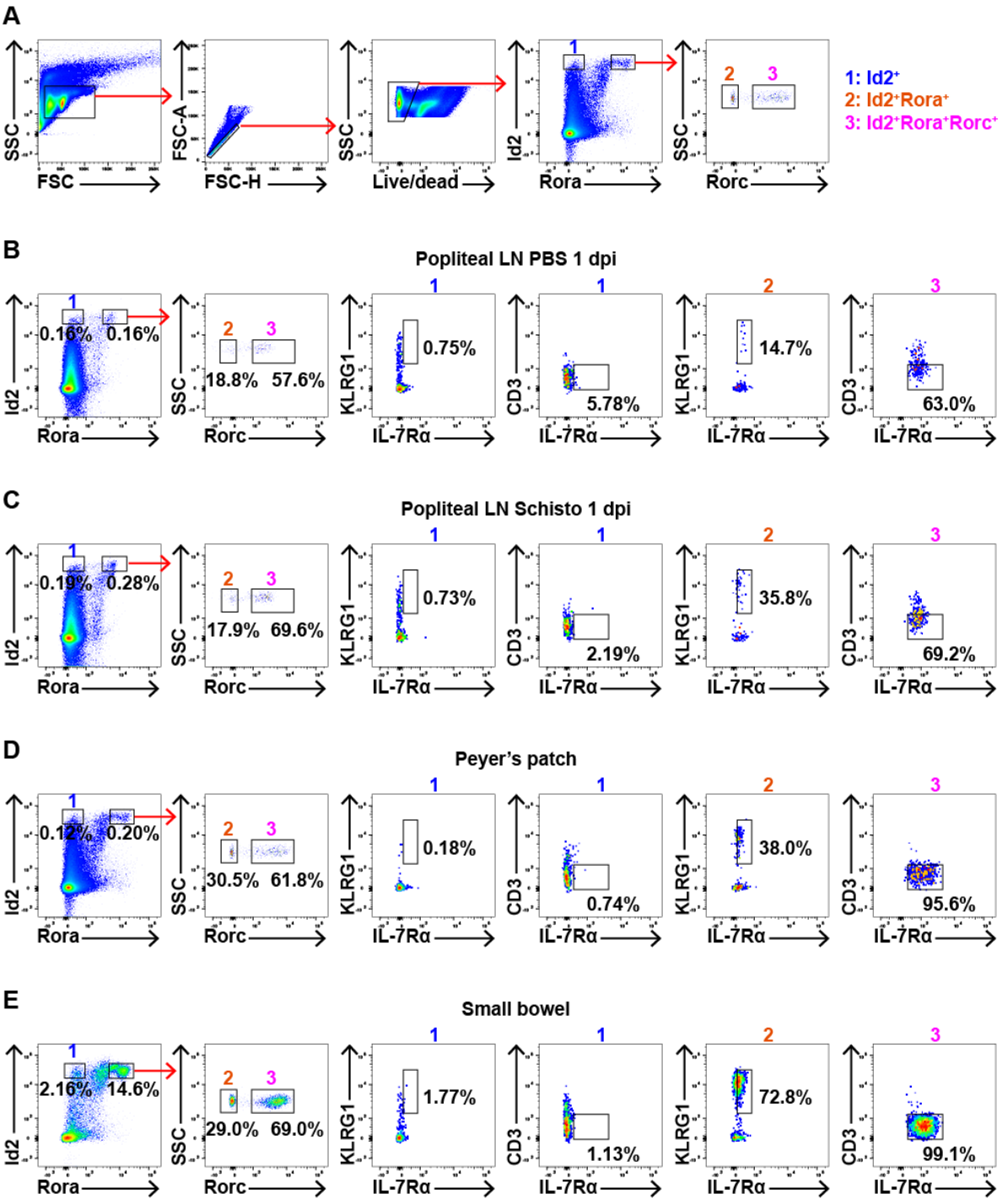

Figure 5.12. Specificity of Id2/Rora/Rorc triple reporter cell populations for ILCs. (A) Flow cytometry plots showing gating strategy for identifying Id2$^+$ (population 1), Id2$^+$Rora$^+$ (population 2) and Id2$^+$Rora$^+$Rorc$^+$ (population 3) cells. (B-E) Flow cytometry plots of (B)

PBS popliteal LN, (C) Schisto popliteal LN, (D) Peyer's patch and (E) small bowel, showing purity of Id2$^+$Rora$^+$ (population 2) for ILC2s (IL-7Rα$^+$KLRG1$^+$), and of Id2$^+$Rora$^+$Rorc$^+$ (population 3) for ILC3s (CD3$^-$IL-7Rα$^+$), with Id2$^+$ (population 1) as control.

5.7.1. Identifying triple reporter cell populations by microscopy

An imaging strategy of sequential single- and two-photon excitation was used to acquire images with the triple reporter fluorophores, with additional CD169 labelling of SCS macrophages in some experiments (Section 3.10.4). This allowed visualisation of the three different cell populations (Id2$^+$, Rora$^+$, Rorc$^+$) of the triple reporter mouse, and most of these cells were situated within T cell rather than B cell areas in the popliteal LN (Figure 5.13A).

In the analysis of these images, 'surfaces' were generated for each cell population (Id2$^+$, Rora$^+$, Rorc$^+$), and dual- or triple-colour cells were manually identified and assigned new surfaces, including Id2$^+$Rora$^+$, Id2$^+$Rora$^+$Rorc$^+$ and Rora$^+$Rorc$^+$ cells. This resulted in cellular maps of multiple cell populations. Id2$^+$Rora$^+$ and Id2$^+$Rora$^+$Rorc$^+$ populations were largely within T cell areas, in both PBS-stimulated (Figure 5.14A) and *S. mansoni*-stimulated (Figure 5.15A) popliteal LNs.

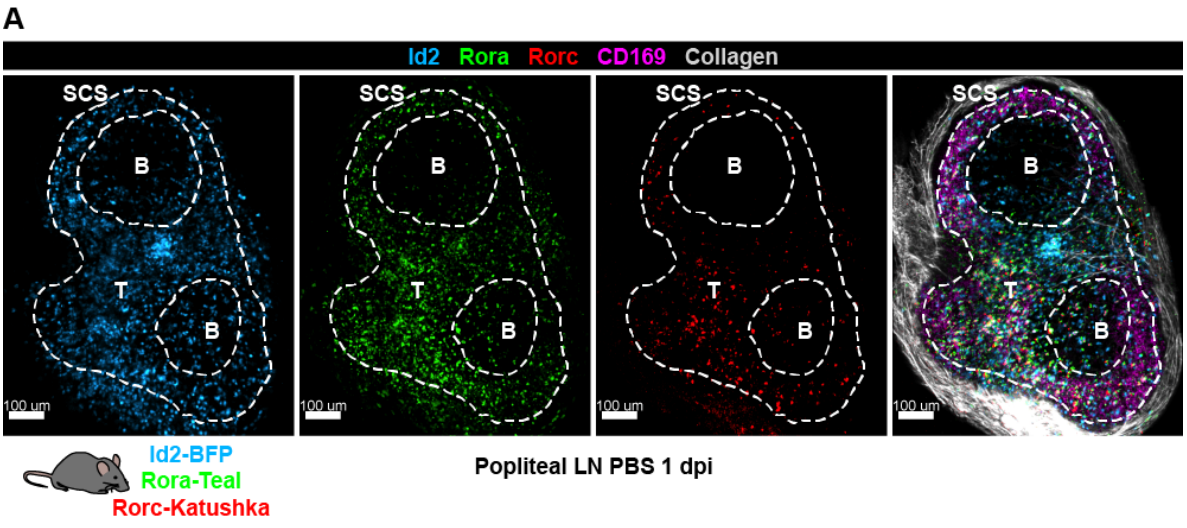

Figure 5.13. Microscopy of Id2/Rora/Rorc triple reporter LN. (A) Intravital image of whole popliteal LN showing Id2$^+$, Rora$^+$ and Rorc$^+$ populations in relation to B and T cell zones and SCS (SCS macrophages labelled with anti-CD169); scale bar 100 μm, Z stack 40 μm.

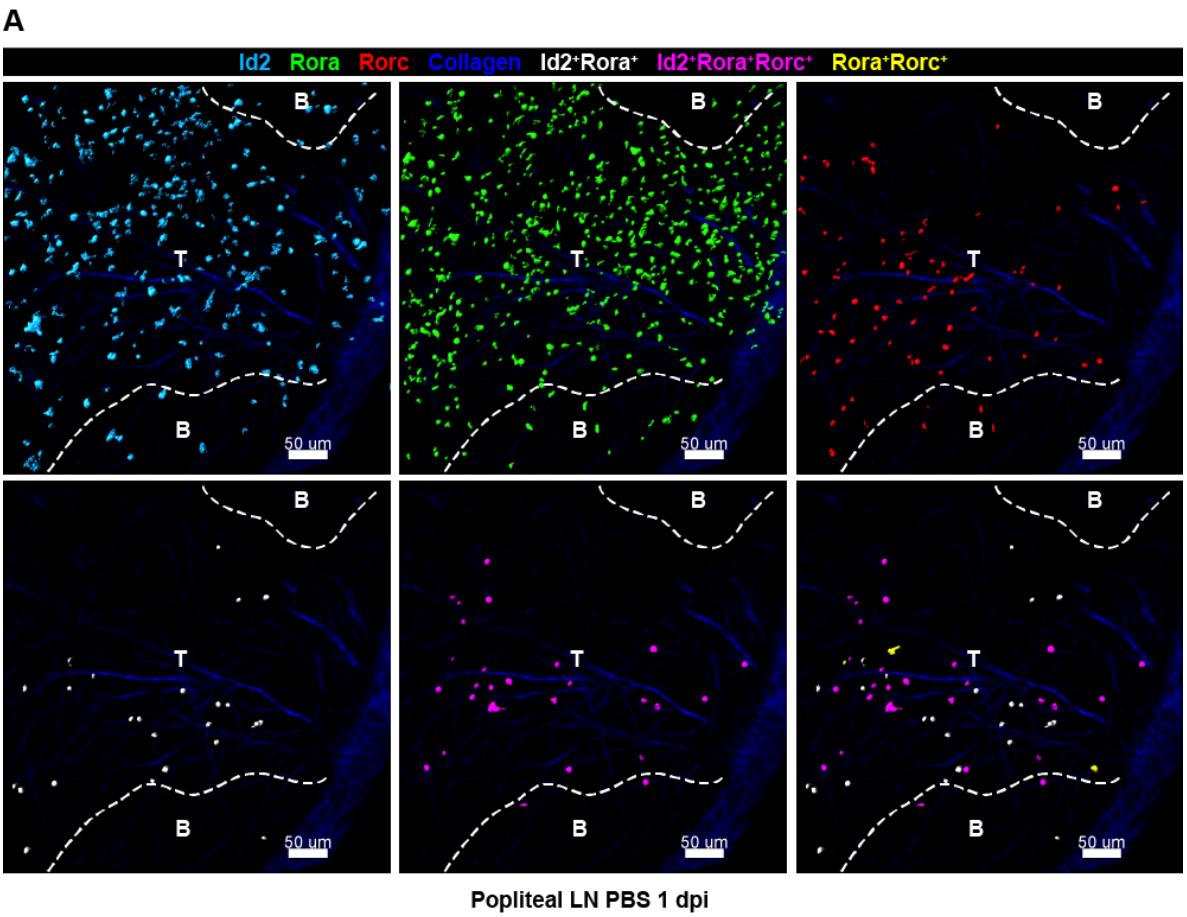

Figure 5.14. Identifying triple reporter cell populations by microscopy in PBS-immunised LN. (A) Image showing surfaces rendered from intravital imaging of popliteal LN 1 day post PBS immunisation, with B and T cell areas outlined (dotted white lines); scale bar 50 µm, Z stack 30 µm.

A

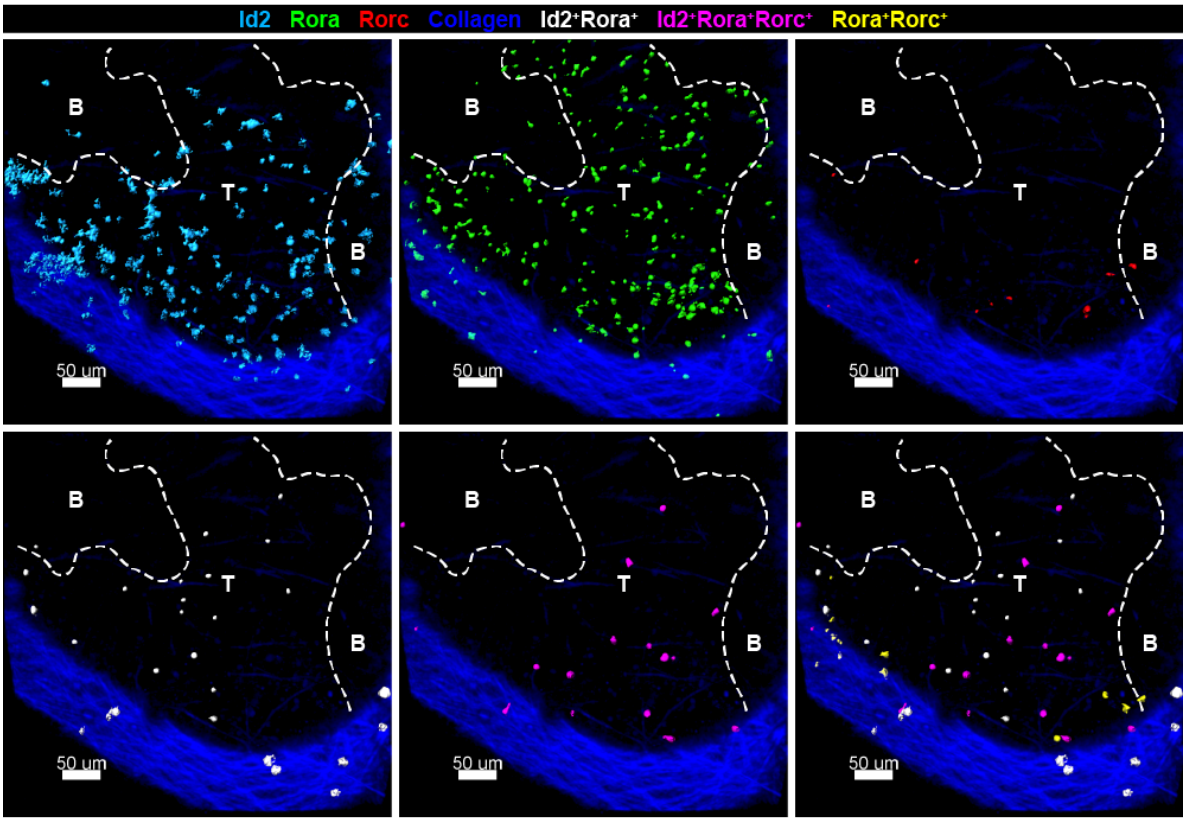

Figure 5.15. Identifying triple reporter cell populations by microscopy in *S. mansoni*-immunised LN. (A) Image showing surfaces rendered from intravital imaging of popliteal LN 1 day post *S. mansoni* immunisation, with B and T cell areas outlined (dotted white lines); scale bar 50 μm, Z stack 36 μm.

5.8. Dynamic behaviour of triple reporter cell populations in popliteal LN

Four populations of cells were analysed: Id2$^+$ (including DCs), Rora$^+$Rorc$^+$ (T cells) (349), Id2$^+$Rora$^+$ (including ILC2s), and Id2$^+$Rora$^+$Rorc$^+$ (ILC3s) (Figure 5.16A). Id2$^+$ cells crawled at the slowest speed and with the least directionality, consistent with them being DCs, previously shown to move slower than T cells in LNs (350). Id2$^+$Rora$^+$ cells moved at lower speed and directionality following *S. mansoni* immunisation. Id2$^+$Rora$^+$Rorc$^+$ ILC3s moved with mean speed similar to that of LN neutrophils but higher than that of Id2$^+$Rora$^+$ cells, with no increase following *S. mansoni* immunisation (Figure 5.16B,C). Id2$^+$Rora$^+$Rorc$^+$ cells were larger than Id2$^+$Rora$^+$ cells (Figure 5.16D,E). The reduction in speed and directionality of Id2$^+$Rora$^+$ cells following a Th2 stimulus would suggest potential interactions with other LN immune cells, for example with Id2$^+$ DCs (Figure 5.17A).

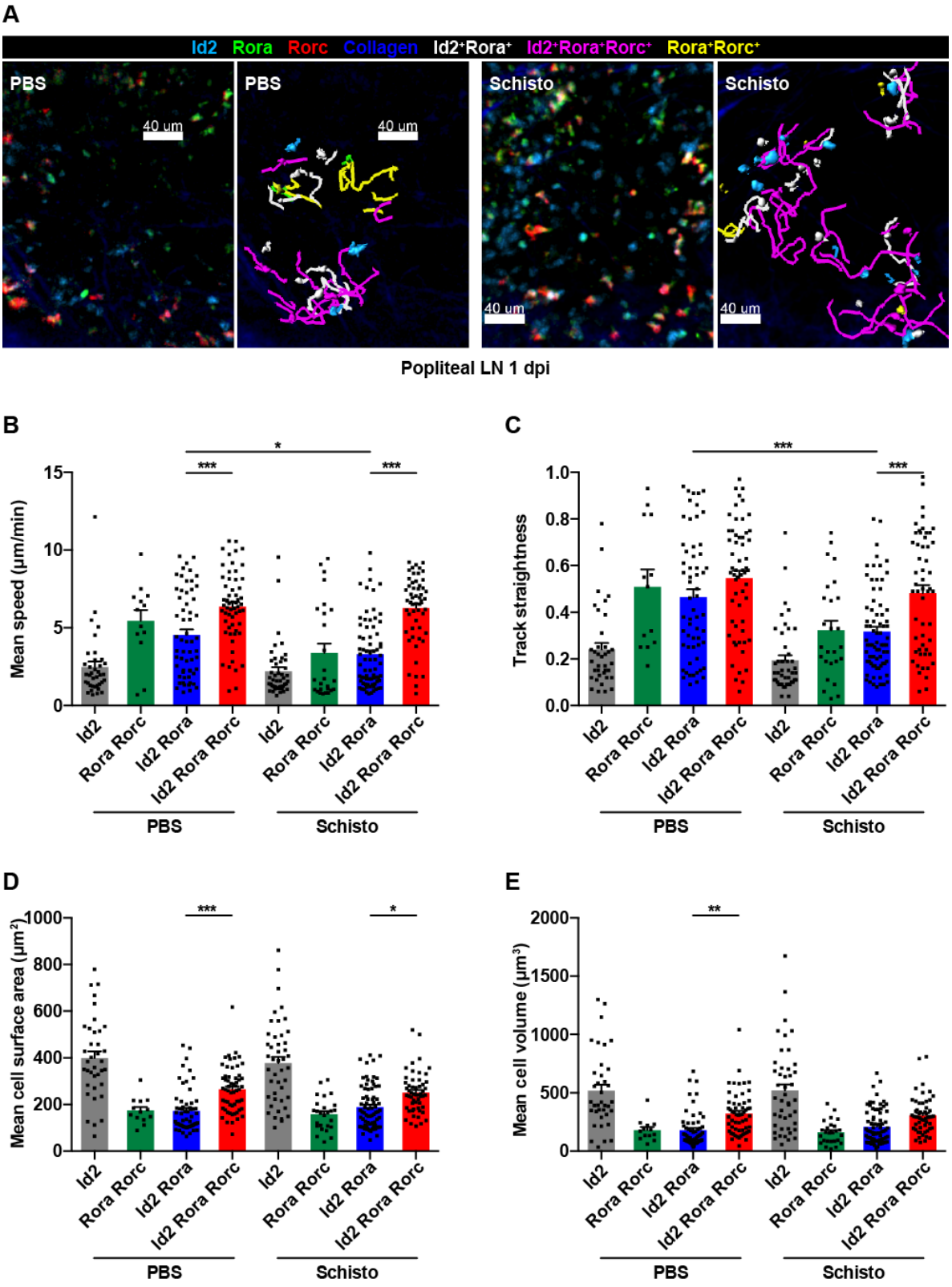

Figure 5.16. Dynamic behaviour of triple reporter cell populations in popliteal LN. (A) Intravital images of triple reporter popliteal LN 1 dpi (PBS or Schisto), with cell tracks shown for Id2$^+$ (cyan), Rora$^+$Rorc$^+$ (yellow), Id2$^+$Rora$^+$ (white) and Id2$^+$Rora$^+$Rorc$^+$ (purple); scale bar 40 µm, Z stack 32 µm. (B-E) Quantification of (B) mean speed, (C) track straightness, (D) mean cell surface area and (E) mean cell volume of cell populations as per (A); *p < 0.05, **p

< 0.01, ***p < 0.001. Pooled data from 5-7 movies from 3-4 mice per condition, with each dot representing one cell track.

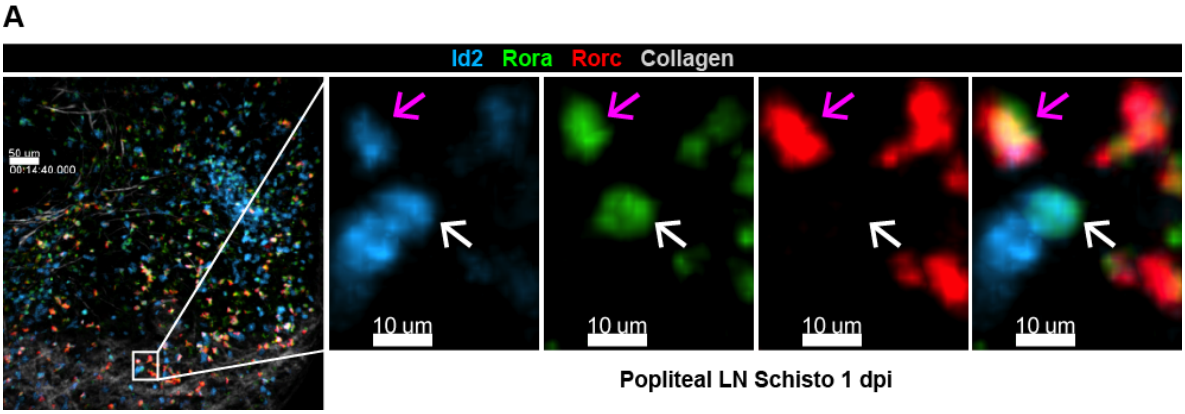

Figure 5.17. Interaction between Id2$^+$ and Id2$^+$Rora$^+$ cells following *S. mansoni* immunisation. (A) Intravital image of popliteal LN (Schisto 1 dpi) showing interaction between Id2$^+$ cell and Id2$^+$Rora$^+$ cell (white arrow), with an adjacent Id2$^+$Rora$^+$Rorc$^+$ cell (purple arrow); scale bar 50 µm (10 µm for magnified white box), Z stack 32 µm.

5.8.1. Relationship of triple reporter cell populations to the SCS

Using subcutaneous footpad injections of anti-CD169 antibody to label popliteal LN SCS macrophages *in vivo*, Id2$^+$Rora$^+$ and Id2$^+$Rora$^+$Rorc$^+$ cells were observed to be present in the SCS at baseline (Figure 5.18A).

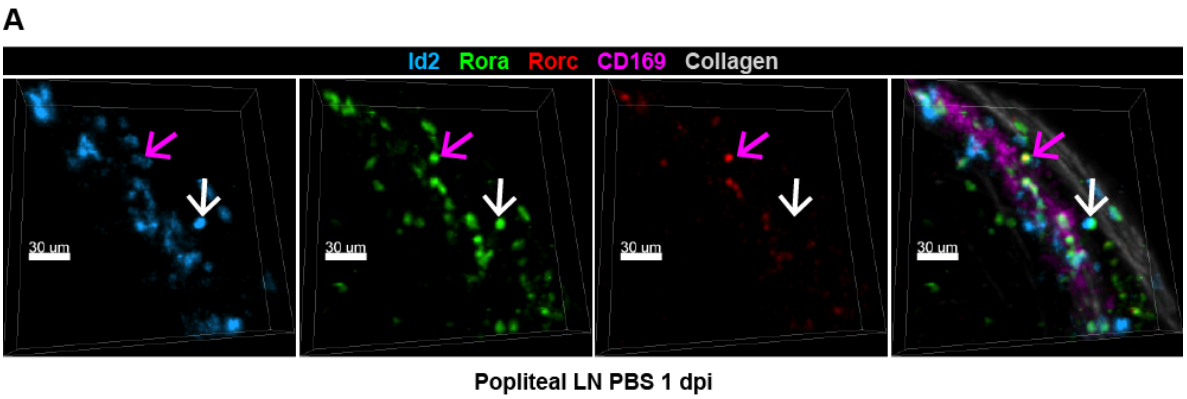

Figure 5.18. Id2$^+$Rora$^+$ and Id2$^+$Rora$^+$Rorc$^+$ cells in SCS of popliteal LN. (A) Intravital image of popliteal LN (PBS 1 dpi), with SCS macrophages labelled *in vivo* by subcutaneous

footpad injection of anti-CD169, showing Id2^{+}Rora^{+} (white arrow) and Id2^{+}Rora^{+}Rorc^{+} (purple arrow) cells in SCS; scalr bar 30 μm, Z stack 30 μm.

Examples of cell trafficking are shown, including Id2^{+}Rora^{+} cell initially co-localising with CD169^{+} SCS macrophage then moving away from the SCS into the LN cortex (Figure 5.19A), and Id2^{+}Rora^{+}Rorc^{+} cell moving along the SCS (Figure 5.19B).

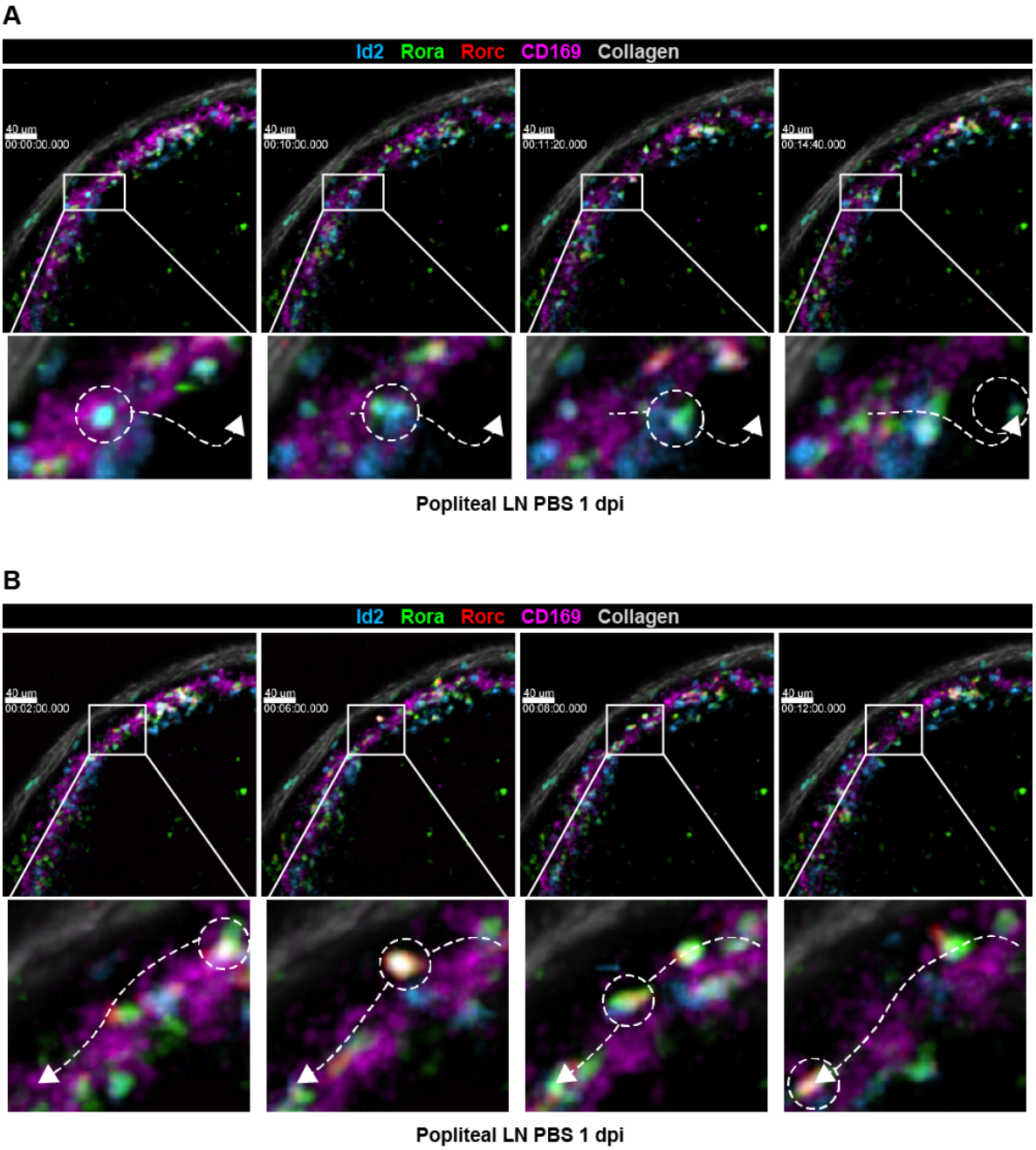

Figure 5.19. Trafficking of Id2^{+}Rora^{+} and Id2^{+}Rora^{+}Rorc^{+} cells in relation to SCS. (A) Intravital image of Id2^{+}Rora^{+} cell (dotted white circle) interacting with SCS macrophage then

moving away from SCS into cortex of popliteal LN (PBS 1 dpi); scale bar 40 μm, Z stack 14 μm. (B) Intravital image of Id2^{+}Rora^{+}Rorc^{+} cell (dotted white circle) crawling along the SCS in popliteal LN (PBS 1 dpi); scale bar 40 μm, Z stack 14 μm.

5.9. Triple reporter cell populations in the footpad

Following *S. mansoni* immunisation, most cells seen in the footpad were Id2^{+} DCs, with few examples of Id2^{+}Rora^{+}Rorc^{+} and Rorc^{+} cells (Figure 5.20A). However, the imaging of Rora-teal cells in the footpad was difficult due to significant background autofluorescence.

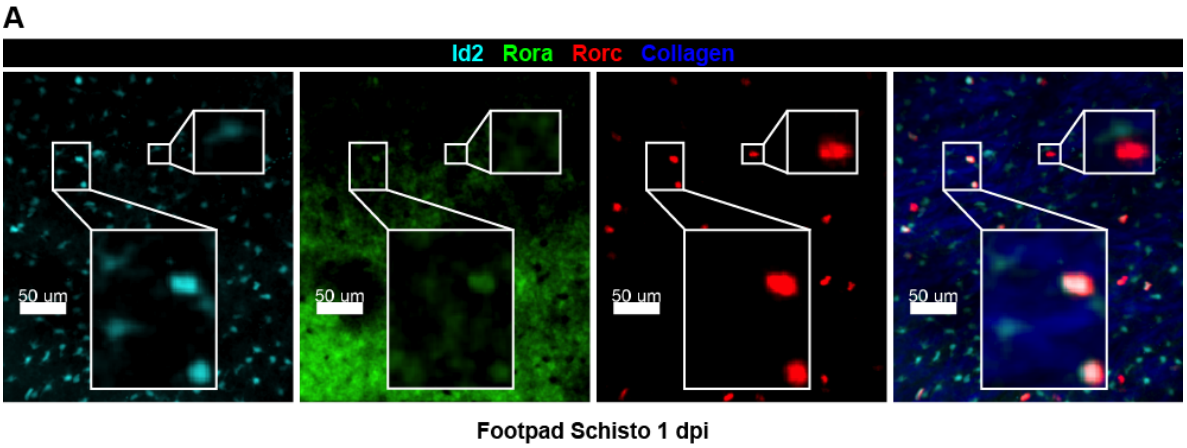

Figure 5.20. Triple reporter cell populations in *S. mansoni*-immunised footpad. (A) Intravital image of footpad of triple reporter mouse day 1 post *S. mansoni* immunisation; scale bar 50 μm, Z stack 55 μm.

5.10. Triple reporter cell populations in Peyer's patch

I also examined the gut of the triple reporter mouse, using the *N. brasiliensis* infection model. In the Peyer's patch, the Id2^{+}, Rora^{+} and Rorc^{+} populations were in similar distributions in both the uninfected (Figure 5.21A) and *N. brasiliensis*-infected (Figure 5.21B) mice. Whilst in the popliteal LN the majority of Rorc^{+} cells were also Id2^{+}Rora^{+}, in the Peyer's patch more Rorc^{+} cells were seen, with some cells appearing dendritic in morphology and situated near blood vessels (Figure 5.22A).

A

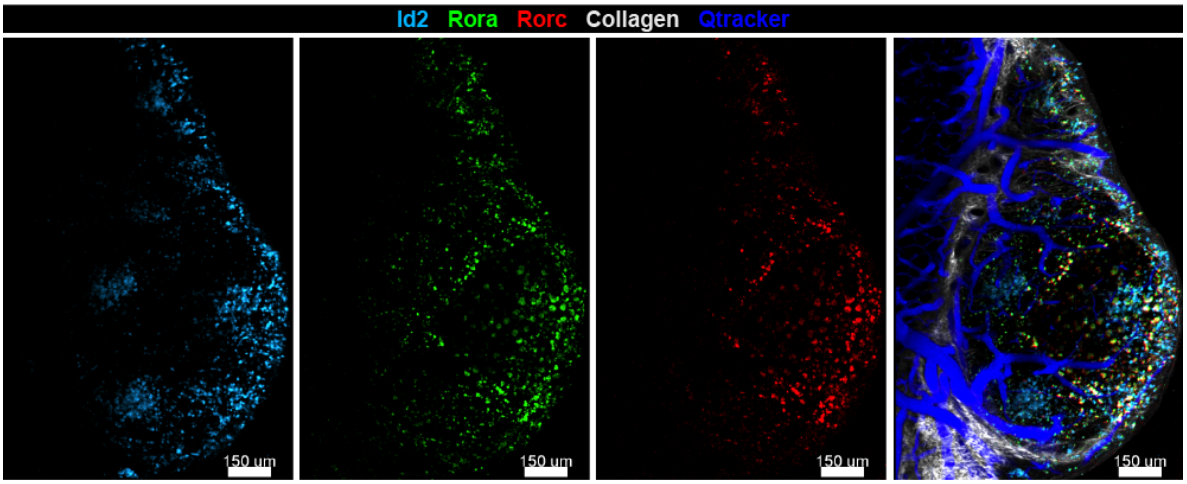

Peyer's patch uninfected

B

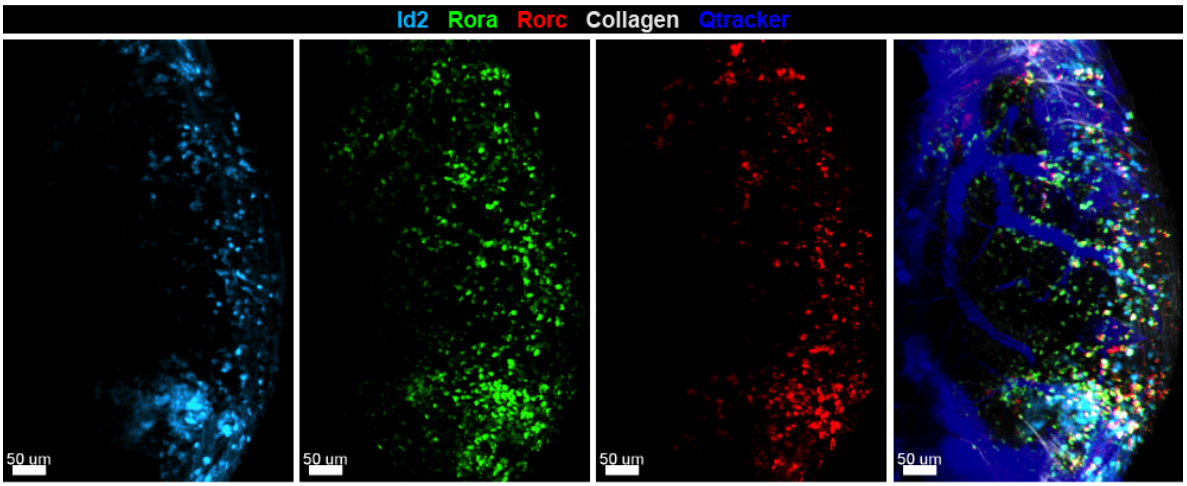

Peyer's patch Nippo 5 dpi

Figure 5.21. Triple reporter cell populations in Peyer's patch. (A) Intravital image of Peyer's patch from uninfected triple reporter; scale bar 150 µm, Z stack 24 µm. (B) Intravital image of Peyer's patch from triple reporter 5 dpi with *N. brasiliensis*; scale bar 50 µm, Z stack 60 µm. Blood vessels were labelled *in vivo* with intravenous Qtracker injection in both.

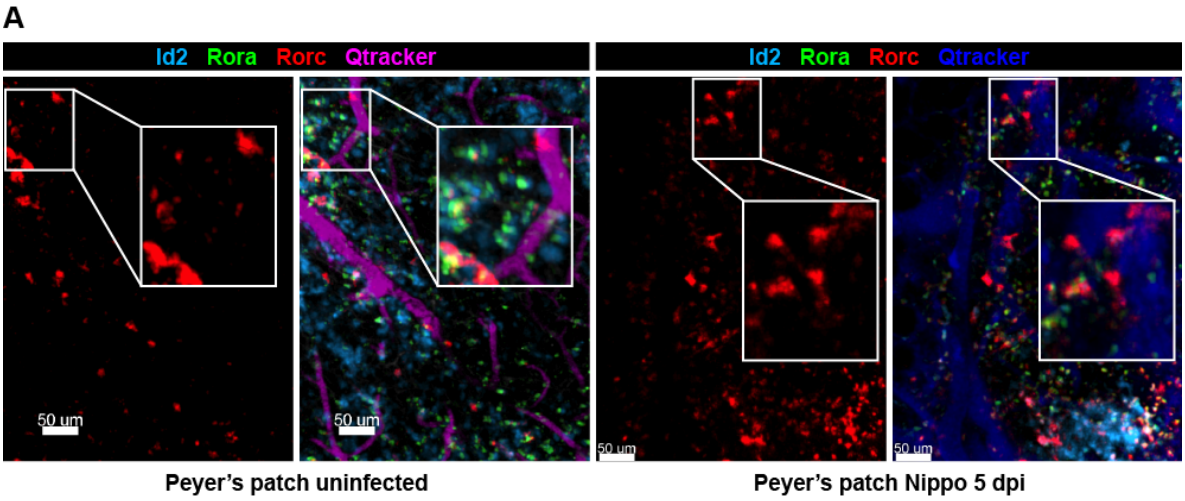

Figure 5.22. Rorc$^+$ cells near blood vessels in Peyer's patch. (A) Intravital images showing Rorc$^+$ cells situated near Qtracker-labelled blood vessels, in both uninfected and 5 dpi Peyer's patch; scale bar 50 μm, Z stack 30 μm.

5.11. Neutrophil expression of RORγt

Whilst RORγt$^+$ ILC3s are present in lymphoid tissues, other cells may also express RORγt. Using a RORγt-GFP reporter mouse, I harvested unstimulated LNs for examination by confocal microscopy and demonstrated the presence of Ly6G$^+$ neutrophils co-expressing RORγt, situated near lymphatic vessels in the popliteal LN (Figure 5.23A).

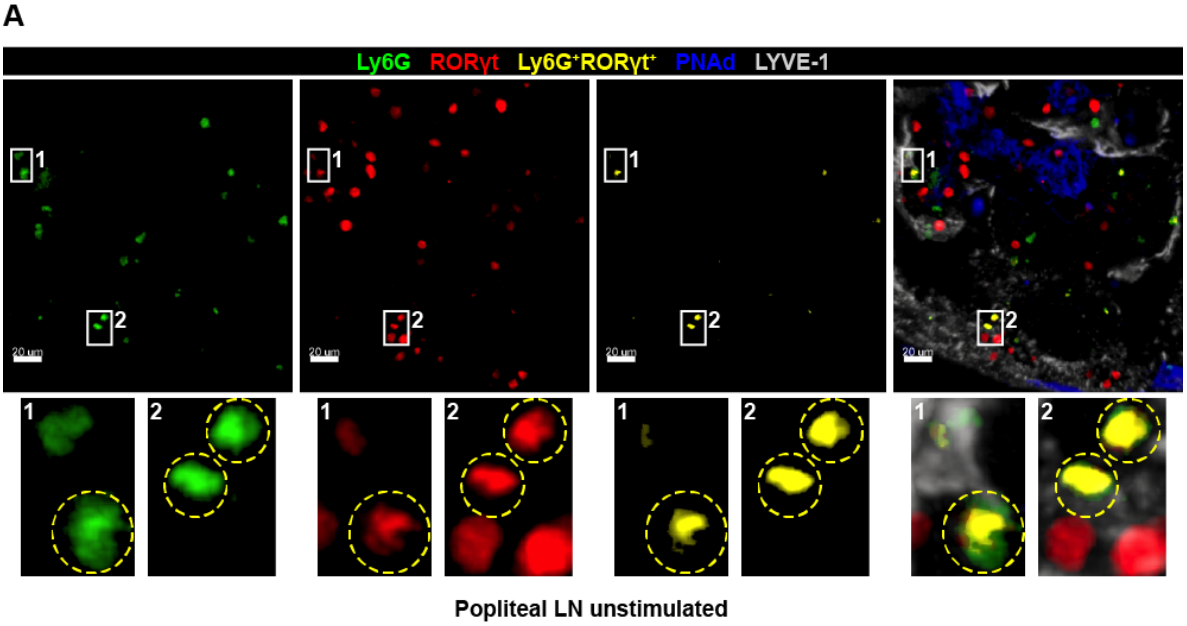

Figure 5.23. Neutrophil expression of RORγt in unstimulated LN. (A) Confocal image of unstimulated popliteal LN of RORγt-GFP reporter, with magnified areas (1 and 2) showing neutrophils with Ly6G and RORγt co-localisation (yellow circles) within LN tissue; scale bar 20 μm, Z stack 18 μm.

5.12. Summary of results

The results I have generated provide data on the dynamic behaviour of ILCs within lymphoid tissues. The CD2/IL-13 double reporter mouse enabled *in vivo* studies of ILC2 behaviour. Using this reporter mouse, two models of type 2 inflammation were studied; *N. brasiliensis* worm infection followed by Peyer's patch and gut imaging, and *S. mansoni* egg footpad immunisation followed by popliteal LN imaging. In both experimental models, the IL-13-producing cells early following stimulation were ILC2s not Th2 cells, confirming the importance of ILC2s in the early response to type 2 inflammatory stimuli.

Within Peyer's patches, the number of IL-13$^+$ ILC2s increased following *N. brasiliensis* infection compared to the number at baseline, with ILC2s located mainly in T cell areas. Intravital imaging of Peyer's patches showed that ILC2s and T cells had similar speed and directionality of movement at baseline; following *N. brasiliensis* infection, ILC2s moved with increased speed and directionality compared to T cells and to uninfected ILC2s, and no interactions were seen between ILC2s and T cells. The cellular size of ILC2s increased following infection, although no cell divisions were observed directly. In the small bowel wall, ILC2s similarly increased in cell number following *N. brasiliensis* infection, moving at higher speed and directionality compared to T cells, but in contrast to the Peyer's patch interactions were observed between ILC2s and T cells within the small bowel wall following infection. In popliteal LNs, ILC2s were located in T cell areas, and following footpad stimulation with UV-killed *S. mansoni* eggs ILC2s increased in number and moved at higher speed compared to T cells, providing evidence of changes in ILC2 number and dynamic behaviour following different type 2 inflammatory stimuli in different tissues.

I also examined the utility of a novel Id2/Rora/Rorc triple reporter mouse for the simultaneous imaging of immune cell subsets. The proportion of Id2$^+$Rora$^+$ cells being ILC2s was variable and lower than expected, limiting the use of this reporter mouse, although the proportion of Id2$^+$Rora$^+$Rorc$^+$ cells being ILC3s was higher. Id2$^+$Rora$^+$ and Id2$^+$Rora$^+$Rorc$^+$ cells were located in T cell areas of popliteal LNs and Peyer's patches, at baseline and post inflammatory challenge. Following *S. mansoni* footpad immunisation, Id2$^+$Rora$^+$ cells in the

popliteal dLN moved with lower speed and directionality, suggesting their interaction with other LN cells.

5.13. Discussion

Overall I demonstrated, using two different helminth experimental models, that early following type 2 inflammatory stimuli ILC2s increased in number in different tissues and were the main source of IL-13, with intravital imaging showing changes such as increased speed, increased directionality and increased cell size post stimulation. Consistent with this, IL-13$^+$ ILC2s did not interact with T cells in lymphoid tissues following inflammatory stimuli, despite their co-location; on the other hand, ILC2-T cell interactions were observed in the small bowel wall following stimulation.

5.13.1. CD2/IL-13 reporter for ILC2 imaging

The CD2-GFP/IL-13-tomato double reporter mouse provided a useful tool for studying ILC2 behaviour *in vivo*. Previous studies have used IL-13 reporter mice to identify ILC2s (237,307). I confirmed by flow cytometry that IL-13$^+$ cells in Peyer's patches and popliteal LNs were ILC2s, being positive for IL-7Rα and ICOS, and negative for markers of other cell types including T cell, eosinophils and granulocytes. GFP fluorescence on CD2$^+$ cells provided an important discriminator between Th2 cells (CD2$^+$IL-13$^+$) and ILC2s (CD2$^-$IL-13$^+$), and in addition provided a population of CD2$^+$IL-13$^-$ T cells that *in vivo* facilitated identification of T cell zones of LNs and acted as controls for quantifying ILC2 dynamic behaviour. One limitation, however, is that not all ILC2s are IL-13$^+$ especially at baseline, and there may be differences in the dynamic behaviour between IL-13$^+$ subsets of ILC2s and ILC2s as a whole group. Nevertheless, some interesting insights into ILC2 behaviour have been generated with this reporter.

In view of the different optimal two-photon excitation wavelengths of GFP and tomato, to avoid issues with repeated multiphoton laser re-tuning during imaging I used single-photon excitation instead (Section 3.10.3). Although single-photon excitation has the theoretical disadvantages of less tissue penetration and more photo-bleaching, in practice I was able to obtain intravital movies with adequate Z depth, whilst avoiding photo-bleaching over the duration of imaging by using low laser power levels. Therefore, despite these technical issues I was still able to obtain good quality *in vivo* data with the CD2/IL-13 double reporter mouse.

5.13.2. ILC2s in early type 2 immune responses

During the imaging of Peyer's patches and popliteal LNs following *N. brasiliensis* infection (day 5 post infection, an early time point following larvae arrival in gut) and *S. mansoni* egg immunisation (day 1 post immunisation) respectively, none of the IL-13$^+$ cells were CD2$^+$, suggesting that at these early time points, ILC2s but not Th2 cells were the major source of IL-13 in lymphoid tissues. IL-13$^+$ ILC2s increased in number, and in Peyer's patches increased in cell size following stimulation, which would be consistent with higher cytokine production. A previous study also showed that ILC2s were the main source of IL-13 early following papain-induced lung inflammation (266). My results demonstrated further evidence of the role of ILC2s early in type 2 inflammatory responses, acting as sentinel effector cells and producing cytokines such as IL-13 to initiate type 2 immune responses prior to Th2 cell activation.

5.13.3. Dynamic behaviour of ILC2s in lymphoid tissues

In Peyer's patches, I showed *in vivo* that early following *N. brasiliensis* infection ILC2s moved with higher speed and directionality compared to T cells and to uninfected ILC2s, and that the cell size of ILC2s increased compared to uninfected ILC2s. These changes in dynamic behaviour potentially suggest that ILC2s activate the early type 2 response via increase in production of cytokines including IL-13. ILC2-derived IL-13 has been shown in other studies to promote a number of cellular responses in non-lymphoid and lymphoid organs, such as DC-mediated recruitment of memory Th2 cells to the lungs (243) and DC migration to and Th2 differentiation in mediastinal dLN following papain-induced lung inflammation (266), and alveolar macrophage activation leading to *N. brasiliensis* killing in the lungs (274).

The increase in ILC2 cell movement may facilitate the distribution of secreted IL-13 to activate other cells. A previous study investigating the influence of T cell-derived IL-2 on Treg activation in LNs showed that IL-2$^+$ cells were present at the centre of Treg clusters, and Treg cells positioned within 100 μm of the centre expressed significantly higher pSTAT5 (representing Treg activation) compared to cells further away (351). In zebrafish, neutrophils showed more directed migration towards zebrafish CXCL8 when within 100 μm of the source but not at further distances (106). These studies suggest that cytokines have a limited area of influence in tissues, and therefore the finding of ILC2s moving with increased speed and directionality following stimulation could enable them to distribute cytokines over wider areas of lymphoid tissues to augment the initiation of type 2 responses.

I sought to expand these findings on ILC2 dynamic behaviour in the gastrointestinal tract to secondary lymphoid organs in other areas by examining LN from a different site with a different experimental model, namely performing intravital imaging of popliteal dLN early (day 1) following footpad immunisation with UV-inactivated *S. mansoni* eggs. This showed that ILC2s had higher speed of movement following *S. mansoni* stimulation compared to PBS stimulation. Although this was in support of the Peyer's patch data, the analysis of the popliteal LN dynamic data was preliminary, and data from more experiments have to be analysed to draw conclusions on the behaviour of ILC2s in this experimental model.

ILC2s and ILC3s have previously been shown to be located in interfollicular zones of mesenteric LN (262). Similarly, I have found ILC2s and ILC3s to be located in T cell areas within Peyer's patches and popliteal LNs. Despite their location within LNs, in Peyer's patches there were only rare incidences of interactions between ILC2s and T cells at baseline, and following *N. brasiliensis* infection no interactions between ILC2s and T cells were observed in any of the intravital movies examined. This was further evidence in support of the role of ILC2s in moving faster and distributing cytokines following stimulation, rather than moving slower and forming cellular interactions, in lymphoid tissues early in the Th2 response.

5.13.4. Dynamic behaviour of ILC2s in small bowel

Whilst the Peyer's patch and popliteal LN intravital data presented above have provided evidence supporting the notion that ILC2s influence immune cells via cytokine production, ILC2s have also been shown to form direct interactions with other immune cells. *In vivo* imaging of the ear skin showed that ILC2s formed brief interactions with mast cells (250). ILC2s have been shown to express MHCII and co-stimulatory molecules, enabling peptide presentation to and activation of antigen-specific T cells *in vitro*, and mediating N. brasiliensis worm expulsion *in vivo* (276).

Examination of the small bowel wall following *N. brasiliensis* infection showed that, similar to Peyer's patches, ILC2s were the main cell population producing IL-13, and IL-13$^+$ ILC2s moved at higher speed and directionality compared to T cells. There was also evidence of ILC2-T cell interaction. This may represent different roles of ILC2s in different tissues following type 2 inflammatory stimuli, whereby in lymphoid tissues ILC2s act mainly as cytokine producers, but in mucosal tissues ILC2s also interact with tissue-resident T cells, with the potential for antigen presentation. ILC2s from different pulmonary compartments showed different surface markers (311), and IL-33 stimulated OX40L expression on lung but not mediastinal LN ILC2s (278). Further studies are required to investigate whether there

are differences in ILC2 chemokine or receptor expression that influence the nature of crosstalk between ILC2 and other immune cells at lymphoid and mucosal tissues.

5.13.5. Id2/Rora/Rorc triple reporter mouse

Using IL-13 to identify ILC2s may not represent the whole ILC2 population, as some ILC2s may have low IL-13 production at baseline. In the small bowel wall, for example, few IL-13$^+$ ILC2s were seen at baseline during imaging. I examined the use of a novel Id2-BFP/Rora-teal/Rorc-katushka triple reporter (224) that would theoretically capture whole ILC subsets, with ILC2s expected to be Id2$^+$Rora$^+$ and ILC3s Id2$^+$Rora$^+$Rorc$^+$. By flow cytometry, the proportion of Id2$^+$Rora$^+$ cells being ILC2s were unfortunately lower than expected in Peyer's patch and popliteal LN. Nevertheless, imaging of popliteal LNs following footpad immunisation showed that Id2$^+$Rora$^+$ cells as a whole group moved at slower speed and directionality following *S. mansoni* challenge, suggesting interactions between these cells, which could be non-ILCs, and other LN cells, as opposed to IL-13$^+$ ILC2s which increased in speed following *S. mansoni* challenge.

There were technical issues with using this triple reporter for intravital imaging, with teal not being a bright fluorophore, and katushka having an optimal two-photon excitation wavelength beyond the tuneable range of the multiphoton laser in our laboratory; in order to overcome these issues I employed a strategy of sequential single- and two-photon excitation during intravital imaging.

I was unable to generate confocal images of harvested triple reporter LNs, as the process of LN fixation resulted in loss of fluorescence signal of the teal fluorophore, and unlike GFP there are no antibodies available against teal to augment the signal on LN sections. Therefore the Id2/Rora/Rorc triple reporter mouse can be used for intravital imaging studies, but not for confocal microscopy after tissue fixation.

The analysis of images from the triple reporter mouse was time-intensive, as I manually identified different cell populations and rendered "surfaces" to generate images of cell subsets. To improve upon this, a computerised algorithm could be applied to the analysis to reduce subjective errors. Such methods have been developed for the analysis of multiple cell types. For example, histo-cytometry utilises deconvolution algorithms, fluorophore compensation, Boolean voxel gating and surface rendering to visualise multiple cell populations with complex combinations of markers (352), and its use could be explored for the analysis of imaging data from the triple reporter mouse. Tissue clearing techniques have also been developed for imaging whole organs made transparent by chemical methods

(353,354), and these have been used in combination with computerised imaging analysis to generate quantitative confocal data with multiple fluorophores in bone marrow (355).

5.13.6. Dynamic behaviour of ILC3s

The Id2/Rora/Rorc triple reporter mouse showed better purity for ILC3s, identified as $Id2^+Rora^+Rorc^+$ cells. Within popliteal LNs, ILC3s were present mainly in T cell areas, consistent with findings from a previous study (262). Currently little data exist on the *in vivo* behaviour of ILC3s, with one study showing that ILC3s exhibited little motility within cryptopatches of the gut during intravital imaging, although there was evidence of ILC3s trafficking into and out of cryptopatches; in this study, ILC3s were visualised using an IL-23-GFP RAG-deficient reporter mouse which lacked adaptive B and T lymphocytes (308). In comparison, the intravital imaging data I presented above showed that ILC3s in the popliteal LN were motile, moving at similar speed to LN neutrophils and at higher speed compared to $Id2^+Rora^+$ cells, in a reporter mouse with intact lymphocytes. In addition, some $Id2^+Rora^+Rorc^+$ cells and $Id2^+Rora^+$ cells were observed to traffick within and out of the SCS.

Due to time constraints I only obtained limited data of triple reporter cell populations in Peyer's patches. In the small bowel lamina propria, the majority of $Id2^+Rora^+$ cells were ILC2s, and almost all $Id2^+Rora^+Rorc^+$ cells were ILC3s, therefore potentially making this a more useful reporter for imaging these ILC subsets simultaneously in the gut. It would be of interest to examine the gut, Peyer's patches and cryptopatches of the triple reporter mouse further, to investigate the behaviour of these ILC subsets using intravital imaging and to compare the results with previously published data more directly.

5.13.7. Neutrophils and ILCs

I showed evidence that neutrophils as well as ILC3s expressed RORγt in unstimulated LNs. $Gr\text{-}1^+$ neutrophils expressed RORγt in a model of liver ischaemic-reperfusion injury (356). Murine BM neutrophils and human peripheral blood neutrophils have been shown to express RORγt and produce IL-17 upon stimulation with IL-6 and IL-23 (357), although a subsequent study was unable to detect IL-17 production by human neutrophils *in vitro* (358). In animal models of asthma with intranasal fungal and protein allergen challenges, both Th2 and Th17 responses were induced (359), and RORγt inhibition, either in RORγt-deficient mice or with the use of pharmacological RORγt blockade, resulted in reduction in both Th2 and Th17 responses, including reduced airway recruitment of eosinophils and neutrophils respectively (360). Furthermore, RORα and RORγt exerted synergistic effects on Th17 differentiation, as shown *in vitro* and *in vivo* using RAG-deficient mice reconstituted with BM cells deficient in

RORγt or in both RORα and RORγt (349). Intradermal administration of killed *N. brasiliensis* larvae to the ear skin has been shown to result in neutrophil recruitment and NETosis, in addition to a Th2 response (361).

These studies suggest common links between neutrophils and ILCs in inflammatory responses, and further investigation of neutrophil-ILC crosstalk in homeostasis and in inflammation may provide insights into the cellular processes and therefore potential therapeutic targets in inflammatory diseases such as asthma and chronic obstructive pulmonary disease that show heterogeneous immunological phenotypes.

5.13.8. Significance of findings

To date there are only few studies on the dynamic behaviour of ILC2s, with *in vivo* imaging showing ILC2s (as CXCR6-GFP cells) in the ear skin moving slower than T cells (250), and *ex vivo* imaging showing ILC2s (as IL-13-GFP cells) in the lungs moving faster and over longer distances than $CD4^+$ T cells (307). Although ILCs are present in LNs, data are lacking on their behaviour in LNs *in vivo*.

With the results detailed above I have generated novel data quantifying the dynamic characteristics of ILC2s in different lymphoid tissues at baseline and following type 2 inflammation. ILC2s have been shown to express MHCII for antigen presentation (37), a process in which one would expect reduction in speed of movement to enable interactions with T cells to occur. In contrast, I showed that in lymphoid tissues ILC2s responded to type 2 stimuli with increased cell number and increased speed and directionality of movement, without forming interactions with T cells, suggesting their role as early cytokine producers. At local sites of inflammation such as small bowel, whilst ILC2s as a group increased speed and directionality of movement, some ILC2s also formed interactions with T cells, potentially suggesting roles additional to cytokine production.

Together these intravital imaging data on cellular dynamics suggest that ILC2s exert varying functions, which may show heterogeneity in lymphoid and non-lymphoid tissues. ILCs are a recently characterised group of cells with diverse effector functions. ILC2s have been shown to be important early effectors of type 2 immune responses, and are involved in a number of chronic inflammatory diseases such as asthma (289,346). Few intravital imaging studies have been performed for the study of ILC2s, and understanding their dynamic behaviour would contribute to knowledge on the role of ILC2s and their influence on innate and adaptive immunity, in lymphoid tissues in homeostasis and in inflammation.

Similarly, little data exist for the dynamic behaviour of ILC3s, with one previous study investigating ILC3s in gut cryptopatches in RAG-deficient mice (308). Utilising the Id2/Rora/Rorc triple reporter mouse, I have presented novel intravital data on the motile nature of ILC3s within LNs. Although the triple reporter mouse has its limitations, it could potentially be a useful tool for the simultaneous imaging of multiple immune cell subsets, including ILC2s and ILC3s in the gut.

5.13.9. Future work

I have shown that, compared to baseline, ILC2s increased in number, size and speed of movement in Peyer's patches following *N. brasiliensis* infection, supportive of ILC2s acting mainly as cytokine producers. The evidence could be strengthened by examination of the fluorescence intensity of IL-13 from intravital images to compare semi-quantitatively the amount of cytokine pre- and post-infection. Whilst manipulating cellular movement specifically on ILC2s *in vivo* would be difficult, I could examine the relationship between ILC2 speed of movement and cytokine production for example by inhibiting motility with cytochalasin and quantifying ILC2 cytokine secretion *in vitro*.

To confirm these findings in a different LN and in a different experimental model, I examined popliteal LNs following either PBS or *S. mansoni* egg foot immunisation; preliminary analysis showed similar changes in cell number and dynamic behaviour with *S. mansoni* immunisation, but data from more experiments have to be analysed in order to draw conclusions on this, and to identify whether there are any cellular interactions between ILC2s and T cells in skin-draining (popliteal) LN compared to gut-draining Peyer's patches. There are differences in tissue activation signals for ILC2s, such as TSLP in the skin and IL-25 in the gut (219). I could investigate whether tissue specific signals impact on the dynamic behaviour of ILC2s in draining LNs, for example by stimulating the footpad with these signals and comparing the dynamics of ILC2s in the draining popliteal LN.

In the small bowel, ILC2s also increased in number and speed of movement suggesting cytokine production, but in contrast to Peyer's patches where no cellular interactions were observed, ILC2-T cell interactions were observed in the small bowel. This may reflect a more diverse role of ILC2s at tissue sites of inflammation. More experiments are required to quantify the relative frequency and duration of interactions between ILC2s and T cells. As ILC2s have been shown in previous studies to express MHCII and present antigen to T cells (276), further experiments could be performed to examine whether these ILC2-T cell interactions represent MHCII-dependent antigen presentation, for example by administering antibody MHCII blockade to CD2/IL-13 reporter mice and observing for differences in ILC2-T

cell interactions, or by transferring antigen-specific fluorescent OTII T cells to IL-13 reporter and stimulating with OVAIC to observe for *in vivo* interactions between ILC2s and antigen-specific T cells.

I have so far examined ILC2 interactions with $CD2^+$ T cells using CD2/IL-13 reporter mice. Further work is required to investigate whether ILC2s interact with other immune cells in the LN, by using the approach of isolating and adoptively transferring the cell type of interest into CD2/IL-13 reporter mice, followed by Peyer's patch or popliteal LN intravital imaging at baseline and post inflammatory stimuli. I could, for example, isolate and transfer B cells either labelled *ex vivo* with cell tracker dye or from fluorescent reporter mice, then examine for interactions between ILC2s and B cells in lymphoid tissues. Similarly, ILC2 interactions with other innate immune cells such as DCs and neutrophils could be studied. I have shown that neutrophils can capture systemic IC for delivery to peripheral LNs (Section 4.10); I could examine by intravital imaging whether these antigen-carrying neutrophils interact with other LN immune cells, including ILC2s, and whether the nature of any interactions differ with different IgG-opsonised antigen, such as IC and opsonised bacteria. For investigating interactions of ILC2s with SCS macrophages, CD169 antibody labelling could be used, for example anti-CD169 injected subcutaneously in the footpad to label SCS macrophages in the draining popliteal LN.

Whilst the ILC2 purity in Peyer's patches and LNs of the Id2-BFP/Rora-teal/Rorc-katushka triple reporter mouse was lower than expected, in the small bowel lamina propria the majority of $Id2^+Rora^+$ cells were ILC2s, and almost all $Id2^+Rora^+Rorc^+$ cells were ILC3s. $Id2^+$ cells include DCs, and although Id2 is not a selective marker, DCs can be distinguished from other $Id2^+$ cells during intravital imaging by their distinctive morphology. My data showing larger cell size and slower speed of movement of $Id2^+$ cells compared to other groups (Section 5.8) would also support most $Id2^+$ cells being DCs. Therefore, although this triple reporter mouse has limitations for ILC2 imaging in lymphoid tissues, it could potentially be of value in the simultaneous imaging of multiple cell subsets in the small bowel, including ILC2s ($Id2^+Rora^+$), ILC3s ($Id2^+Rora^+Rorc^+$) and DCs ($Id2^+$), for example to investigate whether any cellular interactions occur between these innate cell types. With my imaging strategy with this reporter, Qtracker labelling of blood vessels could be used in addition to examine the relation of these cells to blood vessels. However, as stated above, the method of analysis would have to be optimised for future experiments using this reporter.

Chapter 6. Summary and conclusion

6.1. Summary

The innate immune system consists of circulating and tissue-resident cell subsets that form the early host response to infection and tissue injury. Neutrophils are circulating leukocytes that are rapidly recruited from blood to inflammatory tissues, responding to infectious and inflammatory stimuli by expressing a variety of surface receptors for recognition of PAMPs and DAMPs, and exerting their effector function of pathogen killing by methods including phagocytosis, ROS production, degranulation of cytotoxic proteins and NET production. ILCs are a recently characterised group of cells present at mucosal barrier sites such as the skin, lungs and gut with analogous functions to those of Th cell subsets. ILC2s are involved in the initiation of type 2 inflammation, with epithelial alarmins released during tissue damage stimulating ILC2s to produce type 2 cytokines, mediating the early response to helminth infection and allergen-induced inflammation.

In addition to their effector functions, innate immune cells can also interact with adaptive immune cells, for example by processing and presenting antigen to T cells via MHCII, leading to T cell activation. LNs are secondary lymphoid organs packed with immune cells arranged in microanatomical regions, and are ideal sites for enabling these cellular interactions to occur. DCs and macrophages have traditionally been considered professional antigen presenting cells, and DCs can migrate from peripheral tissues into dLNs to interact with lymphocytes; however, other innate immune cells have also been shown to influence adaptive immunity.

Neutrophils are increasingly recognised to have diverse roles beyond their classical effector function of rapid pathogen killing. Following tissue inflammation, whilst some neutrophils undergo apoptosis and efferocytosis, neutrophils have also been shown to migrate to dLNs, where they interact with other LN immune cells such as DCs, SCS macrophages, T cells and B cells, including by MHCII expression and antigen presentation, although studies have shown conflicting results on the overall effect of neutrophils on other LN immune cells. Under homeostatic conditions, it is unclear whether neutrophils similarly migrate into LNs and interact with other immune cells.

I demonstrated that neutrophils were present in unstimulated murine LNs from different body sites. The majority of neutrophils were located within the LN interstitium outside blood and lymphatic vessels, in interfollicular areas near the floor of the SCS. Intravital imaging showed that neutrophils tonically trafficked into LNs at baseline via both blood and lymphatic

vessels, with the mechanism partially dependent on PNAd. Neutrophils were also present in a similar anatomical distribution in LNs from human organ donors. Both human and murine LN neutrophils expressed MHCII at baseline. *Ex vivo*, IC stimulation upregulated neutrophil expression of MHCII and co-stimulatory molecules, and IC-stimulated neutrophils increased antigen-specific $CD4^+$ T cell activation. *In vivo*, neutrophils were capable of early delivery of circulating IC into peripheral LNs, and were observed to interact with SCS macrophages following IC stimulation and with DCs at baseline and following IC stimulation. Overall, these data suggest that neutrophils traffick into LNs under homeostatic conditions, express MHCII at baseline, sample systemic antigen for delivery to LNs, and can potentially interact with other LN immune cells to influence adaptive immunity (Figure 6.1).

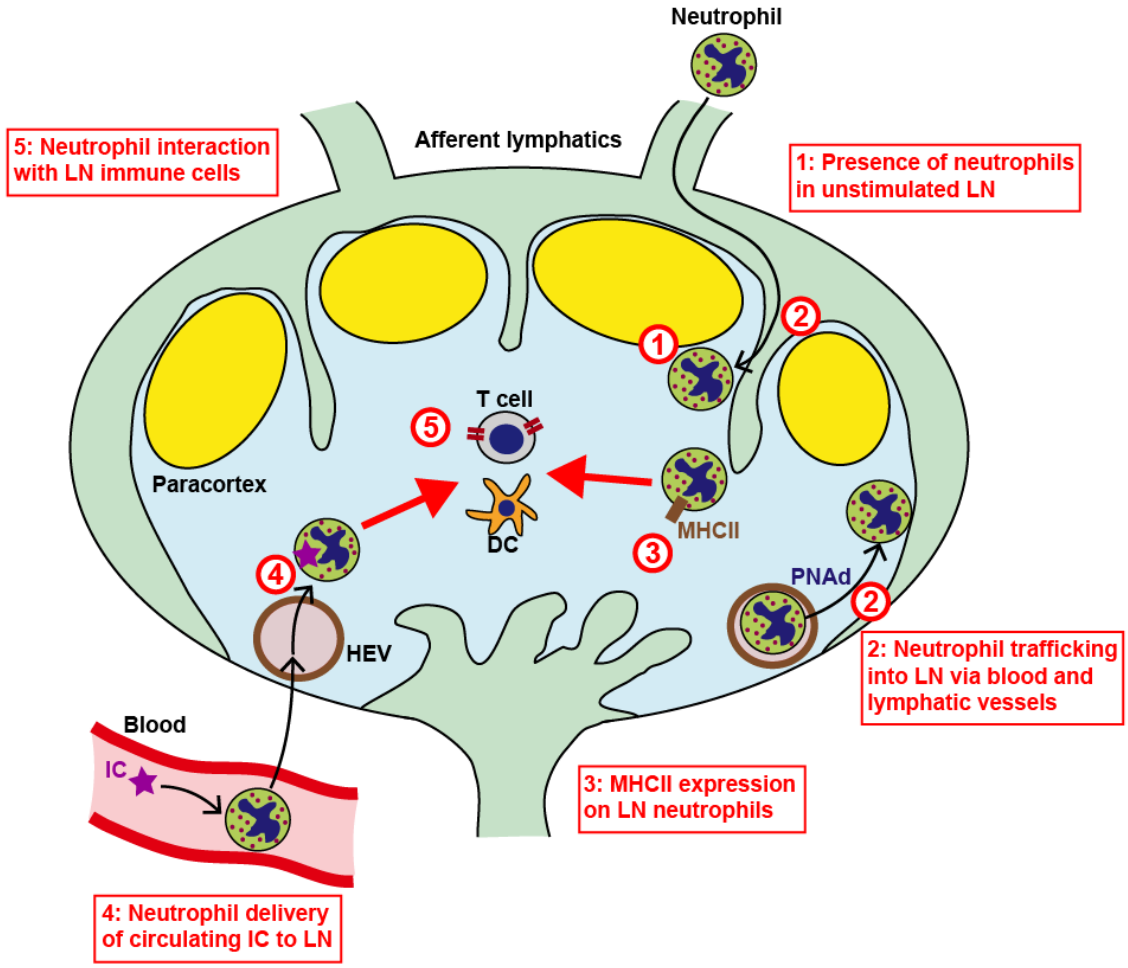

Figure 6.1. The role of LN neutrophils in homeostasis. Summary diagram showing that neutrophils are present in LNs under homeostatic conditions, traffick into LNs via blood and lymphatic vessels, express MHCII at baseline, sample systemic antigen for delivery to LNs, and can potentially interact with other LN immune cells to influence adaptive immunity.

ILCs, like neutrophils, are thought of as early innate effector cells, and whilst neutrophils are traditionally considered to be pathogen killers, ILCs are considered to influence other immune responses mainly via cytokine production. ILC2s are present in LNs and have been shown to exhibit crosstalk with other innate and adaptive immune cells. Whilst a few studies have examined the behaviour of ILC2s in non-lymphoid tissues *in vivo* or *ex vivo*, to date there are little data on the dynamic behaviour of ILC2s in lymphoid tissues *in vivo*.

Using two helminth models of type 2 inflammation, I demonstrated that early following stimulation ILC2s were the main source of IL-13 in lymphoid tissues (Peyer's patches and popliteal LNs) and at local tissue sites of inflammation (small bowel), increasing in cell number and cell size compared to baseline in these tissues. Within lymphoid tissues, ILC2s were located in T cell areas, and intravital imaging showed that ILC2s increased in speed and directionality of movement following inflammatory stimuli, with no interactions observed between ILC2s and T cells, suggesting that in lymphoid tissues ILC2s exhibit dynamic changes early following stimulation to distribute type 2 cytokines. In contrast, in the small bowel wall ILC2s and T cells were observed to interact following stimulation, potentially suggesting broader roles of ILC2s beyond cytokine production. Overall, these data provide novel insights into the dynamic behaviour of ILC2s in lymphoid tissues *in vivo* (Figure 6.2).

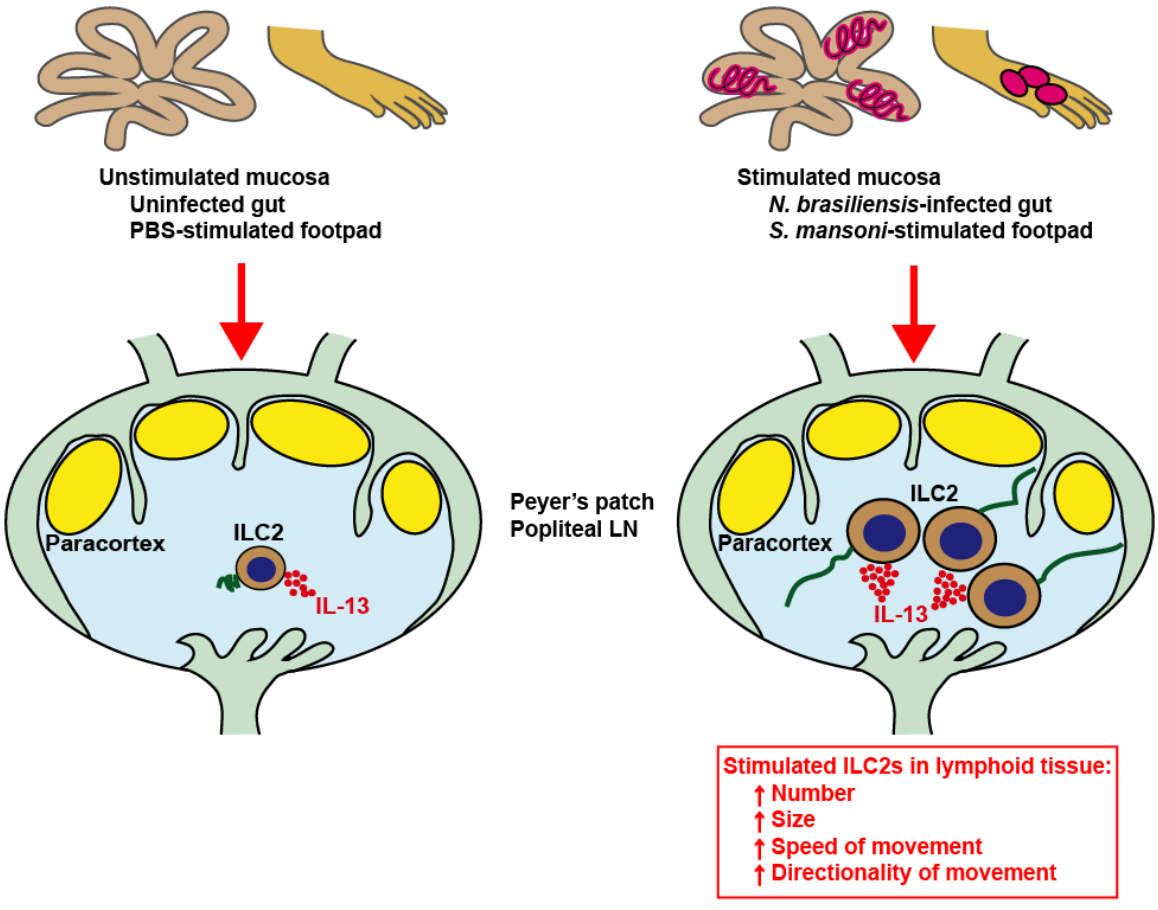

Figure 6.2. The behaviour of ILC2s in homeostasis and inflammation. Summary diagram showing that ILC2s are present in lymphoid tissues such as Peyer's patches and popliteal LNs at baseline, responding to mucosal helminth inflammatory stimuli by increasing in cell number and cell size, and moving with higher speed and directionality.

6.2. Conclusion

Both neutrophils and ILCs have diverse roles beyond their effector functions of pathogen killing and cytokine production. Using different experimental approaches including intravital imaging, I have investigated the dynamic behaviour of neutrophils and ILC2s in peripheral LNs and Peyer's patches, sites of adaptive immune responses. I have demonstrated a novel role of neutrophils in homeostatic immune surveillance, whereby neutrophils routinely patrol LNs at baseline, bringing sampled systemic antigen into LNs for potential antigen presentation with subsequent influence on adaptive immunity. I have characterised the behaviour of ILC2s, with novel *in vivo* data showing changes in ILC2 number and movement dynamics in lymphoid tissues following helminth models of inflammation.

Innate immune cells such as neutrophils and ILC2s are involved in a number of chronic inflammatory diseases, but currently few neutrophil- or ILC2-targeted treatments exist. The data presented above extend the scientific knowledge on the trafficking pattern and dynamic behaviour of these cells within LNs at baseline and following inflammatory stimuli, potentially facilitating the future development of therapeutic approaches to modulate neutrophil- or ILC-driven inflammation in these chronic diseases.

Output

Publication from this thesis

Lok LSC, Dennison TW, Mahbubani KM, Saeb-Parsy K, Chilvers ER, Clatworthy MR. Phenotypically distinct neutrophils patrol uninfected human and mouse lymph nodes. *Proceedings of the National Academy of Sciences of the United States of America* 2019;116(38):19083-9.

Oral presentations from this thesis

Lok LSC, Dennison TW, Chilvers ER, Clatworthy MR. The homeostatic role of lymph node-resident neutrophils in adaptive immunity.
Oral presentation, The Neutrophil conference, Quebec City, Canada, June 2018
Oral Presentation Award

Lok LSC, Stewart B, Chilvers ER, Clatworthy MR. The role of lymph node-resident neutrophils in adaptive immunity. Thorax 2017;72(Suppl 3) A14-5.
Oral presentation, British Thoracic Society Meeting, London, UK, December 2017

Acknowledgements

Firstly, I would like to thank my supervisors, Professor Edwin Chilvers and Professor Menna Clatworthy. Edwin introduced me to the world of academic medicine and the fascinating area of neutrophil biology, and I am grateful to his valuable guidance and mentorship throughout. Menna has spent countless hours teaching me the technique of intravital imaging, and has helped me widen my experience in immunology including studying ILCs; I am privileged to have been supervised by Menna and I am very fortunate to have been given all the time I needed on the microscope to generate many confocal images and intravital movies.

I would like to thank Dr Andrew McKenzie, whose group was one of the first to characterise ILC2s, for the ILC part of my work, providing guidance and support including reporter mice and reagents. I am grateful to past and present members of Andy's laboratory at the LMB, especially Jen Walker, Helen Jolin and Seth Scanlon for their experimental support with the helminth models and imaging sessions. For the human tissue data, I am grateful to Dr Kourosh Saeb-Parsy and members of his team especially Krishnaa Mahbubani for providing surgical samples for my research.

I would like to thank past members of the Chilvers laboratory (now moved to London), including Neda Farahi and Jatinder Juss who taught me much practical knowledge on working with neutrophils, Alison Condliffe (now a Professor at University of Sheffield) who helped me with my Wellcome Trust Fellowship application, and Chrystalla Loutsios and Ros Simmonds for experimental support. I would also like to thank all members of the Clatworthy laboratory. In particular, John Ferdinand and Rebeccah Mathews have helped in many practical ways to make my work possible. Tom Dennison provided me with much needed help with some experiments towards the end of my PhD. Tom Castro has been a true friend and an excellent desk partner, generating many stimulating discussions along the way.

I would like to thank my parents for all the opportunities they have created for me in Macau and in the UK to enable me to reach this stage of my career, and my siblings in Macau and my parents-in-law and siblings-in-law in Japan for their encouragement. Finally, and most importantly, thank you to my wife, Hitomi, for all her personal support in every possible way to see me through completing my PhD and thesis.

References

1. Turvey SE, Broide DH. Innate immunity. *J Allergy Clin Immunol*. 2010;125(2 Suppl 2):S24-32.
2. Takeuchi O, Akira S. Pattern recognition receptors and inflammation. *Cell*. 2010;140(6):805–20.
3. Chaplin DD. Overview of the immune response. *J Allergy Clin Immunol*. 2010;125(2):S3–23.
4. Iwasaki A, Medzhitov R. Control of adaptive immunity by the innate immune system. *Nat Immunol*. 2015;16(4):343–53.
5. Eberl G, Colonna M, Di Santo JP, McKenzie ANJ. Innate lymphoid cells: a new paradigm in immunology. *Science (80-)*. 2015;348(6237):aaa6566.
6. Sonnenberg GF, Artis D. Innate lymphoid cells in the initiation, regulation and resolution of inflammation. *Nat Med*. 2015;21(7):698–708.
7. Karsunky H, Merad M, Cozzio A, Weissman IL, Manz MG. Flt3 ligand regulates dendritic cell development from Flt3+ lymphoid and myeloid-committed progenitors to Flt3+ dendritic cells in vivo. *J Exp Med*. 2003;198(2):305–13.
8. Borregaard N. Neutrophils, from Marrow to Microbes. *Immunity*. 2010;33(5):657–70.
9. Davies LC, Jenkins SJ, Allen JE, Taylor PR. Tissue-resident macrophages. *Nat Immunol*. 2013;14(10):986–95.
10. Gasteiger G, Fan X, Dikiy S, Lee SY, Rudensky AY. Tissue residency of innate lymphoid cells in lymphoid and nonlymphoid organs. *Science (80-)*. 2015;350(6263):981–5.
11. Clatworthy MR, Aronin CEP, Mathews RJ, Morgan NY, Smith KGC, Germain RN. Immune complexes stimulate CCR7-dependent dendritic cell migration to lymph nodes. *Nat Med*. 2014;20(12):1458–63.
12. Voisin M-B, Nourshargh S. Neutrophil trafficking to lymphoid tissues: physiological and pathological implications. *J Pathol*. 2019;247(5):662–71.
13. Roth DB. V(D)J Recombination: Mechanism, Errors, and Fidelity. *Microbiol Spectr*. 2014;2(6):471–3.
14. Bonilla FA, Oettgen HC. Adaptive immunity. *J Allergy Clin Immunol*. 2010;125(2 Suppl 2):S33-40.
15. Trowsdale J, Knight JC. Major Histocompatibility Complex Genomics and Human Disease. *Annu Rev Genomics Hum Genet*. 2013;14(1):301–23.
16. Sharpe AH. Mechanisms of costimulation. *Immunol Rev*. 2009;229(1):5–11.
17. Ruddle NH, Akirav EM. Secondary lymphoid organs: responding to genetic and environmental cues in ontogeny and the immune response. *J Immunol*. 2009;183(4):2205–12.

18. von Andrian UH, Mempel TR. Homing and cellular traffic in lymph nodes. *Nat Rev Immunol*. 2003;3(11):867–78.
19. Weinstein AM, Storkus WJ. Biosynthesis and Functional Significance of Peripheral Node Addressin in Cancer-Associated TLO. *Front Immunol*. 2016;7:301.
20. Okada T, Ngo VN, Ekland EH, Förster R, Lipp M, Littman DR, et al. Chemokine requirements for B cell entry to lymph nodes and Peyer's patches. *J Exp Med*. 2002;196(1):65–75.
21. Bajénoff M, Egen JG, Koo LY, Laugier JP, Brau F, Glaichenhaus N, et al. Stromal Cell Networks Regulate Lymphocyte Entry, Migration, and Territoriality in Lymph Nodes. *Immunity*. 2006;25(6):989–1001.
22. Gasteiger G, Ataide M, Kastenmüller W. Lymph node - an organ for T-cell activation and pathogen defense. *Immunol Rev*. 2016;271(1):200–20.
23. Tripathi SK, Lahesmaa R. Transcriptional and epigenetic regulation of T-helper lineage specification. *Immunol Rev*. 2014;261(1):62–83.
24. Schroeder HW, Cavacini L. Structure and function of immunoglobulins. *J Allergy Clin Immunol*. 2010;125(2 Suppl 2):S41-52.
25. Mandl JN, Liou R, Klauschen F, Vrisekoop N, Monteiro JP, Yates AJ, et al. Quantification of lymph node transit times reveals differences in antigen surveillance strategies of naive CD4+ and CD8+ T cells. *Proc Natl Acad Sci*. 2012;109(44):18036–41.
26. Cyster JG, Schwab SR. Sphingosine-1-Phosphate and Lymphocyte Egress from Lymphoid Organs. *Annu Rev Immunol*. 2012;30:69–94.
27. Alvarez D, Vollmann EH, von Andrian UH. Mechanisms and Consequences of Dendritic Cell Migration. *Immunity*. 2008;29(3):325–42.
28. Gerner MY, Torabi-Parizi P, Germain RN. Strategically Localized Dendritic Cells Promote Rapid T Cell Responses to Lymph-Borne Particulate Antigens. *Immunity*. 2015;42(1):172–85.
29. Kastenmüller W, Torabi-Parizi P, Subramanian N, Lämmermann T, Germain RN. A Spatially-Organized Multicellular Innate Immune Response in Lymph Nodes Limits Systemic Pathogen Spread. *Cell*. 2012;150(6):1235–48.
30. Bajénoff M, Granjeaud S, Guerder S. The strategy of T cell antigen-presenting cell encounter in antigen-draining lymph nodes revealed by imaging of initial T cell activation. *J Exp Med*. 2003;198(5):715–24.
31. Fletcher AL, Lukacs-Kornek V, Reynoso ED, Pinner SE, Bellemare-Pelletier A, Curry MS, et al. Lymph node fibroblastic reticular cells directly present peripheral tissue antigen under steady-state and inflammatory conditions. *J Exp Med*. 2010;207(4):689–97.
32. Baratin M, Simon L, Jorquera A, Ghigo C, Dembele D, Nowak J, et al. T Cell Zone

Resident Macrophages Silently Dispose of Apoptotic Cells in the Lymph Node. *Immunity*. 2017;47(2):349–62.

33. Junt T, Moseman EA, Iannacone M, Massberg S, Lang P a, Boes M, et al. Subcapsular sinus macrophages in lymph nodes clear lymph-borne viruses and present them to antiviral B cells. *Nature*. 2007;450(7166):110–4.
34. Phan TG, Green JA, Gray EE, Xu Y, Cyster JG. Immune complex relay by subcapsular sinus macrophages and noncognate B cells drives antibody affinity maturation. *Nat Immunol*. 2009;10(7):786–93.
35. Qin D, Wu J, Vora KA, Ravetch J V, Szakal AK, Manser T, et al. Fcγ receptor IIB on follicular dendritic cells regulates the B cell recall response. *J Immunol*. 2000;164(12):6268–75.
36. Lin A, Loré K. Granulocytes: New Members of the Antigen-Presenting Cell Family. *Front Immunol*. 2017;8:1781.
37. Withers DR. Innate lymphoid cell regulation of adaptive immunity. *Immunology*. 2016;149(2):123–30.
38. Hampton HR, Chtanova T. The lymph node neutrophil. *Semin Immunol*. 2016;28(2):129–36.
39. Bar-Ephraïm YE, Mebius RE. Innate lymphoid cells in secondary lymphoid organs. *Immunol Rev*. 2016;271(1):185–99.
40. Kolaczkowska E, Kubes P. Neutrophil recruitment and function in health and inflammation. *Nat Rev Immunol*. 2013;13(3):159–75.
41. Vogt KL, Summers C, Chilvers ER, Condliffe AM. Priming and de-priming of neutrophil responses in vitro and in vivo. *Eur J Clin Invest*. 2018;48 Suppl 2:e12967.
42. Gernez Y, Tirouvanziam R, Chanez P. Neutrophils in chronic inflammatory airway diseases: Can we target them and how? *Eur Respir J*. 2010;35(3):467–9.
43. Cowland JB, Borregaard N. Granulopoiesis and granules of human neutrophils. *Immunol Rev*. 2016;273(1):11–28.
44. Walker F, Zhang H, Matthews V, Weinstock J, Nice EC, Ernst M, et al. IL6/sIL6R complex contributes to emergency granulopoietic responses in G-CSF– and GM-CSF– deficient mice. *Blood*. 2008;111(8):3978–85.
45. Day RB, Link DC. Regulation of neutrophil trafficking from the bone marrow. *Cell Mol Life Sci*. 2012;69(9):1415–23.
46. Summers C, Rankin SM, Condliffe AM, Singh N, Peters AM, Chilvers ER. Neutrophil kinetics in health and disease. *Trends Immunol*. 2010;31(8):318–24.
47. Yipp BG, Kim JH, Lima R, Zbytnuik LD, Petri B, Swanlund N, et al. The Lung is a Host Defense Niche for Immediate Neutrophil-Mediated Vascular Protection. *Sci Immunol*. 2017;2(10):eaam8929.
48. Summers C, Singh NR, White JF, Mackenzie IM, Johnston A, Solanki C, et al.

Pulmonary retention of primed neutrophils: a novel protective host response, which is impaired in the acute respiratory distress syndrome. *Thorax*. 2014;69(7):623–9.

49. Mestas J, Hughes CCW. Of mice and not men: differences between mouse and human immunology. *J Immunol*. 2004;172(5):2731–8.
50. Martin C, Burdon PC., Bridger G, Gutierrez-Ramos J-C, Williams TJ, Rankin SM. Chemokines Acting via CXCR2 and CXCR4 Control the Release of Neutrophils from the Bone Marrow and Their Return following Senescence. *Immunity*. 2003;19(4):583–93.
51. Eash KJ, Greenbaum AM, Gopalan PK, Link DC. CXCR2 and CXCR4 antagonistically regulate neutrophil trafficking from murine bone marrow. *J Clin Invest*. 2010;120(7):2423–31.
52. Devi S, Wang Y, Chew WK, Lima R, N AG, Mattar CN, et al. Neutrophil mobilization via plerixafor-mediated CXCR4 inhibition arises from lung demargination and blockade of neutrophil homing to the bone marrow. *J Exp Med*. 2013;210(11):2321–36.
53. Casanova-Acebes M, Pitaval C, Weiss LA, Nombela-Arrieta C, Chèvre R, A-González N, et al. Rhythmic modulation of the hematopoietic niche through neutrophil clearance. *Cell*. 2013;153(5):1025–35.
54. Furze RC, Rankin SM. The role of the bone marrow in neutrophil clearance under homeostatic conditions in the mouse. *FASEB J*. 2008;22(9):3111–9.
55. Broxmeyer HE, Orschell CM, Clapp DW, Hangoc G, Cooper S, Plett PA, et al. Rapid mobilization of murine and human hematopoietic stem and progenitor cells with AMD3100, a CXCR4 antagonist. *J Exp Med*. 2005;201(8):1307–18.
56. Ley K, Hoffman HM, Kubes P, Cassatella MA, Zychlinsky A, Hedrick CC, et al. Neutrophils: New insights and open questions. *Sci Immunol*. 2018;3(30):eaat4579.
57. Lok LSC, Farahi N, Juss JK, Loutsios C, Solanki CK, Peters AM, et al. Effects of tocilizumab on neutrophil function and kinetics. *Eur J Clin Invest*. 2017;47(10):736–45.
58. Adrover JM, Del Fresno C, Crainiciuc G, Cuartero MI, Casanova-Acebes M, Weiss LA, et al. A Neutrophil Timer Coordinates Immune Defense and Vascular Protection. *Immunity*. 2019;50(2):390-402.e10.
59. Cheretakis C, Leung R, Sun CX, Dror Y, Glogauer M. Timing of neutrophil tissue repopulation predicts restoration of innate immune protection in a murine bone marrow transplantation model. *Blood*. 2006;108(8):2821–6.
60. Lord BI, Molineux G, Pojda Z, Souza LM, Mermod JJ, Dexter TM. Myeloid cell kinetics in mice treated with recombinant interleukin-3, granulocyte colony-stimulating factor (CSF), or granulocyte-macrophage CSF in vivo. *Blood*. 1991;77(10):2154–9.
61. Basu S, Hodgson G, Katz M, Dunn AR. Evaluation of role of G-CSF in the production, survival, and release of neutrophils from bone marrow into circulation. *Blood*. 2002;100(3):854–61.

62. Farahi N, Singh NR, Heard S, Loutsios C, Summers C, Solanki CK, et al. Use of 111-Indium–labeled autologous eosinophils to establish the in vivo kinetics of human eosinophils in healthy subjects. *Blood*. 2012;120(19):4068–71.
63. Lahoz-Beneytez J, Elemans M, Zhang Y, Ahmed R, Salam A, Block M, et al. Human neutrophil kinetics: modeling of stable isotope labeling data supports short blood neutrophil half-lives. *Blood*. 2016;127(26):3431–8.
64. Tak T, Tesselaar K, Pillay J, Borghans JAM, Koenderman L. What's your age again? Determination of human neutrophil half-lives revisited. *J Leukoc Biol*. 2013;94(4):595–601.
65. Pillay J, Braber I Den, Vrisekoop N, Kwast LM, de Boer RJ, Borghans JAM, et al. In vivo labeling with 2H2O reveals a human neutrophil lifespan of 5.4 days. *Blood*. 2010;116(4):625–7.
66. Beura LK, Hamilton SE, Bi K, Schenkel JM, Odumade OA, Casey KA, et al. Normalizing the environment recapitulates adult human immune traits in laboratory mice. *Nature*. 2016;532(7600):512–6.
67. Zhang D, Chen G, Manwani D, Mortha A, Xu C, Faith JJ, et al. Neutrophil ageing is regulated by the microbiome. *Nature*. 2015;525(7570):528–32.
68. Deshmukh HS, Liu Y, Menkiti OR, Mei J, Dai N, O'Leary CE, et al. The microbiota regulates neutrophil homeostasis and host resistance to Escherichia coli K1 sepsis in neonatal mice. *Nat Med*. 2014;20(5):524–30.
69. Kanther M, Tomkovich S, Xiaolun S, Grosser MR, Koo J, Flynn EJ, et al. Commensal microbiota stimulate systemic neutrophil migration through induction of Serum amyloid A. *Cell Microbiol*. 2014;16(7):1053–67.
70. Colotta F, Re F, Polentarutti N, Sozzani S, Mantovani A. Modulation of granulocyte survival and programmed cell death by cytokines and bacterial products. *Blood*. 1992;80(8):2012–20.
71. Kim M-H, Granick JL, Kwok C, Walker NJ, Borjesson DL, Curry FE, et al. Neutrophil survival and c-kit+ -progenitor proliferation in Staphylococcus aureus–infected skin wounds promote resolution. *Blood*. 2011;117(12):3343–52.
72. Juss JK, House D, Amour A, Begg M, Herre J, Storisteanu DML, et al. Acute respiratory distress syndrome neutrophils have a distinct phenotype and are resistant to phosphoinositide 3-kinase inhibition. *Am J Respir Crit Care Med*. 2016;194(8):961–73.
73. Futosi K, Fodor S, Mocsai A. Neutrophil cell surface receptors and their intracellular signal transduction pathways. *Int Immunopharmacol*. 2013;17(3):638–50.
74. Akira S, Takeda K. Toll-like receptor signalling. *Nat Rev Immunol*. 2004;4(7):499–511.
75. Hayashi F, Means TK, Luster AD. Toll-like receptors stimulate human neutrophil function. *Blood*. 2003;102(7):2660–9.

76. Applequist SE, Wallin RPA, Ljunggren H-G. Variable expression of Toll-like receptor in murine innate and adaptive immune cell lines. *Int Immunol*. 2002;14(9):1065–74.
77. Selvaraj P, Fifadara N, Nagarajan S, Cimino A, Wang G. Functional Regulation of Human Neutrophil Fc γ Receptors. *Immunol Res*. 2004;29(1–3):219–30.
78. Smith KGC, Clatworthy MR. FcγRIIB in autoimmunity and infection: evolutionary and therapeutic implications. *Nat Rev Immunol*. 2010;10(5):328–43.
79. Bruhns P. Properties of mouse and human IgG receptors and their contribution to disease models. *Blood*. 2012;119(24):5640–9.
80. van Mirre E, Breunis WB, Geissler J, Hack CE, de Boer M, Roos D, et al. Neutrophil responsiveness to IgG, as determined by fixed ratios of mRNA levels for activating and inhibitory Fc RII (CD32), is stable over time and unaffected by cytokines. *Blood*. 2006;108(2):584–90.
81. Belostocki K, Pricop L, Redecha PB, Aydin A, Leff L, Harrison MJ, et al. Infliximab treatment shifts the balance between stimulatory and inhibitory Fcγ receptor type II isoforms on neutrophils in patients with rheumatoid arthritis. *Arthritis Rheum*. 2008;58(2):384–8.
82. Lee PY, Wang J-X, Parisini E, Dascher CC, Nigrovic PA. Ly6 family proteins in neutrophil biology. *J Leukoc Biol*. 2013;94(4):585–94.
83. Wang JX, Bair AM, King SL, Shnayder R, Huang YF, Shieh CC, et al. Ly6G ligation blocks recruitment of neutrophils via a β2-integrin- dependent mechanism. *Blood*. 2012;120(7):1489–98.
84. Hasenberg A, Hasenberg M, Männ L, Neumann F, Borkenstein L, Stecher M, et al. Catchup: a mouse model for imaging-based tracking and modulation of neutrophil granulocytes. *Nat Methods*. 2015;12(5):445–52.
85. Hume DA. Applications of myeloid-specific promoters in transgenic mice support in vivo imaging and functional genomics but do not support the concept of distinct macrophage and dendritic cell lineages or roles in immunity. *J Leukoc Biol*. 2011;89(4):525–38.
86. Pillay J, Tak T, Kamp VM, Koenderman L. Immune suppression by neutrophils and granulocytic myeloid-derived suppressor cells: similarities and differences. *Cell Mol Life Sci*. 2013;70(20):3813–27.
87. Lakschevitz FS, Hassanpour S, Rubin A, Fine N, Sun C, Glogauer M. Identification of neutrophil surface marker changes in health and inflammation using high-throughput screening flow cytometry. *Exp Cell Res*. 2016;342(2):200–9.
88. Nguyen GT, Green ER, Mecsas J. Neutrophils to the ROScue: Mechanisms of NADPH Oxidase Activation and Bacterial Resistance. *Front Cell Infect Microbiol*. 2017;7:373.
89. Warnatsch A, Tsourouktsoglou T-D, Branzk N, Wang Q, Reincke S, Herbst S, et al.

Reactive Oxygen Species Localization Programs Inflammation to Clear Microbes of Different Size. *Immunity*. 2017;46(3):421–32.

90. Miralda I, Uriarte SM, McLeish KR. Multiple Phenotypic Changes Define Neutrophil Priming. *Front Cell Infect Microbiol*. 2017;7:217.
91. Murray J, Barbara JAJ, Dunkley SA, Lopez AF, van Ostade X, Condliffe AM, et al. Regulation of Neutrophil Apoptosis by Tumor Necrosis Factor-a: Requirement for TNFR55 and TNFR75 for Induction of Apoptosis In Vitro. *Blood*. 1997;90(7):2772–83.
92. Richer BC, Salei N, Laskay T, Seeger K. Changes in Neutrophil Metabolism upon Activation and Aging. *Inflammation*. 2018;41(2):710–21.
93. Kitchen E, Rossi AG, Condliffe AM, Haslett C, Chilvers ER. Demonstration of Reversible Priming of Human Neutrophils Using Platelet-Activating Factor. *Blood*. 1996;88(11):4330–7.
94. Faurschou M, Borregaard N. Neutrophil granules and secretory vesicles in inflammation. *Microbes Infect*. 2003;5(14):1317–27.
95. Häger M, Cowland JB, Borregaard N. Neutrophil granules in health and disease. *J Intern Med*. 2010;268(1):25–34.
96. Sørensen OE, Borregaard N. Neutrophil extracellular traps — the dark side of neutrophils. *J Clin Invest*. 2016;126(5):1612–20.
97. Branzk N, Lubojemska A, Hardison SE, Wang Q, Gutierrez MG, Brown GD, et al. Neutrophils sense microbe size and selectively release neutrophil extracellular traps in response to large pathogens. *Nat Immunol*. 2014;15(11):1017–25.
98. Sangaletti S, Tripodo C, Chiodoni C, Guarnotta C, Cappetti B, Casalini P, et al. Neutrophil extracellular traps mediate transfer of cytoplasmic neutrophil antigens to myeloid dendritic cells toward ANCA induction and associated autoimmunity. *Blood*. 2012;120(15):3007–18.
99. De Filippo K, Henderson RB, Laschinger M, Hogg N. Neutrophil chemokines KC and macrophage-inflammatory protein-2 are newly synthesized by tissue macrophages using distinct TLR signaling pathways. *J Immunol*. 2008;180(6):4308–15.
100. Marki A, Buscher K, Mikulski Z, Pries A, Ley K. Rolling neutrophils form tethers and slings under physiologic conditions in vivo. *J Leukoc Biol*. 2018;103(1):67–70.
101. Ng LG, Qin JS, Roediger B, Wang Y, Jain R, Cavanagh LL, et al. Visualizing the neutrophil response to sterile tissue injury in mouse dermis reveals a three-phase cascade of events. *J Invest Dermatol*. 2011;131(10):2058–68.
102. Lämmermann T, Afonso P V, Angermann BR, Wang JM, Kastenmüller W, Parent C a, et al. Neutrophil swarms require LTB4 and integrins at sites of cell death in vivo. *Nature*. 2013;498(7454):371–5.
103. Huang C, Niethammer P. Tissue Damage Signaling Is a Prerequisite for Protective Neutrophil Recruitment to Microbial Infection in Zebrafish. *Immunity*. 2018;48(5):1006-

1013.e6.
104. Niethammer P, Grabher C, Look AT, Mitchison TJ. A tissue-scale gradient of hydrogen peroxide mediates rapid wound detection in zebrafish. *Nature*. 2009;459(7249):996–9.
105. Deng Q, Harvie EA, Huttenlocher A. Distinct signalling mechanisms mediate neutrophil attraction to bacterial infection and tissue injury. *Cell Microbiol*. 2012;14(4):517–28.
106. Sarris M, Masson JB, Maurin D, Van Der Aa LM, Boudinot P, Lortat-Jacob H, et al. Inflammatory Chemokines Direct and Restrict Leukocyte Migration within Live Tissues as Glycan-Bound Gradients. *Curr Biol*. 2012;22(24):2375–82.
107. Greenlee-Wacker MC. Clearance of apoptotic neutrophils and resolution of inflammation. *Immunol Rev*. 2016;273(1):357–70.
108. Hughes J, Johnson RJ, Mooney A, Hugo C, Gordon K, Savill J. Neutrophil fate in experimental glomerular capillary injury in the rat. Emigration exceeds in situ clearance by apoptosis. *Am J Pathol*. 1997;150(1):223–34.
109. Mathias JR, Perrin BJ, Liu TX, Kanki J, Look AT, Huttenlocher A. Resolution of inflammation by retrograde chemotaxis of neutrophils in transgenic zebrafish. *J Leukoc Biol*. 2006;80(6):1281–8.
110. Ellett F, Elks PM, Robertson AL, Ogryzko N V., Renshaw SA. Defining the phenotype of neutrophils following reverse migration in zebrafish. *J Leukoc Biol*. 2015;98(6):975–81.
111. Holmes GR, Anderson SR, Dixon G, Robertson AL, Reyes-Aldasoro CC, Billings SA, et al. Repelled from the wound, or randomly dispersed? Reverse migration behaviour of neutrophils characterized by dynamic modelling. *J R Soc Interface*. 2012;9(77):3229–39.
112. Colom B, Bodkin J V., Beyrau M, Woodfin A, Ody C, Rourke C, et al. Leukotriene B4-Neutrophil Elastase Axis Drives Neutrophil Reverse Transendothelial Cell Migration In Vivo. *Immunity*. 2015;42(6):1075–86.
113. Yang C-W, Strong BSI, Miller MJ, Unanue ER. Neutrophils influence the level of antigen presentation during the immune response to protein antigens in adjuvants. *J Immunol*. 2010;185(5):2927–34.
114. Hampton HR, Bailey J, Tomura M, Brink R, Chtanova T. Microbe-dependent lymphatic migration of neutrophils modulates lymphocyte proliferation in lymph nodes. *Nat Commun*. 2015;6:7139.
115. Buckley CD, Ross EA, McGettrick HM, Osborne CE, Haworth O, Schmutz C, et al. Identification of a phenotypically and functionally distinct population of long-lived neutrophils in a model of reverse endothelial migration. *J Leukoc Biol*. 2006;79(2):303–11.

116. Woodfin A, Voisin M-B, Beyrau M, Colom B, Caille D, Diapouli F-M, et al. The junctional adhesion molecule JAM-C regulates polarized transendothelial migration of neutrophils in vivo. *Nat Immunol*. 2011;12(8):761–9.
117. Wu D, Zeng Y, Fan Y, Wu J, Mulatibieke T, Ni J, et al. Reverse-migrated neutrophils regulated by JAM-C are involved in acute pancreatitis-associated lung injury. *Sci Rep*. 2016;6:20545.
118. Wang J, Hossain M, Thanabalasuriar A, Gunzer M, Meininger C, Kubes P. Visualizing the function and fate of neutrophils in sterile injury and repair. *Science (80-)*. 2017;358(6359):111–6.
119. Abadie V, Badell E, Douillard P, Ensergueix D, Leenen PJM, Tanguy M, et al. Neutrophils rapidly migrate via lymphatics after Mycobacterium bovis BCG intradermal vaccination and shuttle live bacilli to the draining lymph nodes. *Blood*. 2005;106(5):1843–50.
120. Rigby DA, Ferguson DJP, Johnson LA, Jackson DG. Neutrophils rapidly transit inflamed lymphatic vessel endothelium via integrin-dependent proteolysis and lipoxin-induced junctional retraction. *J Leukoc Biol*. 2015;98(6):897–912.
121. Arokiasamy S, Zakian C, Dilliway J, Wang W, Nourshargh S, Voisin M-B. Endogenous TNFα orchestrates the trafficking of neutrophils into and within lymphatic vessels during acute inflammation. *Sci Rep*. 2017;7(1):44189.
122. de Veer M, Kemp J, Chatelier J, Elhay MJ, Meeusen ENT. The kinetics of soluble and particulate antigen trafficking in the afferent lymph, and its modulation by aluminum-based adjuvant. *Vaccine*. 2010;28(40):6597–602.
123. Maletto BA, Ropolo AS, Alignani DO, Liscovsky M V., Ranocchia RP, Moron VG, et al. Presence of neutrophil-bearing antigen in lymphoid organs of immune mice. *Blood*. 2006;108(9):3094–102.
124. Castell SD, Harman MF, Morón G, Maletto BA, Pistoresi-Palencia MC. Neutrophils Which Migrate to Lymph Nodes Modulate CD4+ T Cell Response by a PD-L1 Dependent Mechanism. *Front Immunol*. 2019;10:105.
125. Abadie V, Bonduelle O, Duffy D, Parizot C, Verrier B, Combadière B. Original encounter with antigen determines antigen-presenting cell imprinting of the quality of the immune response in mice. *PLoS One*. 2009;4(12):e8159.
126. Duffy D, Perrin H, Abadie V, Benhabiles N, Boissonnas A, Liard C, et al. Neutrophils transport antigen from the dermis to the bone marrow, initiating a source of memory CD8+ T cells. *Immunity*. 2012;37(5):917–29.
127. Liang F, Lindgren G, Sandgren KJ, Thompson EA, Francica JR, Seubert A, et al. Vaccine priming is restricted to draining lymph nodes and controlled by adjuvant-mediated antigen uptake. *Sci Transl Med*. 2017;9(393):eaal2094.
128. Hor JL, Heath WR, Mueller SN. Neutrophils are dispensable in the modulation of T cell

immunity against cutaneous HSV-1 infection. *Sci Rep*. 2017;7:41091.

129. Kamenyeva O, Boularan C, Kabat J, Cheung GYC, Cicala C, Yeh AJ, et al. Neutrophil Recruitment to Lymph Nodes Limits Local Humoral Response to Staphylococcus aureus. McLoughlin RM, editor. *PLOS Pathog*. 2015;11(4):e1004827.
130. Bogoslowski A, Butcher EC, Kubes P. Neutrophils recruited through high endothelial venules of the lymph nodes via PNAd intercept disseminating Staphylococcus aureus. *Proc Natl Acad Sci*. 2018;115(10):2449–54.
131. Gorlino C V, Ranocchia RP, Harman MF, García I a, Crespo MI, Morón G, et al. Neutrophils exhibit differential requirements for homing molecules in their lymphatic and blood trafficking into draining lymph nodes. *J Immunol*. 2014;193(4):1966–74.
132. Brackett CM, Muhitch JB, Evans SS, Gollnick SO. IL-17 Promotes Neutrophil Entry into Tumor-Draining Lymph Nodes following Induction of Sterile Inflammation. *J Immunol*. 2013;191(8):4348–57.
133. Beauvillain C, Cunin P, Doni A, Scotet M, Jaillon S, Loiry ML, et al. CCR7 is involved in the migration of neutrophils to lymph nodes. *Blood*. 2011;117(4):1196–204.
134. Andersson H, Andersson B, Eklund D, Ngoh E, Persson A, Svensson K, et al. Apoptotic neutrophils augment the inflammatory response to Mycobacterium tuberculosis infection in human macrophages. *PLoS One*. 2014;9(7):e101514.
135. Yatim N, Cullen S, Albert ML. Dying cells actively regulate adaptive immune responses. *Nat Rev Immunol*. 2017;17(4):262–75.
136. Uhl B, Vadlau Y, Zuchtriegel G, Nekolla K, Sharaf K, Gaertner F, et al. Aged neutrophils contribute to the first line of defense in the acute inflammatory response. *Blood*. 2016;128(19):2327–37.
137. Kim JH, Podstawka J, Lou Y, Li L, Lee EKS, Divangahi M, et al. Aged polymorphonuclear leukocytes cause fibrotic interstitial lung disease in the absence of regulation by B cells. *Nat Immunol*. 2018;19(2):192–201.
138. Fox S, Leitch AE, Duffin R, Haslett C, Rossi AG. Neutrophil apoptosis: Relevance to the innate immune response and inflammatory disease. *J Innate Immun*. 2010;2(3):216–27.
139. Bogoslowski A, Wijeyesinghe S, Lee W-Y, Chen C-S, Alanani S, Jenne C, et al. Neutrophils Recirculate through Lymph Nodes to Survey Tissues for Pathogens. *J Immunol*. 2020;204(9):2552–61.
140. Gray EE, Cyster JG. Lymph node macrophages. *J Innate Immun*. 2012;4(5–6):424–36.
141. Chtanova T, Schaeffer M, Han SJ, van Dooren GG, Nollmann M, Herzmark P, et al. Dynamics of Neutrophil Migration in Lymph Nodes during Infection. *Immunity*. 2008;29(3):487–96.
142. Sagoo P, Garcia Z, Breart B, Lemaître F, Michonneau D, Albert ML, et al. In vivo

imaging of inflammasome activation reveals a subcapsular macrophage burst response that mobilizes innate and adaptive immunity. *Nat Med*. 2016;22(1):64–71.

143. Gaya M, Castello A, Montaner B, Rogers N, Reis e Sousa C, Bruckbauer A, et al. Inflammation-induced disruption of SCS macrophages impairs B cell responses to secondary infection. *Science (80-)*. 2015;347(6222):667–72.
144. Megiovanni AM, Sanchez F, Robledo-Sarmiento M, Morel C, Gluckman JC, Boudaly S. Polymorphonuclear neutrophils deliver activation signals and antigenic molecules to dendritic cells: a new link between leukocytes upstream of T lymphocytes. *J Leukoc Biol*. 2006;79(5):977–88.
145. Hedlund S, Persson A, Vujic A, Che KF, Stendahl O, Larsson M. Dendritic cell activation by sensing Mycobacterium tuberculosis-induced apoptotic neutrophils via DC-SIGN. *Hum Immunol*. 2010;71(6):535–40.
146. van Gisbergen KPJM, Sanchez-Hernandez M, Geijtenbeek TBH, van Kooyk Y. Neutrophils mediate immune modulation of dendritic cells through glycosylation-dependent interactions between Mac-1 and DC-SIGN. *J Exp Med*. 2005;201(8):1281–92.
147. Scapini P, Laudanna C, Pinardi C, Allavena P, Mantovani A, Sozzani S, et al. Neutrophils produce biologically active macrophage inflammatory protein-3alpha (MIP-3alpha)/CCL20 and MIP-3beta/CCL19. *Eur J Immunol*. 2001;31(7):1981–8.
148. Charmoy M, Brunner-Agten S, Aebischer D, Auderset F, Launois P, Milon G, et al. Neutrophil-derived CCL3 is essential for the rapid recruitment of dendritic cells to the site of Leishmania major inoculation in resistant mice. *PLoS Pathog*. 2010;6(2):e1000755.
149. Tamassia N, Bianchetto-Aguilera F, Arruda-Silva F, Gardiman E, Gasperini S, Calzetti F, et al. Cytokine production by human neutrophils: Revisiting the “dark side of the moon”. *Eur J Clin Invest*. 2018;48 Suppl 2:e12952.
150. Park SJ, Burdick MD, Mehrad B. Neutrophils mediate maturation and efflux of lung dendritic cells in response to Aspergillus fumigatus germ tubes. *Infect Immun*. 2012;80(5):1759–65.
151. Kreisel D, Sugimoto S, Zhu J, Nava R, Li W, Okazaki M, et al. Emergency granulopoiesis promotes neutrophil-dendritic cell encounters that prevent mouse lung allograft acceptance. *Blood*. 2011;118(23):6172–82.
152. Krishnamoorthy N, Douda DN, Brüggemann TR, Ricklefs I, Duvall MG, Abdulnour RE, et al. Neutrophil cytoplasts induce TH17 differentiation and skew inflammation toward neutrophilia in severe asthma. *Sci Immunol*. 2018;3(26):eaao4747.
153. Patel DF, Peiró T, Bruno N, Vuononvirta J, Akthar S, Puttur F, et al. Neutrophils restrain allergic airway inflammation by limiting ILC2 function and monocyte–dendritic cell antigen presentation. *Sci Immunol*. 2019;4(41):eaax7006.

154. Morel C, Badell E, Abadie V, Robledo M, Setterblad N, Gluckman JC, et al. Mycobacterium bovis BCG-infected neutrophils and dendritic cells cooperate to induce specific T cell responses in humans and mice. *Eur J Immunol*. 2008;38(2):437–47.
155. Alfaro C, Suarez N, Oñate C, Perez-Gracia JL, Martinez-Forero I, Hervas-Stubbs S, et al. Dendritic Cells Take up and Present Antigens from Viable and Apoptotic Polymorphonuclear Leukocytes. Bertoletti A, editor. *PLoS One*. 2011;6(12):e29300.
156. Ribeiro-Gomes FL, Peters NC, Debrabant A, Sacks DL. Efficient capture of infected neutrophils by dendritic cells in the skin inhibits the early anti-leishmania response. *PLoS Pathog*. 2012;8(2):e1002536.
157. Odobasic D, Kitching a R, Yang Y, Sullivan KMO, Muljadi RCM, Edgtton KL, et al. Neutrophil myeloperoxidase regulates T-cell-driven tissue inflammation in mice by inhibiting dendritic cell function. *Blood*. 2013;121(20):4195–204.
158. Doz E, Lombard R, Carreras F, Buzoni-Gatel D, Winter N. Mycobacteria-infected dendritic cells attract neutrophils that produce IL-10 and specifically shut down Th17 CD4 T cells through their IL-10 receptor. *J Immunol*. 2013;191(7):3818–26.
159. Clayton AR, Prue RL, Harper L, Drayson MT, Savage COS. Dendritic cell uptake of human apoptotic and necrotic neutrophils inhibits CD40, CD80, and CD86 expression and reduces allogeneic T cell responses: Relevance to systemic vasculitis. *Arthritis Rheum*. 2003;48(8):2362–74.
160. Cross A, Bucknall RC, Cassatella MA, Edwards SW, Moots RJ. Synovial fluid neutrophils transcribe and express class II major histocompatibility complex molecules in rheumatoid arthritis. *Arthritis Rheum*. 2003;48(10):2796–806.
161. Vono M, Lin A, Norrby-Teglund A, Koup RA, Liang F, Loré K. Neutrophils acquire the capacity for antigen presentation to memory CD4+ T cells in vitro and ex vivo. *Blood*. 2017;129(14):1991–2001.
162. Fanger NA, Liu C, Guyre PM, Wardwell K, O'Neil J, Guo TL, et al. Activation of human T cells by major histocompatability complex class II expressing neutrophils: proliferation in the presence of superantigen, but not tetanus toxoid. *Blood*. 1997;89(11):4128–35.
163. Radsak M, Iking-Konert C, Stegmaier S, Andrassy K, Hänsch GM. Polymorphonuclear neutrophils as accessory cells for T-cell activation: Major histocompatibility complex class II restricted antigen-dependent induction of T-cell proliferation. *Immunology*. 2000;101(4):521–30.
164. Pliyev BK, Sumarokov AB, Buriachkovskaia LI, Menshikov M. Extracellular acidosis promotes neutrophil transdifferentiation to MHC class II-expressing cells. *Cell Immunol*. 2011;271(2):214–8.
165. Sandilands GP, Ahmed Z, Perry N, Davison M, Lupton A, Young B. Cross-linking of neutrophil CD11b results in rapid cell surface expression of molecules required for

antigen presentation and T-cell activation. *Immunology*. 2005;114(3):354–68.

166. Li K-J, Wu C-H, Shen C-Y, Kuo Y-M, Yu C-L, Hsieh S-C. Membrane Transfer from Mononuclear Cells to Polymorphonuclear Neutrophils Transduces Cell Survival and Activation Signals in the Recipient Cells via Anti-Extrinsic Apoptotic and MAP Kinase Signaling Pathways. *PLoS One*. 2016;11(6):e0156262.
167. Culshaw S, Millington OR, Brewer JM, McInnes IB. Murine neutrophils present Class II restricted antigen. *Immunol Lett*. 2008;118(1):49–54.
168. Ostanin D V, Kurmaeva E, Furr K, Bao R, Hoffman J, Berney S, et al. Acquisition of antigen-presenting functions by neutrophils isolated from mice with chronic colitis. *J Immunol*. 2012;188(3):1491–502.
169. Sharma S, Davis RE, Srivastva S, Nylén S, Sundar S, Wilson ME. A Subset of Neutrophils Expressing Markers of Antigen-Presenting Cells in Human Visceral Leishmaniasis. *J Infect Dis*. 2016;214(10):1531–8.
170. Polak D, Hafner C, Briza P, Kitzmüller C, Elbe-Bürger A, Samadi N, et al. A novel role for neutrophils in IgE-mediated allergy: Evidence for antigen presentation in late-phase reactions. *J Allergy Clin Immunol*. 2019;143(3):1143-1152.e4.
171. Davey MS, Morgan MP, Liuzzi AR, Tyler CJ, Khan MWA, Szakmany T, et al. Microbe-Specific Unconventional T Cells Induce Human Neutrophil Differentiation into Antigen Cross-Presenting Cells. *J Immunol*. 2014;193(7):3704–16.
172. Geng S, Matsushima H, Okamoto T, Yao Y, Lu R, Takashima A. Reciprocal regulation of development of neutrophil- Dendritic cell hybrids in mice by IL-4 and interferon-gamma. *PLoS One*. 2013;8(11):e82929.
173. Geng S, Matsushima H, Okamoto T, Yao Y, Lu R, Page K, et al. Emergence, origin, and function of neutrophil-dendritic cell hybrids in experimentally induced inflammatory lesions in mice. *Blood*. 2013;121(10):1690–700.
174. Matsushima H, Geng S, Lu R, Okamoto T, Yao Y, Mayuzumi N, et al. Neutrophil differentiation into a unique hybrid population exhibiting dual phenotype and functionality of neutrophils and dendritic cells. *Blood*. 2013;121(10):1677–89.
175. Fites JS, Gui M, Kernien JF, Negoro P, Dagher Z, Sykes DB, et al. An unappreciated role for neutrophil-DC hybrids in immunity to invasive fungal infections. *PLoS Pathog*. 2018;14(5):e1007073.
176. Oehler L, Majdic O, Pickl WF, Stöckl J, Riedl E, Drach J, et al. Neutrophil granulocyte-committed cells can be driven to acquire dendritic cell characteristics. *J Exp Med*. 1998;187(7):1019–28.
177. Iking-Konert C, Ostendorf B, Sander O, Jost M, Wagner C, Joosten L, et al. Transdifferentiation of polymorphonuclear neutrophils to dendritic-like cells at the site of inflammation in rheumatoid arthritis: evidence for activation by T cells. *Ann Rheum Dis*. 2005;64(10):1436–42.

178. Singhal S, Bhojnagarwala PS, O'Brien S, Moon EK, Garfall AL, Rao AS, et al. Origin and Role of a Subset of Tumor-Associated Neutrophils with Antigen-Presenting Cell Features in Early-Stage Human Lung Cancer. *Cancer Cell*. 2016;30(1):120–35.
179. Abi Abdallah DS, Egan CE, Butcher BA, Denkers EY. Mouse neutrophils are professional antigen-presenting cells programmed to instruct Th1 and Th17 T-cell differentiation. *Int Immunol*. 2011;23(5):317–26.
180. Potter NS, Harding C V. Neutrophils process exogenous bacteria via an alternate class I MHC processing pathway for presentation of peptides to T lymphocytes. *J Immunol*. 2001;167(5):2538–46.
181. Beauvillain C, Delneste Y, Scotet M, Peres A, Gascan H, Guermonprez P, et al. Neutrophils efficiently cross-prime naive T cells in vivo. *Blood*. 2007;110(8):2965–73.
182. Yang F, Feng C, Zhang X, Lu J, Zhao Y. The Diverse Biological Functions of Neutrophils, Beyond the Defense Against Infections. *Inflammation*. 2017;40(1):311–23.
183. Governa V, Trella E, Mele V, Tornillo L, Amicarella F, Cremonesi E, et al. The Interplay Between Neutrophils and CD8+ T Cells Improves Survival in Human Colorectal Cancer. *Clin Cancer Res*. 2017;23(14):3847–58.
184. Lim K, Hyun YM, Lambert-Emo K, Capece T, Bae S, Miller R, et al. Neutrophil trails guide influenza-specific CD8+ T cells in the airways. *Science (80-)*. 2015;349(6252):aaa4352.
185. Pillay J, Kamp VM, van Hoffen E, Visser T, Tak T, Lammers J-W, et al. A subset of neutrophils in human systemic inflammation inhibits T cell responses through Mac-1. *J Clin Invest*. 2012;122(1):327–36.
186. Musich T, Rahman MA, Mohanram V, Miller-Novak L, Demberg T, Venzon DJ, et al. Neutrophil Vaccination Dynamics and Their Capacity To Mediate B Cell Help in Rhesus Macaques. *J Immunol*. 2018;201(8):2287–302.
187. Huard B, McKee T, Bosshard C, Durual S, Matthes T, Myit S, et al. APRIL secreted by neutrophils binds to heparan sulfate proteoglycans to create plasma cell niches in human mucosa. *J Clin Invest*. 2008;118(8):2887–95.
188. Puga I, Cols M, Barra CM, He B, Cassis L, Gentile M, et al. B cell–helper neutrophils stimulate the diversification and production of immunoglobulin in the marginal zone of the spleen. *Nat Immunol*. 2012;13(2):170–80.
189. Nagelkerke SQ, Aan De Kerk DJ, Jansen MH, Van Den Berg TK, Kuijpers TW. Failure to detect functional neutrophil B Helper cells in the human spleen. *PLoS One*. 2014;9(2):e88377.
190. Bird AK, Chang M, Barnard J, Goldman BI, Meednu N, Rangel-Moreno J, et al. Neutrophils Slow Disease Progression in Murine Lupus via Modulation of Autoreactive Germinal Centers. *J Immunol*. 2017;199(2):458–66.

191. Jee J, Bonnegarde-Bernard A, Duverger A, Iwakura Y, Cormet-Boyaka E, Martin TL, et al. Neutrophils negatively regulate induction of mucosal IgA responses after sublingual immunization. *Mucosal Immunol*. 2015;8(4):735–45.
192. Parsa R, Lund H, Georgoudaki A-M, Zhang X-M, Ortlieb Guerreiro-Cacais A, Grommisch D, et al. BAFF-secreting neutrophils drive plasma cell responses during emergency granulopoiesis. *J Exp Med*. 2016;213(8):1537–53.
193. Massena S, Christoffersson G, Vagesjo E, Seignez C, Gustafsson K, Binet F, et al. Identification and characterization of VEGF-A – responsive neutrophils expressing CD49d , VEGFR1 , and CXCR4 in mice and humans. *Blood*. 2015;126(17):2016–26.
194. Leliefeld PHC, Pillay J, Vrisekoop N, Heeres M, Tak T, Kox M, et al. Differential antibacterial control by neutrophil subsets. *Blood Adv*. 2018;2(11):1344–55.
195. Deniset JF, Kubes P. Neutrophil heterogeneity: Bona fide subsets or polarization states? *J Leukoc Biol*. 2018;103(5):829–38.
196. Silvestre-Roig C, Fridlender ZG, Glogauer M, Scapini P. Neutrophil Diversity in Health and Disease. *Trends Immunol*. 2019;40(7):565–83.
197. Thomas DC. How the phagocyte NADPH oxidase regulates innate immunity. *Free Radic Biol Med*. 2018;125:44–52.
198. Németh T, Mócsai A, Lowell CA. Neutrophils in animal models of autoimmune disease. *Semin Immunol*. 2016;28(2):174–86.
199. Mortaz E, Alipoor SD, Adcock IM, Mumby S, Koenderman L. Update on Neutrophil Function in Severe Inflammation. *Front Immunol*. 2018;9:2171.
200. Scozzi D, Ibrahim M, Menna C, Krupnick AS, Kreisel D, Gelman AE. The role of neutrophils in transplanted organs. *Am J Transplant*. 2017;17(2):328–35.
201. Hoenderdos K, Condliffe A. The neutrophil in chronic obstructive pulmonary disease. *Am J Respir Cell Mol Biol*. 2013;48(5):531–9.
202. Farahi N, Loutsios C, Tregay N, Wright AKA, Berair R, Lok LSC, et al. In vivo imaging reveals increased eosinophil uptake in the lungs of obese asthmatic patients. *J Allergy Clin Immunol*. 2018;142(5):1659-1662.e8.
203. Peiró T, Patel DF, Akthar S, Gregory LG, Pyle CJ, Harker JA, et al. Neutrophils drive alveolar macrophage IL-1β release during respiratory viral infection. *Thorax*. 2018;73(6):546–56.
204. Vermeren S, Karmakar U, Rossi AG. Immune complex-induced neutrophil functions: A focus on cell death. *Eur J Clin Invest*. 2018;48 Suppl 2:e12948.
205. Fossati G, Bucknall RC, Edwards SW. Insoluble and soluble immune complexes activate neutrophils by distinct activation mechanisms: changes in functional responses induced by priming with cytokines. *Ann Rheum Dis*. 2002;61(1):13–9.
206. Sadik CD, Kim ND, Iwakura Y, Luster AD. Neutrophils orchestrate their own recruitment in murine arthritis through C5aR and FcγR signaling. *Proc Natl Acad Sci*.

2012;109(46):E3177–85.
207. Willcocks LC, Lyons PA, Clatworthy MR, Robinson JI, Yang W, Newland SA, et al. Copy number of FCGR3B, which is associated with systemic lupus erythematosus, correlates with protein expression and immune complex uptake. *J Exp Med*. 2008;205(7):1573–82.
208. Looney MR, Su X, Ziffle JA Van, Lowell CA, Matthay MA. Neutrophils and their Fcγ receptors are essential in a mouse model of transfusion-related acute lung injury. *J Clin Invest*. 2006;116(6):1615–23.
209. Schett G, Neurath MF. Resolution of chronic inflammatory disease: universal and tissue-specific concepts. *Nat Commun*. 2018;9(1):3261.
210. Casanova-Acebes M, Nicolás-Ávila JA, Li JL, García-Silva S, Balachander A, Rubio-Ponce A, et al. Neutrophils instruct homeostatic and pathological states in naive tissues. *J Exp Med*. 2018;215(11):2778–95.
211. Tomay F, Wells K, Duong L, Tsu JW, Dye DE, Radley-Crabb HG, et al. Aged neutrophils accumulate in lymphoid tissues from healthy elderly mice and infiltrate T- and B-cell zones. *Immunol Cell Biol*. 2018;96(8):831–40.
212. Klose CSN, Artis D. Innate lymphoid cells as regulators of immunity, inflammation and tissue homeostasis. *Nat Immunol*. 2016;17(7):765–74.
213. Spits H, Artis D, Colonna M, Diefenbach A, Di Santo JP, Eberl G, et al. Innate lymphoid cells — a proposal for uniform nomenclature. *Nat Rev Immunol*. 2013;13(2):145–9.
214. Wang S, Xia P, Chen Y, Qu Y, Xiong Z, Ye B, et al. Regulatory Innate Lymphoid Cells Control Innate Intestinal Inflammation. *Cell*. 2017;171(1):201-216.e18.
215. Mjösberg J, Spits H. Human innate lymphoid cells. *J Allergy Clin Immunol*. 2016;138(5):1265–76.
216. Lim AI, Li Y, Lopez-Lastra S, Stadhouders R, Paul F, Casrouge A, et al. Systemic Human ILC Precursors Provide a Substrate for Tissue ILC Differentiation. *Cell*. 2017;168(6):1086-1100.e10.
217. Symowski C, Voehringer D. Interactions between Innate Lymphoid Cells and Cells of the Innate and Adaptive Immune System. *Front Immunol*. 2017;8:1422.
218. Monticelli L a., Sonnenberg GF, Abt MC, Alenghat T, Ziegler CGK, Doering TA, et al. Innate lymphoid cells promote lung-tissue homeostasis after infection with influenza virus. *Nat Immunol*. 2011;12(11):1045–54.
219. von Moltke J, Ji M, Liang H-E, Locksley RM. Tuft-cell-derived IL-25 regulates an intestinal ILC2–epithelial response circuit. *Nature*. 2016;529(7585):221–5.
220. Xu W, Cherrier DE, Chea S, Vosshenrich C, Serafini N, Petit M, et al. An Id2RFP-Reporter Mouse Redefines Innate Lymphoid Cell Precursor Potentials. *Immunity*. 2019;50(4):1054-1068.e3.

221. Constantinides MG, McDonald BD, Verhoef PA, Bendelac A. A committed precursor to innate lymphoid cells. *Nature*. 2014;508(7496):397–401.
222. Scoville SD, Freud AG, Caligiuri MA. Cellular pathways in the development of human and murine innate lymphoid cells. *Curr Opin Immunol*. 2019;56:100–6.
223. Ghaedi M, Steer CA, Martinez-Gonzalez I, Halim TYF, Abraham N, Takei F. Common-Lymphoid-Progenitor-Independent Pathways of Innate and T Lymphocyte Development. *Cell Rep*. 2016;15(3):471–80.
224. Walker JA, Clark PA, Crisp A, Barlow JL, Szeto A, Ferreira ACF, et al. Polychromic Reporter Mice Reveal Unappreciated Innate Lymphoid Cell Progenitor Heterogeneity and Elusive ILC3 Progenitors in Bone Marrow. *Immunity*. 2019;51(1):104-118.e7.
225. Vonarbourg C, Mortha A, Bui VL, Hernandez PP, Kiss EA, Hoyler T, et al. Regulated expression of nuclear receptor RORγt confers distinct functional fates to NK cell receptor-expressing RORγt(+) innate lymphocytes. *Immunity*. 2010;33(5):736–51.
226. Ohne Y, Silver JS, Thompson-Snipes L, Collet MA, Blanck JP, Cantarel BL, et al. IL-1 is a critical regulator of group 2 innate lymphoid cell function and plasticity. *Nat Immunol*. 2016;17(6):646–55.
227. Lim AI, Menegatti S, Bustamante J, Le Bourhis L, Allez M, Rogge L, et al. IL-12 drives functional plasticity of human group 2 innate lymphoid cells. *J Exp Med*. 2016;213(4):569–83.
228. Bal SM, Bernink JH, Nagasawa M, Groot J, Shikhagaie MM, Golebski K, et al. IL-1β, IL-4 and IL-12 control the fate of group 2 innate lymphoid cells in human airway inflammation in the lungs. *Nat Immunol*. 2016;17(6):636–45.
229. Bernink JH, Ohne Y, Teunissen MBM, Wang J, Wu J, Krabbendam L, et al. c-Kit-positive ILC2s exhibit an ILC3-like signature that may contribute to IL-17-mediated pathologies. *Nat Immunol*. 2019;20(8):992–1003.
230. Mombaerts P, Iacomini J, Johnson RS, Herrup K, Tonegawa S, Papaioannou VE. RAG-1-deficient mice have no mature B and T lymphocytes. *Cell*. 1992;68(5):869–77.
231. Cording S, Medvedovic J, Lécuyer E, Aychek T, Déjardin F, Eberl G. Mouse models for the study of fate and function of innate lymphoid cells. *Eur J Immunol*. 2018;48(8):1271–80.
232. Robinette ML, Fuchs A, Cortez VS, Lee JS, Wang Y, Durum SK, et al. Transcriptional programs define molecular characteristics of innate lymphoid cell classes and subsets. *Nat Immunol*. 2015;16(3):306–17.
233. Fort MM, Cheung J, Yen D, Li J, Zurawski SM, Lo S, et al. IL-25 induces IL-4, IL-5, and IL-13 and Th2-associated pathologies in vivo. *Immunity*. 2001;15(6):985–95.
234. Fallon PG, Ballantyne SJ, Mangan NE, Barlow JL, Dasvarma A, Hewett DR, et al. Identification of an interleukin (IL)-25-dependent cell population that provides IL-4, IL-5, and IL-13 at the onset of helminth expulsion. *J Exp Med*. 2006;203(4):1105–16.

235. Moro K, Yamada T, Tanabe M, Takeuchi T, Ikawa T, Kawamoto H, et al. Innate production of TH2 cytokines by adipose tissue-associated c-Kit+Sca-1+ lymphoid cells. *Nature*. 2010;463(7280):540–4.
236. Price AE, Liang H-E, Sullivan BM, Reinhardt RL, Eisley CJ, Erle DJ, et al. Systemically dispersed innate IL-13-expressing cells in type 2 immunity. *Proc Natl Acad Sci U S A*. 2010;107(25):11489–94.
237. Neill DR, Wong SH, Bellosi A, Flynn RJ, Daly M, Langford TKA, et al. Nuocytes represent a new innate effector leukocyte that mediates type-2 immunity. *Nature*. 2010;464(7293):1367–70.
238. Kabata H, Moro K, Koyasu S. The group 2 innate lymphoid cell (ILC2) regulatory network and its underlying mechanisms. *Immunol Rev*. 2018;286(1):37–52.
239. Moro K, Ealey KN, Kabata H, Koyasu S. Isolation and analysis of group 2 innate lymphoid cells in mice. *Nat Protoc*. 2015;10(5):792–806.
240. Li BWS, Stadhouders R, de Bruijn MJW, Lukkes M, Beerens DMJM, Brem MD, et al. Group 2 Innate Lymphoid Cells Exhibit a Dynamic Phenotype in Allergic Airway Inflammation. *Front Immunol*. 2017;8:1684.
241. Ricardo-Gonzalez RR, Van Dyken SJ, Schneider C, Lee J, Nussbaum JC, Liang H-E, et al. Tissue signals imprint ILC2 identity with anticipatory function. *Nat Immunol*. 2018;19(10):1093–9.
242. Klein Wolterink RGJ, Serafini N, van Nimwegen M, Vosshenrich CAJ, de Bruijn MJW, Fonseca Pereira D, et al. Essential, dose-dependent role for the transcription factor Gata3 in the development of IL-5+ and IL-13+ type 2 innate lymphoid cells. *Proc Natl Acad Sci U S A*. 2013;110(25):10240–5.
243. Halim TYF, Hwang YY, Scanlon ST, Zaghouani H, Garbi N, Fallon PG, et al. Group 2 innate lymphoid cells license dendritic cells to potentiate memory TH2 cell responses. *Nat Immunol*. 2016;17(1):57–64.
244. Mjösberg J, Bernink J, Golebski K, Karrich JJ, Peters CP, Blom B, et al. The transcription factor GATA3 is essential for the function of human type 2 innate lymphoid cells. *Immunity*. 2012;37(4):649–59.
245. Halim TYF, MacLaren A, Romanish MT, Gold MJ, McNagny KM, Takei F. Retinoic-acid-receptor-related orphan nuclear receptor alpha is required for natural helper cell development and allergic inflammation. *Immunity*. 2012;37(3):463–74.
246. Wong SH, Walker JA, Jolin HE, Drynan LF, Hams E, Camelo A, et al. Transcription factor RORα is critical for nuocyte development. *Nat Immunol*. 2012;13(3):229–36.
247. Walker JA, Oliphant CJ, Englezakis A, Yu Y, Clare S, Rodewald H-R, et al. Bcl11b is essential for group 2 innate lymphoid cell development. *J Exp Med*. 2015;212(6):875–82.
248. Lei A-H, Xiao Q, Liu G-Y, Shi K, Yang Q, Li X, et al. ICAM-1 controls development and

function of ILC2. *J Exp Med*. 2018;215(8):2157–74.

249. Allen JE, Sutherland TE. Host protective roles of type 2 immunity: Parasite killing and tissue repair, flip sides of the same coin. *Semin Immunol*. 2014;26(4):329–40.
250. Roediger B, Kyle R, Yip KH, Sumaria N, Guy T V, Kim BS, et al. Cutaneous immunosurveillance and regulation of inflammation by group 2 innate lymphoid cells. *Nat Immunol*. 2013;14(6):564–73.
251. Li Y, Chen S, Chi Y, Yang Y, Chen X, Wang H, et al. Kinetics of the accumulation of group 2 innate lymphoid cells in IL-33-induced and IL-25-induced murine models of asthma: a potential role for the chemokine CXCL16. *Cell Mol Immunol*. 2019;16(1):86–97.
252. Stier MT, Zhang J, Goleniewska K, Cephus JY, Rusznak M, Wu L, et al. IL-33 promotes the egress of group 2 innate lymphoid cells from the bone marrow. *J Exp Med*. 2018;215(1):263–81.
253. Karta MR, Rosenthal PS, Beppu A, Vuong CY, Miller M, Das S, et al. β2 integrins rather than β1 integrins mediate Alternaria-induced group 2 innate lymphoid cell trafficking to the lung. *J Allergy Clin Immunol*. 2018;141(1):329-338.e12.
254. Kim MH, Taparowsky EJ, Kim CH. Retinoic Acid Differentially Regulates the Migration of Innate Lymphoid Cell Subsets to the Gut. *Immunity*. 2015;43(1):107–19.
255. Gour N, Smole U, Yong H-M, Lewkowich IP, Yao N, Singh A, et al. C3a is required for ILC2 function in allergic airway inflammation. *Mucosal Immunol*. 2018;11(6):1653–62.
256. Tait Wojno ED, Monticelli L a, Tran S V, Alenghat T, Osborne LC, Thome JJ, et al. The prostaglandin D2 receptor CRTH2 regulates accumulation of group 2 innate lymphoid cells in the inflamed lung. *Mucosal Immunol*. 2015;8(6):1313–23.
257. Maric J, Ravindran A, Mazzurana L, Van Acker A, Rao A, Kokkinou E, et al. Cytokine-induced endogenous production of prostaglandin D2 is essential for human group 2 innate lymphoid cell activation. *J Allergy Clin Immunol*. 2019;143(6):2202-2214.e5.
258. Huang Y, Guo L, Qiu J, Chen X, Hu-Li J, Siebenlist U, et al. IL-25-responsive, lineage-negative KLRG1(hi) cells are multipotential "inflammatory" type 2 innate lymphoid cells. *Nat Immunol*. 2015;16(2):161–9.
259. Huang Y, Mao K, Chen X, Sun M, Kawabe T, Li W, et al. S1P-dependent interorgan trafficking of group 2 innate lymphoid cells supports host defense. *Science (80-)*. 2018;359(6371):114–9.
260. Germain RN, Huang Y. ILC2s - resident lymphocytes pre-adapted to a specific tissue or migratory effectors that adapt to where they move? *Curr Opin Immunol*. 2019;56:76–81.
261. Kim CH, Hashimoto-Hill S, Kim M. Migration and Tissue Tropism of Innate Lymphoid Cells. *Trends Immunol*. 2016;37(1):68–79.
262. Mackley EC, Houston S, Marriott CL, Halford EE, Lucas B, Cerovic V, et al. CCR7-

dependent trafficking of RORγ^{+} ILCs creates a unique microenvironment within mucosal draining lymph nodes. *Nat Commun*. 2015;6:5862.

263. Walker JA, McKenzie ANJ. TH2 cell development and function. *Nat Rev Immunol*. 2018;18(2):121–33.
264. Mirchandani AS, Besnard A-G, Yip E, Scott C, Bain CC, Cerovic V, et al. Type 2 innate lymphoid cells drive CD4+ Th2 cell responses. *J Immunol*. 2014;192(5):2442–8.
265. Halim TYF. Group 2 innate lymphoid cells in disease. *Int Immunol*. 2016;28(1):13–22.
266. Halim TYF, Steer CA, Mathä L, Gold MJ, Martinez-Gonzalez I, McNagny KM, et al. Group 2 innate lymphoid cells are critical for the initiation of adaptive T helper 2 cell-mediated allergic lung inflammation. *Immunity*. 2014;40(3):425–35.
267. Kumagai K, Lewandowski R, Jackson-Humbles DN, Li N, Van Dyken SJ, Wagner JG, et al. Ozone-Induced Nasal Type 2 Immunity in Mice Is Dependent on Innate Lymphoid Cells. *Am J Respir Cell Mol Biol*. 2016;54(6):782–91.
268. Li BWS, de Bruijn MJW, Tindemans I, Lukkes M, KleinJan A, Hoogsteden HC, et al. T cells are necessary for ILC2 activation in house dust mite-induced allergic airway inflammation in mice. *Eur J Immunol*. 2016;46(6):1392–403.
269. Ogasawara N, Poposki JA, Klingler AI, Tan BK, Weibman AR, Hulse KE, et al. IL-10, TGF-β, and glucocorticoid prevent the production of type 2 cytokines in human group 2 innate lymphoid cells. *J Allergy Clin Immunol*. 2018;141(3):1147-1151.e8.
270. Shimokawa C, Kanaya T, Hachisuka M, Ishiwata K, Hisaeda H, Kurashima Y, et al. Mast Cells Are Crucial for Induction of Group 2 Innate Lymphoid Cells and Clearance of Helminth Infections. *Immunity*. 2017;46(5):863–74.
271. Kim BS, Wang K, Siracusa MC, Saenz SA, Brestoff JR, Monticelli LA, et al. Basophils promote innate lymphoid cell responses in inflamed skin. *J Immunol*. 2014;193(7):3717–25.
272. Drake LY, Iijima K, Kita H. Group 2 innate lymphoid cells and CD4+ T cells cooperate to mediate type 2 immune response in mice. *Allergy*. 2014;69(10):1300–7.
273. Liu B, Lee J-B, Chen C-Y, Hershey GKK, Wang Y-H. Collaborative interactions between type 2 innate lymphoid cells and antigen-specific CD4+ Th2 cells exacerbate murine allergic airway diseases with prominent eosinophilia. *J Immunol*. 2015;194(8):3583–93.
274. Bouchery T, Kyle R, Camberis M, Shepherd A, Filbey K, Smith A, et al. ILC2s and T cells cooperate to ensure maintenance of M2 macrophages for lung immunity against hookworms. *Nat Commun*. 2015;6(1):6970.
275. Drake LY, Iijima K, Bartemes K, Kita H. Group 2 Innate Lymphoid Cells Promote an Early Antibody Response to a Respiratory Antigen in Mice. *J Immunol*. 2016;197(4):1335–42.
276. Oliphant CJ, Hwang YY, Walker JA, Salimi M, Wong SH, Brewer JM, et al. MHCII-

mediated dialog between group 2 innate lymphoid cells and CD4(+) T cells potentiates type 2 immunity and promotes parasitic helminth expulsion. *Immunity*. 2014;41(2):283–95.

277. von Burg N, Turchinovich G, Finke D. Maintenance of Immune Homeostasis through ILC/T Cell Interactions. *Front Immunol*. 2015;6:416.
278. Halim TYF, Rana BMJ, Walker JA, Kerscher B, Knolle MD, Jolin HE, et al. Tissue-Restricted Adaptive Type 2 Immunity Is Orchestrated by Expression of the Costimulatory Molecule OX40L on Group 2 Innate Lymphoid Cells. *Immunity*. 2018;48(6):1195-1207.e6.
279. Maazi H, Patel N, Sankaranarayanan I, Suzuki Y, Rigas D, Soroosh P, et al. ICOS:ICOS-ligand interaction is required for type 2 innate lymphoid cell function, homeostasis, and induction of airway hyperreactivity. *Immunity*. 2015;42(3):538–51.
280. Hardman CS, Chen Y-L, Salimi M, Jarrett R, Johnson D, Järvinen VJ, et al. CD1a presentation of endogenous antigens by group 2 innate lymphoid cells. *Sci Immunol*. 2017;2(18):eaan5918.
281. Hepworth MR, Monticelli LA, Fung TC, Ziegler CGK, Grunberg S, Sinha R, et al. Innate lymphoid cells regulate CD4+ T-cell responses to intestinal commensal bacteria. *Nature*. 2013;498(7452):113–7.
282. Melo-Gonzalez F, Kammoun H, Evren E, Dutton EE, Papadopoulou M, Bradford BM, et al. Antigen-presenting ILC3 regulate T cell-dependent IgA responses to colonic mucosal bacteria. *J Exp Med*. 2019;216(4):728–42.
283. Muir R, Osbourn M, Dubois A V, Doran E, Small DM, Monahan A, et al. Innate Lymphoid Cells are the Predominant Source of Interleukin-17A During the Early Pathogenesis of Acute Respiratory Distress Syndrome. *Am J Respir Crit Care Med*. 2016;193(4):407–16.
284. Cai T, Qiu J, Ji Y, Li W, Ding Z, Suo C, et al. IL-17-producing ST2+ group 2 innate lymphoid cells play a pathogenic role in lung inflammation. *J Allergy Clin Immunol*. 2019;143(1):229-244.e9.
285. Xu J, Guardado J, Hoffman R, Xu H, Namas R, Vodovotz Y, et al. IL33-mediated ILC2 activation and neutrophil IL5 production in the lung response after severe trauma: A reverse translation study from a human cohort to a mouse trauma model. *PLoS Med*. 2017;14(7):e1002365.
286. Liang Y, Yi P, Yuan DMK, Jie Z, Kwota Z, Soong L, et al. IL-33 induces immunosuppressive neutrophils via a type 2 innate lymphoid cell/IL-13/STAT6 axis and protects the liver against injury in LCMV infection-induced viral hepatitis. *Cell Mol Immunol*. 2019;16(2):126–37.
287. Mindt BC, Fritz JH, Duerr CU. Group 2 Innate Lymphoid Cells in Pulmonary Immunity and Tissue Homeostasis. *Front Immunol*. 2018;9:840.

288. Smith SG, Chen R, Kjarsgaard M, Huang C, Oliveria J-P, O'Byrne PM, et al. Increased numbers of activated group 2 innate lymphoid cells in the airways of patients with severe asthma and persistent airway eosinophilia. *J Allergy Clin Immunol*. 2016;137(1):75-86.e8.
289. Chen R, Smith SG, Salter B, El-Gammal A, Oliveria JP, Obminski C, et al. Allergen-induced Increases in Sputum Levels of Group 2 Innate Lymphoid Cells in Subjects with Asthma. *Am J Respir Crit Care Med*. 2017;196(6):700–12.
290. Ortega HG, Liu MC, Pavord ID, Brusselle GG, FitzGerald JM, Chetta A, et al. Mepolizumab Treatment in Patients with Severe Eosinophilic Asthma. *N Engl J Med*. 2014;371(13):1198–207.
291. Golebski K, Ros XR, Nagasawa M, van Tol S, Heesters BA, Aglmous H, et al. IL-1β, IL-23, and TGF-β drive plasticity of human ILC2s towards IL-17-producing ILCs in nasal inflammation. *Nat Commun*. 2019;10(1):2162.
292. Silver JS, Kearley J, Copenhaver AM, Sanden C, Mori M, Yu L, et al. Inflammatory triggers associated with exacerbations of COPD orchestrate plasticity of group 2 innate lymphoid cells in the lungs. *Nat Immunol*. 2016;17(6):626–35.
293. Kearley J, Silver JS, Sanden C, Liu Z, Berlin AA, White N, et al. Cigarette smoke silences innate lymphoid cell function and facilitates an exacerbated type I interleukin-33-dependent response to infection. *Immunity*. 2015;42(3):566–79.
294. Hams E, Armstrong ME, Barlow JL, Saunders SP, Schwartz C, Cooke G, et al. IL-25 and type 2 innate lymphoid cells induce pulmonary fibrosis. *Proc Natl Acad Sci U S A*. 2014;111(1):367–72.
295. Brestoff JR, Kim BS, Saenz SA, Stine RR, Monticelli LA, Sonnenberg GF, et al. Group 2 innate lymphoid cells promote beiging of white adipose tissue and limit obesity. *Nature*. 2015;519(7542):242–6.
296. Rak GD, Osborne LC, Siracusa MC, Kim BS, Wang K, Bayat A, et al. IL-33-Dependent Group 2 Innate Lymphoid Cells Promote Cutaneous Wound Healing. *J Invest Dermatol*. 2015;136(2):487–96.
297. Rauber S, Luber M, Weber S, Maul L, Soare A, Wohlfahrt T, et al. Resolution of inflammation by interleukin-9-producing type 2 innate lymphoid cells. *Nat Med*. 2017;23(8):938–44.
298. Chun TT, Chung C-S, Fallon EA, Hutchins NA, Clarke E, Rossi A-L, et al. Group 2 Innate Lymphoid Cells (ILC2s) Are Key Mediators of the Inflammatory Response in Polymicrobial Sepsis. *Am J Pathol*. 2018;188(9):2097–108.
299. Geier CB, Kraupp S, Bra D, Eibl MM, Farmer JR, Csomos K, et al. Reduced numbers of circulating group 2 innate lymphoid cells in patients with common variable immunodeficiency. *Eur J Immunol*. 2017;47(11):1959–69.
300. Vély F, Barlogis V, Vallentin B, Neven B, Piperoglou C, Ebbo M, et al. Evidence of

innate lymphoid cell redundancy in humans. *Nat Immunol*. 2016;17(11):1291–9.
301. Cameron GJM, Cautivo KM, Loering S, Jiang SH, Deshpande A V., Foster PS, et al. Group 2 Innate Lymphoid Cells Are Redundant in Experimental Renal Ischemia-Reperfusion Injury. *Front Immunol*. 2019;10:826.
302. Rankin LC, Girard-Madoux MJH, Seillet C, Mielke LA, Kerdiles Y, Fenis A, et al. Complementarity and redundancy of IL-22-producing innate lymphoid cells. *Nat Immunol*. 2016;17(2):179–86.
303. Urban JF, Noben-Trauth N, Donaldson DD, Madden KB, Morris SC, Collins M, et al. IL-13, IL-4Ralpha, and Stat6 are required for the expulsion of the gastrointestinal nematode parasite Nippostrongylus brasiliensis. *Immunity*. 1998;8(2):255–64.
304. Marsland BJ, Kurrer M, Reissmann R, Harris NL, Kopf M. Nippostrongylus brasiliensis infection leads to the development of emphysema associated with the induction of alternatively activated macrophages. *Eur J Immunol*. 2008;38(2):479–88.
305. Hams E, Aviello G, Fallon PG. The schistosoma granuloma: friend or foe? *Front Immunol*. 2013;4:89.
306. Pearce EJ, M Kane C, Sun J, J Taylor J, McKee AS, Cervi L. Th2 response polarization during infection with the helminth parasite Schistosoma mansoni. *Immunol Rev*. 2004;201:117–26.
307. Puttur F, Denney L, Gregory LG, Vuononvirta J, Oliver R, Entwistle LJ, et al. Pulmonary environmental cues drive group 2 innate lymphoid cell dynamics in mice and humans. *Sci Immunol*. 2019;4(36):eaav7638.
308. Pearson C, Thornton EE, McKenzie B, Schaupp A-L, Huskens N, Griseri T, et al. ILC3 GM-CSF production and mobilisation orchestrate acute intestinal inflammation. *Elife*. 2016;5:e10066.
309. Mohrs M, Shinkai K, Mohrs K, Locksley RM. Analysis of Type 2 Immunity In Vivo with a Bicistronic IL-4 Reporter. *Immunity*. 2001;15(2):303–11.
310. Nussbaum JC, Van Dyken SJ, von Moltke J, Cheng LE, Mohapatra A, Molofsky AB, et al. Type 2 innate lymphoid cells control eosinophil homeostasis. *Nature*. 2013;502(7470):245–8.
311. Entwistle LJ, Gregory LG, Oliver RA, Branchett WJ, Puttur F, Lloyd CM. Pulmonary Group 2 Innate Lymphoid Cell Phenotype Is Context Specific: Determining the Effect of Strain, Location, and Stimuli. *Front Immunol*. 2020;10(January):3114.
312. Eberl G, Marmon S, Sunshine M-J, Rennert PD, Choi Y, Littman DR. An essential function for the nuclear receptor RORγt in the generation of fetal lymphoid tissue inducer cells. *Nat Immunol*. 2004;5(1):64–73.
313. Perry SW, Burke RM, Brown EB. Two-Photon and Second Harmonic Microscopy in Clinical and Translational Cancer Research. *Ann Biomed Eng*. 2012;40(2):277–91.
314. Drobizhev M, Makarov NS, Tillo SE, Hughes TE, Rebane A. Two-photon absorption

properties of fluorescent proteins. *Nat Methods*. 2011;8(5):393–9.
315. Clatworthy MR. Two-photon microscopy for imaging germinal centers and T follicular helper cells. *Methods Mol Biol*. 2015;1291:63–75.
316. Stein J V., F Gonzalez S. Dynamic intravital imaging of cell-cell interactions in the lymph node. *J Allergy Clin Immunol*. 2017;139(1):12–20.
317. Li JL, Goh CC, Keeble JL, Qin JS, Roediger B, Jain R, et al. Intravital multiphoton imaging of immune responses in the mouse ear skin. *Nat Protoc*. 2012;7(2):221–34.
318. Looney MR, Thornton EE, Sen D, Lamm WJ, Glenny RW, Krummel MF. Stabilized imaging of immune surveillance in the mouse lung. *Nat Methods*. 2011;8(1):91–6.
319. Hasegawa T, Kikuta J, Ishii M. Imaging the Bone-Immune Cell Interaction in Bone Destruction. *Front Immunol*. 2019;10:596.
320. Liou HLR, Myers JT, Barkauskas DS, Huang AY. Intravital Imaging of the Mouse Popliteal Lymph Node. *J Vis Exp*. 2012;(60):e3720.
321. Faust N, Varas F, Kelly LM, Heck S, Graf T. Insertion of enhanced green fluorescent protein into the lysozyme gene creates mice with green fluorescent granulocytes and macrophages. *Blood*. 2000;96(2):719–26.
322. Schaefer BC, Schaefer ML, Kappler JW, Marrack P, Kedl RM. Observation of antigen-dependent CD8+ T-cell/ dendritic cell interactions in vivo. *Cell Immunol*. 2001;214(2):110–22.
323. Lindquist RL, Shakhar G, Dudziak D, Wardemann H, Eisenreich T, Dustin ML, et al. Visualizing dendritic cell networks in vivo. *Nat Immunol*. 2004;5(12):1243–50.
324. Anderson KG, Mayer-Barber K, Sung H, Beura L, James BR, Taylor JJ, et al. Intravascular staining for discrimination of vascular and tissue leukocytes. *Nat Protoc*. 2014;9(1):209–22.
325. Ekpenyong AE, Toepfner N, Fiddler C, Herbig M, Li W, Cojoc G, et al. Mechanical deformation induces depolarization of neutrophils. *Sci Adv*. 2017;3(6):e1602536.
326. Heesters BA, Chatterjee P, Kim Y-A, Gonzalez SF, Kuligowski MP, Kirchhausen T, et al. Endocytosis and Recycling of Immune Complexes by Follicular Dendritic Cells Enhances B Cell Antigen Binding and Activation. *Immunity*. 2013;38(6):1164–75.
327. Eissing N, Heger L, Baranska A, Cesnjevar R, Büttner-Herold M, Söder S, et al. Easy performance of 6-color confocal immunofluorescence with 4-laser line microscopes. *Immunol Lett*. 2014;161(1):1–5.
328. Drobizhev M, Tillo S, Makarov N, Hughes T, Rebane A. Absolute two-photon absorption spectra and two-photon brightness of orange and red fluorescent proteins. *J Phys Chem B*. 2009;113(4):855–9.
329. Boxio R, Bossenmeyer-Pourie C, Steinckwich N, Dournon C, Nube O. Mouse bone marrow contains large numbers of functionally competent neutrophils. *J Leukoc Biol*. 2004;75(4):604–11.

330. Ubags NDJ, Suratt BT. Isolation and Characterization of Mouse Neutrophils. *Methods Mol Biol*. 2018;1809:45–57.
331. Haslett C, Guthrie L a, Kopaniak MM, Johnston RB, Henson PM. Modulation of multiple neutrophil functions by preparative methods or trace concentrations of bacterial lipopolysaccharide. *Am J Pathol*. 1985;119(1):101–10.
332. Steinert EM, Schenkel JM, Fraser KA, Beura LK, Manlove LS, Igyártó BZ, et al. Quantifying Memory CD8 T Cells Reveals Regionalization of Immunosurveillance. *Cell*. 2015;161(4):737–49.
333. Moran I, Nguyen A, Khoo WH, Butt D, Bourne K, Young C, et al. Memory B cells are reactivated in subcapsular proliferative foci of lymph nodes. *Nat Commun*. 2018;9(1):3372.
334. Basu S, Hodgson G, Zhang HH, Katz M, Quilici C, Dunn AR. "Emergency" granulopoiesis in G-CSF-deficient mice in response to Candida albicans infection. *Blood*. 2000;95(12):3725–33.
335. Barnden MJ, Allison J, Heath WR, Carbone FR. Defective TCR expression in transgenic mice constructed using cDNA-based α- and β-chain genes under the control of heterologous regulatory elements. *Immunol Cell Biol*. 1998;76(1):34–40.
336. Geerdink RJ, Hennus MP, Westerlaken GHA, Abrahams AC, Albers KI, Walk J, et al. LAIR-1 limits neutrophil extracellular trap formation in viral bronchiolitis. *J Allergy Clin Immunol*. 2018;141(2):811–4.
337. Kumawat K, Geerdink RJ, Hennus MP, Roda MA, van Ark I, Leusink-Muis T, et al. LAIR-1 Limits Neutrophilic Airway Inflammation. *Front Immunol*. 2019;10:842.
338. Zhou J, Nefedova Y, Lei A, Gabrilovich D. Neutrophils and PMN-MDSC: Their biological role and interaction with stromal cells. *Semin Immunol*. 2018;35(December):19–28.
339. Campbell EL, Bruyninckx WJ, Kelly CJ, Glover LE, McNamee EN, Bowers BE, et al. Transmigrating neutrophils shape the mucosal microenvironment through localized oxygen depletion to influence resolution of inflammation. *Immunity*. 2014;40(1):66–77.
340. Pliyev BK, Dimitrieva T V., Savchenko VG. Cytokine-mediated induction of MHC class II in human neutrophils is dependent on NADPH oxidase activity. *Eur J Cell Biol*. 2015;94(1):67–70.
341. Farahi N, Loutsios C, Tregay N, Summers C, Lok LSC, Ruparelia P, et al. Radiolabelled leucocytes in human pulmonary disease. *Br Med Bull*. 2018;127(1):69–82.
342. Coxon A, Rieu P, Barkalow FJ, Askari S, Sharpe AH, von Andrian UH, et al. A Novel Role for the β2 Integrin CD11b/CD18 in Neutrophil Apoptosis: A Homeostatic Mechanism in Inflammation. *Immunity*. 1996;5(6):653–66.
343. Förster R, Schubel A, Breitfeld D, Kremmer E, Renner-Müller I, Wolf E, et al. CCR7

Coordinates the Primary Immune Response by Establishing Functional Microenvironments in Secondary Lymphoid Organs. *Cell*. 1999;99(1):23–33.

344. Spitzer MH, Nolan GP. Mass Cytometry: Single Cells, Many Features. *Cell*. 2016;165(4):780–91.
345. Gasteiger G, D'Osualdo A, Schubert DA, Weber A, Bruscia EM, Hartl D. Cellular Innate Immunity: An Old Game with New Players. *J Innate Immun*. 2017;9(2):111–25.
346. Hurrell BP, Shafiei Jahani P, Akbari O. Social Networking of Group Two Innate Lymphoid Cells in Allergy and Asthma. *Front Immunol*. 2018;9:2694.
347. Cherrier M, Sawa S, Eberl G. Notch, Id2, and RORγt sequentially orchestrate the fetal development of lymphoid tissue inducer cells. *J Exp Med*. 2012;209(4):729–40.
348. Jackson JT, Hu Y, Liu R, Masson F, D'Amico A, Carotta S, et al. Id2 expression delineates differential checkpoints in the genetic program of CD8α+ and CD103+ dendritic cell lineages. *EMBO J*. 2011;30(13):2690–704.
349. Yang XO, Pappu BP, Nurieva R, Akimzhanov A, Kang HS, Chung Y, et al. T helper 17 lineage differentiation is programmed by orphan nuclear receptors ROR alpha and ROR gamma. *Immunity*. 2008;28(1):29–39.
350. Miller MJ, Hejazi AS, Wei SH, Cahalan MD, Parker I. T cell repertoire scanning is promoted by dynamic dendritic cell behavior and random T cell motility in the lymph node. *Proc Natl Acad Sci*. 2004;101(4):998–1003.
351. Liu Z, Gerner MY, Van Panhuys N, Levine AG, Rudensky AY, Germain RN. Immune homeostasis enforced by co-localized effector and regulatory T cells. *Nature*. 2015;528(7581):225–30.
352. Gerner MY, Kastenmuller W, Ifrim I, Kabat J, Germain RN. Histo-Cytometry: A Method for Highly Multiplex Quantitative Tissue Imaging Analysis Applied to Dendritic Cell Subset Microanatomy in Lymph Nodes. *Immunity*. 2012;37(2):364–76.
353. Erturk A, Becker K, Jahrling N, Mauch CP, Hojer CD, Egen JG, et al. Three-dimensional imaging of solvent-cleared organs using 3DISCO. *Nat Protoc*. 2012;7(11):1983–95.
354. Susaki EA, Tainaka K, Perrin D, Yukinaga H, Kuno A, Ueda HR. Advanced CUBIC protocols for whole-brain and whole-body clearing and imaging. *Nat Protoc*. 2015;10(11):1709–27.
355. Coutu DL, Kokkaliaris KD, Kunz L, Schroeder T. Multicolor quantitative confocal imaging cytometry. *Nat Methods*. 2018;15(1):39–46.
356. Tan Z, Jiang R, Wang X, Wang Y, Lu L, Liu Q, et al. RORγt+IL-17+ neutrophils play a critical role in hepatic ischemia-reperfusion injury. *J Mol Cell Biol*. 2013;5(2):143–6.
357. Taylor PR, Roy S, Leal SM, Sun Y, Howell SJ, Cobb BA, et al. Activation of neutrophils by autocrine IL-17A-IL-17RC interactions during fungal infection is regulated by IL-6, IL-23, RORγt and dectin-2. *Nat Immunol*. 2014;15(2):143–51.

358. Tamassia N, Arruda-Silva F, Calzetti F, Lonardi S, Gasperini S, Gardiman E, et al. A Reappraisal on the Potential Ability of Human Neutrophils to Express and Produce IL-17 Family Members In Vitro: Failure to Reproducibly Detect It. *Front Immunol*. 2018;9:795.
359. Lim H, Kim YU, Yun K, Drouin SM, Chung Y. Distinct regulation of Th2 and Th17 responses to allergens by pulmonary antigen presenting cells in vivo. *Immunol Lett*. 2013;156(1–2):140–8.
360. Na H, Lim H, Choi G, Kim B-K, Kim S-H, Chang Y-S, et al. Concomitant suppression of TH2 and TH17 cell responses in allergic asthma by targeting retinoic acid receptor-related orphan receptor γt. *J Allergy Clin Immunol*. 2018;141(6):2061-2073.e5.
361. Pellefigues C, Tang S-C, Schmidt A, White RF, Lamiable O, Connor LM, et al. Toll-Like Receptor 4, but Not Neutrophil Extracellular Traps, Promote IFN Type I Expression to Enhance Th2 Responses to Nippostrongylus brasiliensis. *Front Immunol*. 2017;8:1575.